United States
Environmental Protection
Agency

Environmental Sciences Research
Laboratory
Research Triangle Park NC 27711

EPA-600/7-80-025
February 1980

Research and Development

EPA

Aerosol Source Characterization Study in St. Louis

Trace Element Analysis

RESEARCH REPORTING SERIES

Research reports of the Office of Research and Development, U.S. Environmental Protection Agency, have been grouped into nine series. These nine broad categories were established to facilitate further development and application of environmental technology. Elimination of traditional grouping was consciously planned to foster technology transfer and a maximum interface in related fields. The nine series are:

1. Environmental Health Effects Research
2. Environmental Protection Technology
3. Ecological Research
4. Environmental Monitoring
5. Socioeconomic Environmental Studies
6. Scientific and Technical Assessment Reports (STAR)
7. Interagency Energy-Environment Research and Development
8. "Special" Reports
9. Miscellaneous Reports

This report has been assigned to the INTERAGENCY ENERGY-ENVIRONMENT RESEARCH AND DEVELOPMENT series. Reports in this series result from the effort funded under the 17-agency Federal Energy/Environment Research and Development Program. These studies relate to EPA's mission to protect the public health and welfare from adverse effects of pollutants associated with energy systems. The goal of the Program is to assure the rapid development of domestic energy supplies in an environmentally-compatible manner by providing the necessary environmental data and control technology. Investigations include analyses of the transport of energy-related pollutants and their health and ecological effects; assessments of, and development of, control technologies for energy systems; and integrated assessments of a wide range of energy-related environmental issues.

This document is available to the public through the National Technical Information Service, Springfield, Virginia 22161.

EPA-600/7-80-025
February 1980

AEROSOL SOURCE CHARACTERIZATION STUDY IN ST. LOUIS

Trace Element Analysis

by

Kenneth A. Hardy

Department of Physical Sciences
Florida International University
Miami, Florida 33199

Contract No. 68-02-2406

Project Officer

Ronald K. Patterson

Atmospheric Chemistry and Physics Division
Environmental Sciences Research Laboratory
Research Triangle Park, North Carolina 27711

ENVIRONMENTAL SCIENCES RESEARCH LABORATORY
OFFICE OF RESEARCH AND DEVELOPMENT
U.S. ENVIRONMENTAL PROTECTION AGENCY
RESEARCH TRIANGLE PARK, NORTH CAROLINA 27711

DISCLAIMER

This report has been reviewed by the Environmental Sciences Research Laboratory, U.S. Environmental Protection Agency and approved for publication. Approval does not signify that the contents necessarily reflect the views and policies of the U.S. Environmental Protection Agency, nor does mention of trade names or commercial products constitute endorsement or recommendation for use.

ABSTRACT

The aerosol in St. Louis was sampled in July 1975 to better characterize the aerosol in an urban environment with moderate dispersion characteristics and heavy industrial activity. Two sampling sites were chosen, one in downtown St. Louis and a second close to the industrialized section in south St. Louis.

Sampling devices at each site included a five-stage cascade impactor and a streaker sampler to give the time distribution of trace elements. A wind-direction-sensitive sampling system controlling four five-stage cascade impactors was installed at one site. Size and time distributions of trace elements heavier than silicon were determined by proton induced x-ray emission at Florida State University.

Aerosol source coefficients show that the aerosol from the downtown site is primarily from coal (60-80%), cement dust (17%), steel manufacturing (6-7%) and auto emissions (3%). The aerosol from the industrialized site is primarily due to coal combustion products and dust (75%), and cement dust (15%); while auto emissions and heavy industrial processes account for ∿5% of the aerosol mass. Determining the directional distribution of the aerosol trace elements allowed pinpointing of strong local sources.

This report was submitted in fulfillment of Contract No. 68-02-2406 by Florida International University under the sponsorship of the U.S. Environmental Protection Agency. This report covers the period June 1976, to June 1979, and work was completed as of December 1979.

CONTENTS

FIGURES

TABLES

SECTION 1

INTRODUCTION

The aerosol in St. Louis has been intensively studied in the past several years (Johansson et al., 1975). St. Louis is the tenth largest city in the United States and is situated on the Mississippi River in gently rolling topography. St. Louis is the site of much heavy industry, involving approximately 35% of the population. Industries such as coking, primary metal and steel production, transportation equipment manufacturing, metal fabrication and heavy machinery contribute to the particulate problem in St. Louis.

In order to aid in the characterization of an atmospheric aerosol, knowledge of the trace element concentrations as a function of particle size, time and meteorological conditions, in addition to the normally measured parameters such as total aerosol mass is necessary. A study was undertaken in July 1975, with the cooperation of the Aerosol Research Branch of the United States Environmental Protection Agency in order to aid in the characterization of the aerosol in St. Louis, Missouri.

In this study two sampling sites were chosen. A site in a downtown commercial area at 14th and Market Streets, the St. Louis Municipal Court site and a site in the heavy industrial area in south St. Louis, at 8227 S. Broadway, the St. Louis Fire Station site at Broadway and Hurck.

Sampling devices at each station included a five-stage Battelle design cascade impactor (Mitchell et al., 1959) a streaker sampler giving two-hour time resolution (Nelson et al., 1975) and a high volume sampler to measure total aerosol mass. In addition, a wind direction sensitive sampling system, operating from Battelle impactors was operated at each site during different time periods. Each one of the four wind direction sensitive Battelle impactors operated only when the wind was blowing from a selected ninety degree sector and above a predetermined velocity (approximately 8 kph). The four quadrants were centered around the northeast, southeast, southwest and northwest directions. The cascade impactors classify particulates into six size ranges of d<.25, .25<d<.5, .5<d<1., 1<d<2, 2<d<4 and 4<d micrometers, equivalent aerodynamic diameter (Mitchell et al., 1959). The streaker is a continuous sampling device utilizing .4μm nucleopore filters that can give two-hour time resolution from a $.12m^3$ sample. (Nelson et al., 1959) the streaker and cascade impactor samples were analyzed by proton induced x-ray emission (Johansson et al., 1972) at Florida State University.

SECTION 2

DATA EVALUATION

WEATHER CONDITIONS

The weather conditions during the sampling period were monitored by the National Weather Service and four additional radiosonds per day flown by the Environmental Protection Agency. The pertinent data is summarized in Table 1.

Inspection of the table shows generally light winds from the south to southwest and a morning inversion that, with the exception of two days, persisted through the day.

TABLE 1

WEATHER CONDITIONS DURING THE SAMPLING PERIOD

Date	Average Wind Speed Km/Hr	Average Wind Direction Degrees	Inversion A.M.	Inversion P.M.	Precipitation in In.
7/15/75	8.7	190	Yes	No	0
7/16/75	12.5	150	Yes	Yes	0
7/17/75	10.8	180	Yes	Yes	.06
7/18/75	11.4	200	Yes	Yes	.30
7/19/75	15.8	220	Yes	Yes	.09
7/20/75	7.9	280	Yes	No	0
7/21/75	5.5	340	Yes	Yes	0
7/22/75	6.8	100	Yes	Yes	0
7/23/75	13.7	180	Yes	Yes	.20
7/24/75	9.2	300	Yes	No	0

SIZE DISTRIBUTION DATA

The mass weighted mean diameter is useful to characterize the elemental size distributions. It is defined as

$$\bar{d} = \frac{\sum_{i=1}^{6} m_i d_i}{\sum_{i=1}^{6} m_i}$$

where the summation indices 1, specifies the stage of the cascade impactor, m_i is the mass collected on that stage and d_i the average equivalent aerodynamic diameter of the particulates collected on stage i. The assignment of the average diameter is somewhat arbitrary, as stages one and six are open ended. The diameters used in the calculation were .19, .37, .75, 1.5, 3.0, 6.0 micro-meters for stages 6 through 1, respectively. The data shown in Table 2 is useful to compare different samples collected with similar devices. The error in these figures is approximately ±20%.

Mass weighted mean diameter was not calculated for all sets of size distribution data analyzed. Four sets from the municipal court site, and nine sets from the Fire Station site. These size distributions are presented in figure 2 to figure 92. The mass weighted mean diameter was only calculated for complete data sets, that is, data sets with no missing stages. Table 3 shows the collection dates for the size distribution samples.

TABLE 2

MASS WEIGHTED MEAN DIAMETER

Micro Meters

ELEMENT	SLMC 7/17/75	SLMC N.E. 7/16/75	SLMC S.E. 7/17/75	SLMC S.W. 7/16/75	SLMC N.W. 7/16/75	SLFS 7/16/75	SLFS N.E. 7/17/75	SLFS E. 7/18/75	SLFS S.W. 7/18/75
P	1.91	1.07	1.12	1.08	1.42	1.29	2.0	1.67	1.45
S	.86	.69	.70	.63	1.69	.52	.86	.86	.58
Cl	3.61	1.42	2.01	1.54	2.97	2.91	4.09	1.42	3.61
K	2.28	1.71	2.44	2.51	2.60	3.14	2.98	1.35	2.67
Ca	4.26	3.36	4.26	3.29	3.19	4.39	4.24	2.05	4.24
Ti	3.42	2.13	2.97	1.33	2.10	2.92	3.02	2.91	3.42
V	1.16	-	-	-	-	1.77	-	2.13	-
Cr	2.36	1.61	-	.71	-	-	2.74	2.32	-
Mn	2.37	1.40	2.46	1.13	1.29	1.61	3.29	1.61	2.22
Fe	3.37	2.31	3.30	1.92	2.31	2.94	3.71	1.82	3.08
Ni	3.10	-	2.36	-	-	-	-	1.02	2.79
Cu	1.52	1.97	1.15	-	2.19	1.30	1.93	.63	2.63
Zn	1.57	2.12	1.49	2.06	1.90	1.82	2.30	1.19	2.25
Br	1.48	1.48	1.86	1.12	2.33	1.65	1.87	1.84	.83
Pb	1.21	.81	1.01	.66	1.67	1.09	.96	2.09	.76

TABLE 3

COLLECTION DATES, SIZE DISTRIBUTION SAMPLES

Date	Municipal Court Samples	Fire Station Samples
7/15/75 Tuesday		SLFS-A
7/16/75 Wednesday	SLMC-B	SLFS-B*
7/17/75 Thursday	SLMC-C*	SLFS-C
7/18/75 Friday	SLMC-D	SLFS-D
7/19/75 Saturday	SLMC-E	SLFS-E
7/20/75 Sunday		SLFS-F
7/21/75 Monday		SLFS-G
7/22/75 Tuesday		
7/23/75 Wednesday		SLFS-I
7/24/75 Thursday		SLFS-J

SLMC (St. Louis Municipal Court)

SLFS (St. Louis Fire Station)

*Signifies that only the elemental ratios are useful as the air flow data for this sample is unreliable.

CALCULATION OF SOURCE COEFFICIENTS

A useful way of analyzing air particulate data is the computation of the aerosol source coefficients (Miller et al.). The concentration of air particulate matter at a sampling site due to several sources can be written

$$C_i = \sum_j \alpha_{ij} \gamma_{ij} m_j$$

where j indicates the source of the particulate matter. C_i is the concentration of an element i (nanograms/meter^3) at the collection site, α_{ij} is the fractional composition of element i emitted by source j, m_j is the mass of particulate matter attributable to source j, γ_{ij} is the coefficient of fractionization, which describes the loss of element i between the source and the sampling station. The m_j's may be determined from the experimentally observed concentrations by a linear least squares criteria. The quantity minimized, Q, is given by:

$$Q = \sum_i \frac{x_i - \sum_j \alpha_{ij} \gamma_{ij} m_j}{\sigma_i}$$

which takes the error (σ_i) in the observed concentration (x_i) into account. In general, the γ_{ij} coefficients are not known, but can be assumed to close to 1. The α_{ij} coefficients, which describe the composition of an aerosol emitted by a source j are known for anthropogenic sources but less well known for natural sources. In the calculations presented here, γ_{ij} is taken to be 1.

The method is satisfactory for total particulate matter, however less satisfactory for particulate matter classified by size, as the fractional composition for particulate matter as a function of particle size is not well known. Table 4 shows the assumed source fractional composition for the major components of the aerosol in St. Louis. In the calculation it was assumed that the aerosol was primarily due to six major sources; steel, cement dust, automotive emissions, fuel oil fly ash, soil, and coal. In the composition of fuel oil fly ash, a 10% conversion of SO_2 to particulate matter was assumed.

Aerosol source coefficients were calculated from cascade impactor data by summing the elemental mass deposited on each stage. Only sets of impactor data including all six stages were used for the calculation of source coefficients. Aerosol source coefficients were also calculated from the time distribution data by averaging the data obtained from each streaker. The agreement between the aerosol mass calculated from the aerosol source coefficients and the observed total aerosol mass, from high volume filters, is not encouraging. However, since the calculated aerosol composition agrees with that measured by the cascade impactors and streaker sampler the results of the calculation are meaningful. The deviation between the calculated and measured total mass can be attributed to two factors: (1) the efficiency of the high volume sampler with respect to particle size is different than that of the cascade impactor and the streaker, and thereby samples a larger fraction of the aerosol mass; and (2) the composition of the St. Louis aerosol is much more complex than the assumed composition, consisting of many small sources that contribute to the aerosol mass measured by the high volume sampler.

Table 5 compares the calculated total masses from the impactor and streaker samples to the measured total aerosol masses obtained from the high volume sampler. Table 6 shows source coefficients

TABLE 4

ASSUMED FRACTIONAL ELEMENTAL COMPOSITION OF THE MAJOR SOURCES OF THE ST. LOUIS AEROSOL

Element	Steel[a]	Cement[b]	Automobile[c]	Fuel Oil Fly Ash[d]	Soil[e]	Coal[f]
P	0	0	0	0	0	0
S	0	$.10x10^{-1}$	$.10x10^{0}$	$.39x10^{0}$	$8x10^{-4}$	0
Cl	0	0	$.69x10^{-1}$	0	0	0
K	0	$.80x10^{-3}$	0	$.39x10^{-2}$	$1.8x10^{-2}$	$3.3x10^{-2}$
Ca	$8.9x10^{-2}$	$.46x10^{0}$	$.48x10^{-1}$	$.18x10^{-2}$	$5.6x10^{-3}$	$3.8x10^{-2}$
Ti	0	$.18x10^{-2}$	0	$.13x10^{-3}$	$3.8x10^{-3}$	$1x10^{-2}$
V	0	0	0	$.11x10^{-1}$	$7x10^{-5}$	$8x10^{-4}$
Cr	0	0	0	$.53x10^{-3}$	$5x10^{-5}$	$6.5x10^{-4}$
Mn	$3.5x10^{-2}$	$.30x10^{-3}$	0	$.13x10^{-3}$	$8x10^{-4}$	$3.4x10^{-4}$
Fe	$2.2x10^{-1}$	$.21x10^{-1}$	$.82x10^{-1}$	$.11x10^{-1}$	$2x10^{-2}$	$1x10^{-1}$
Ni	0	0	0	$.25x10^{-1}$	$5x10^{-5}$	$3.7x10^{-4}$
Cu	0	0	0	$.66x10^{-3}$	$3x10^{-5}$	$3.1x10^{-4}$
Zn	$3.4x10^{-2}$	0	$.12x10^{-1}$	$.12x10^{-3}$	$1x10^{-4}$	$5.2x10^{-3}$
Br	0	0	$.15x10^{0}$	$.13x10^{-3}$	0	0
Pb	0	0	$.41x10^{0}$	$.79x10^{-3}$	$5x10^{-5}$	$9x10^{-4}$

(a) Gatz, D. F., Symposium on Atom Diffusion, American Meteor Soc, Boston, 1974.
(b) Standards for Portland Cement. ASTM-C-150.
(c) Cahill, T. A., Feeney, P. J., Report to California Air Resources Board ARB 502, 1973.
(d) Winchester, J. A., De Saedelier, G. G., Nondestructive Activation Analysis, Amsterdam, 1975.
(e) McClelland, J., U.S. Department of Agriculture, Private Comm.
(f) Heisler, S. L., EPA Progress Report, R802160-03-0, 1975.

calculated from the impactor data. It should be noted that the assumed composition of coal and soil are similar (Table 4) and the source coefficient calculation will not be sensitive to this difference. Table 6 also shows the source coefficients calculated from the averaged streaker data. To calculate these source coefficients, the elemental abundances were averaged over all the data points from a streaker, and these abundances used to calculate the source coefficients. As with the impactor data, the total aerosol mass calculated does not agree with that measured by the high volume sampler. (Table 5)

TABLE 5

TOTAL AEROSOL MASS

Impactor Samples

Sample	Date	Total Mass Calculated (μg/m^3)	Mass (μg/m^3)	% Calculated Mass / HiVol Mass x 100
SLFS B	7/16/75	9.4	139.2	6.8
SLMC C	7/17/75	16.4	115.4	14.4
SLFS G	7/21/75	8.4	80.8	10.5
Streaker Samples				
SLFS	7/15/75	6.8	124.5	5.5
SLFS	7/22/75	16.8	124.5	13.5
SLMC	7/22/75	18.0	97.2	18.5

TABLE 6

SOURCE COEFFICIENTS (%)

Data Set	Date	Steel	Cement	Coal	Fuel Oil Fly Ash	Soil	Automobile
				From Impactor Data			
SLFS B	7/16/75	5.4	23.5	-	.6	69	1.7
SLFS C	7/17/75	6.3	17	60	-	11	3.8
SLFS G	7/21/75	48	3.4	33	.4	-	14
				From Streaker Data			
SLFS	7/15/75	13.8	-	79.5	-	-	6.6
SLFS	7/22/75	4.5	14.7	75.2	2.9	-	2.5
SLMC	7/22/75	7.2	-	88.6	.9	-	3.1

HIGH VOLUME FILTER ANALYSIS

The high volume sampler filters were analyzed by the U. S. Environmental Protection Agency for SO_4, NO_3, C, N, Na^+ and K^+. The filters were weighed by the City of St. Louis, Division of Air Pollution Control. These results are presented in Table 7 and Table 8 (private communication, R. Patterson, 1976.) In addition, organic extractions were performed by ultrasonic agitation (Mendenhall et al., 1978.)

TABLE 7

HIGH VOLUME FILTER ANALYSIS
(Municipal Court)

($\mu g/m^3$)

Date	Mass	C	N	SO_4	NO_3	Na^+	NH_4^+	K^+
7/15	98.2	6.4	.6	14.3	3.6	6.6	.3	.6
7/16	115.4	7.2	1.1	24.3	6.3	9.5	1.8	--
7/17	115.4	7.3	.5	25.8	20.7	7.1	--	.8
7/18	88.4	6.4	.4	14.6	4	8.8	--	.4
7/19	51.9	3.6	.3	9.6	2.7	5.8	--	.2
7/20	95.	4.9	.4	11.4	4.5	7.7	--	.4
7/21	118.4	6.1	.7	16.7	4.8	6.5	.9	--
7/22	99.8	5.9	.6	24.1	29.3	9.	.6	--
7/23	109.1	--	--	--	--	--	--	--
7/24	62.4	4.	.4	12.1	4.	8.3	--	.2
7/25	41.2	--	--	--	--	--	--	--
7/26	114.2	6.5	1.8	29.6	5.3	7.6	4.4	--
7/27	72.4	3.7	1.1	22.1	1.2	6.1	2.7	--
7/28	135.4	5.1	.6	17.7	4.5	7.6	--	--
7/29	80.9	3.3	.7	21.2	1.5	7.4	3.4	--
7/30	152.3	9.	2.3	45.4	1.7	7.5	2.9	--
7/31	102.6	4.9	.5	22.3	1.5	8.	--	--

TABLE 8

HIGH VOLUME FILTER ANALYSIS

ST. LOUIS FIRE STATION
($\mu g/m^3$)

Date	Mass	C	N	SO_4	NO_3	Na^+	NH_4^+	K^+
7/15	126.5	7.3	.4	13.6	1.7	5	.3	--
7/16	139.2	7.3	.6	21.1	3.3	7	.4	--
7/17	171.1	10.4	.4	26.3	3.1	6.8	--	.2
7/18	183.9	7.1	.4	23.6	2.	7.5	.4	--
7/19	85.5	3.6	.1	13	1.8	5.7	--	.3
7/20	64.4	3.7	.3	11	2.5	6.5	--	.3
7/21	80.8	4.9	.4	21.2	3.6	6	--	.2
7/22	83.7	5.5	.3	14.6	3.6	6.7	--	.1
7/23	214.4	--	--	--	--	--	--	--
7/24	57.3	3.2	.2	10.9	3.2	6.8	--	.3
7/25	131.3	--	--	--	--	--	--	--
7/26	107.6	6.8	.7	27.2	3.3	8.4	.6	--
7/27	123.8	7.1	1.5	43	1.1	11.3	3.8	--
7/28	127.6	7.3	.4	37.5	2.3	8.2	1.8	--
7/29	141.4	8.4	.8	25.6	3.2	8.9	--	.5
7/30	134.1	7.2	1.4	37	1.3	8.9	3.0	--
7/31	93.9	6.2	.3	17.7	2.6	7.9	--	.4

DIRECTIONAL DISTRIBUTION OF PARTICULATE MATTER

The directional distribution of the elemental concentration of particulate matter may be determined by combining the information obtained from the streaker samplers with meteorological information.

The wind direction as a function of time was taken from the Department of Commerce weather summary for the St. Louis area. The elemental concentration as a function of time from the streaker samples was combined with the wind direction as a function of time to yield a directional distribution of the elemental concentration of particulate matter. The streaker samples were sorted into thirty six groups, each group corresponding to a ten degree sector of wind direction. The elemental concentrations were averaged over these groups to yield the directional distributions.

SECTION 3

SITE-BY-SITE DATA SUMMARY

ST. LOUIS FIRE STATION (SLFS), BROADWAY AND HURCK

The Broadway and Hurck sampling site is located in close proximity to fifteen major point sources (Fig. 1) which emit a total of 486,000 tons/year of SO_2. The directional distribution of particulate matter taken during the period 7/15/75 to 7/22/75 indicate sources of Cl, K, Ca, Ti, V, Fe, Mn, and Zn in a direction S.W. of the sampling site. The directional distributions of Br and Pb are similar except for a strong source of Pb south of the sampling site. Cr is observed to have a source N.E. of the sampling site, in the direction of the majority of steel fabricating industries, while Cu and Ni have sources to the S.E. of the sampling site. Directional distributions taken during the week starting 7/22/75 are more isotropic; however, Ti, V, Cr, and Fe show sources to the west of the sampling site, Cu has a source S.W. of the sampling site, while Br and Pb originate primarily south of the sampling site.

The wind direction sensitive size distribution data were taken in sectors centered around E, S, W. S.W. and N.E. The wind direction sensing device was located so that interference from trees and tall buildings would not affect the aerosol collection devices or the sensitivity of the wind direction sensing instruments. The size distributions are similar for P, S, Cl, and K, however there is a marked difference in the size distribution for calcium from the east. Calcium distribution from the W, N.E., S, and S.W. have distributions typical of abrasive sources, while the distribution from the east shows a distribution typical of a combustion source. A distribution of this type would be expected from a coal burning power plant.

The size distributions of copper indicate a different distribution in a S.W. direction (typical of an abrasive source) while the other directions are typical of combustion sources. The Pb distributions are similar except for the easterly direction, which indicates a source of large particulate Pb in that direction. It must be noted that the first collection stage from the impactor sampling the southerly direction did not indicate any Pb or Br, so the distribution from the south is somewhat uncertain.

The time distribution of the elemental composition of particulate matter for the Broadway and Hurck site shows a large peak on 7/23/75 from 1000 to 2300 hrs in the elements Ti, V, Mn and Fe. Computer calculations for near surface trajectories were made every four hours during this period. Arrival times for these air parcels were 0700, 1100, 1500, 1900 and 2300. The air parcel that arrived at 0700 (before the incident of high titanium concentration) traveled in a north westerly direction. The air parcels that arrived at 1100 and 1500 traveled in a northerly direction, while the parcel arriving at 1900 traveled in a northeasterly direction. The parcel that arrived at 2300 traveled from the west. The magnitudes of the peaks obtained at 14th and Market and the peak observed at Broadway and Hurck indicate a source close to the Broadway and Hurck site. The aerosol source coefficients were calculated for the time period 0800-2300 on 7/23/75, by averaging the time distribution data for this time interval. The results indicate that 70% of the observed aerosol was due to coal, 20% due to cement dust, 5% due to processes associated with steel manufacturing and 3% due to auto emissions. This analysis accounts for only 2% of the observed titanium, therefore, there must be an additional source of titanium close to the Broadway and Hurck site. These results are in good agreement with the conclusions reached by Draftz using microscopical analysis on aerosol samples taken on 7/23. The elemental size distributions observed on 7/23 are markedly different (for several elements) than those observed on other days in the sampling period. Titanium, V, Mn and Fe show a higher percentage of the observed mass in the large particulate fractions on 7/23 than on other days. In addition, K has an enhanced large particulate size distribution. Unfortunately stage five was missing from this sample, so the mass weighted mean diameter was not calculated.

Of the elemental size distributions observed at the Broadway and Hurck site, the distributions observed on 7/16 and 7/21 are typical.

The elements P, Cl, K, Ca, Fe and Zn exhibit bimodal size distributions with a large fraction of the mass collected on stages 1 and 6. Sulfur, Mn, Br and Pb have small particle enhanced size distributions, and Ti has a large particle enhanced size distribution. In summary, the data analyzed from Broadway and Hurck indicate that a large percentage of the aerosol mass observed at the sampling site (approximately 75%) is due to coal combustion and coal dust. Cement dust accounts for about 15% of the aerosol mass, while automotive emissions and heavy industrial processes account for small percentages (approximately 5% each.) The bimodal distribution for elements contained in coal (and soil) indicate that the large diameter ($d>3\mu m$) particulates originate from coal dust.

The similarity in the elemental composition of the local soil and coal, do not enable a definitive distinction between these two sources. There is a large source of Ti near the sampling site that cannot be accounted for. Draftz concluded that the Ti is probably combined as TiO_2.

ST. LOUIS MUNICIPAL COURT

The St. Louis Municipal Court sampling site is located in the heart of the commercial district in downtown St. Louis. It lies south of the area of heavy industry (steel and metal fabrication) near Alton, Ill. (approximately 10 km), west of coal burning power plants in east St. Louis, and north of the industrialized area in south St. Louis (approximately 8 km).

The time distributions of particulate matter at the Municipal Court exhibits two incidents of high elemental concentrations in some trace elements. From 0000 to 1200 on 7/23/75 there were large increases in the concentration of Cl, Zn, Cu and Pb. The period from 1800 on 7/23/75 to 2000 on 7/24/75 showed increases in the concentration of P, S, Cl and K. From 0600 on 7/24/75 to 1400 on 7/24/75 there was a sharp increase in the level of Mn observed at the sampling site. During the period 0000 to 1200 on 7/23/75 the wind direction varied around the southeast (120° to 160°) but switched to the southwest (220°) by 1500. During this incident (the increase in Pb concentration) there was no increase in the concentrations of Br so the increase in Pb cannot be attributed to automobile emission. The wind direction sensitive size distribution for Cu and Zn were markedly different in the sector centered on the southeast than in the other directions. The size distribution observed from the southeasterly direction is a small particle enhanced distribution for these elements. The source of these particulates is probably industrial emissions from the nonferrous metal plants southeast of the city.

During the period from 1800 on 7/23/75 to 2000 on 7/24/75, the winds were from the southwest to the northwest. There was an increase in potassium concentration observed at the Municipal Court site during this interval. As there was no increase in the Ca concentration during this time, this increase cannot be attributed to dust or soil.

The directional distribution of particulate matter indicates a source of P, S, Cl, Mn and Ni to the northeast. Likely sources would be the heavy industry located from Granite City to Wood River. The wind direction sensitive size distributions support this conclusion as the size distribution of P, S and Cl in the air parcel from the N.E. are different, being a distribution typical of a combustion source. Titanium and V have strong sources to the northwest of the sampling site. The wind direction sensitive size distribution of Ti is large particulate favored, in the air parcel from the N.W. sector, leading to a conclusion that paint pigments are the likely source of the Ti. A strong source of Cr is located south of the sampling site as indicated by the directional distributions of the particulate matter. Nickel particulates originated northeast of the sampling site in the direction of the steel mills in Granite City while the Cu and Zn have sources to the southwest.

Four sets of elemental size distributions from the Municipal Court site were analyzed. Only one set was complete. The size distribution indicates that S, V, Br and Pb originated from combustion sources while Cl, K, Ca, Ti, V, Cr, Mn and Fe originated from abrasive processes. In summary, the aerosol source coefficients show that the aerosol at the Municipal Court sampling site is primarily from coal (60-80%), cement dust (17%), steel manufacturing (6-7%) and auto emissions (3%).

CONCLUSION

The aerosol in St. Louis is a complex mixture of particulate matter from many urban and industrial sources. This study indicates that sampling at several sites in an urban environment with multiple sampling devices is necessary to characterize the aerosol.

The elemental concentration of the aerosol as a function of time is particularily useful when combined with suitable meteorological information, as this data allows the determination of directional distributions of particulate matter. The calculation of aerosol source coefficients requires better knowledge of the source compositions for the various point sources that may be of interest in the area being investigated. Knowledge of the elemental aerosol source composition as a function of particle size would be particularily useful.

REFERENCES

American Society for Testing and Materials. Standards for Portland Cement. ASTM-C-150.

Andersen, A. A. 1966. A Sampler for Respiratory Health Hazard Assessment. Am. Ind. Hyg. Assn. J. 27:160-165.

Cahill, T. A. and P. J. Feeney, 1973. Report to California Air Resources Board: Contribution of Freeway Traffic to Airborne Particulate Matter. ARB 502. University of California, Davis.

DeJong, G., D. Watts, L. Spiller and R. Patterson, 1978. Programmable Instrument for Controlling Atmospheric Sampling. JAPCA. 28(4):373-376.

Draftz, R. G. and Severin, K., Aerosol Characterization Study in St. Louis-Microscopical Analysis. U. S. Environmental Protection Agency, Research Triangle Park, North Carolina. (In print)

Gatz, D. F., Symposium on Atomic Diffusion. American Meteorological Soc. 1974.

Epstein, B. S. and D. A. Lynn, 1976. National Assessment of the Urban Particulate Problem, XIV. EPA-450/3-76-026L. U. S. Environmental Protection Agency, Research Triangle Park, North Carolina.

Heifler, S. L., EPA Progress Report R802160-03-0, 1975.

Johansson, T. B., R. Akselsson, and S. A. E. Johansson, 1972. Proton Induced X-ray Emission Spectroscopy in Elemental Trace Analysis. Adv. X-ray Anal. 15:373-387.

Johansson, T. B., R. E. Van Grieken, J. W. Nelson and J. W. Winchester. Elemental Trace Analysis of Small Samples by Proton-Induced X-ray Emission. Anal. Chem., 47, 855-860, 1975.

Mendenhall, G., P. Jones, P. Stink and W. Margard. Organic Characterization of Aerosols and Vapor Phase Compounds in Urban Atmospheres. EPA-600/3-78-031. U. S. Environmental Protection Agency, Research Triangle Park, North Carolina.

Miller, M. S., S. K. Friedlander, and G. M. Hedy. A Chemical Element Balance for the Pasadena Aerosol. J. Coll. Interface Sci. 30:165.

Mitchell, R. I. and J. M. Pilcher, 1959. Improved Cascade Impactor for Measuring Aerosol Particle Sizes. Ind. Eng. Chem. 51:1039-1042.

Nelson, J. W., B. Jensen, G. G. Desaedeleer, K. R. Akselsson, and J. W. Winchester, 1975. Automatic Time Sequence Filter Sampling for Rapid Multi-Element Analysis by Proton Induced X-ray Emission. Adv. X-ray Anal. 19.

Parsons, A. A., 1897. Florida Agricultural Experimental Station Bulletin No. 3. Gainesville, Florida.

Winchester, J. W. and G. G. Desaedeleer, 1975. Nondestructive Activation Analysis, Proceedings. Amsterdam.

Figure 1 Map of St. Louis with Major Point Sources

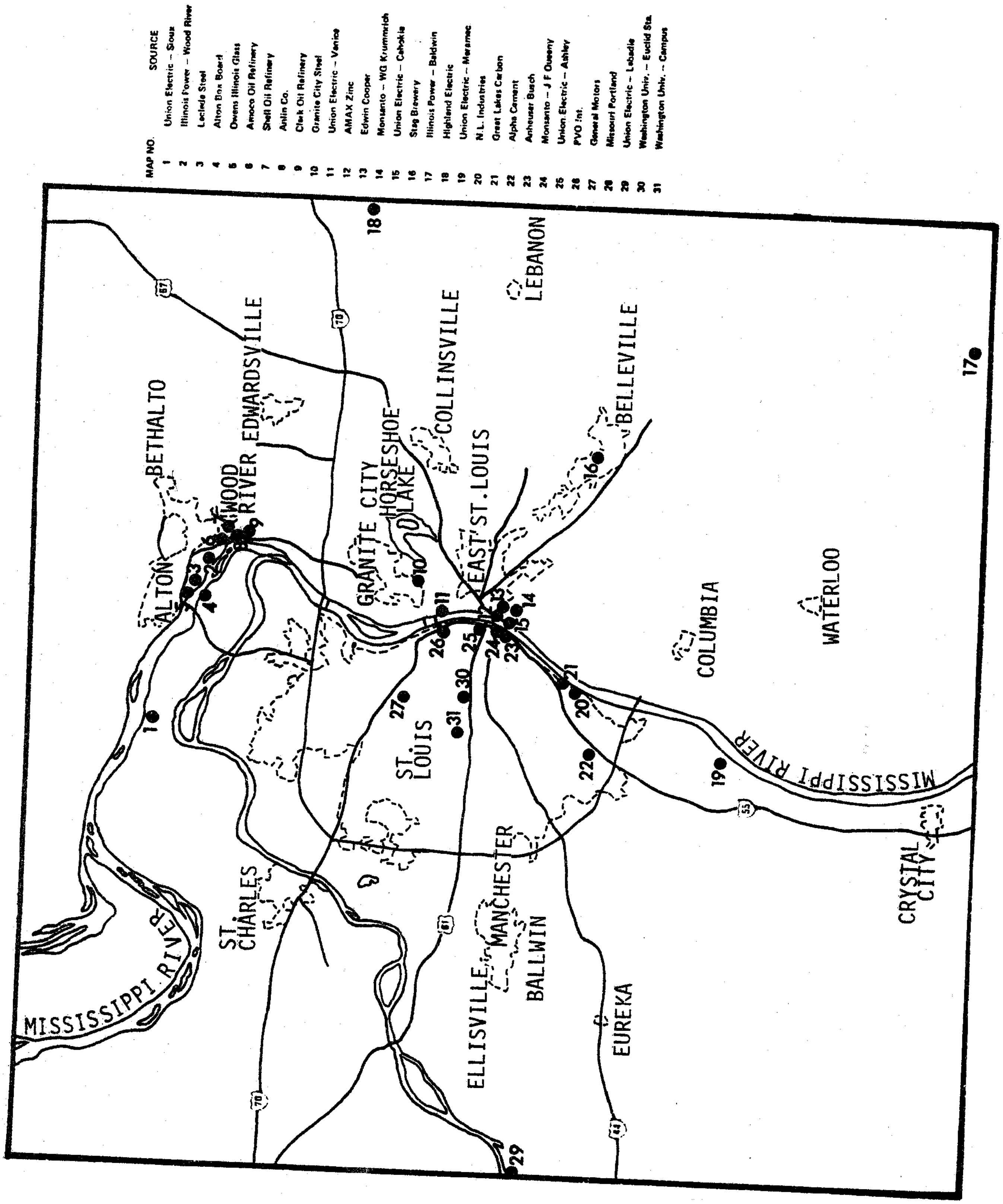

Figure 2 St. Louis Fire Station A. Size Distribution P

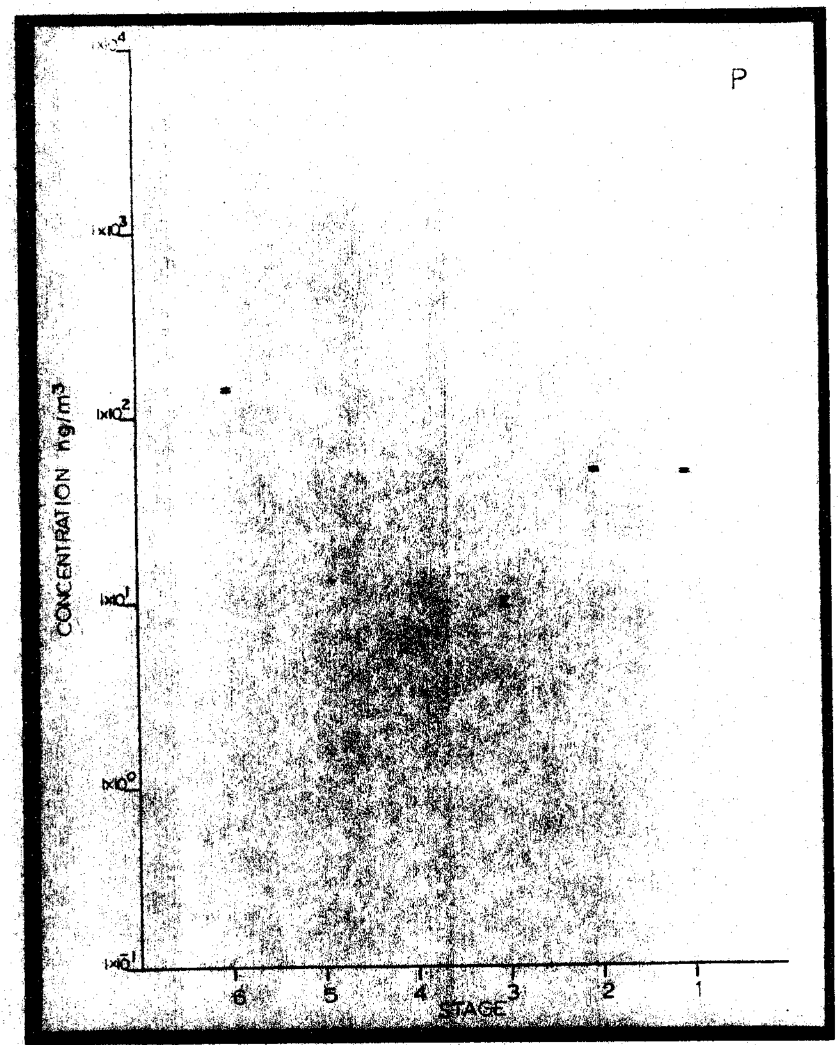

Figure 3 St. Louis Fire Station A. Size Distribution S

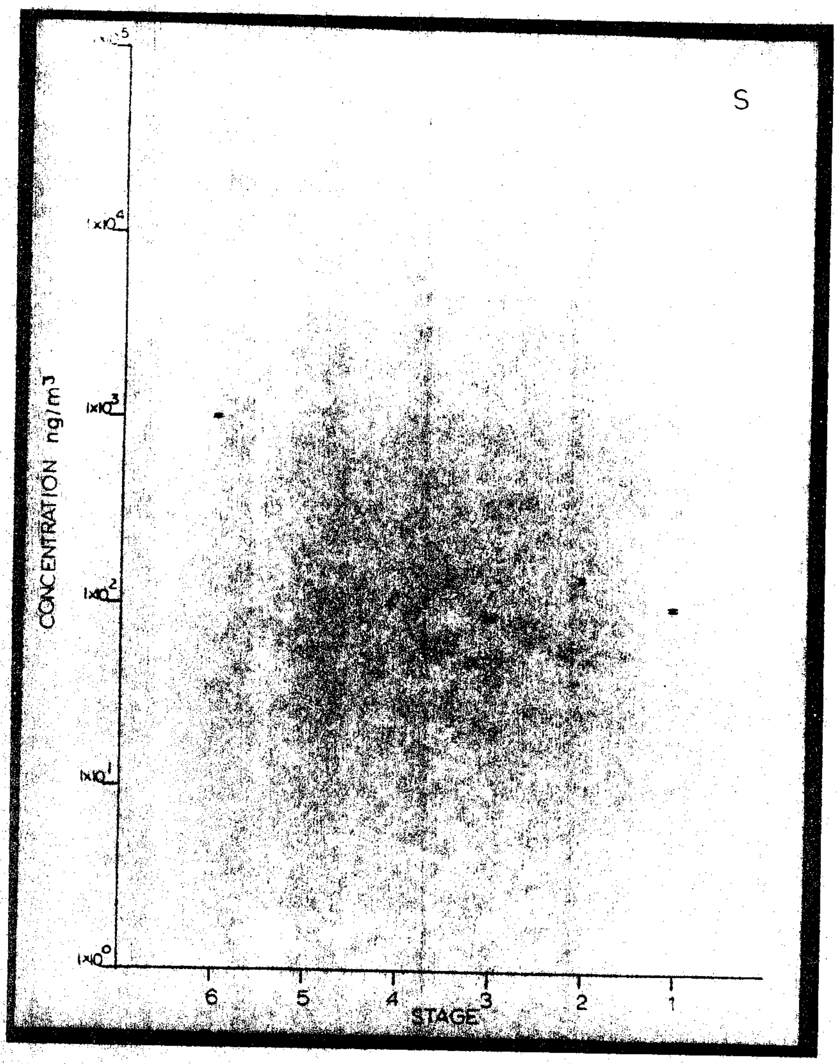

Figure 4 St. Louis Fire Station A. Size Distribution Cl

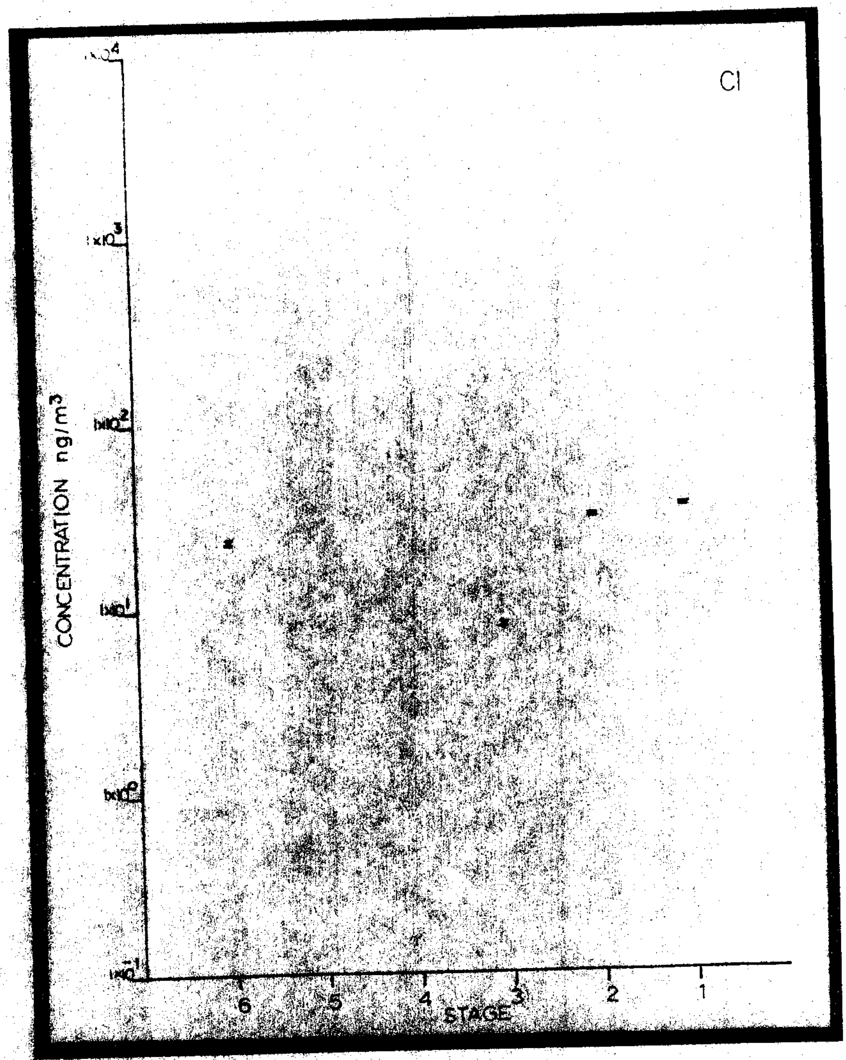

Figure 5 St. Louis Fire Station A. Size Distribution K

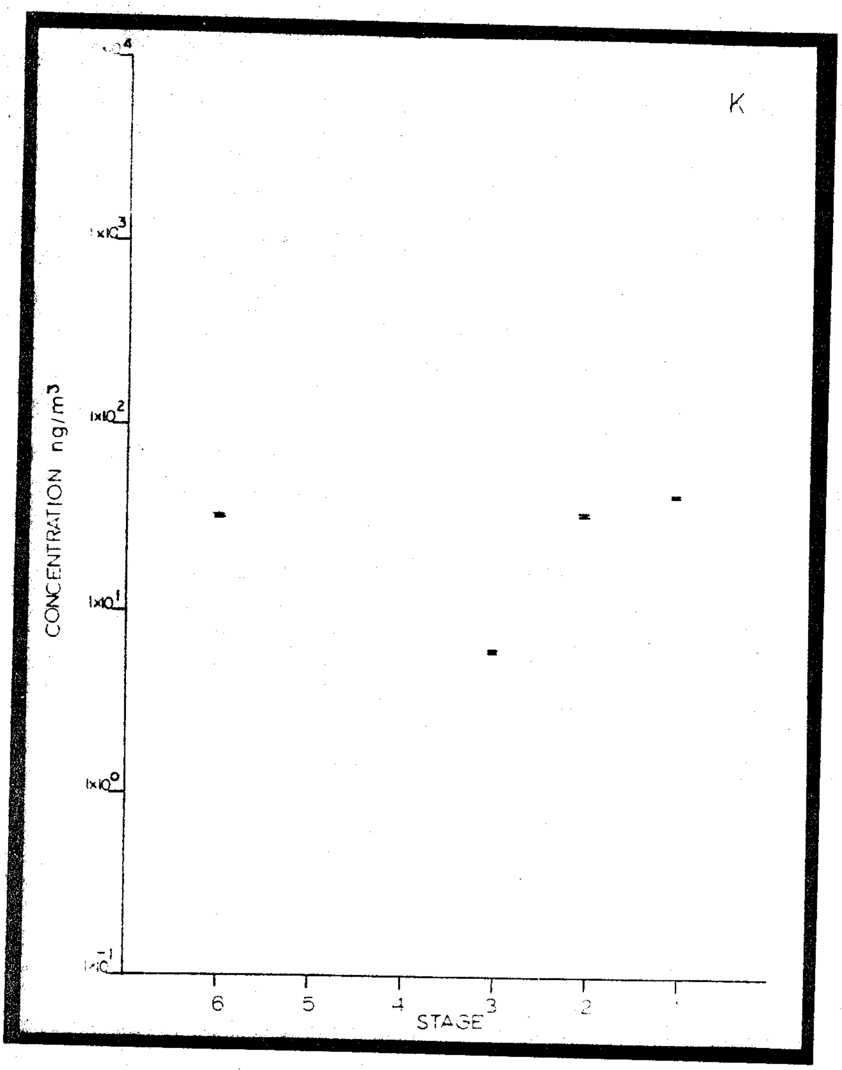

Figure 6 St. Louis Fire Station A. Size Distribution Ca

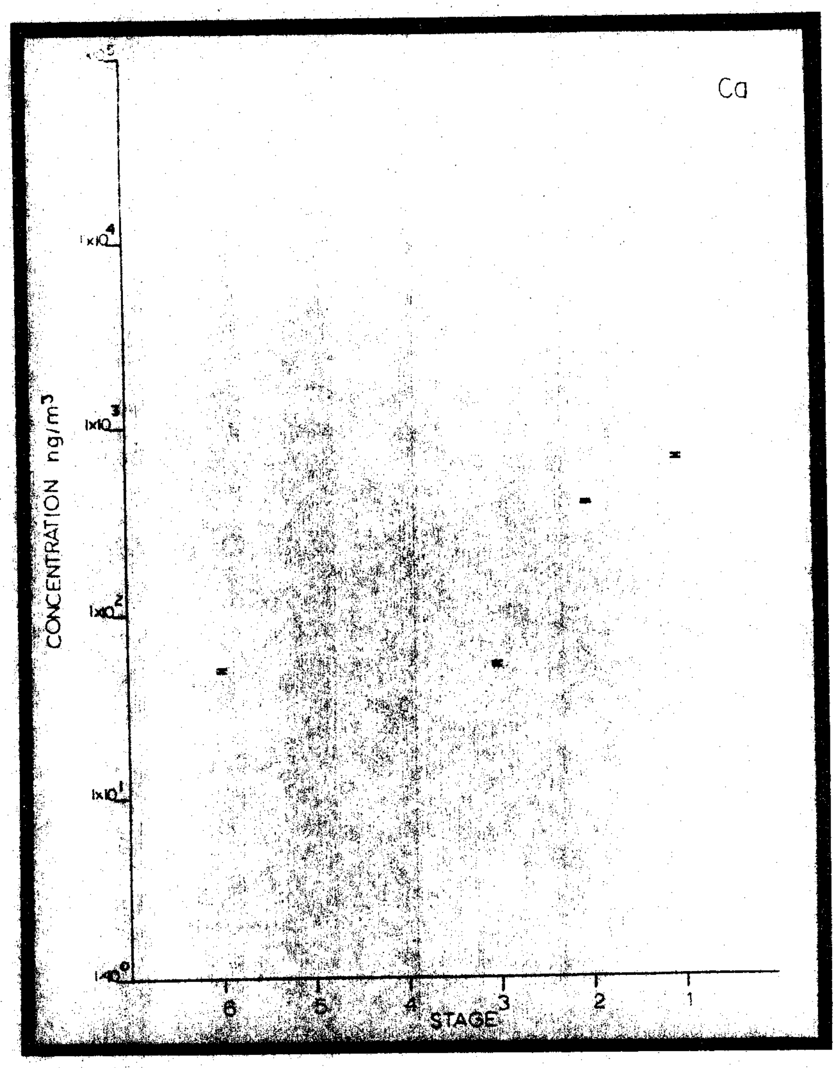

Figure 7 St. Louis Fire Station A. Size Distribution Ti

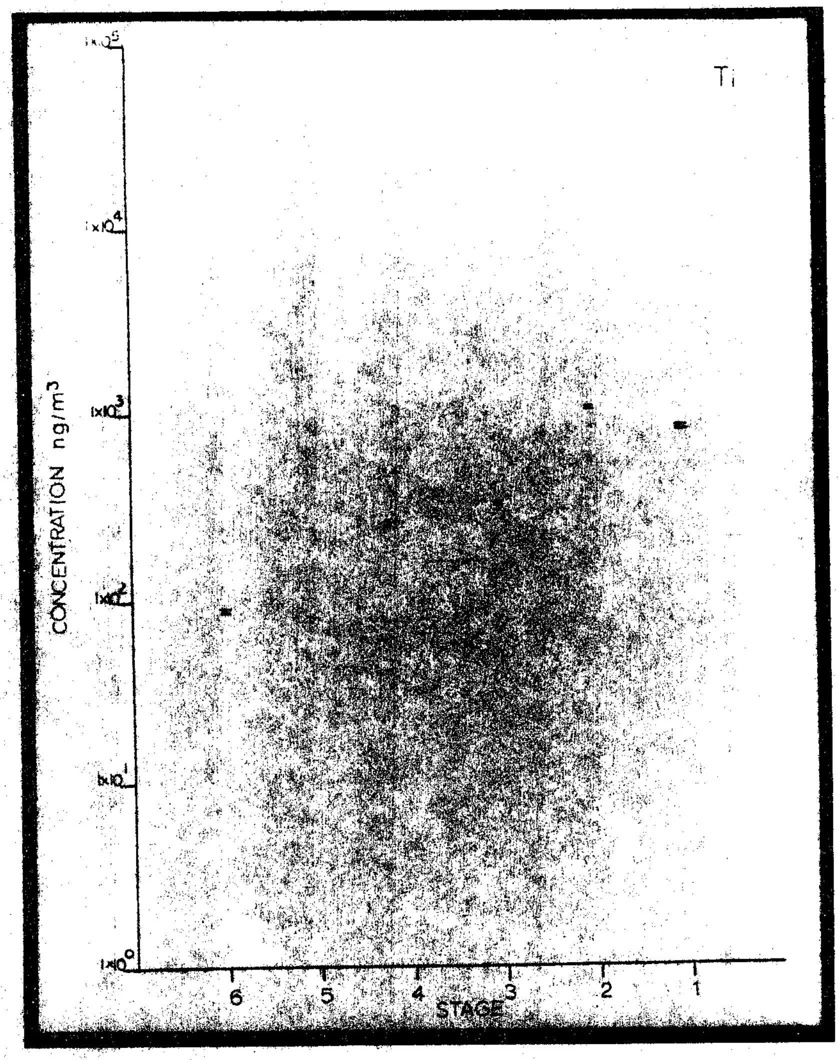

Figure 8 St. Louis Fire Station A. Size Distribution V

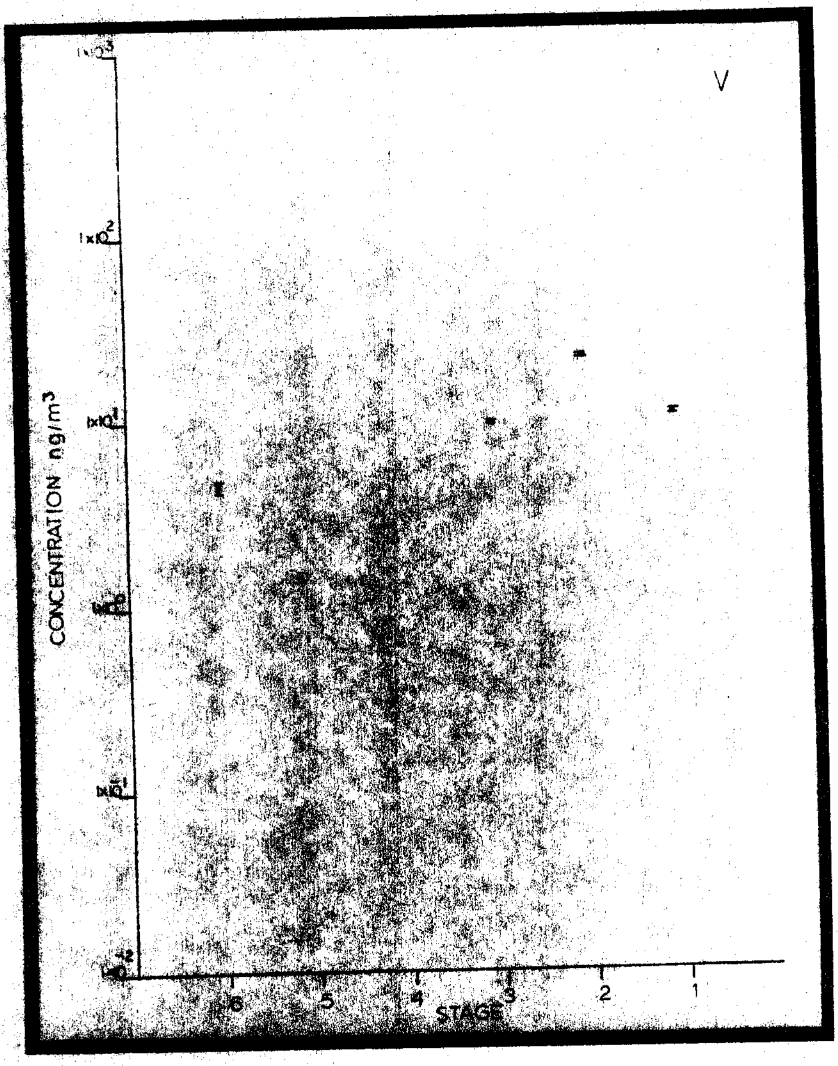

Figure 9 St. Louis Fire Station A. Size Distribution Mn

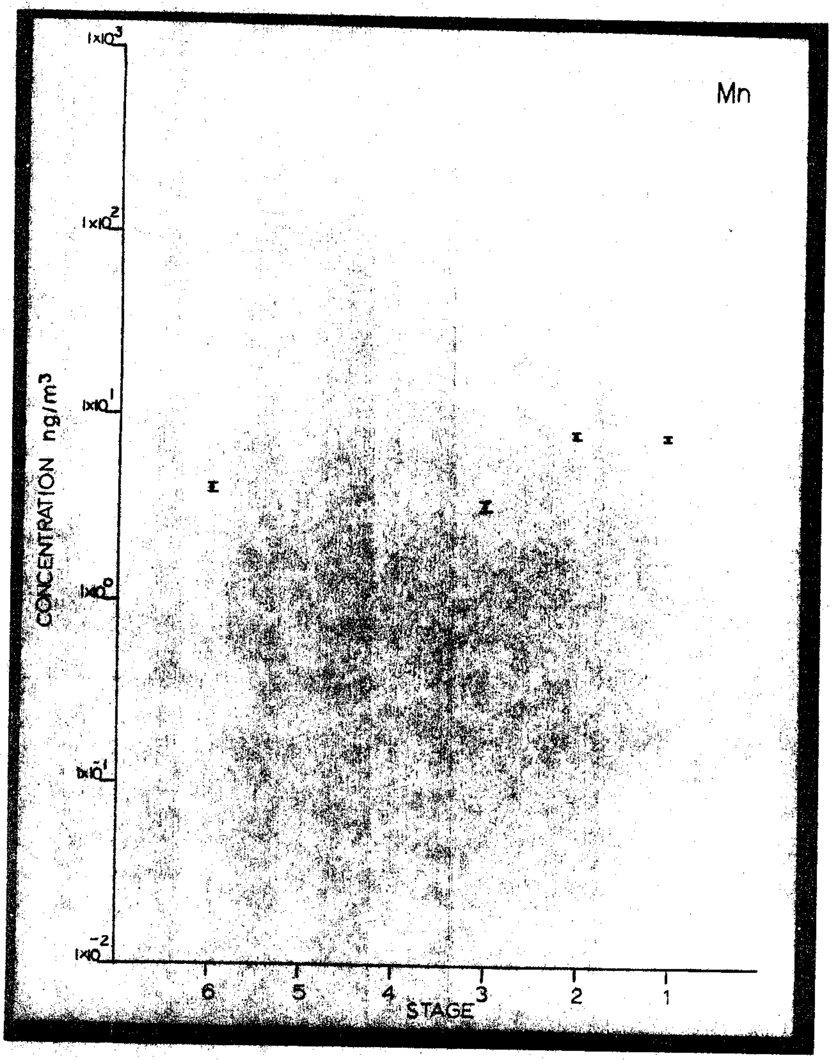

Figure 10 St. Louis Fire Station A. Size Distribution Fe

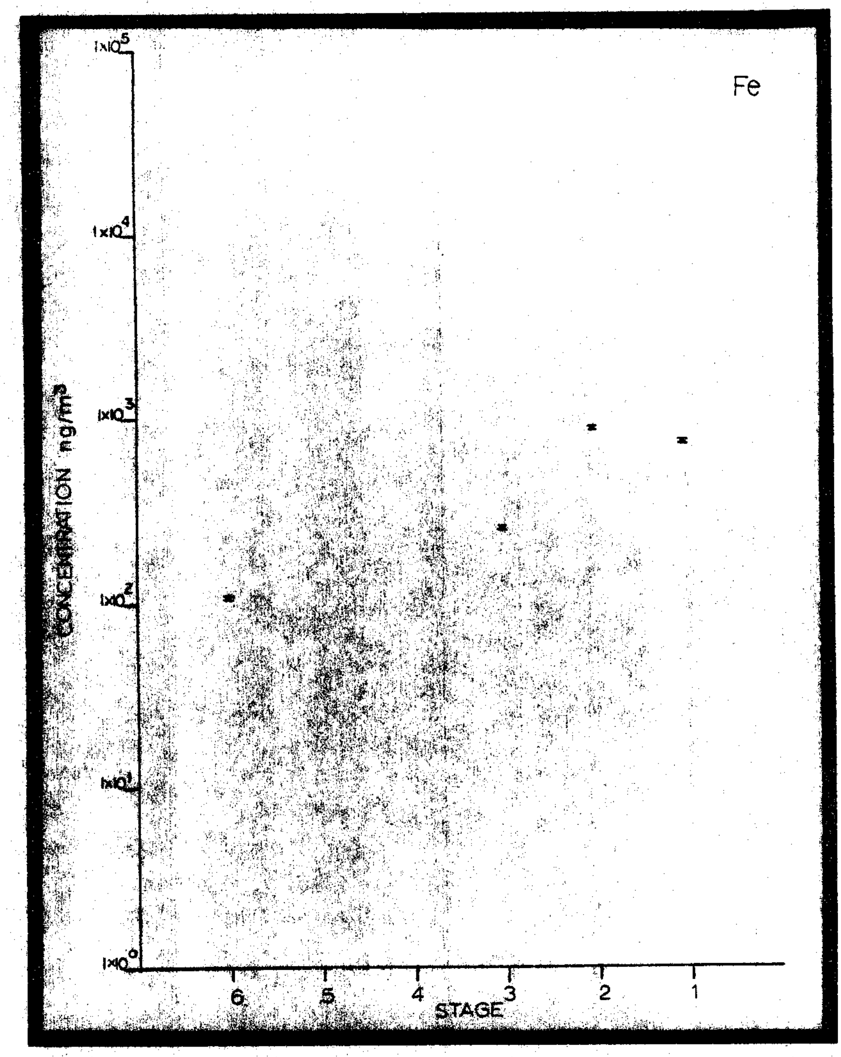

Figure 11 St. Louis Fire Station A. Size Distribution Cu

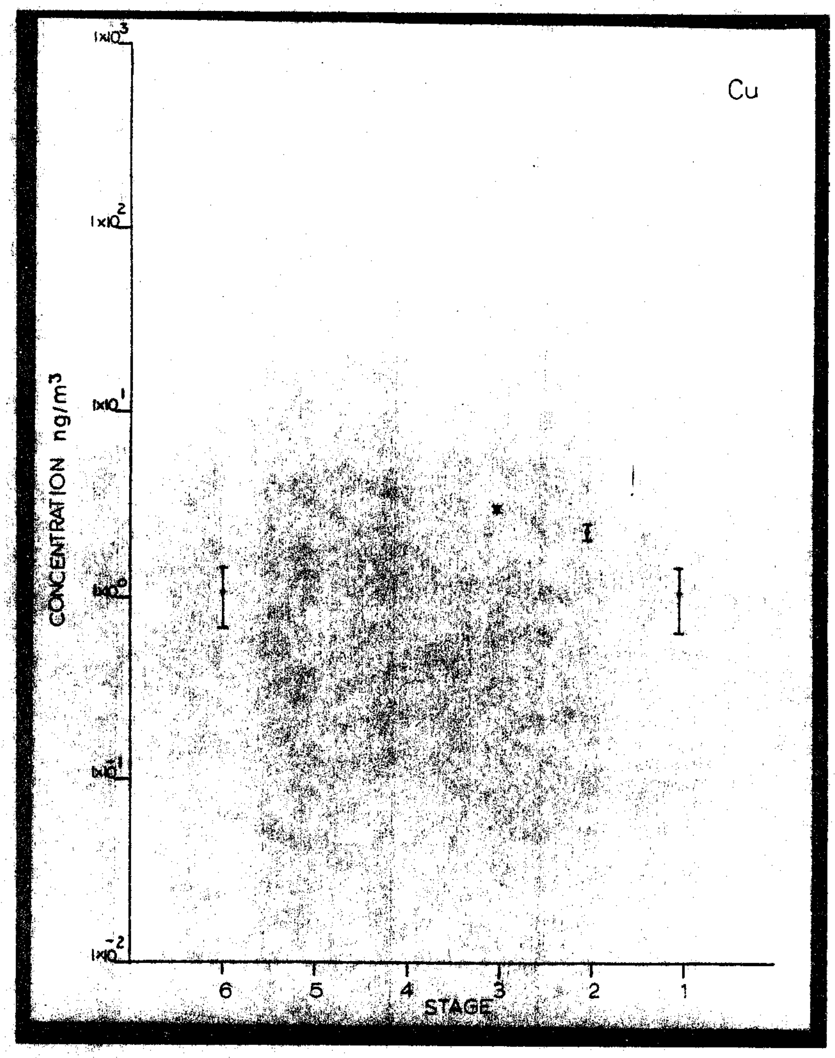

Figure 12 St. Louis Fire Station A. Size Distribution Zn

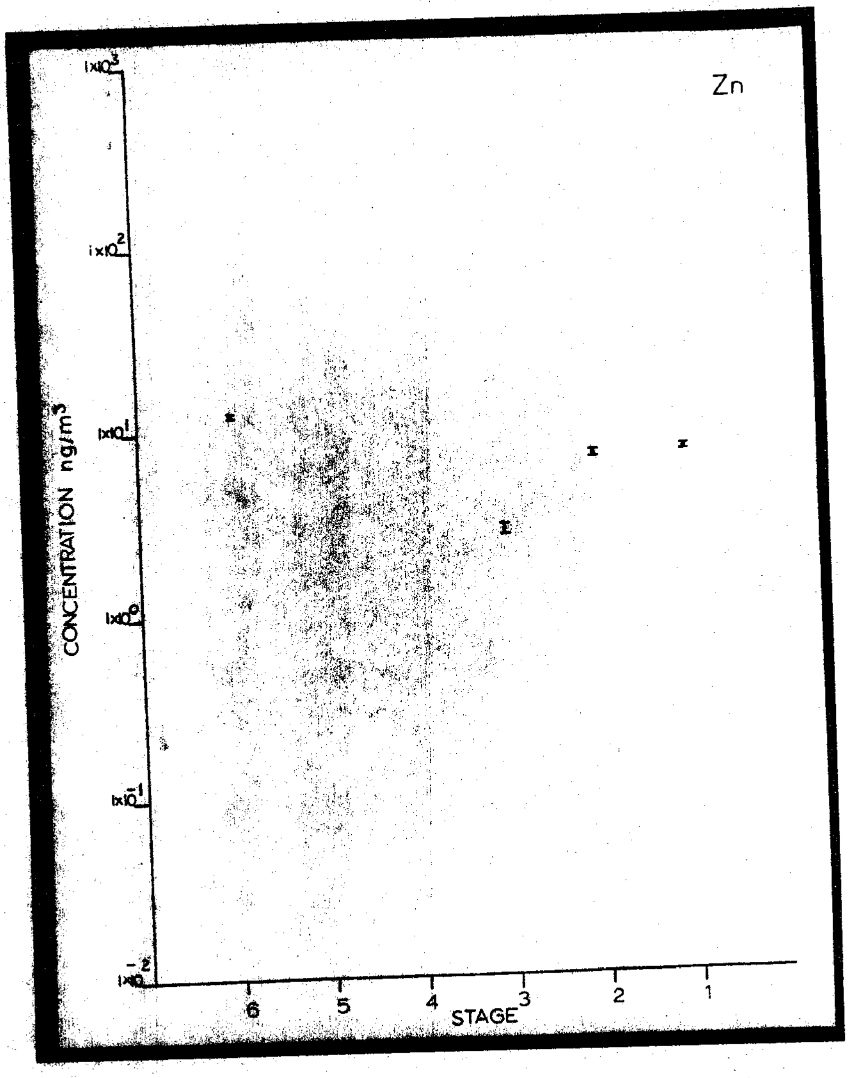

Figure 13 St. Louis Fire Station A. Size Distribution Pb

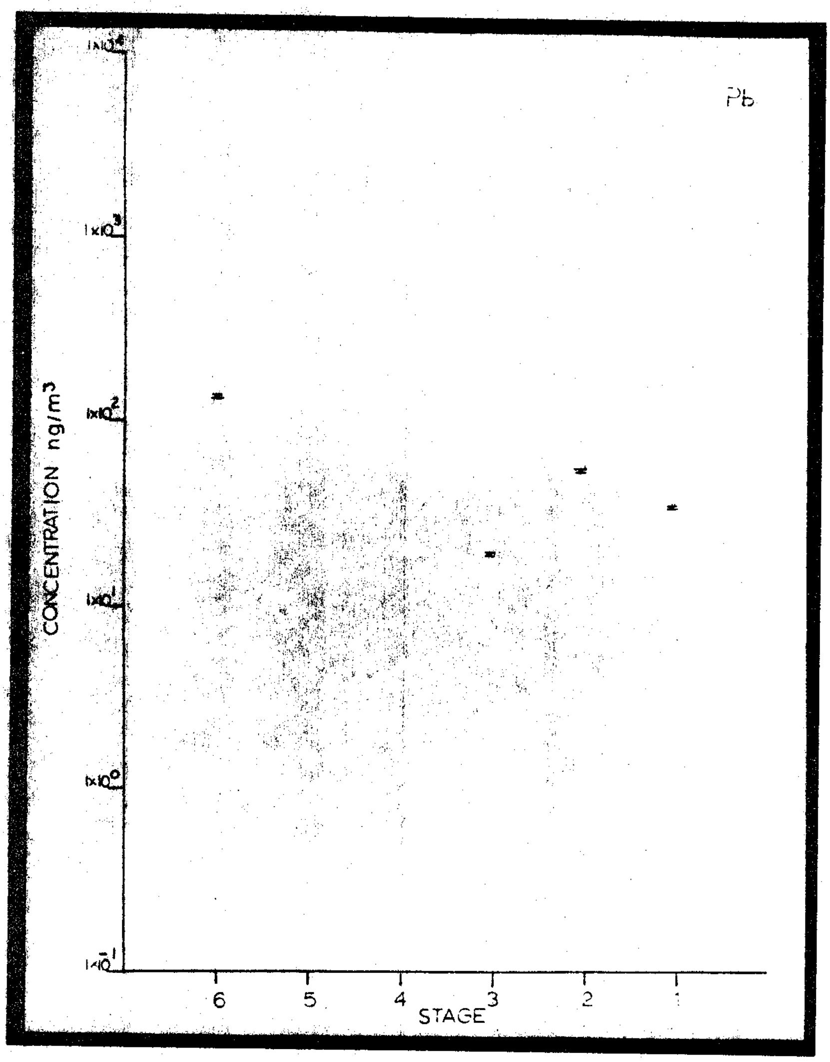

Figure 14 St. Louis Fire Station B. Size Distribution P

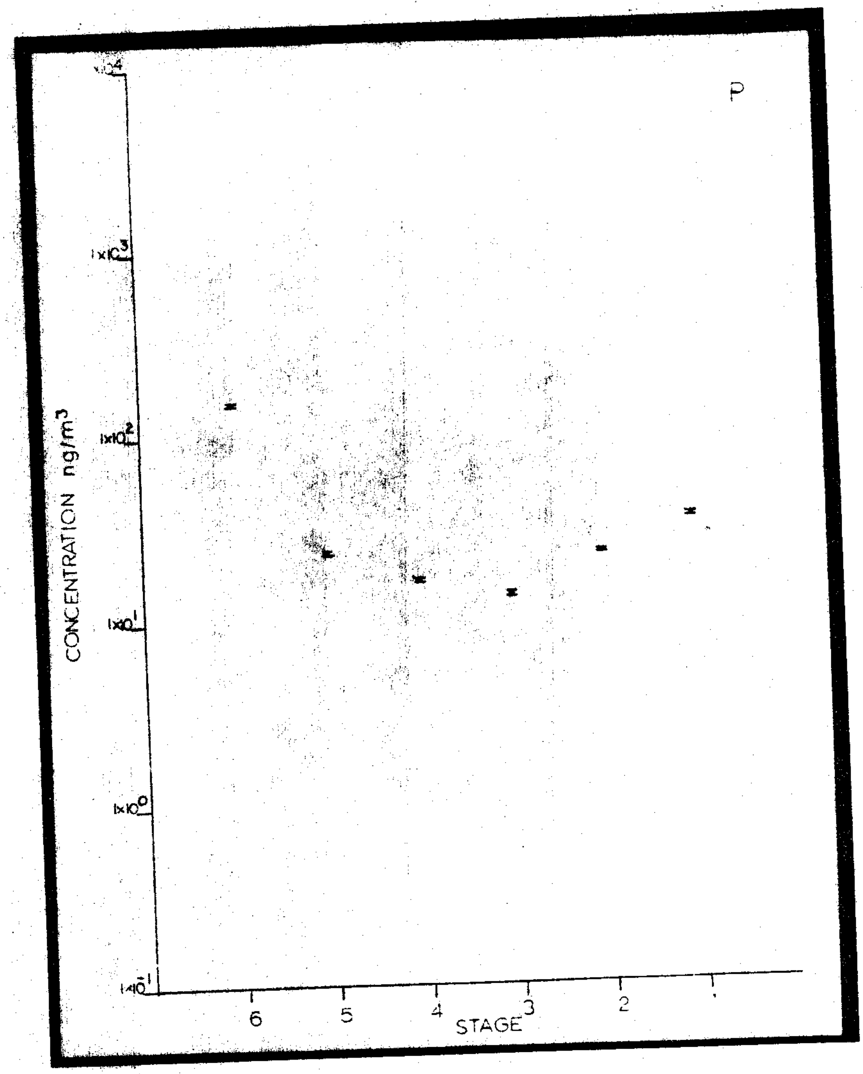

Figure 15 St. Louis Fire Station B. Size Distribution S

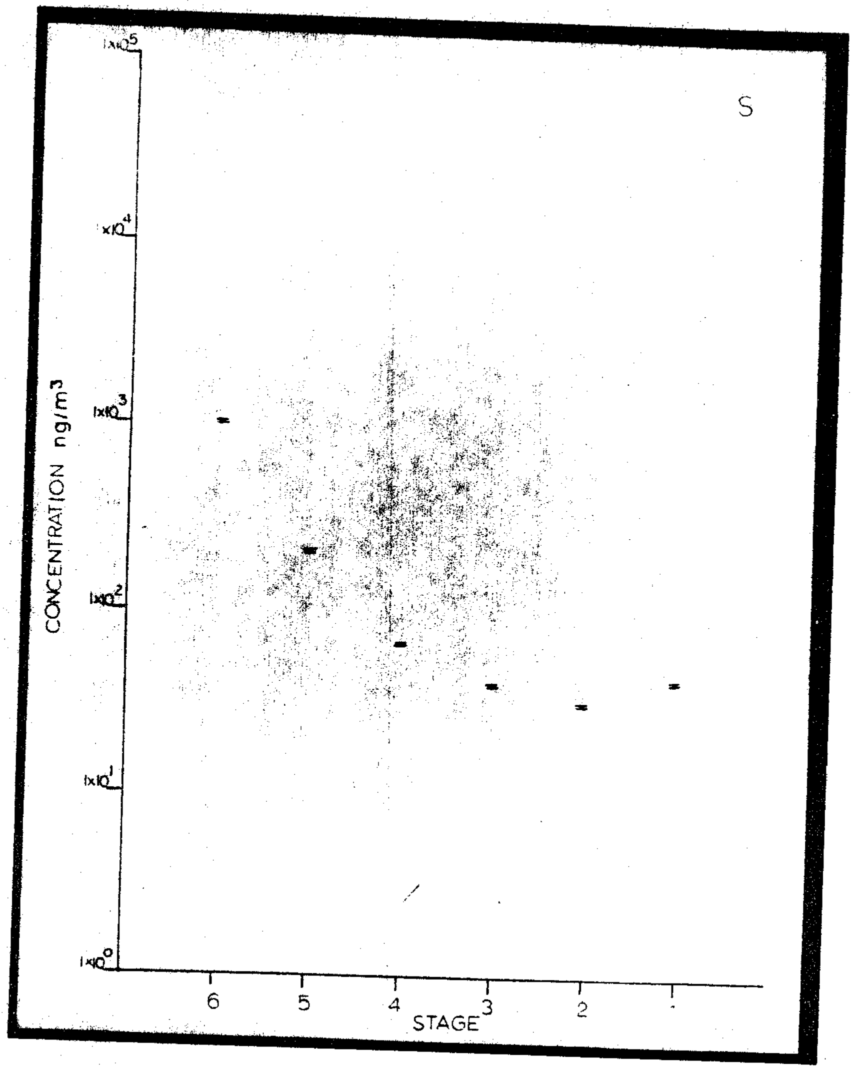

Figure 16 St. Louis Fire Station B. Size Distribution Cl

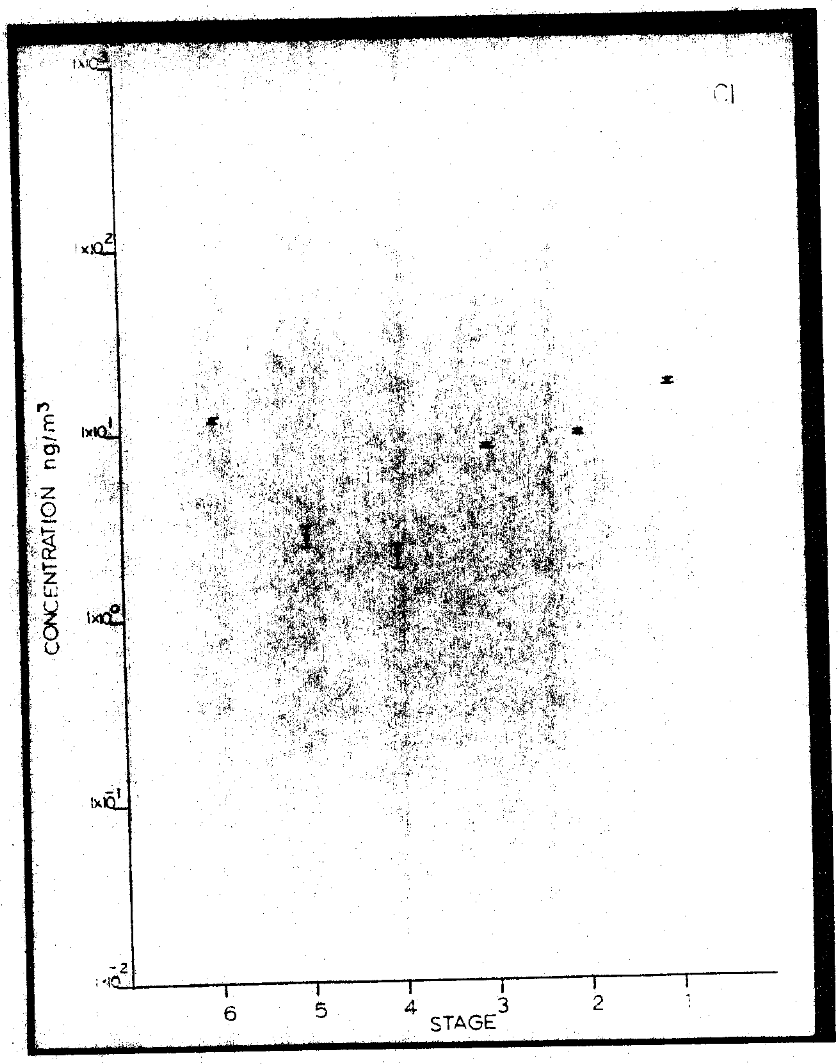

Figure 17 St. Louis Fire Station B. Size Distribution K

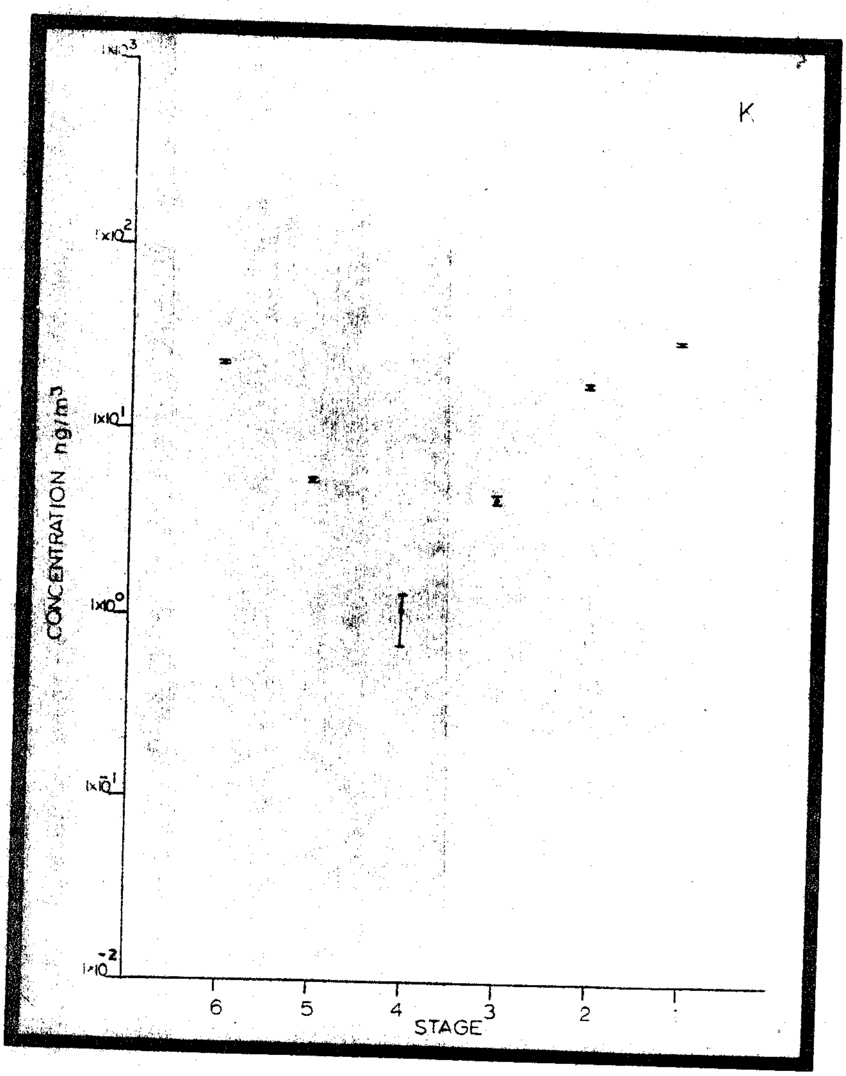

Figure 18 St. Louis Fire Station B. Size Distribution Ca

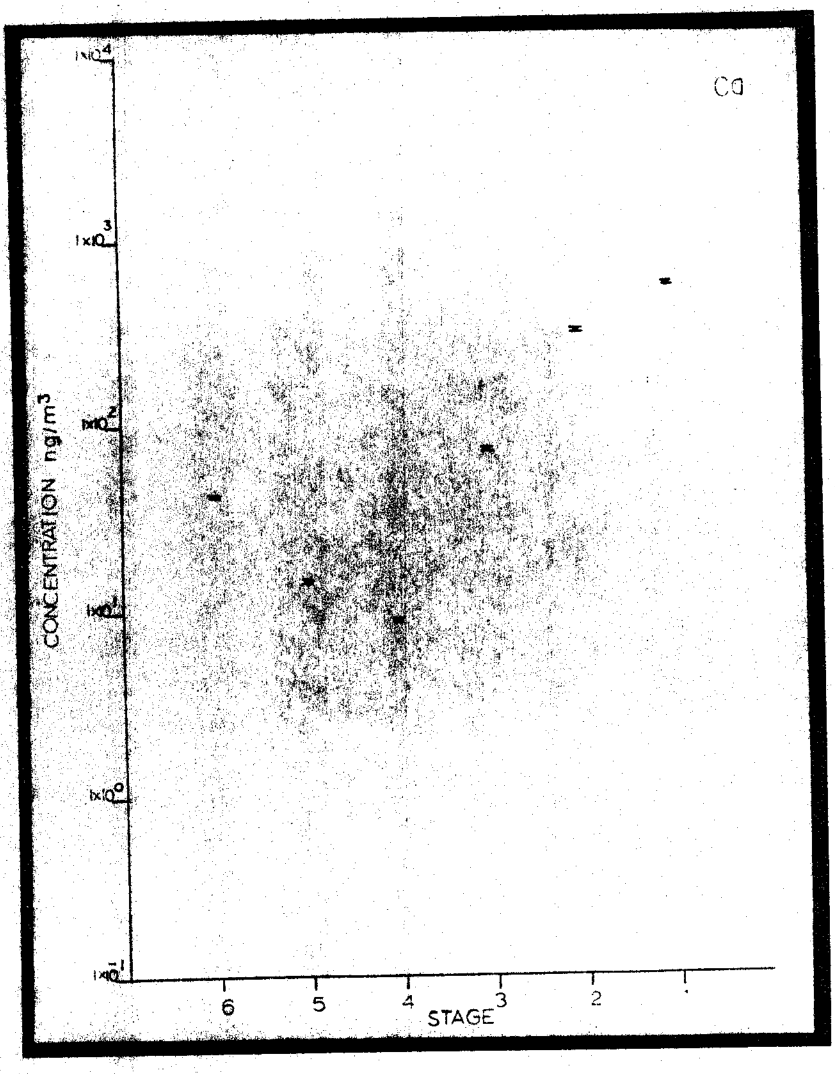

Figure 19 St. Louis Fire Station B. - Size Distribution Ti

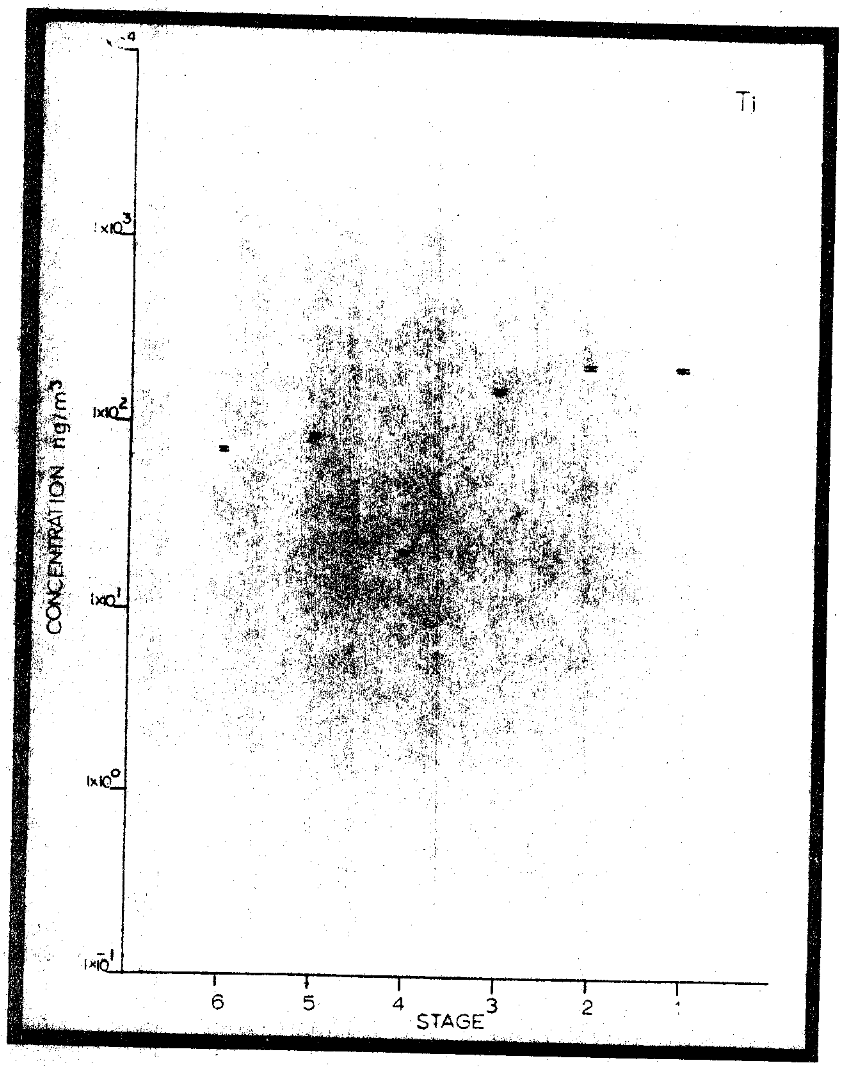

Figure 20 St. Louis Fire Station B. Size Distribution V

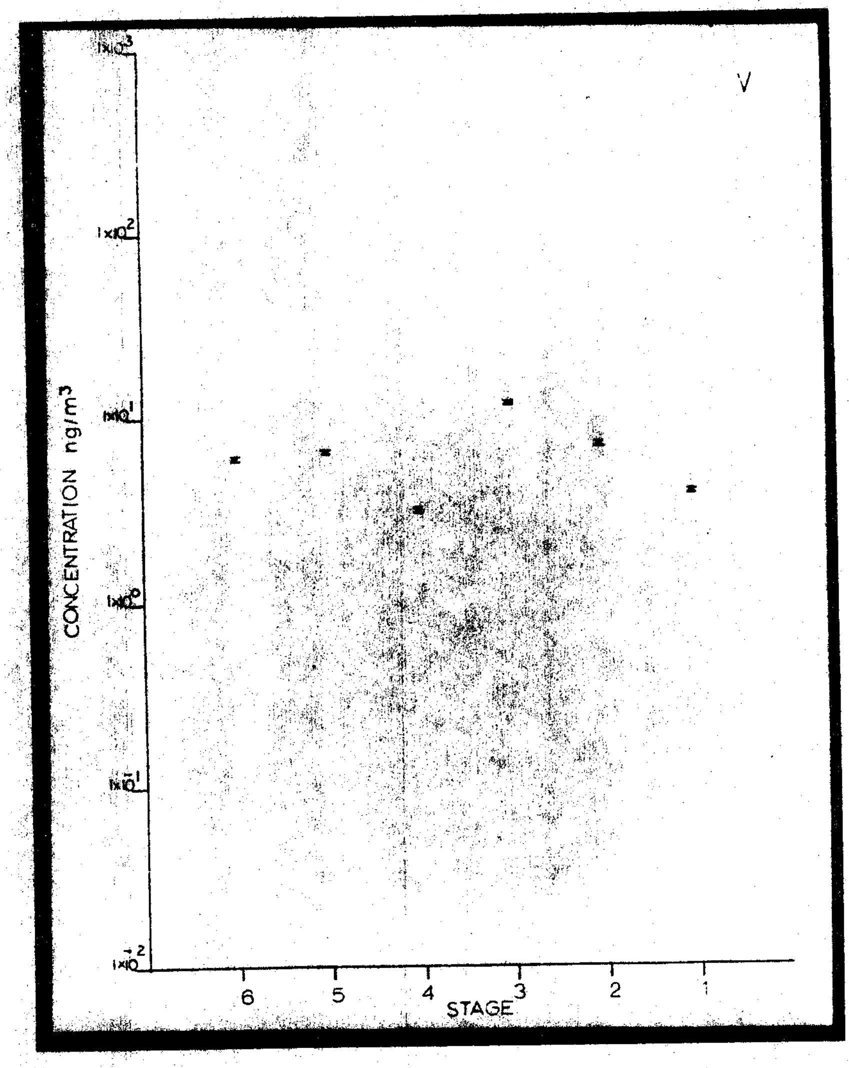

Figure 21 St. Louis Fire Station B. Size Distribution Mn

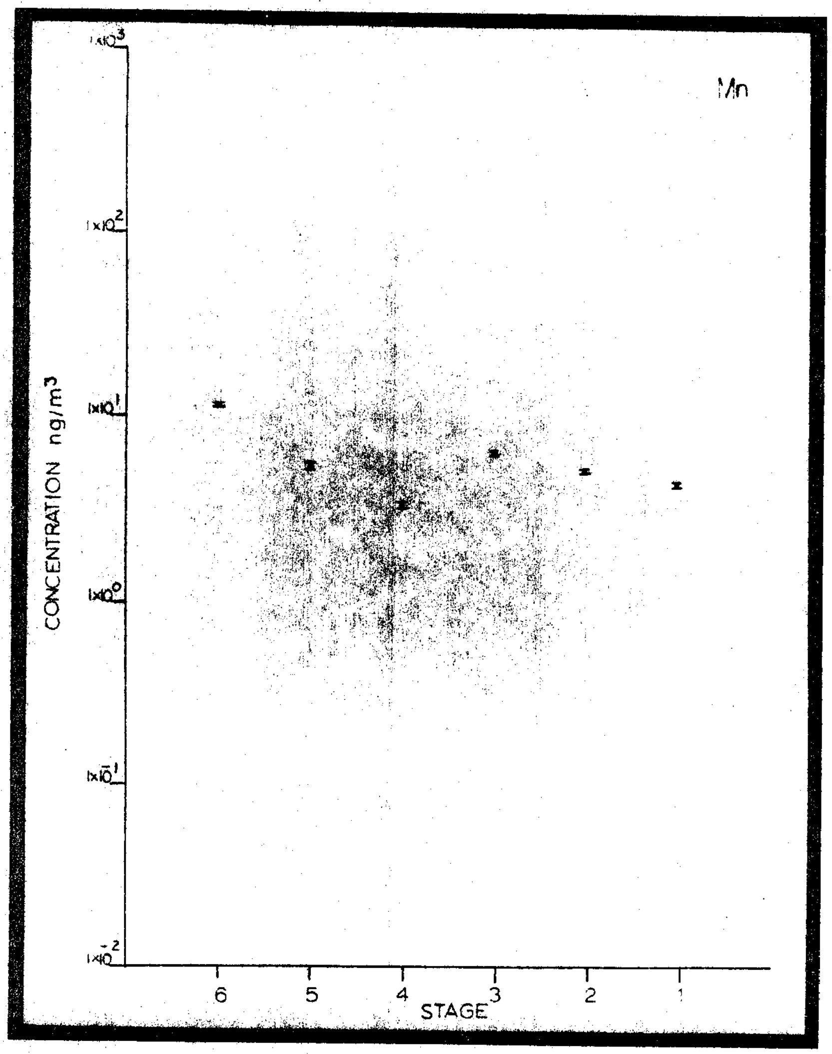

Figure 22 St. Louis Fire Station B. Size Distribution Fe

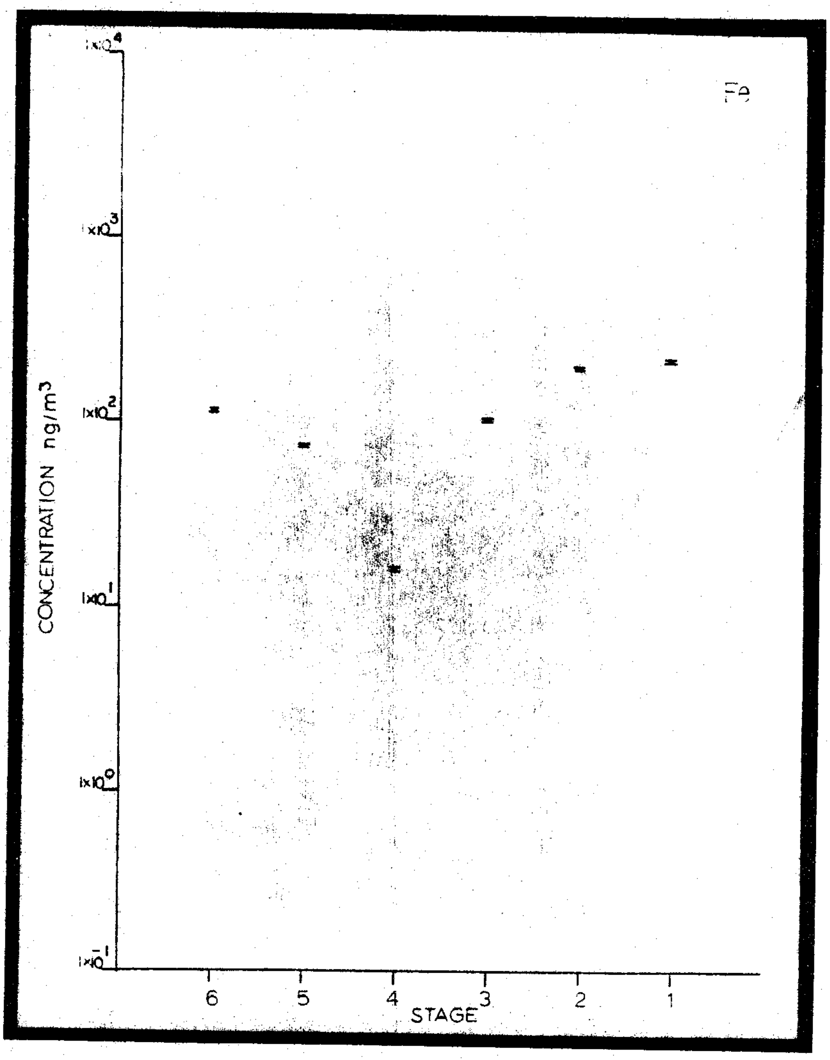

Figure 23 St. Louis Fire Station B. Size Distribution Cu

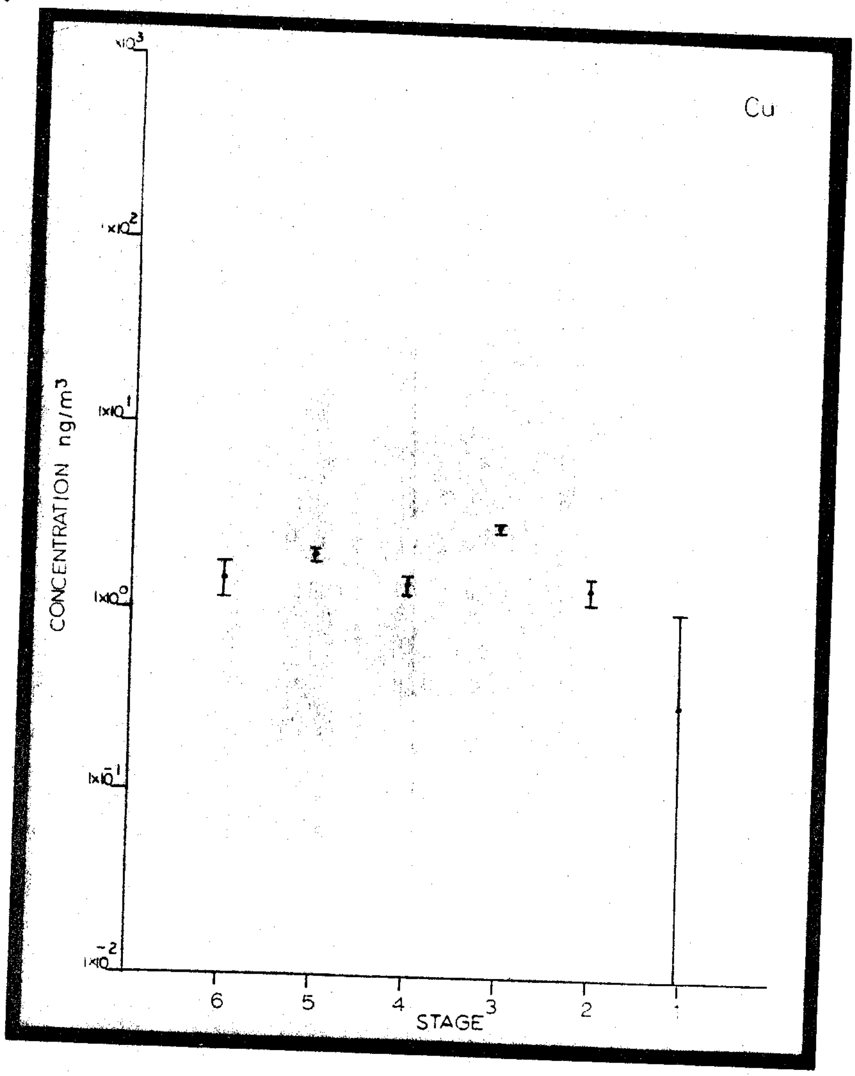

Figure 24 St. Louis Fire Station B. Size Distribution Zn

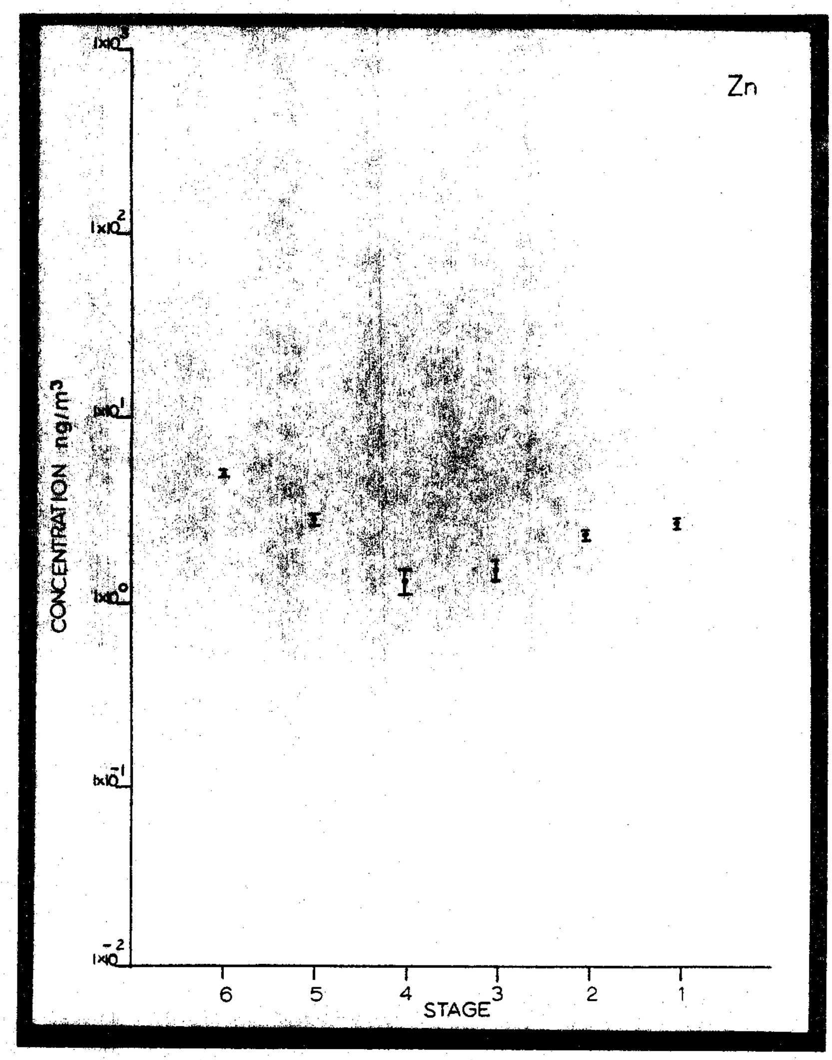

Figure 25 St. Louis Fire Station B. Size Distribution Br

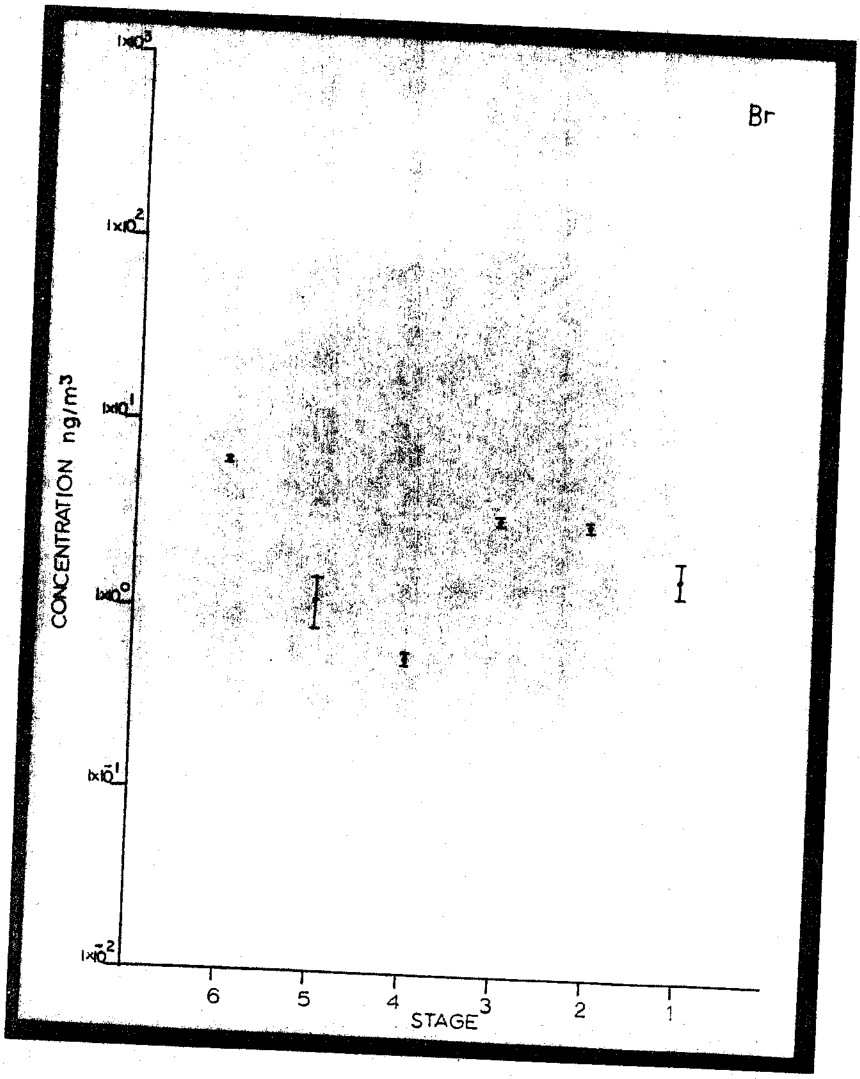

Figure 26 St. Louis Fire Station B. Size Distribution Pb

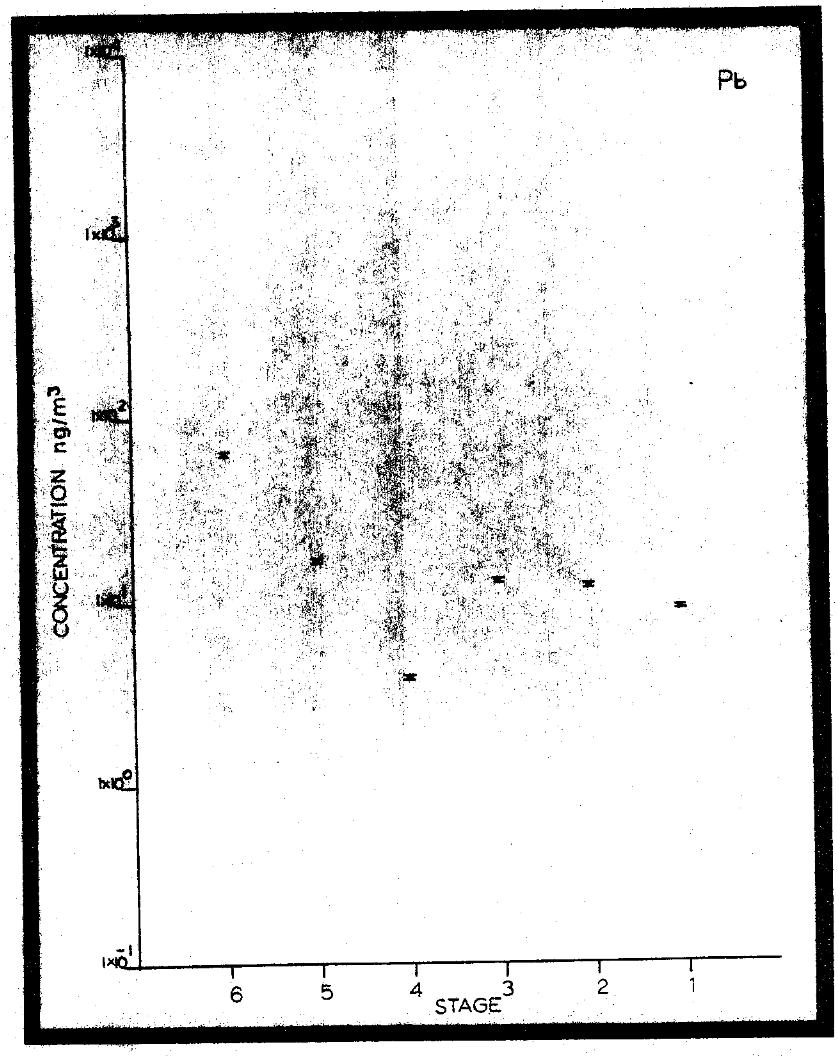

Figure 27   St. Louis Fire Station D. Size Distribution P

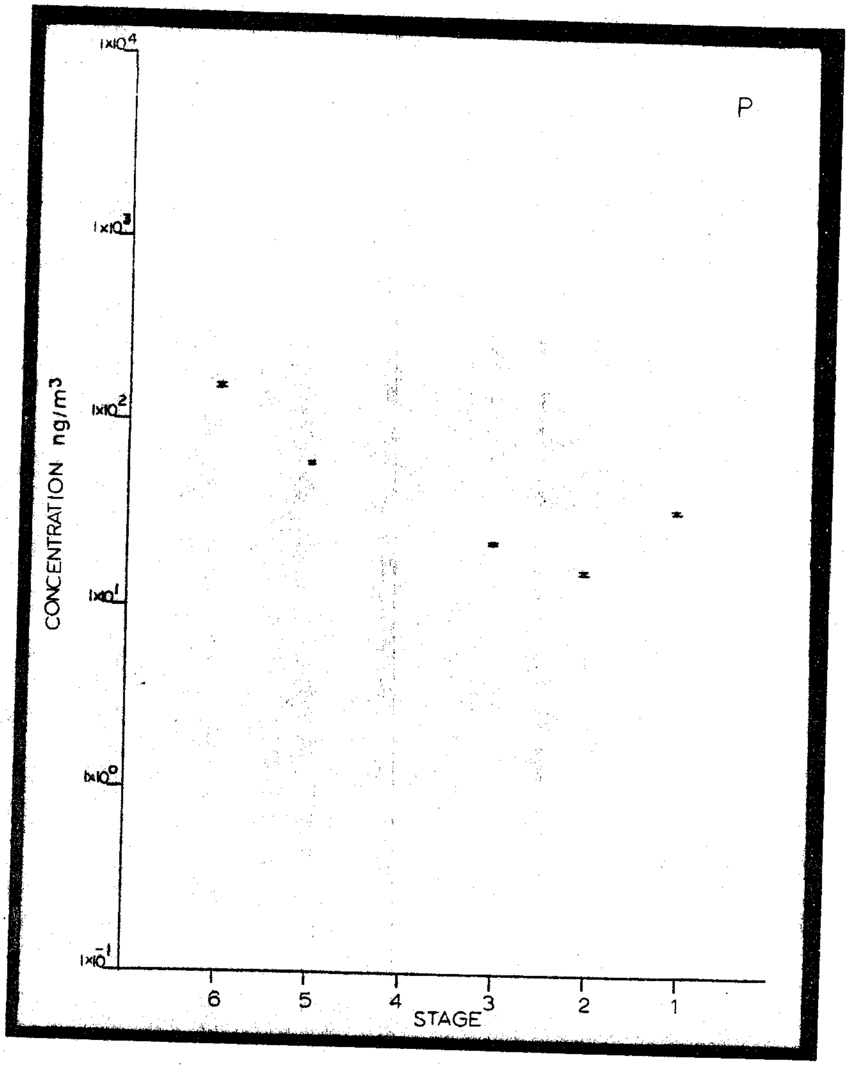

Figure 28 St. Louis Fire Station D. Size Distribution S

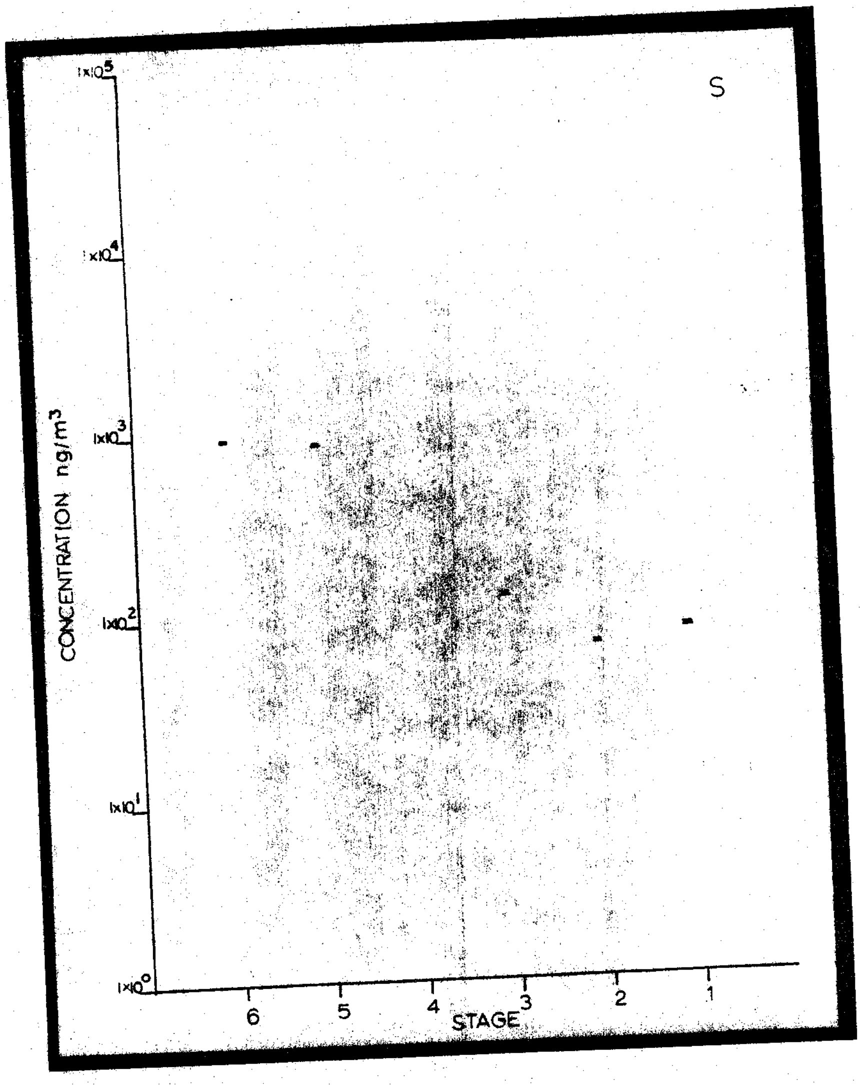

Figure 29 St. Louis Fire Station D. Size Distribution Cl

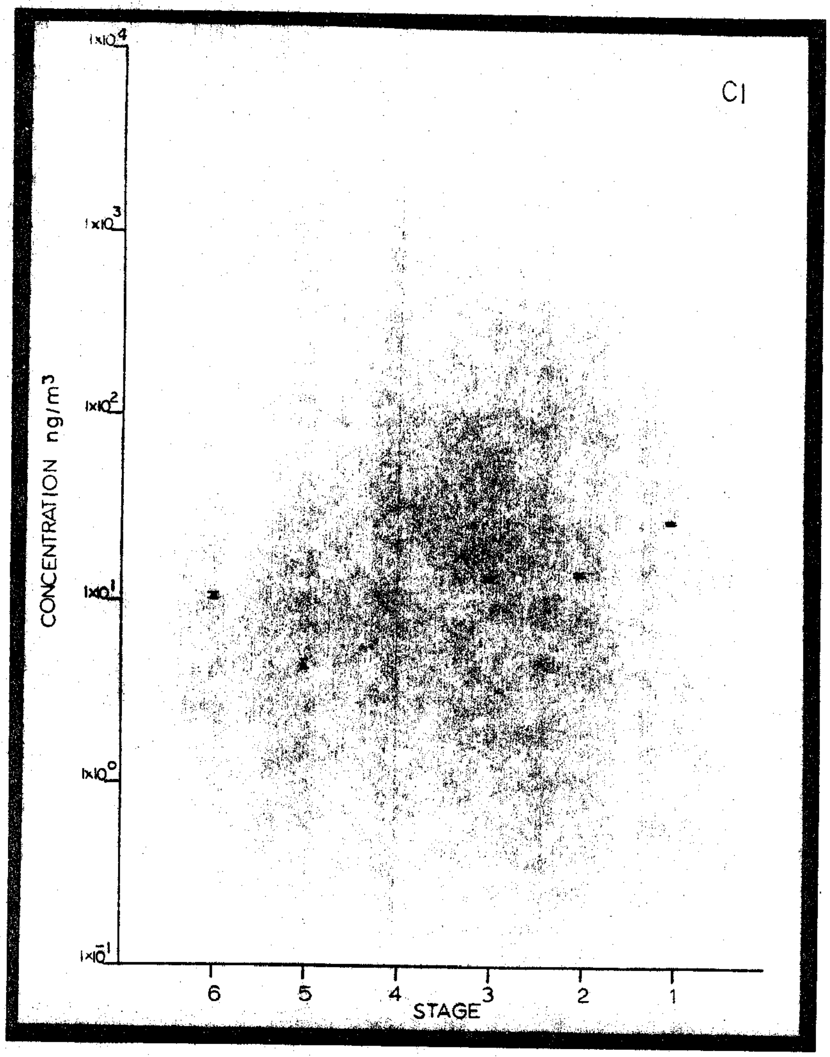

Figure 30   St. Louis Fire Station D. Size Distribution K

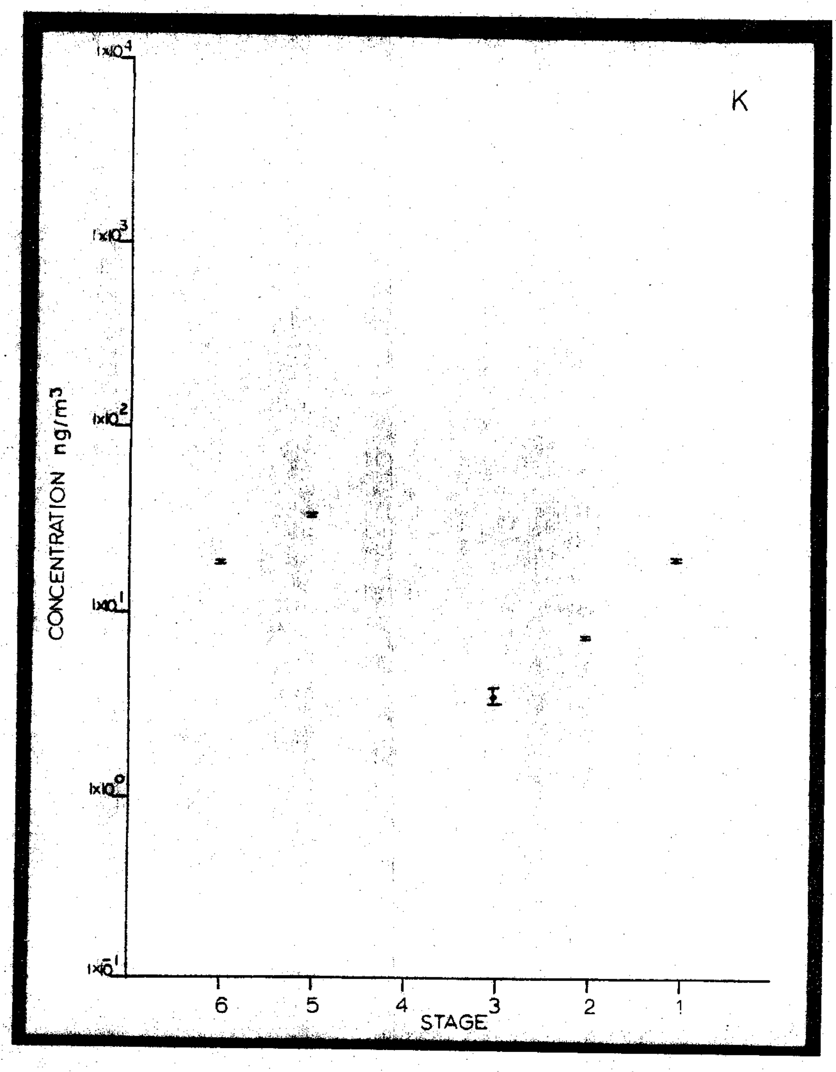

Figure 31 St. Louis Fire Station D. Size Distribution Ca

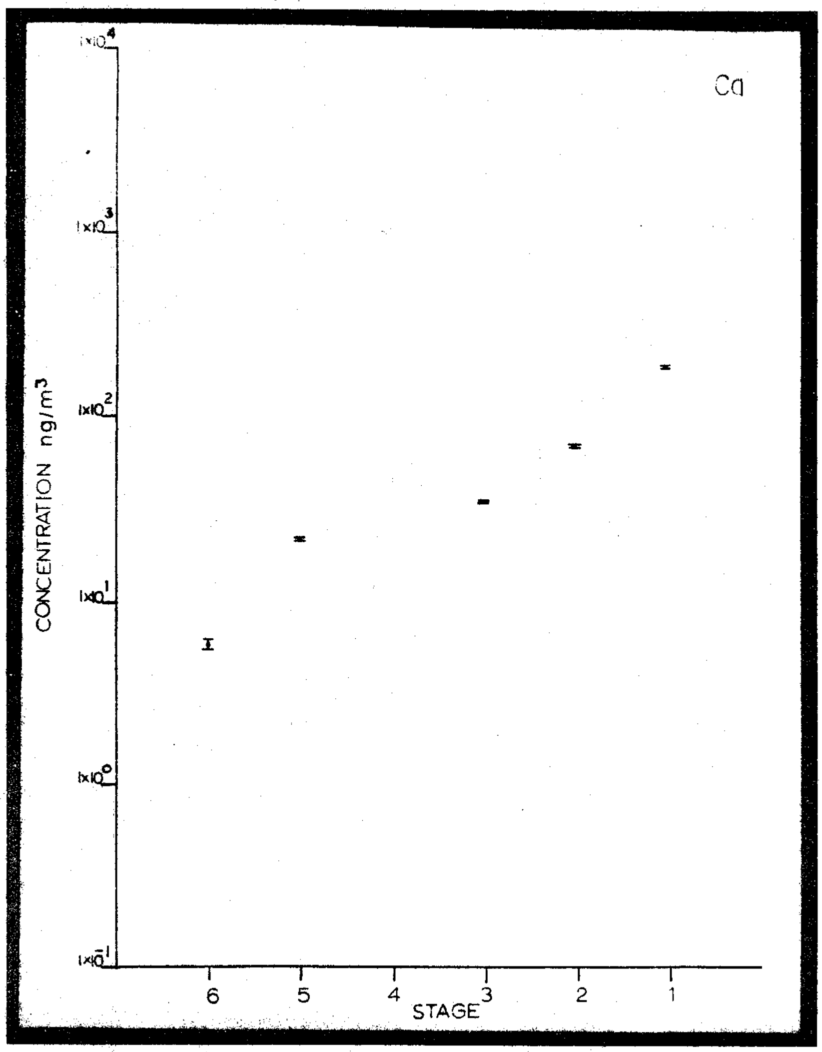

Figure 32 St. Louis Fire Station D. Size Distribution Ti

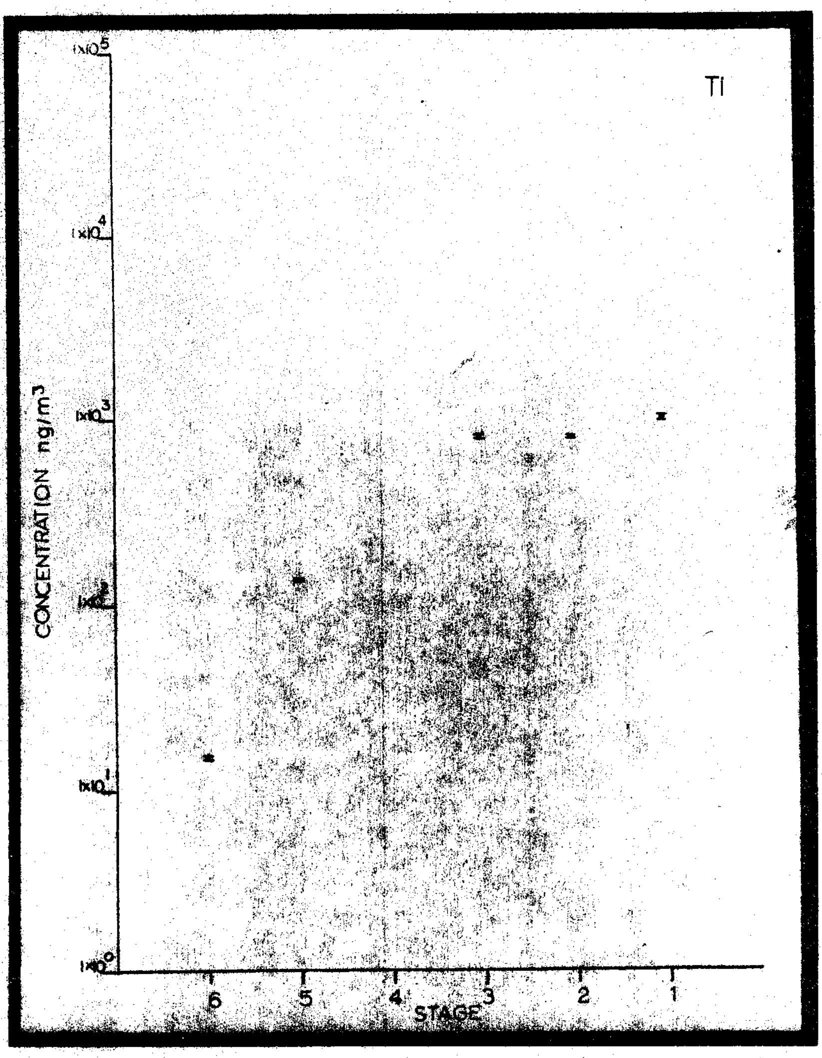

Figure 33 St. Louis Fire Station D. Size Distribution V

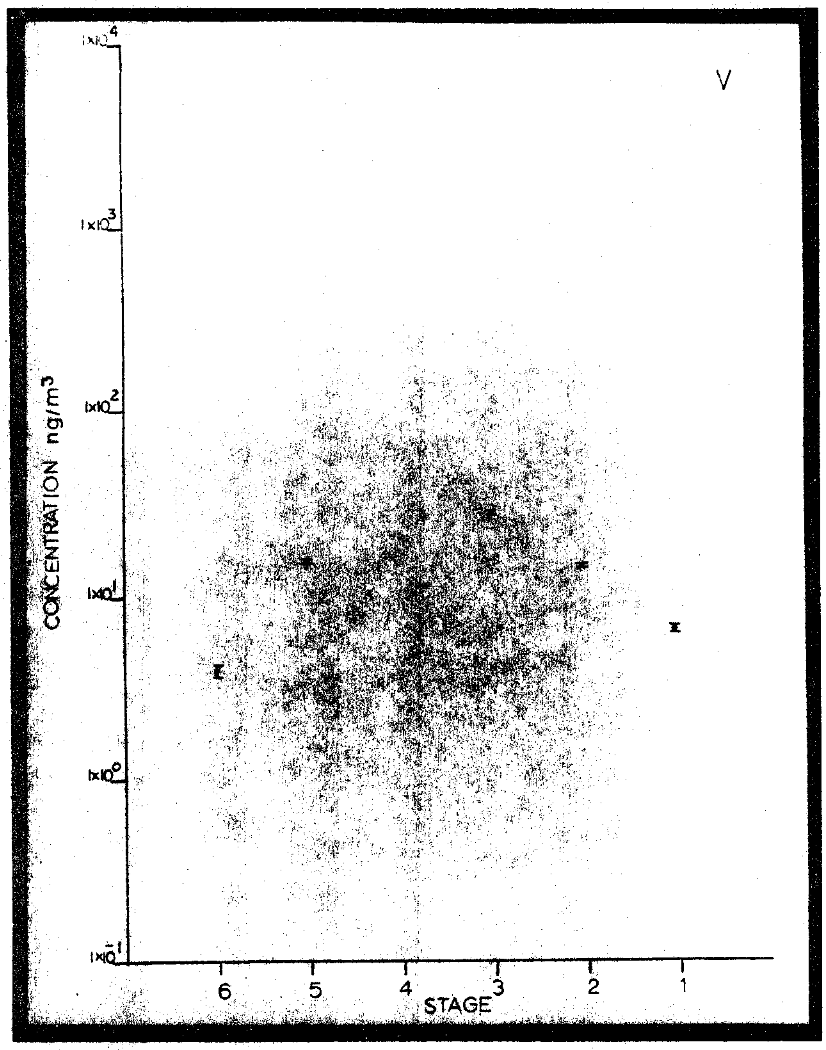

Figure 34 St. Louis Fire Station D. Size Distribution Mn

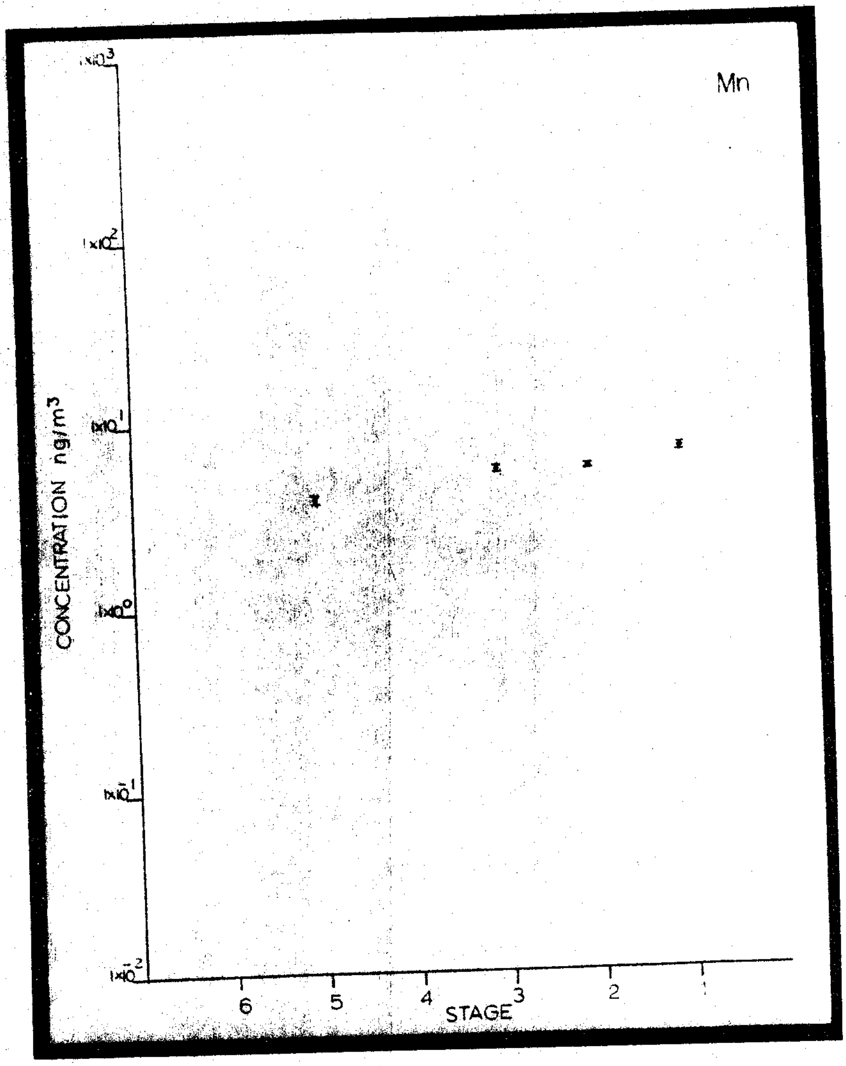

Figure 35 St. Louis Fire Station D. Size Distribution Fe

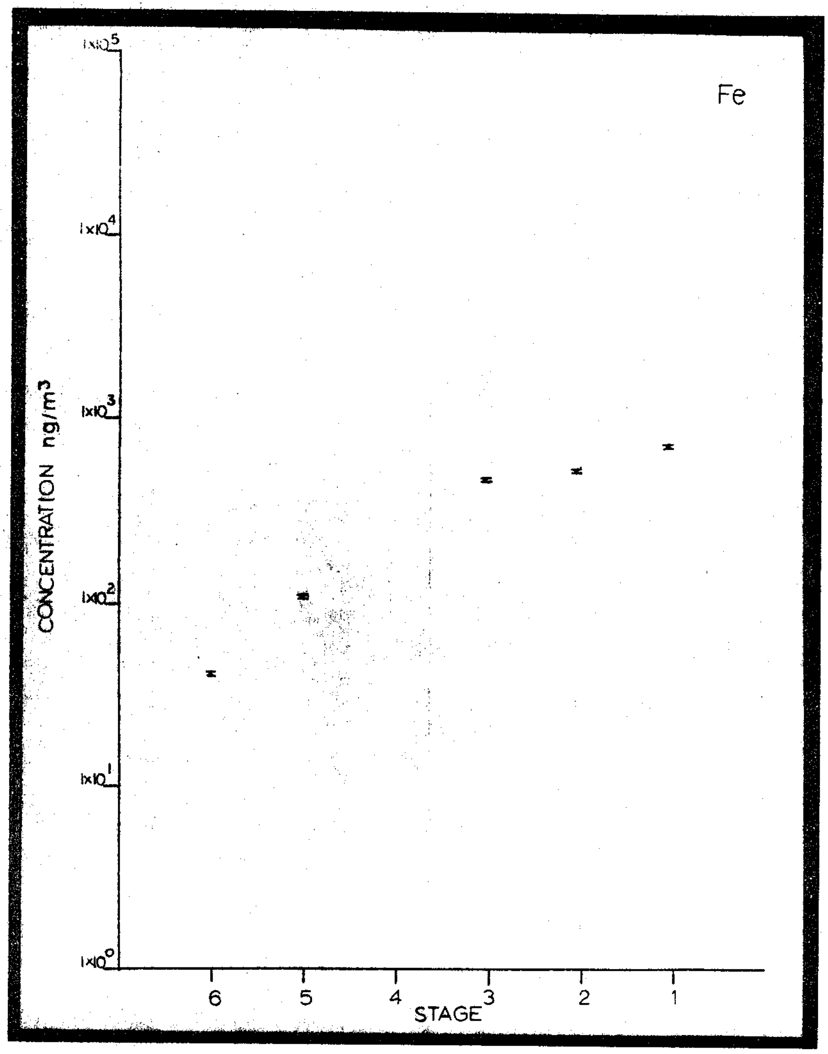

Figure 36 St. Louis Fire Station D. Size Distribution Cu

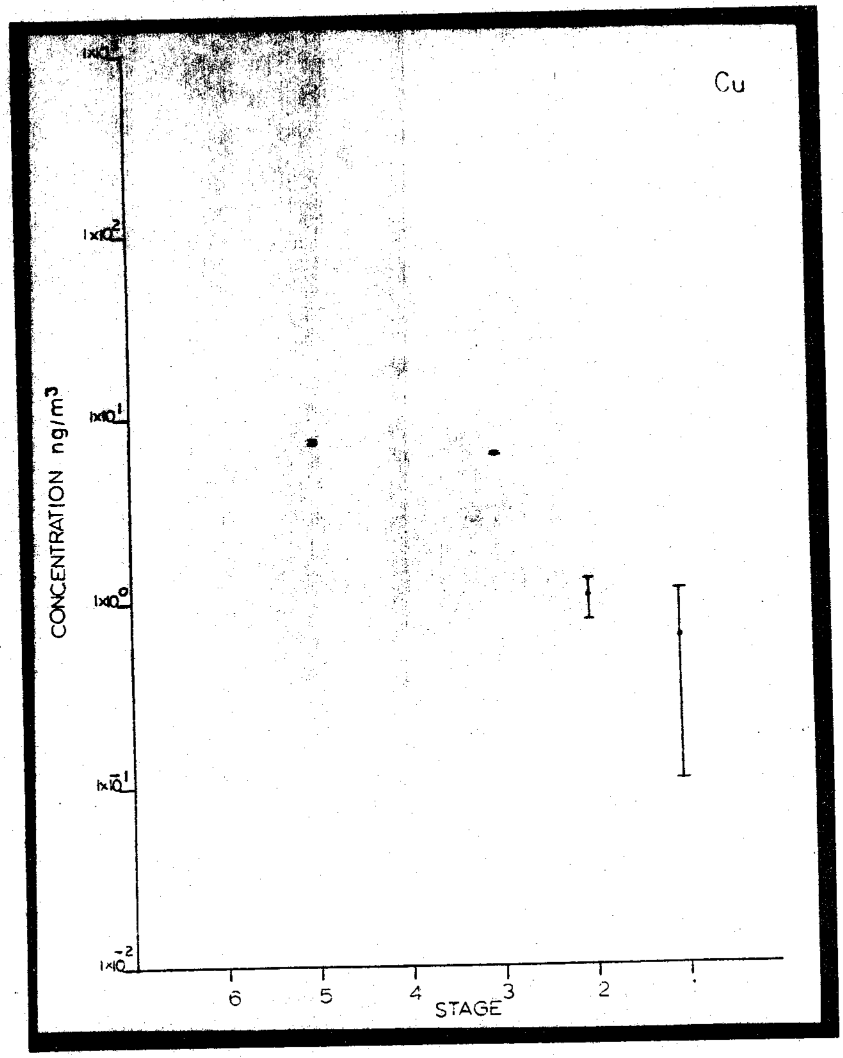

Figure 37 St. Louis Fire Station D. Size Distribution Zn

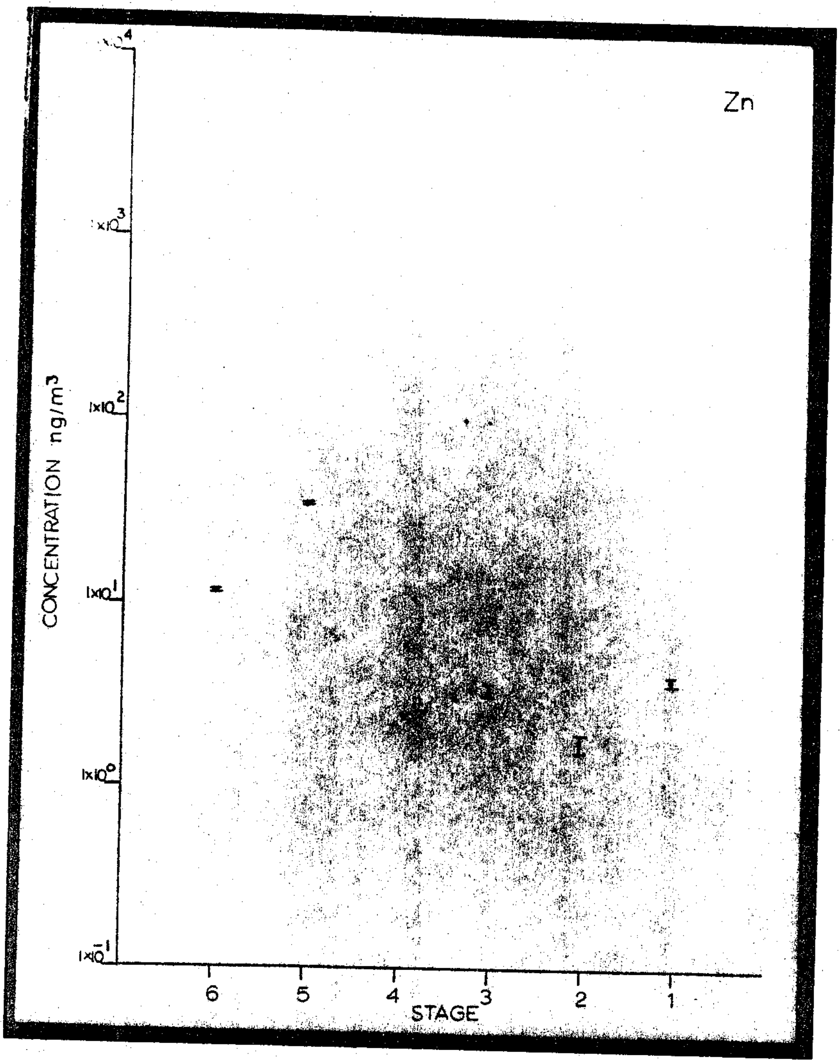

Figure 38 St. Louis Fire Station D. Size Distribution Br

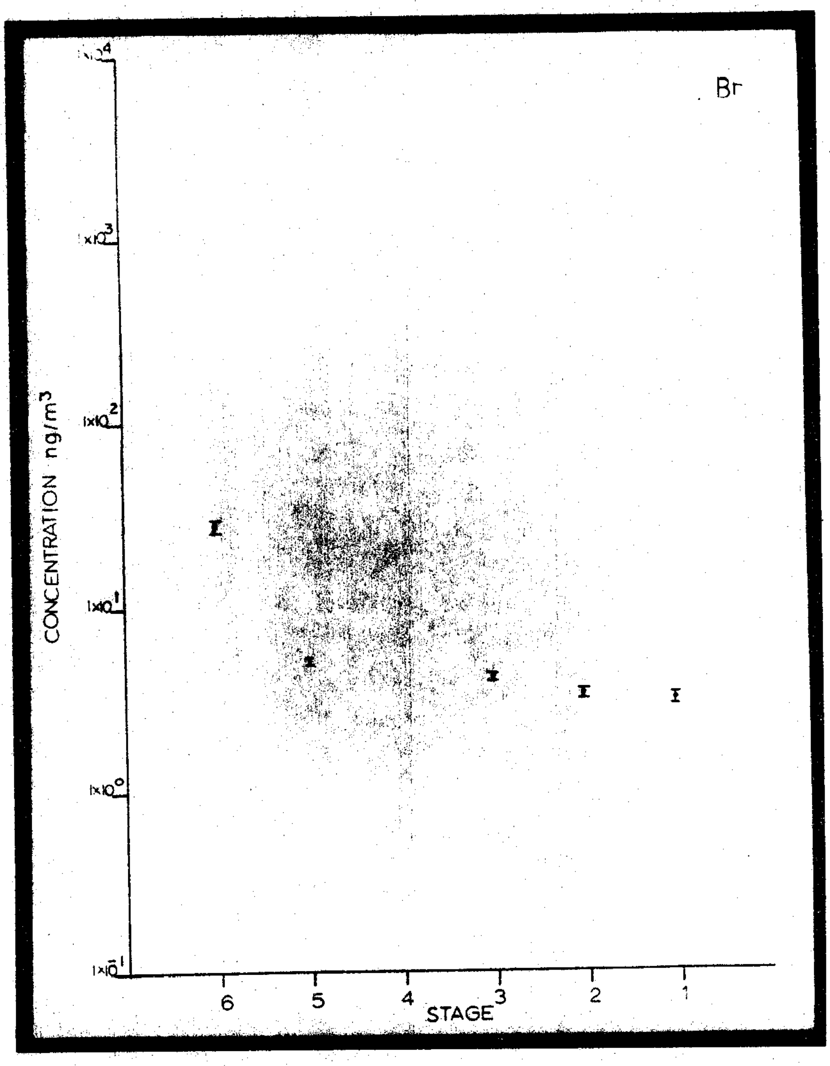

Figure 39 St. Louis Fire Station D. Size Distribution Pb

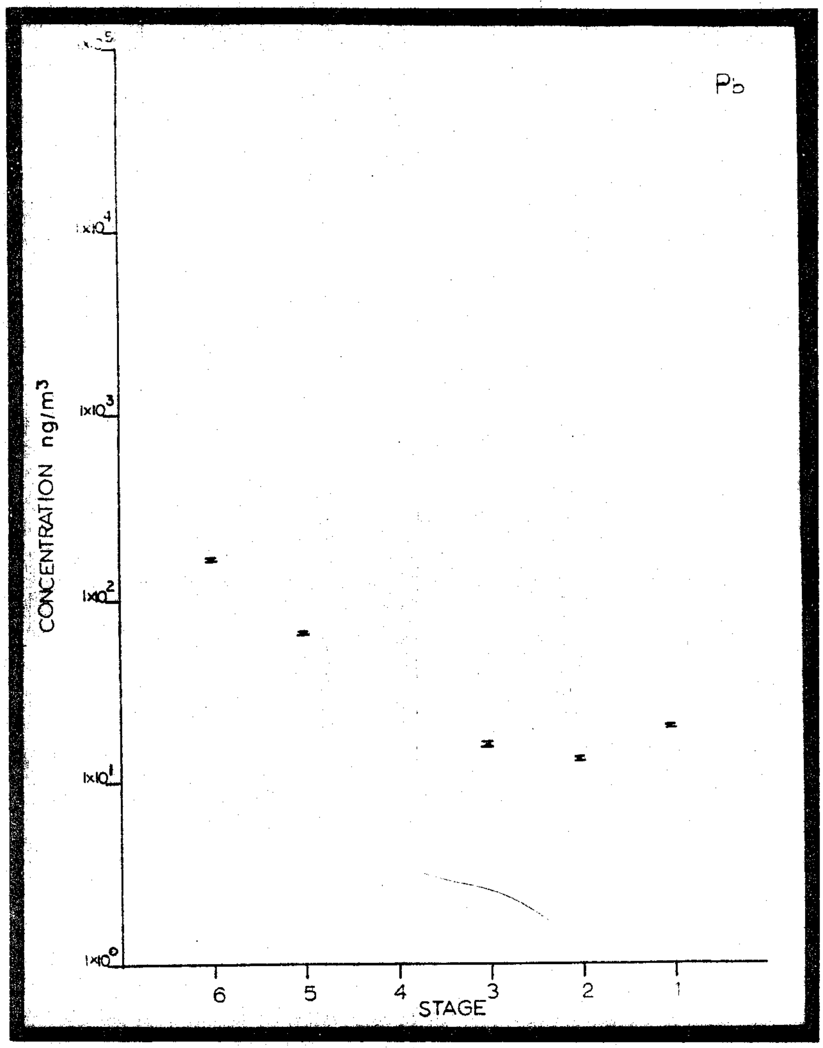

Figure 40 St. Louis Fire Station G. Size Distribution P

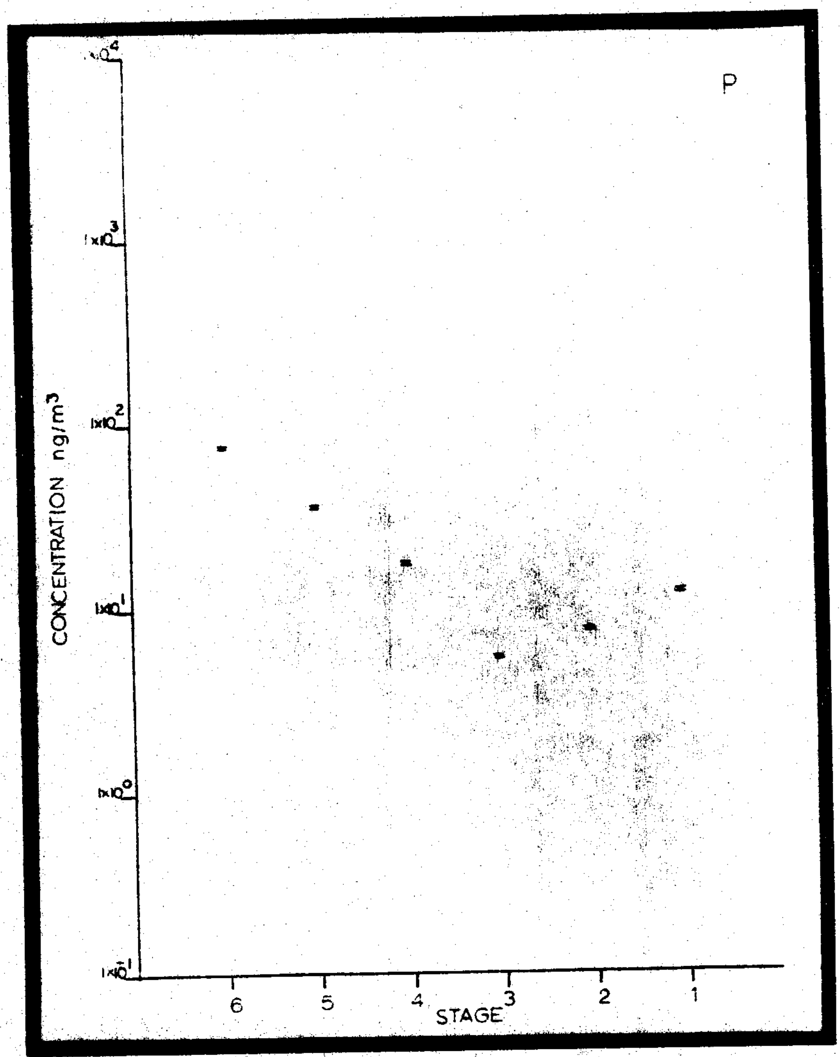

Figure 41 St. Louis Fire Station G. Size Distribution S

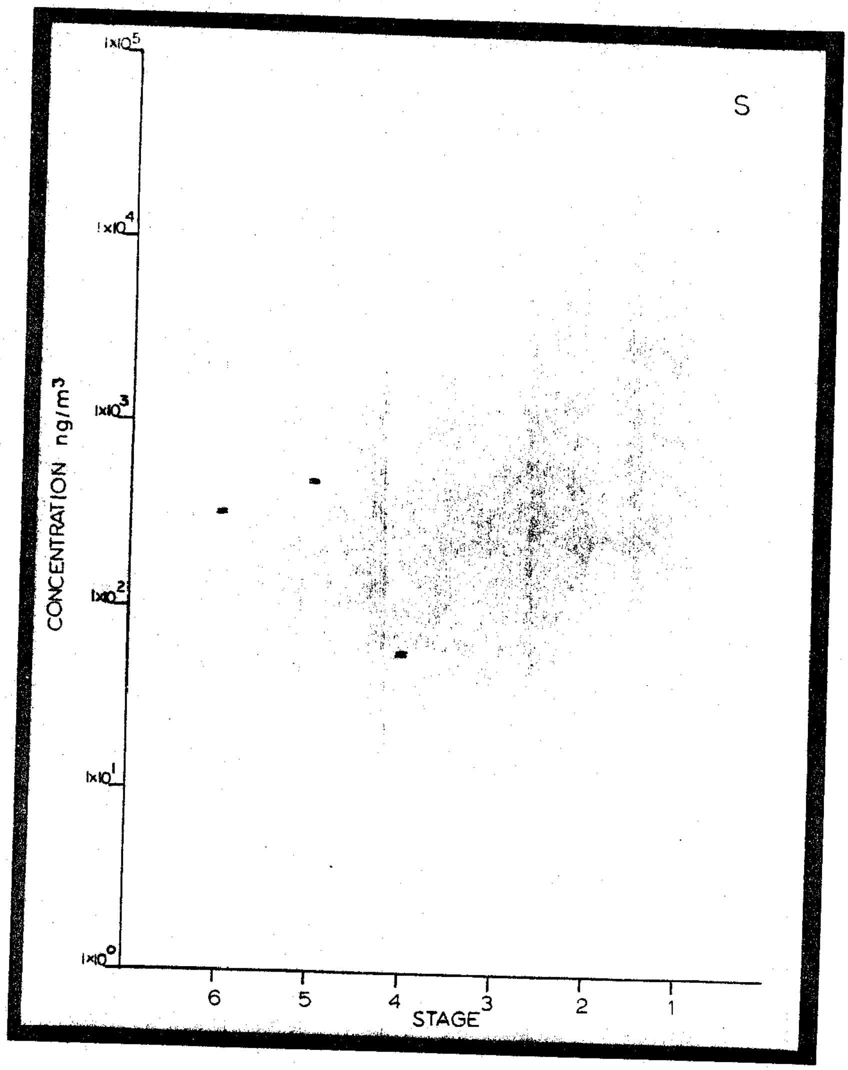

Figure 42 St. Louis Fire Station G. Size Distribution Cl

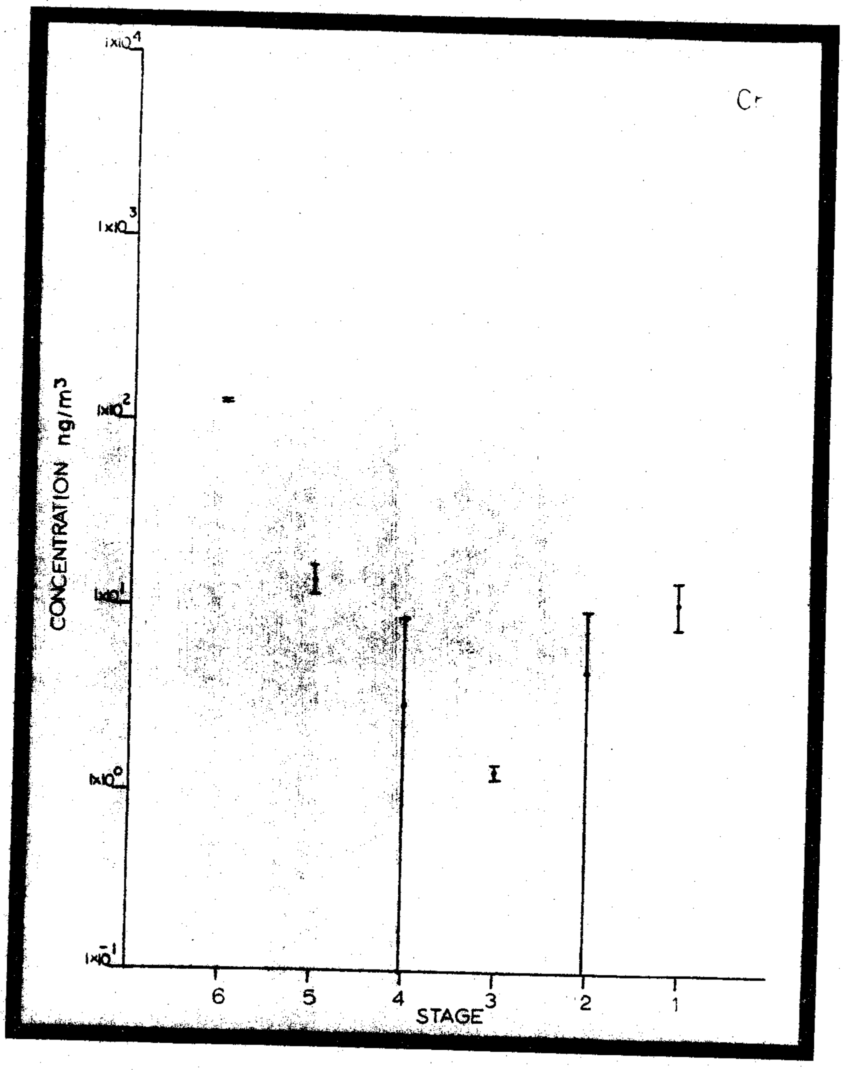

Figure 43 St. Louis Fire Station G. Size Distribution K

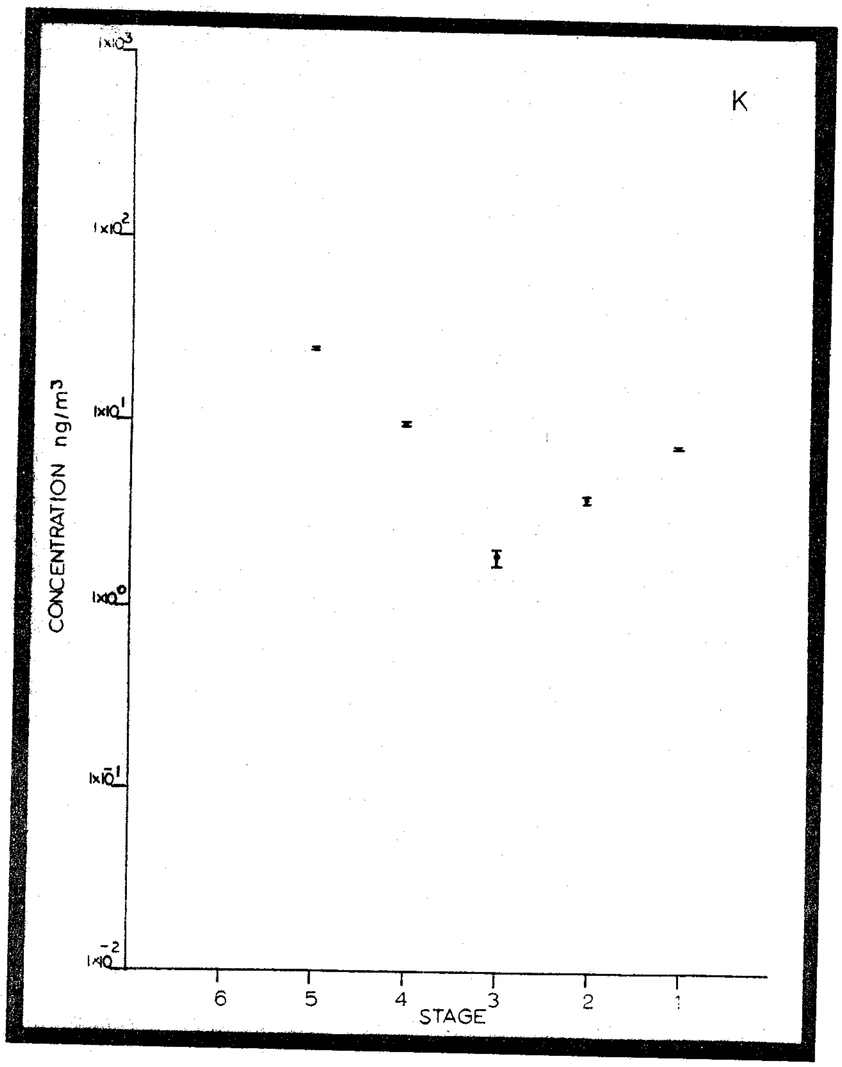

Figure 44 St. Louis Fire Station G. Size Distribution Ca

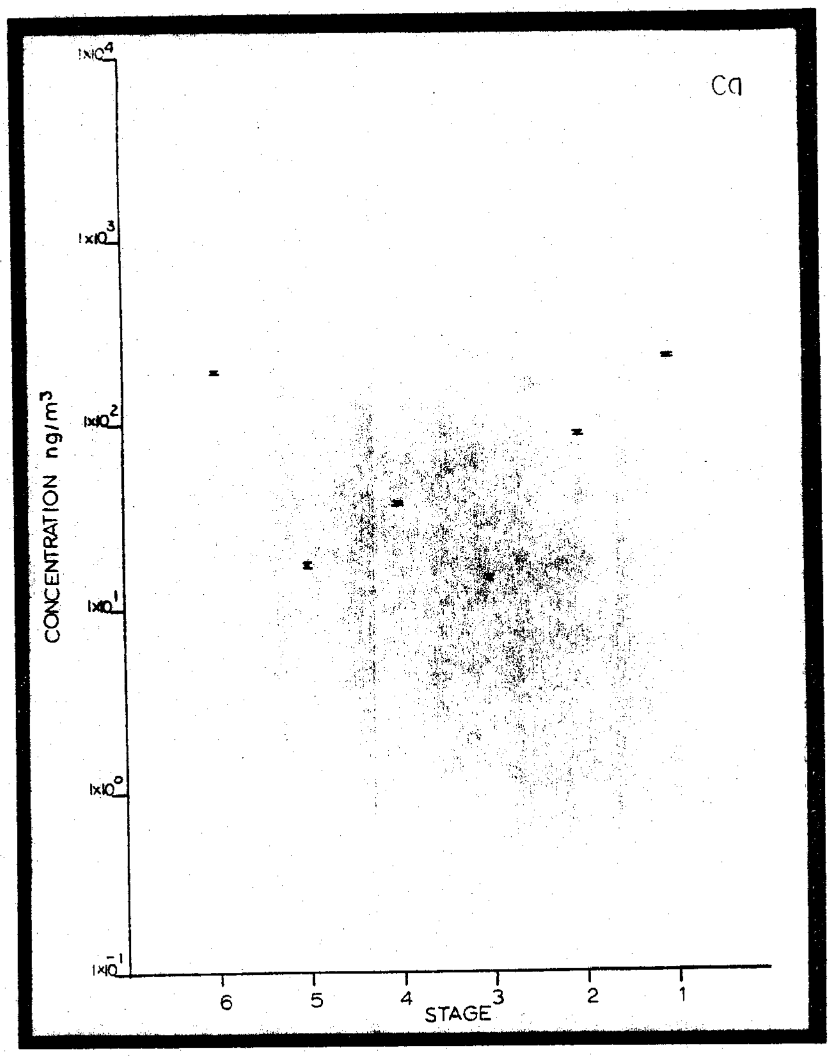

Figure 45 St. Louis Fire Station G. Size Distribution Ti

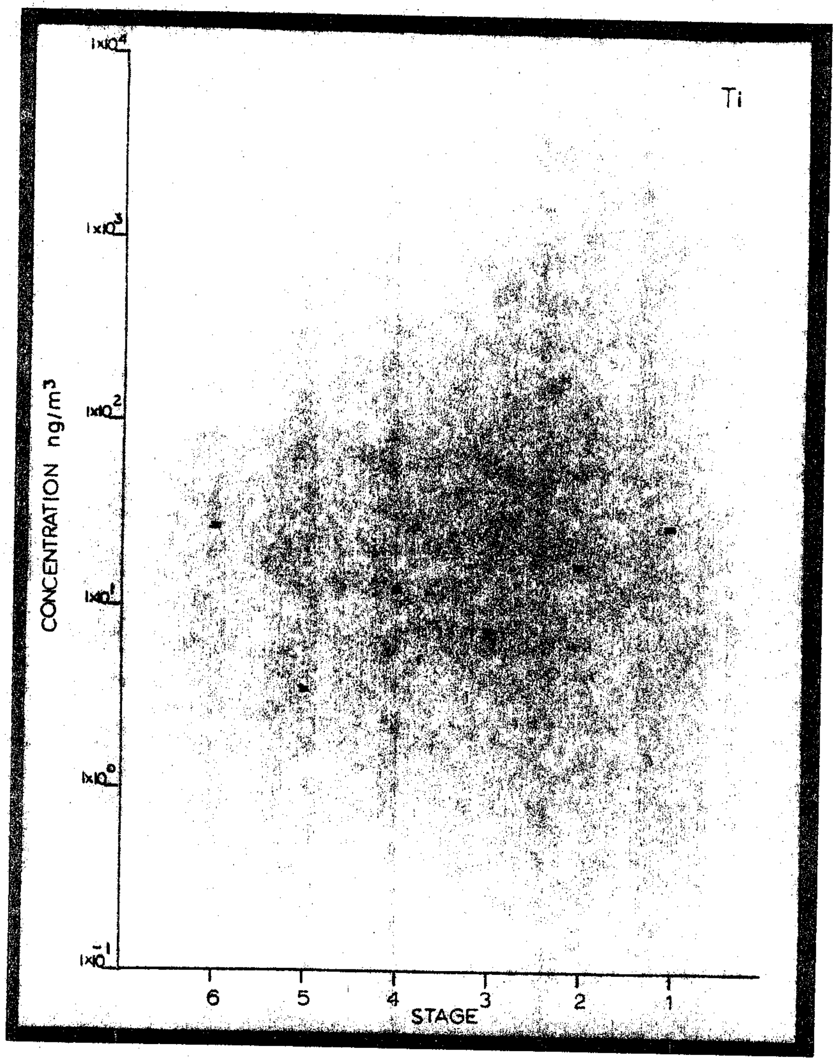

Figure 46 St. Louis Fire Station G. Size Distribution V

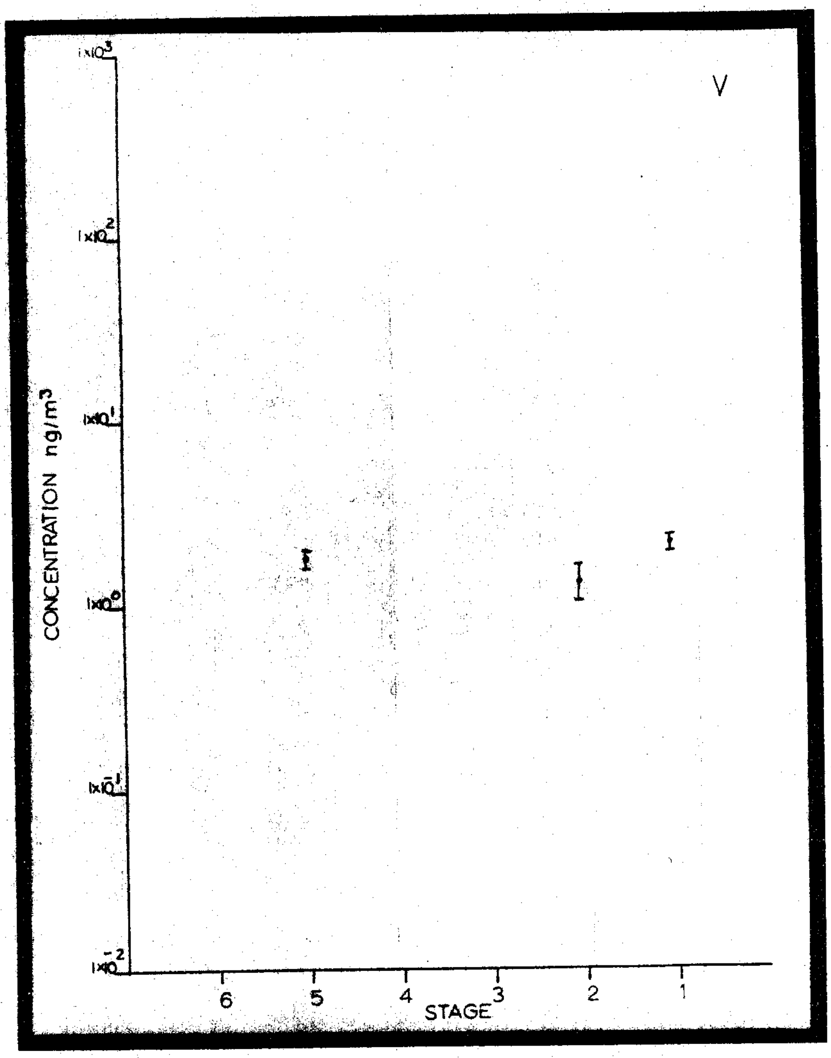

Figure 47 St. Louis Fire Station G. Size Distribution Mn

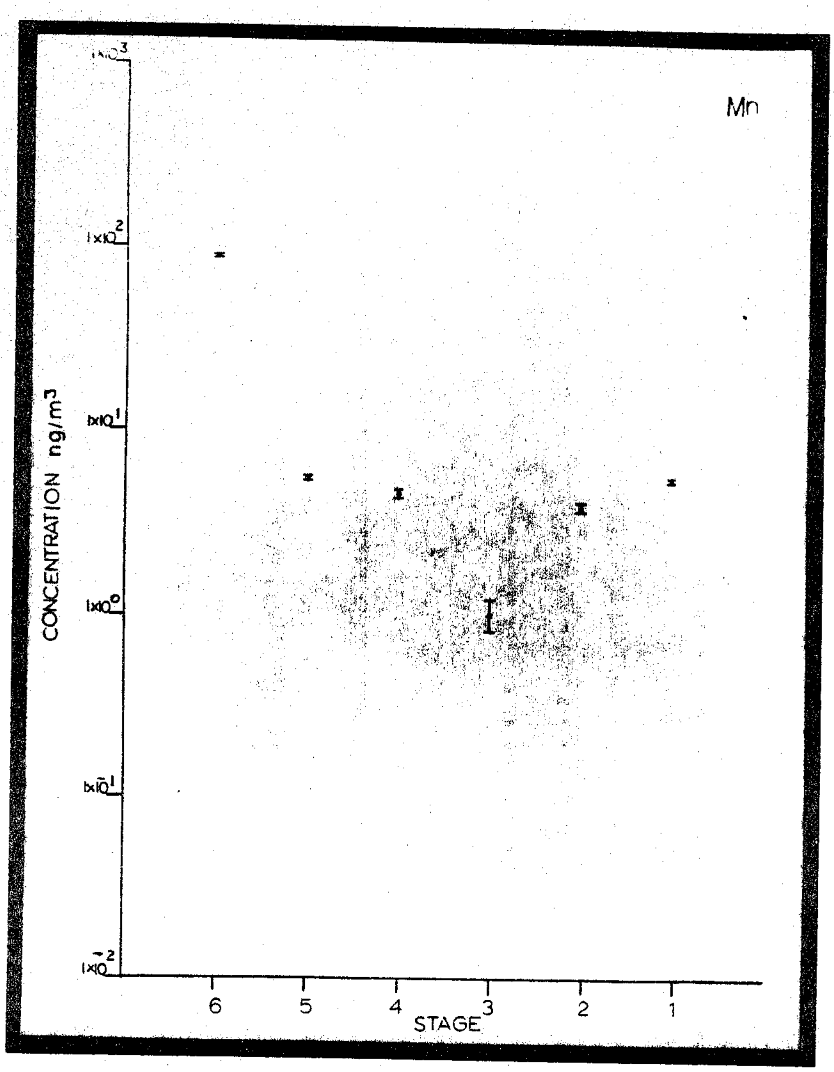

Figure 48 St. Louis Fire Station G. Size Distribution Fe

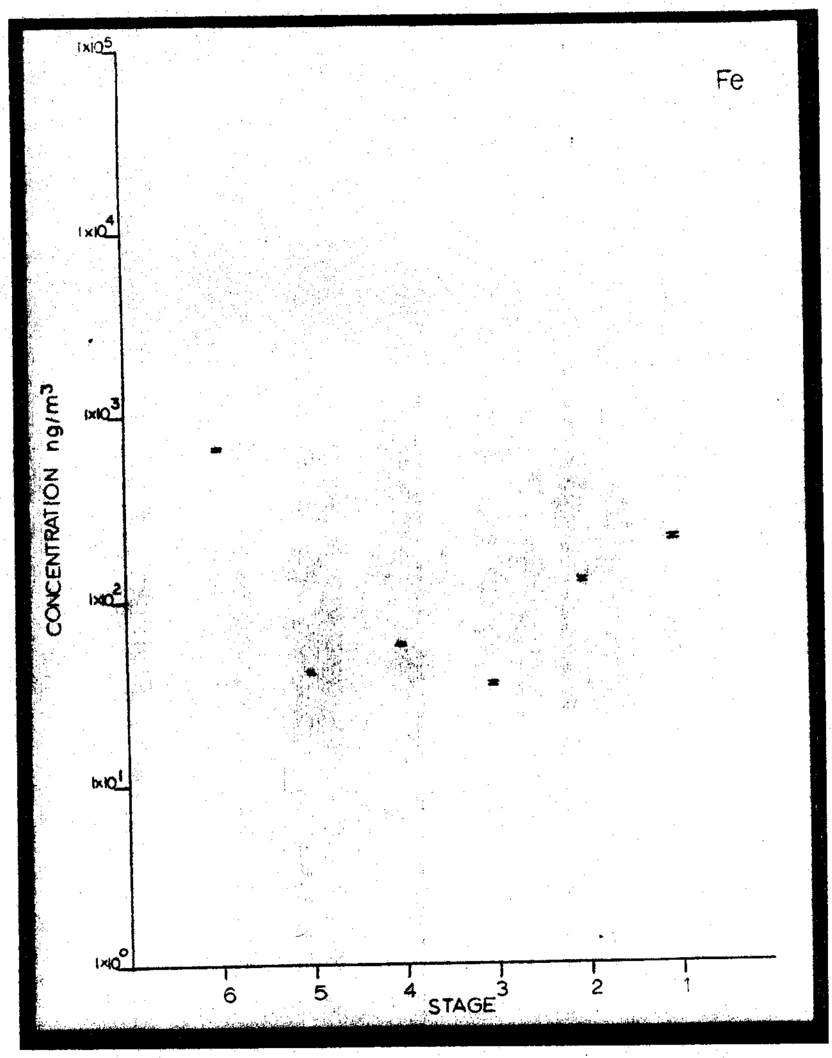

Figure 49   St. Louis Fire Station G. Size Distribution Cu

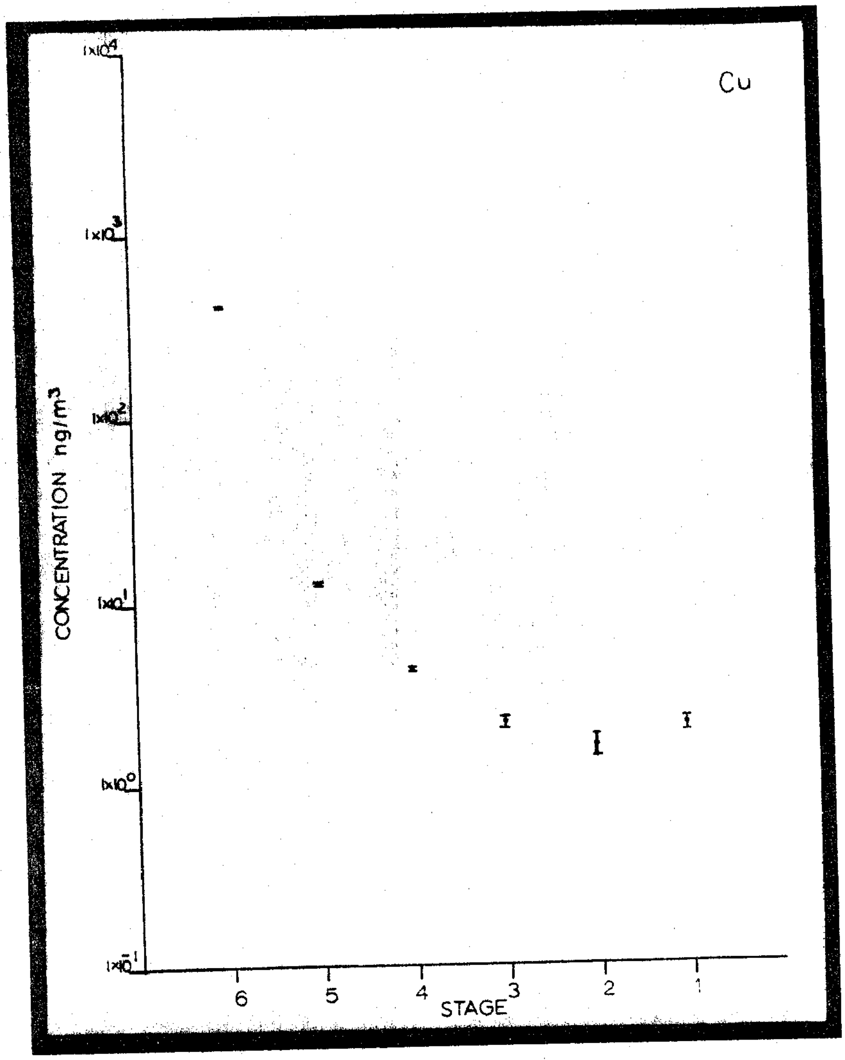

Figure 50 St. Louis Fire Station G. Size Distribution Zn

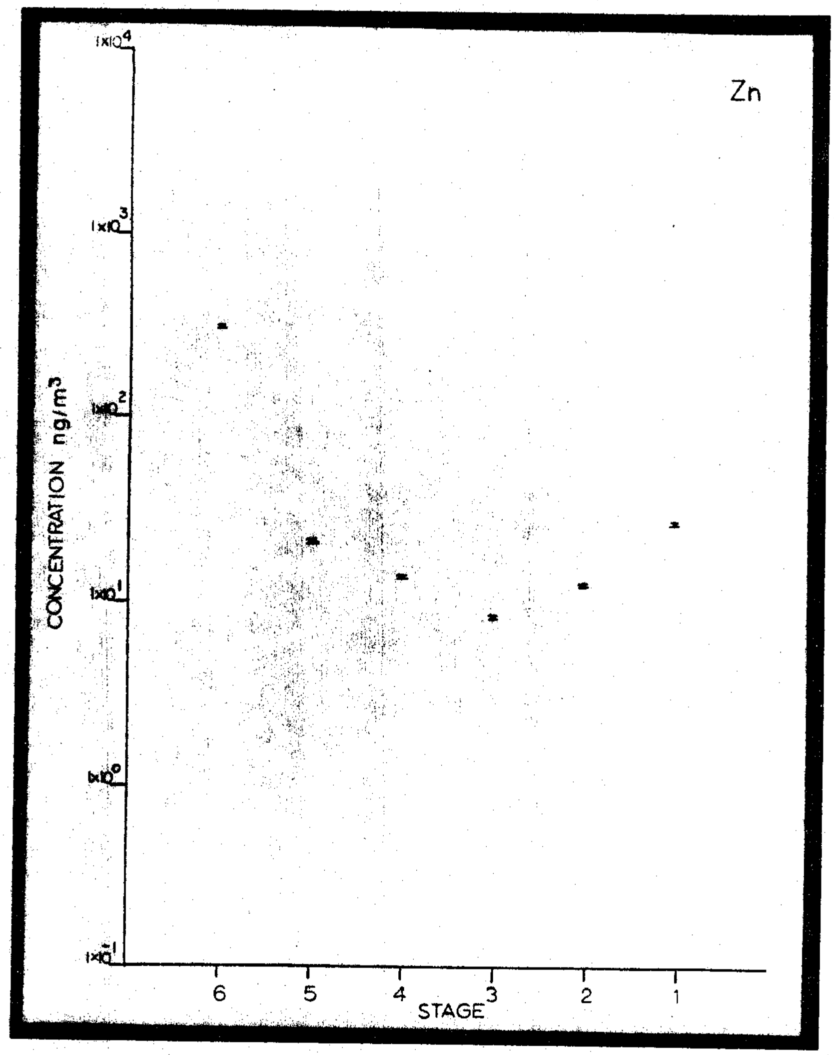

Figure 51 St. Louis Fire Station G. Size Distribution Br

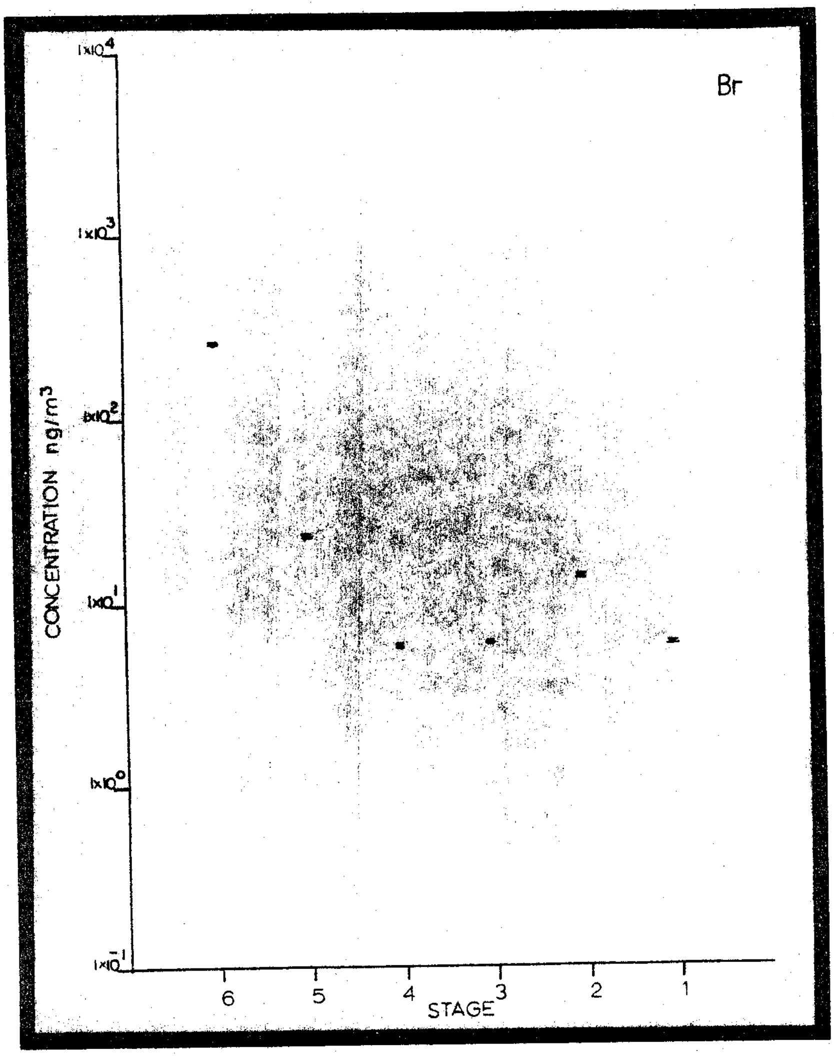

Figure 52 St. Louis Fire Station G. Size Distribution Pb

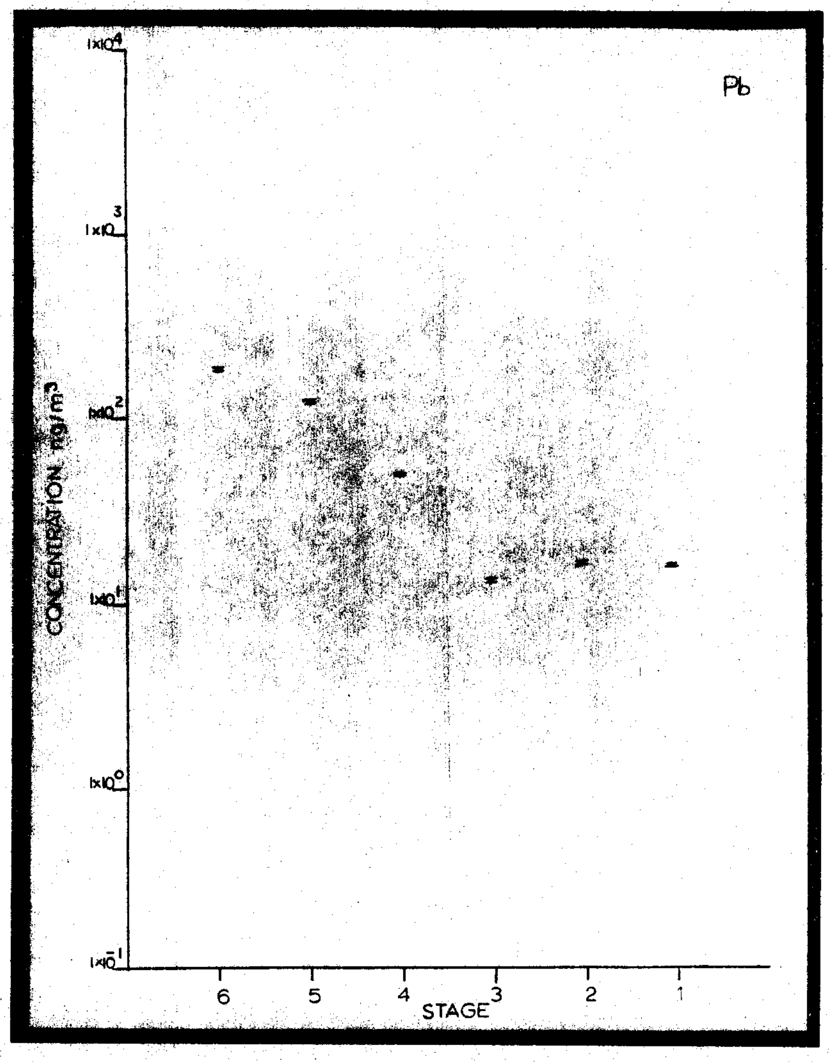

Figure 53 St. Louis Fire Station I. Size Distribution P

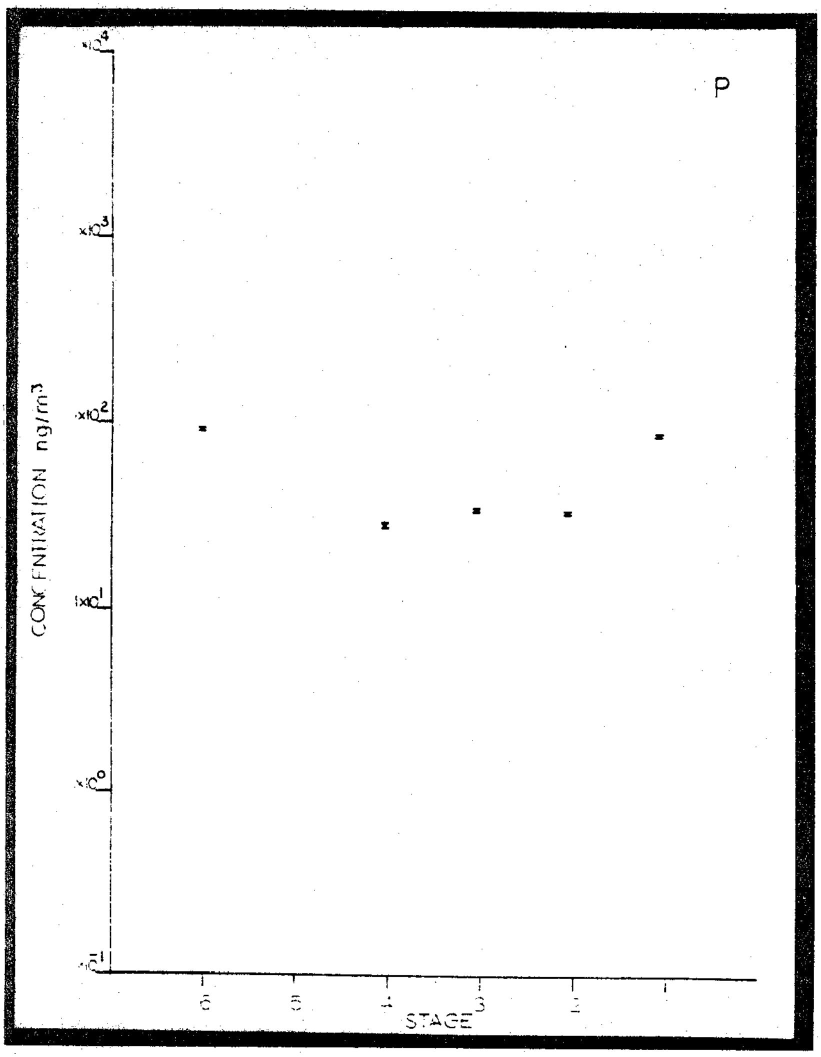

Figure 54 St. Louis Fire Station I. Size Distribution S

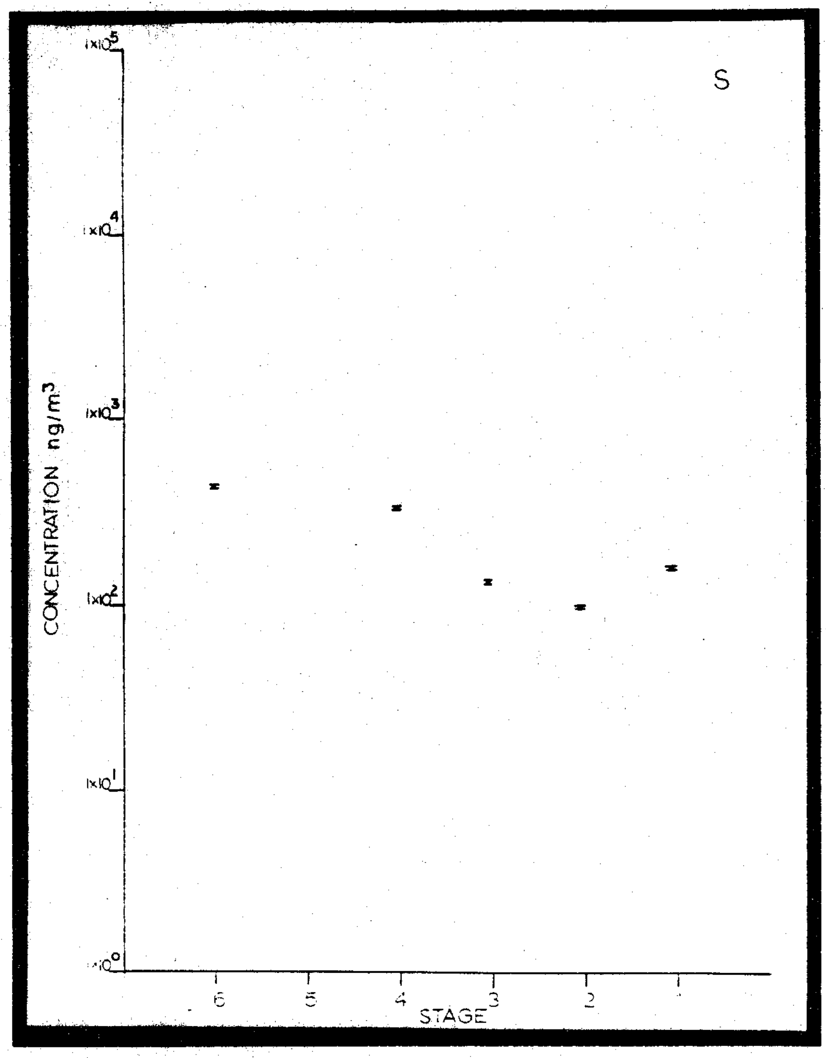

Figure 55   St. Louis Fire Station I. Size Distribution Cl

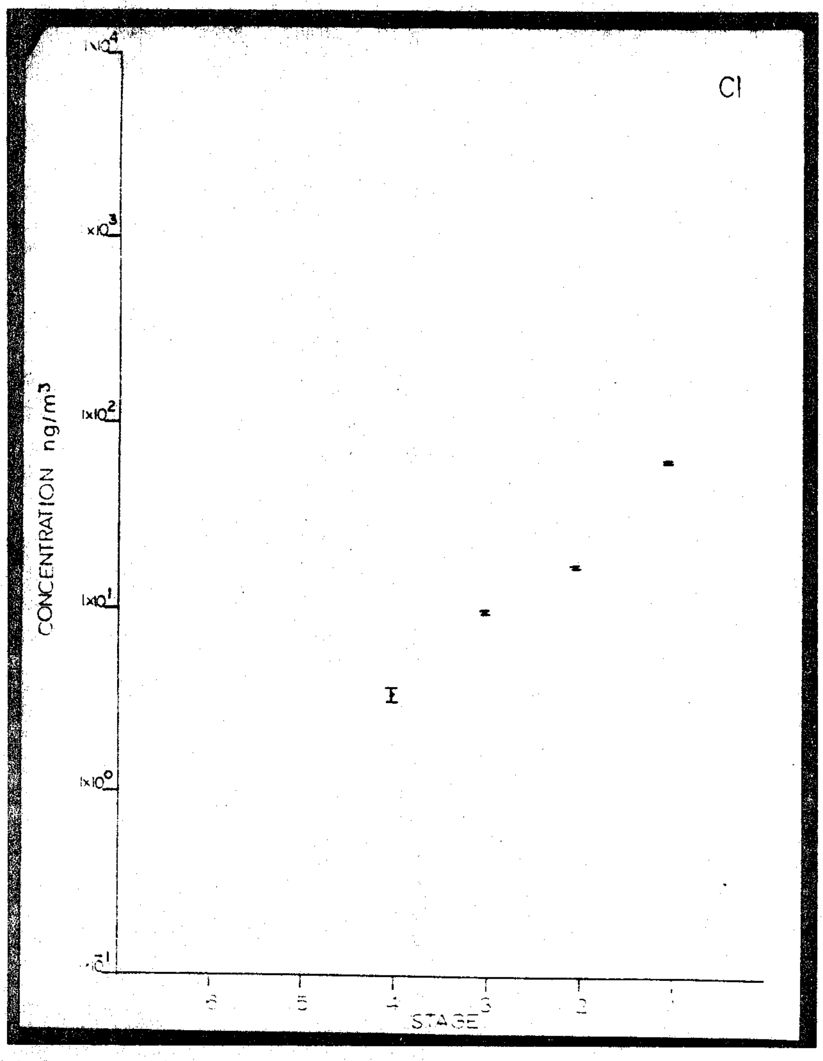

Figure 56 St. Louis Fire Station I. Size Distribution K

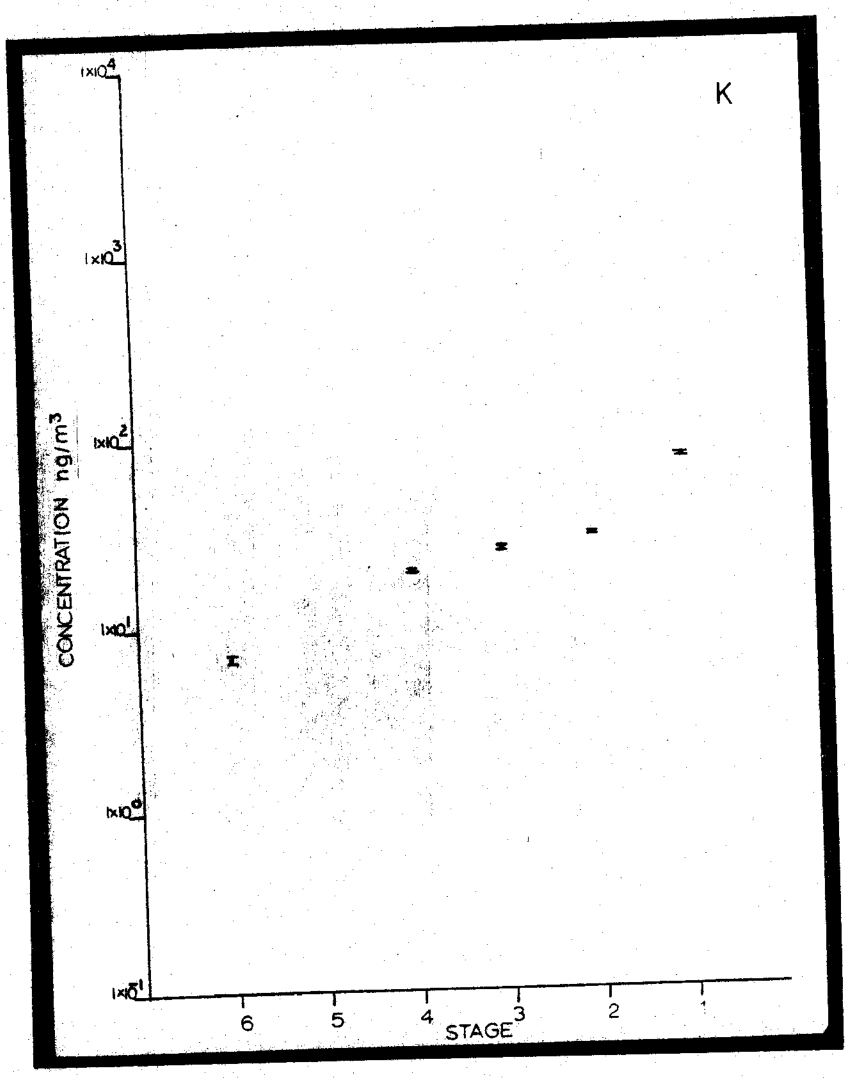

Figure 57 St. Louis Fire Station I. Size Distribution Ca

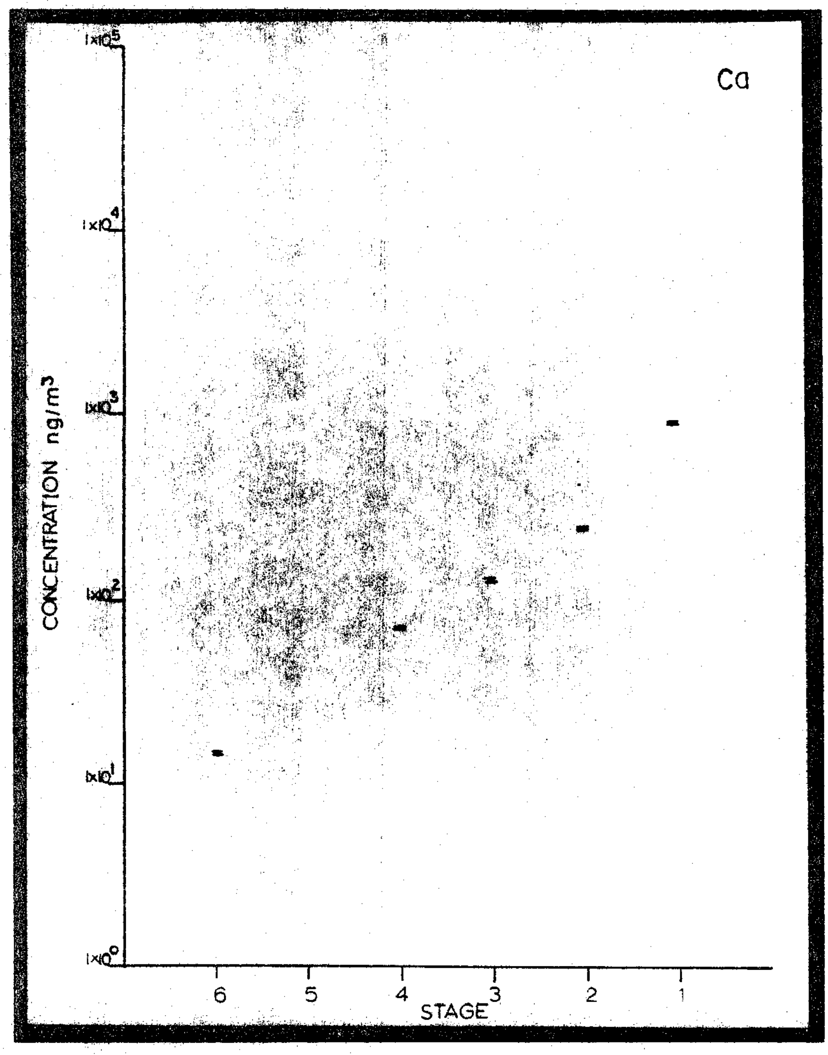

Figure 58 St. Louis Fire Station I. Size Distribution Ti

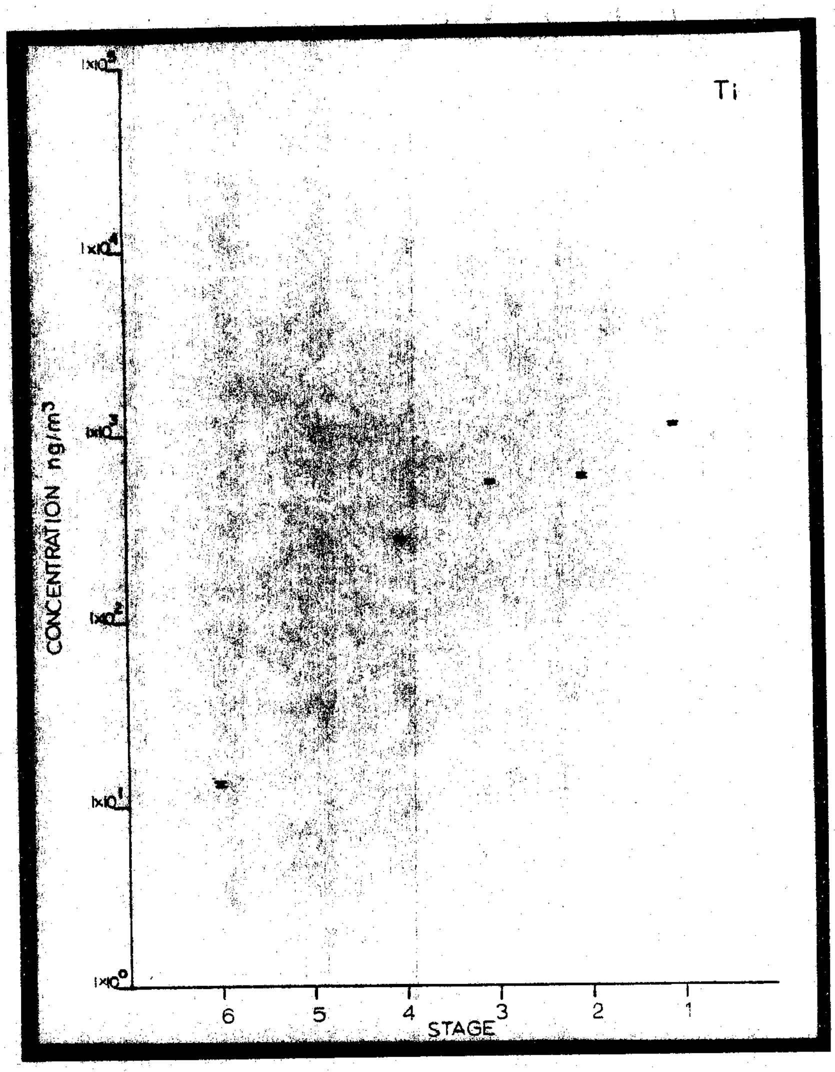

Figure 59 St. Louis Fire Station I. Size Distribution V

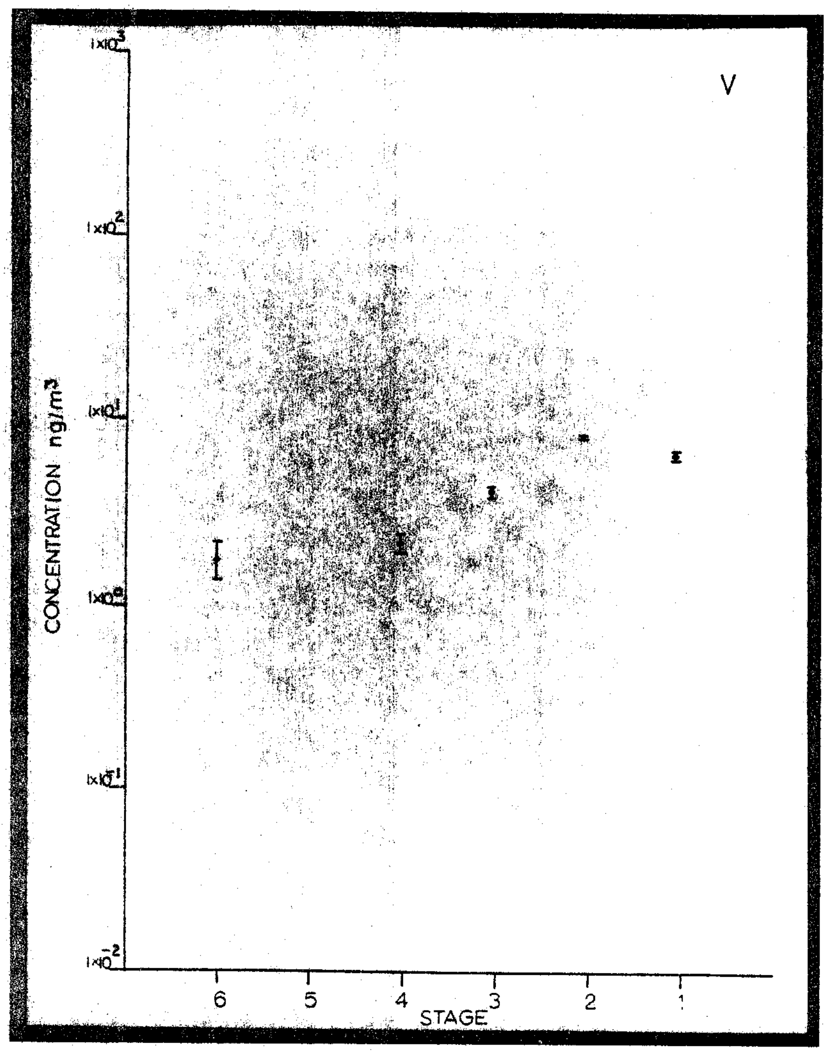

Figure 60 St. Louis Fire Station I. Size Distribution Mn

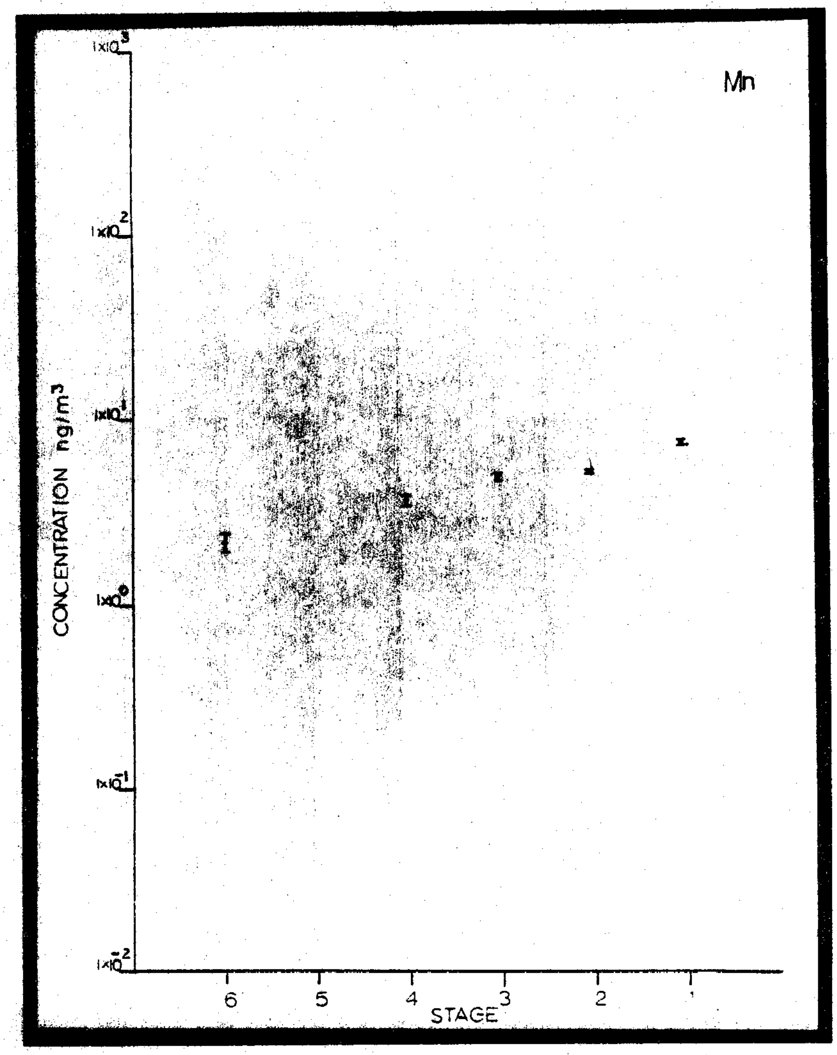

Figure 61 St. Louis Fire Station I. Size Distribution Fe

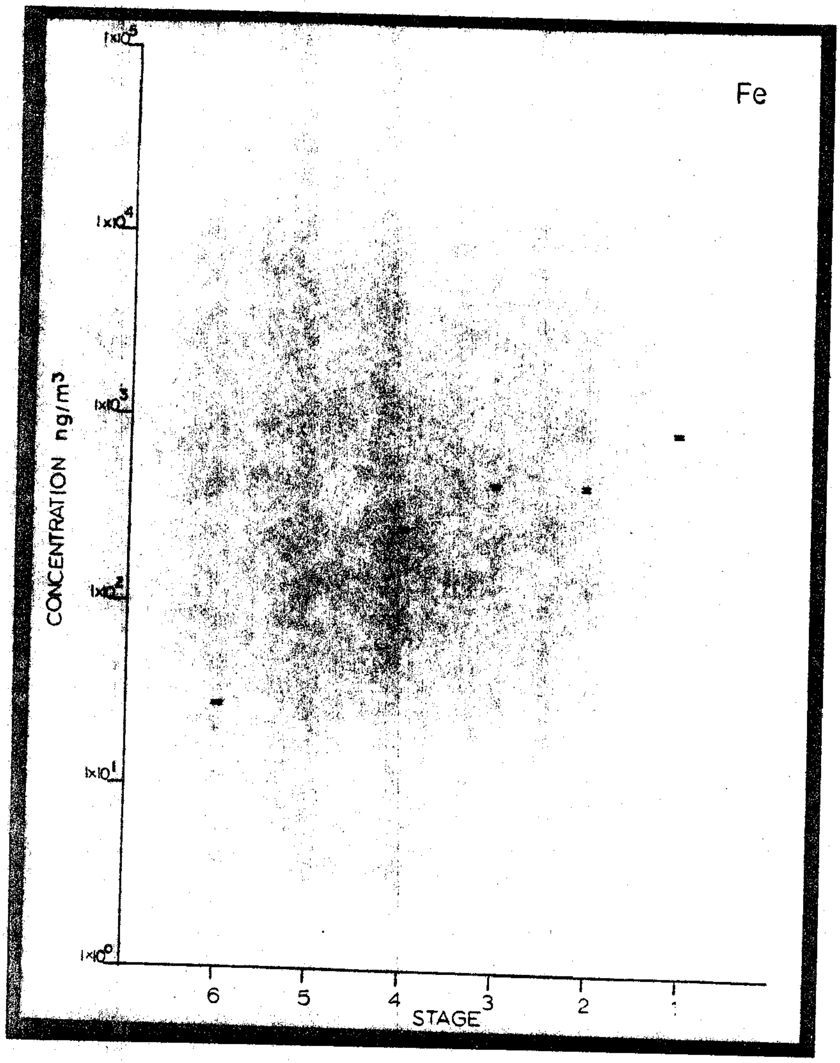

Figure 62 St. Louis Fire Station I. Size Distribution Cu

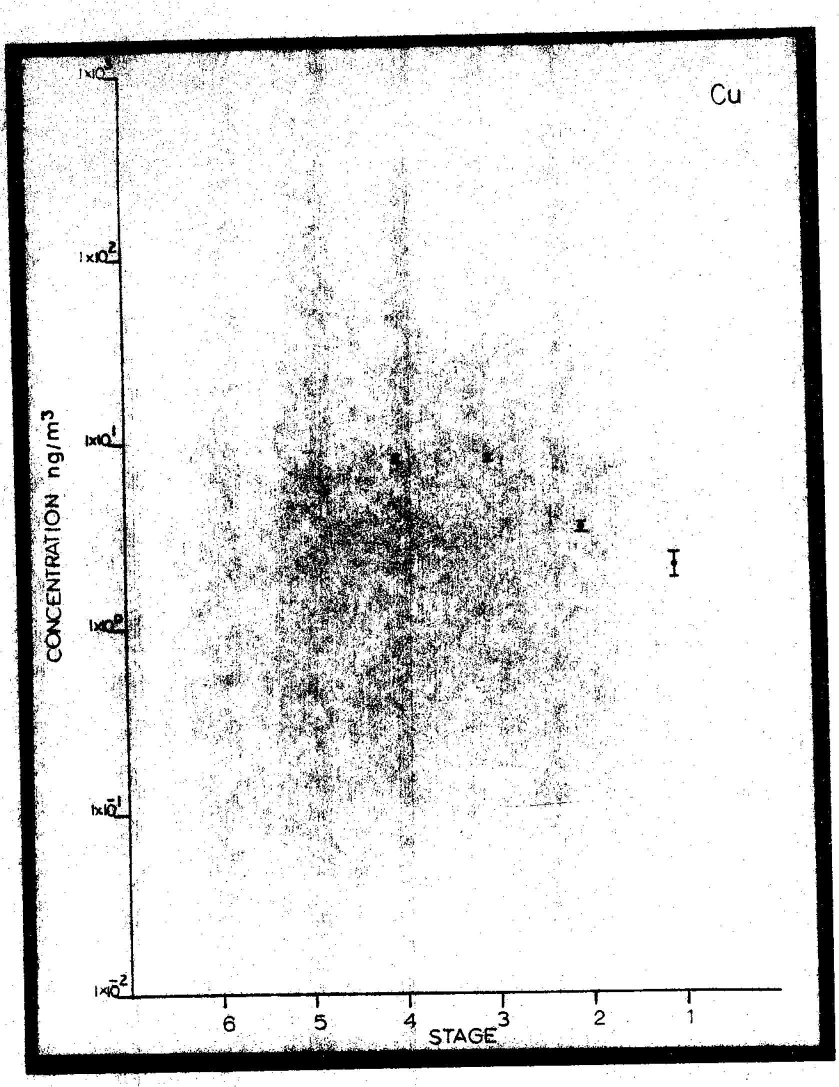

Figure 63 St. Louis Fire Station I. Size Distribution Zn

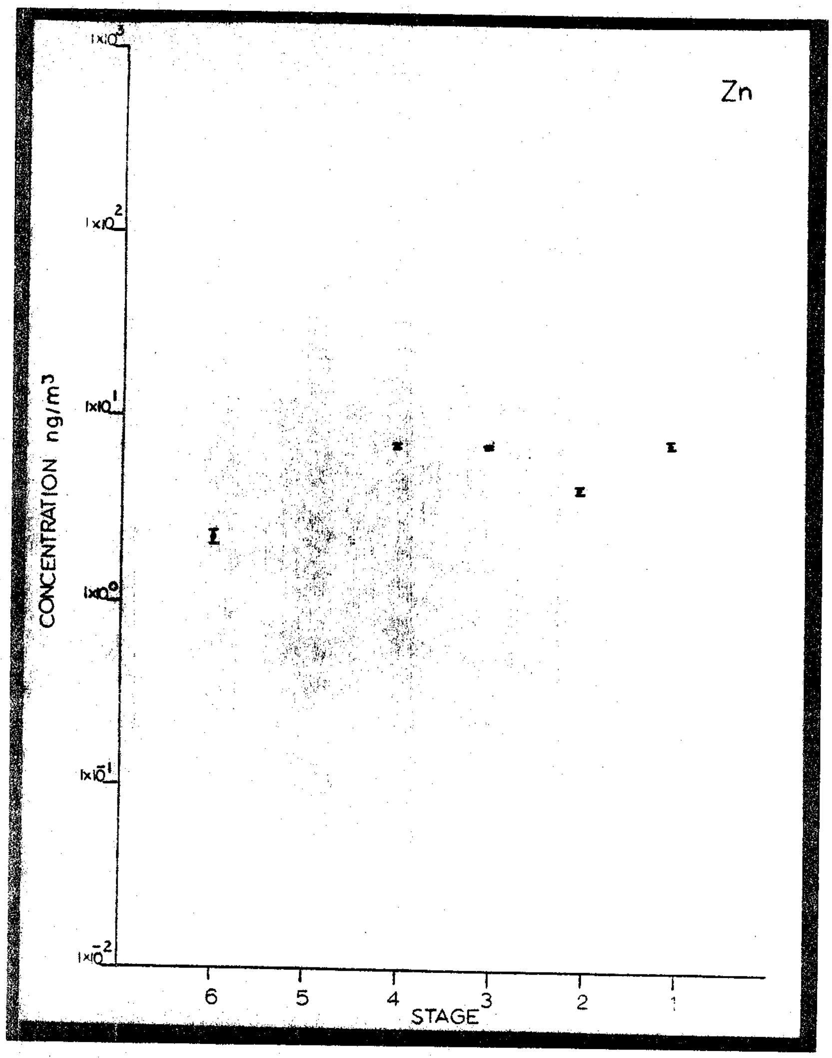

Figure 64 St. Louis Fire Station I. Size Distribution Br

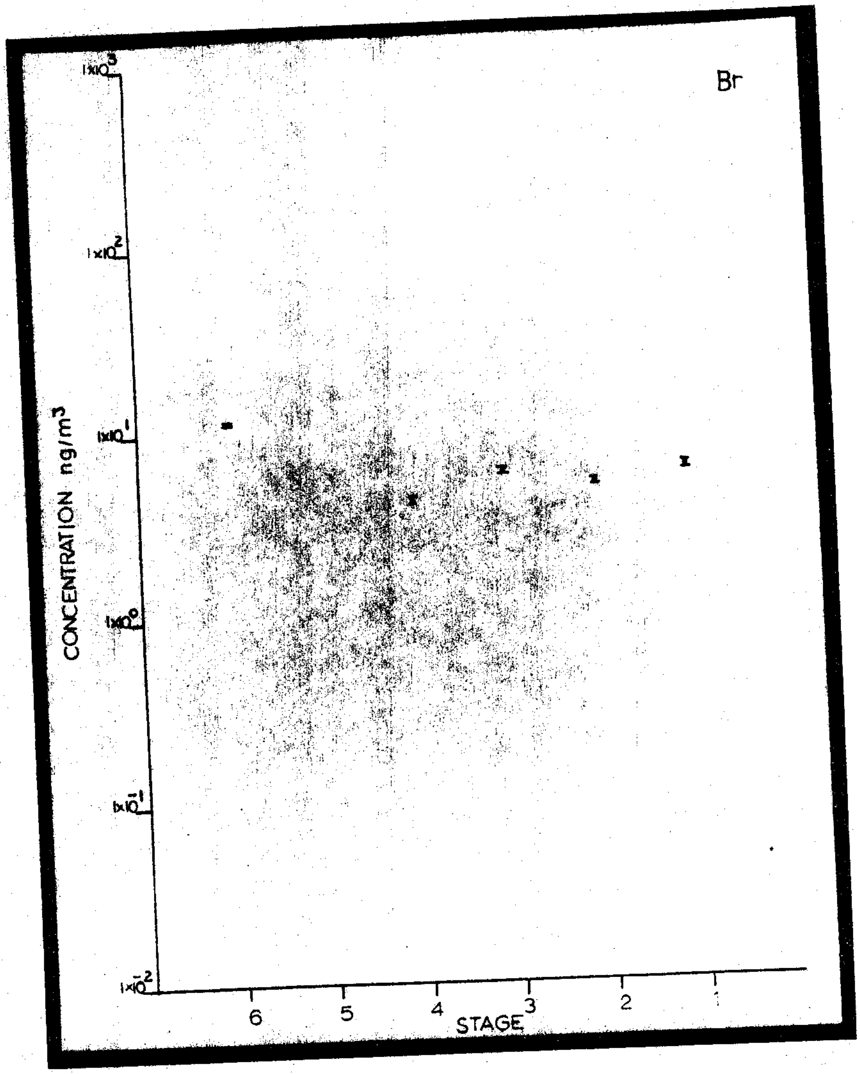

Figure 65 St. Louis Fire Station I. Size Distribution Pb

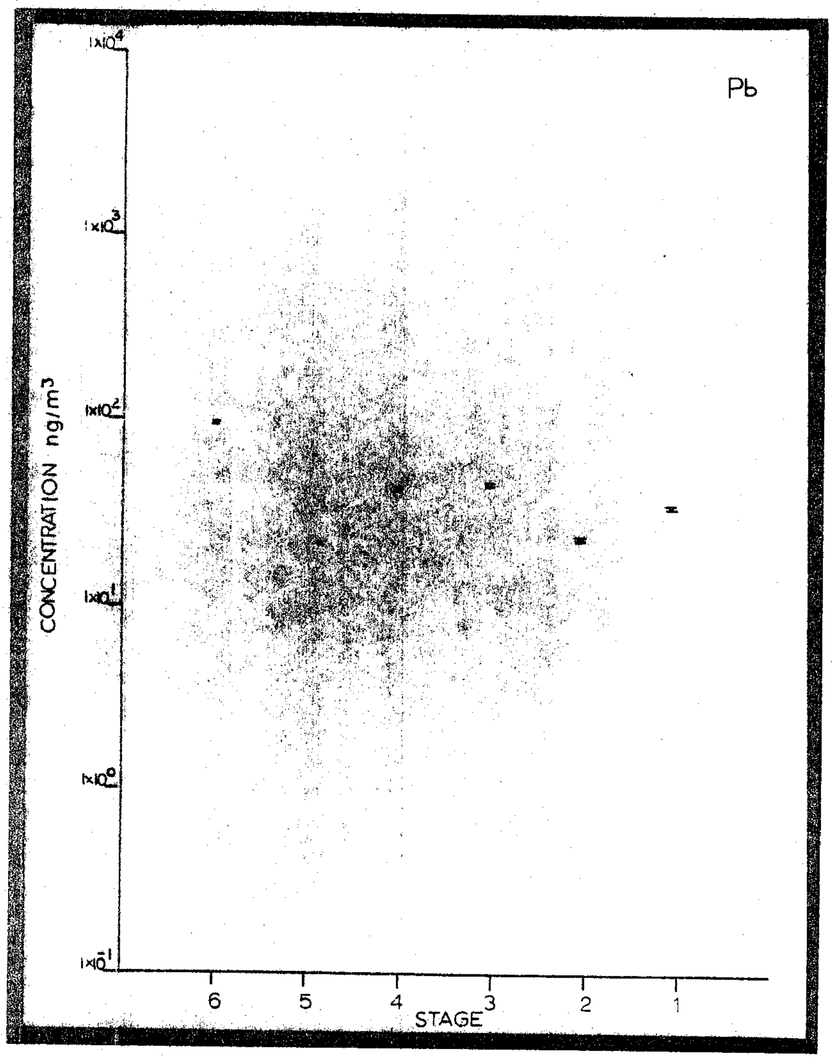

Figure 66 St. Louis Municipal Court B. Size Distribution P

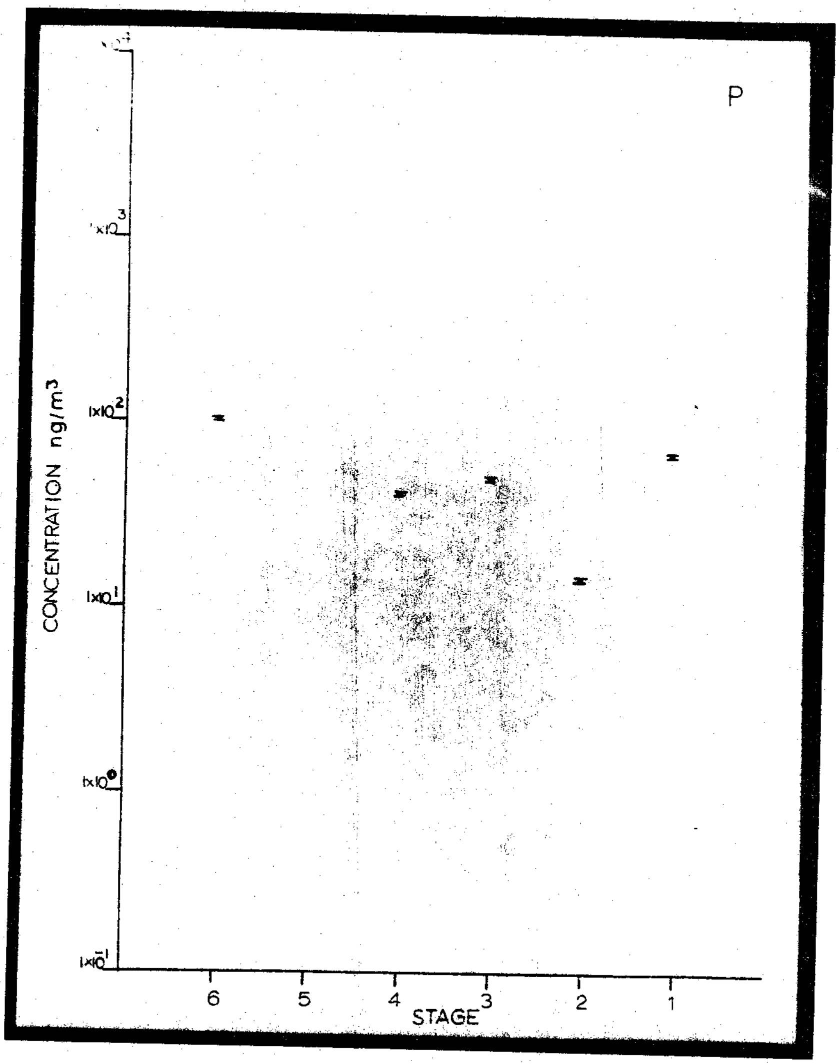

Figure 67 St. Louis Municipal Court B. Size Distribution S

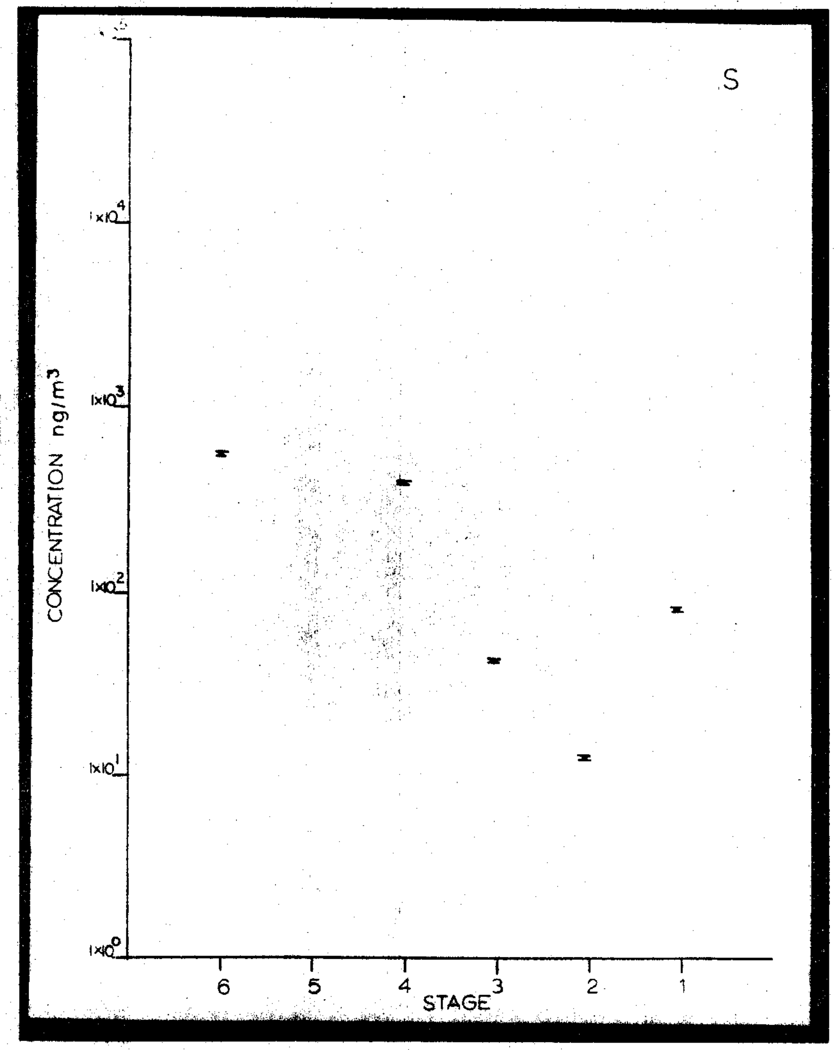

Figure 68 St. Louis Municipal Court B. Size Distribution Cl

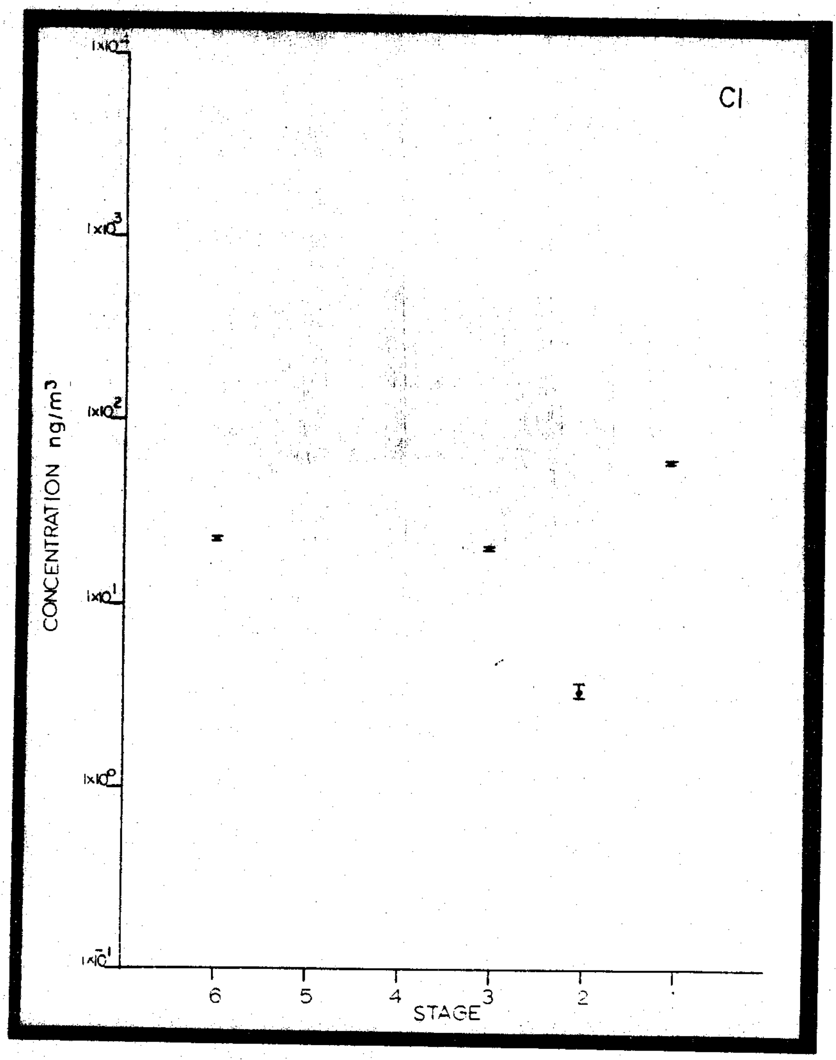

Figure 69 St. Louis Municipal Court B. Size Distribution K

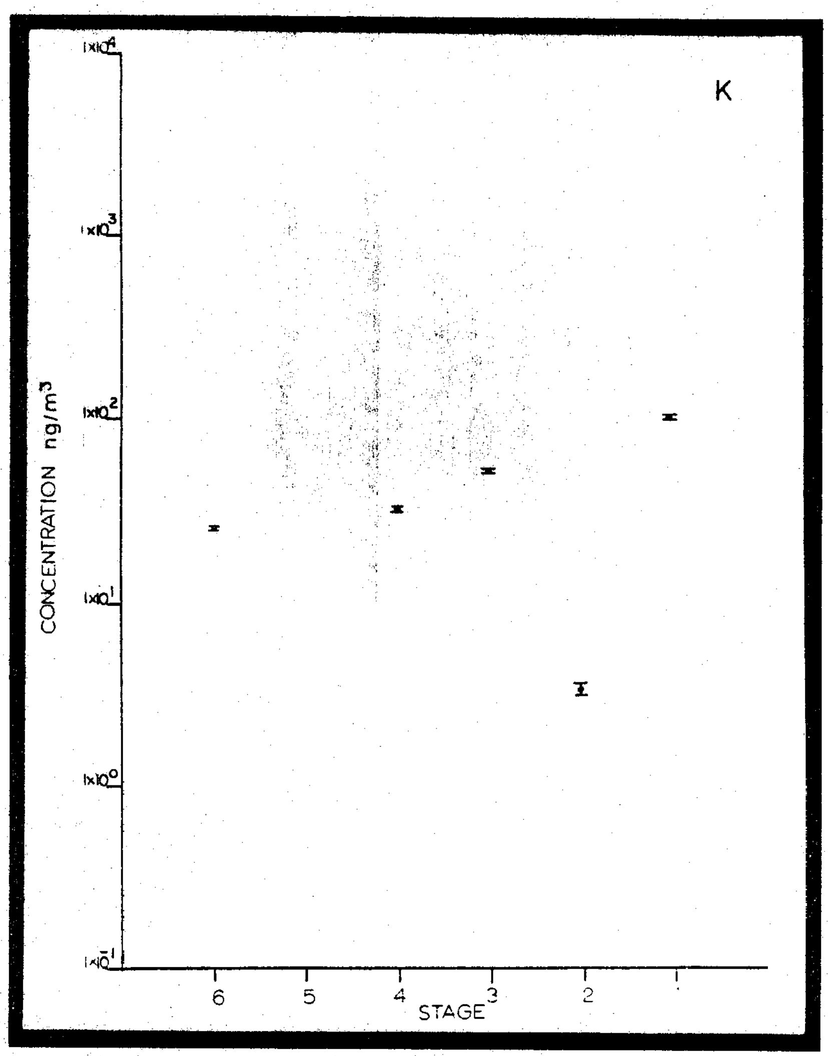

Figure 70 St. Louis Municipal Court B. Size Distribution Ca

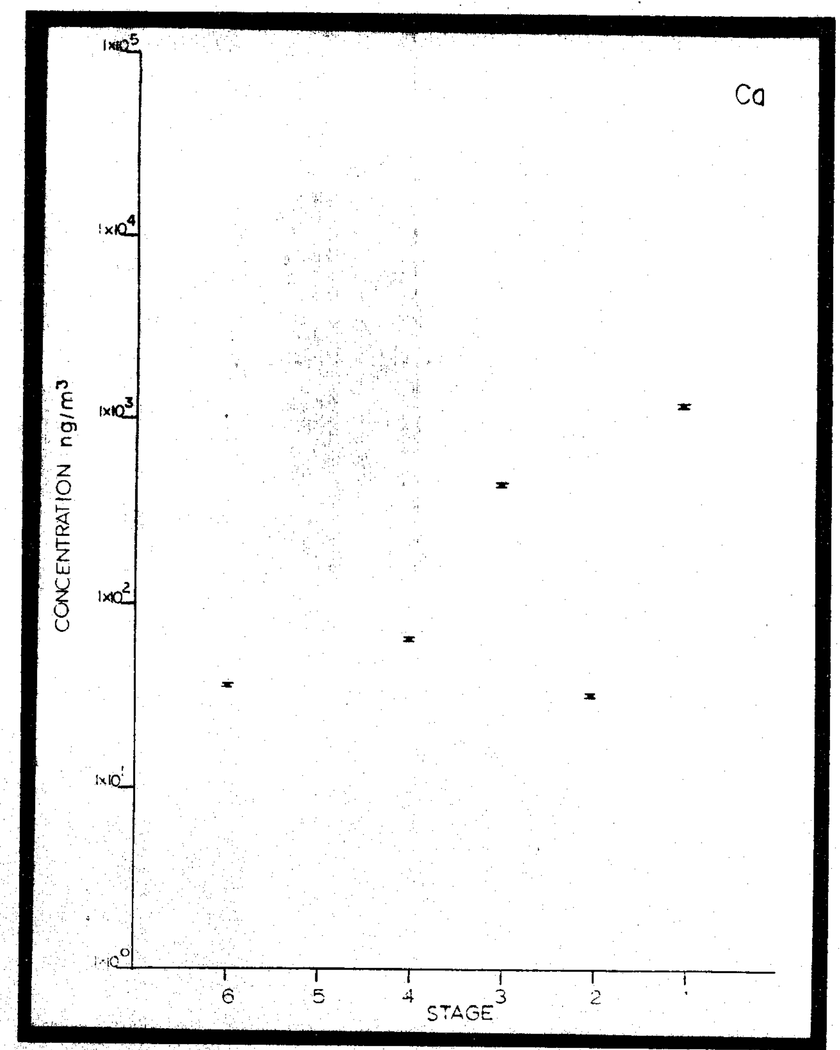

Figure 71 St. Louis Municipal Court B. Size Distribution Ti

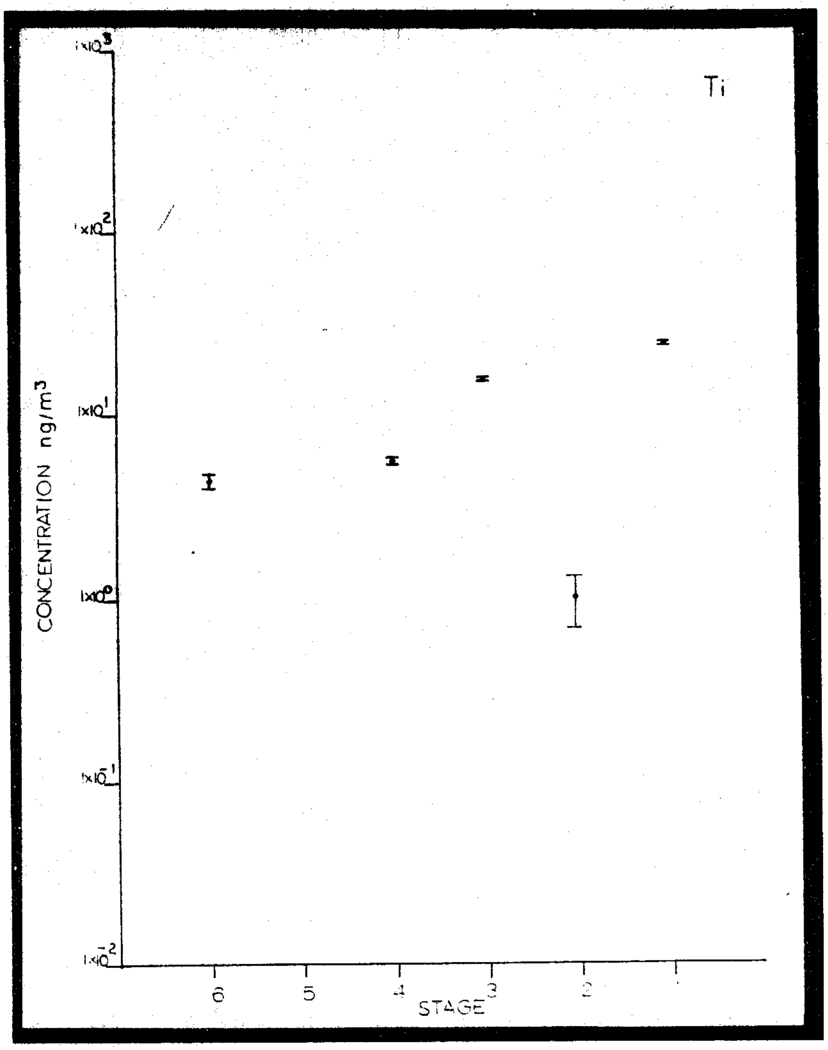

Figure 72 St. Louis Municipal Court B. Size Distribution V

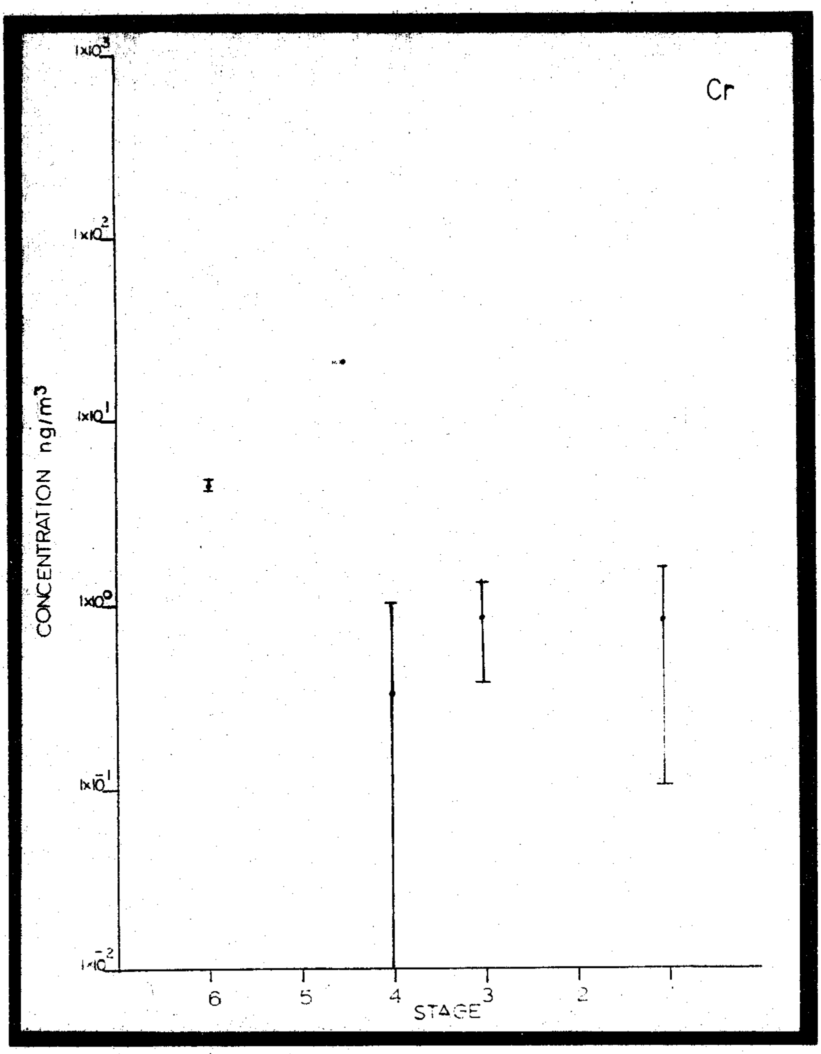

Figure 73 St. Louis Municipal Court B. Size Distribution Mn

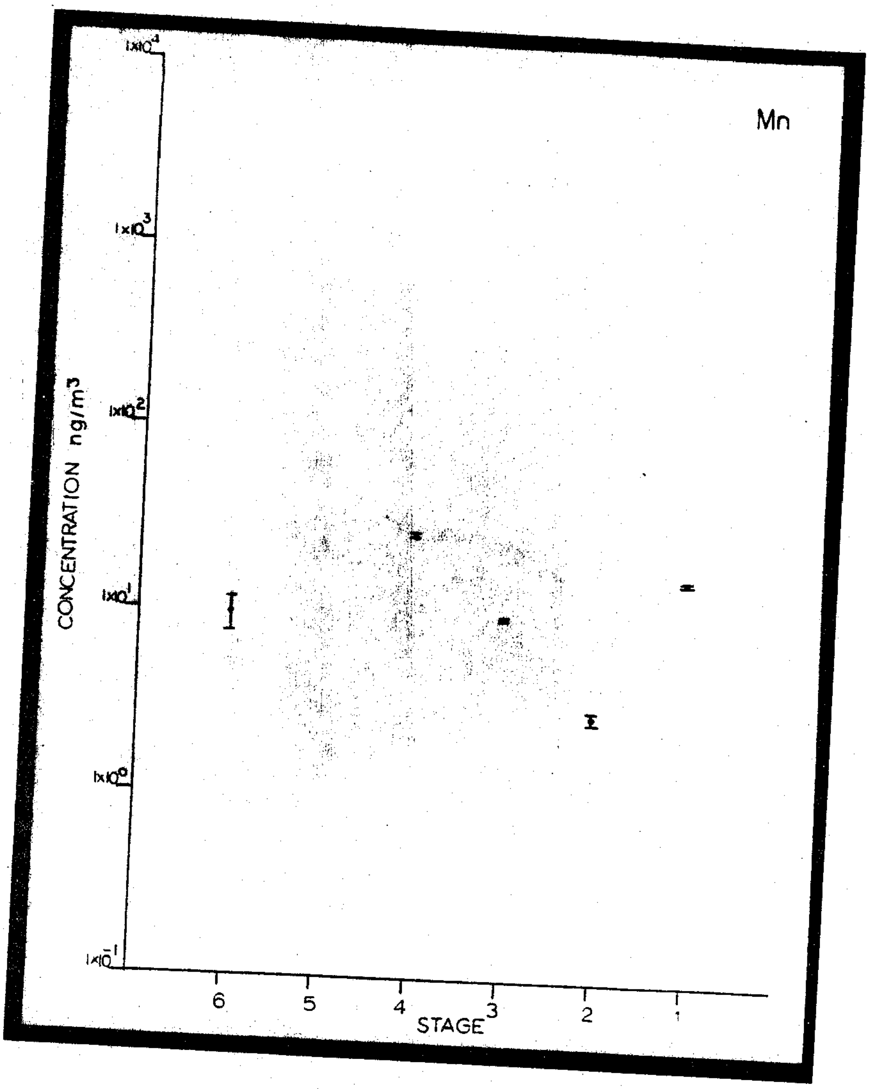

Figure 74 St. Louis Municipal Court B. Size Distribution Fe

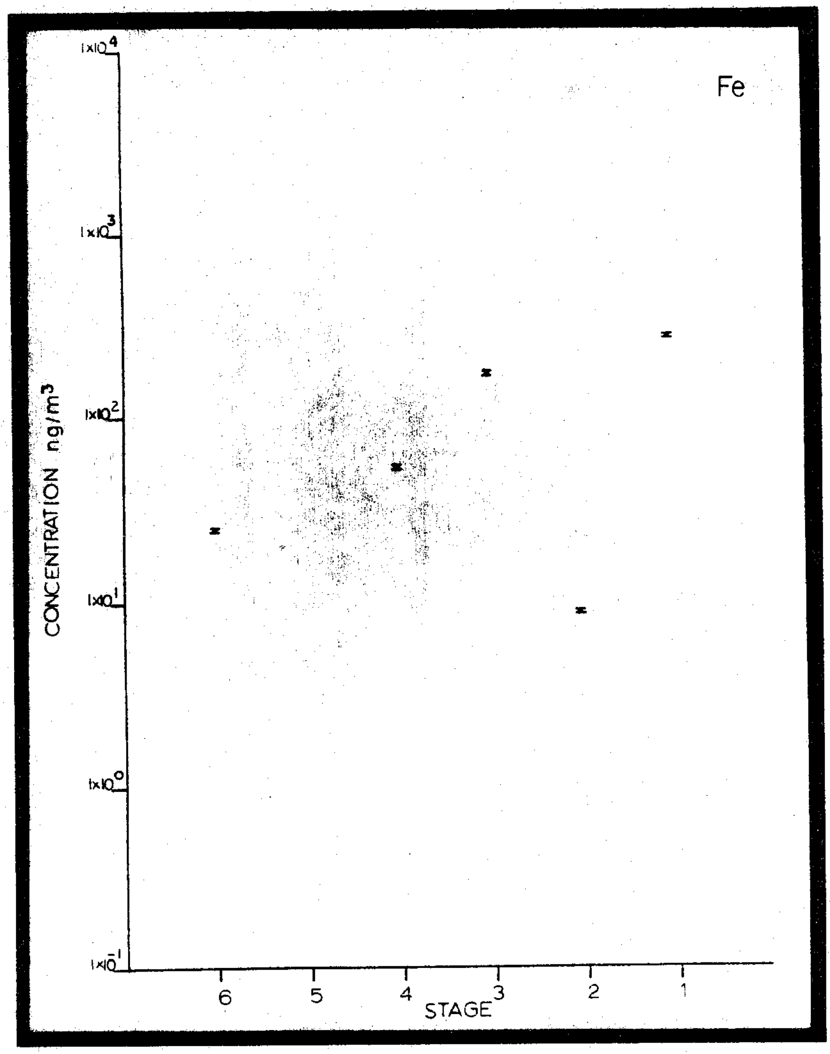

Figure 75 St. Louis Municipal Court B. Size Distribution Cu

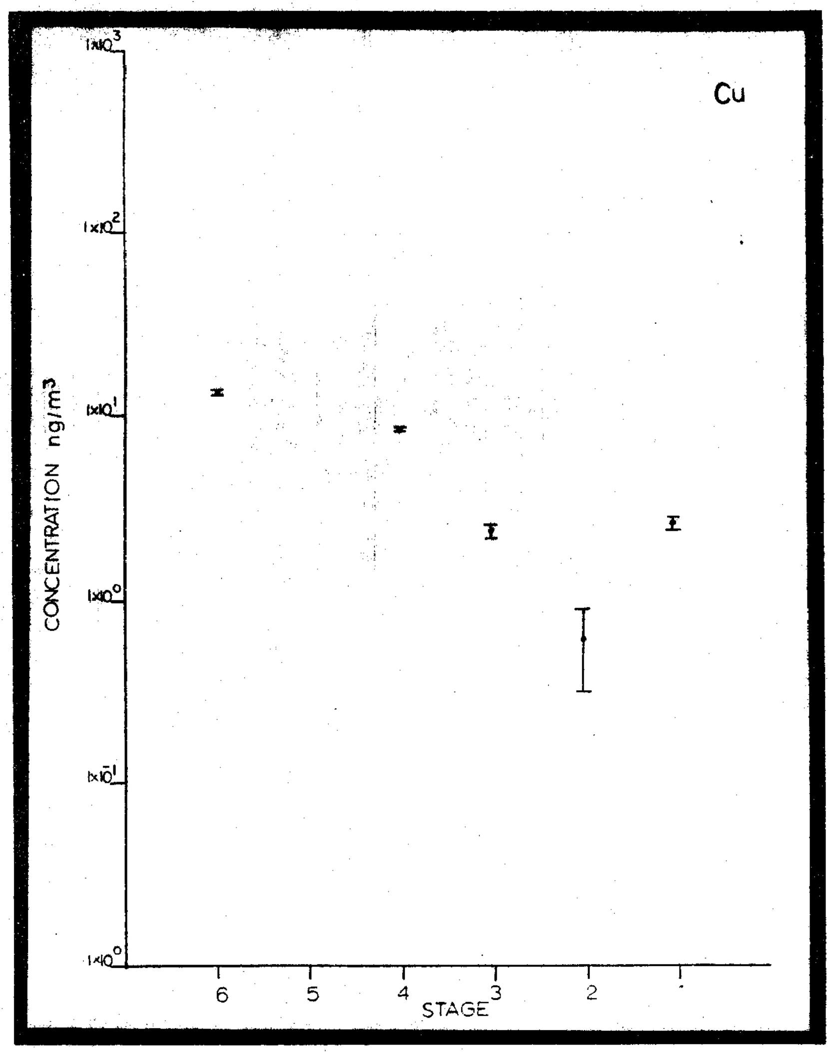

Figure 76 St. Louis Municipal Court B. Size Distribution Zn

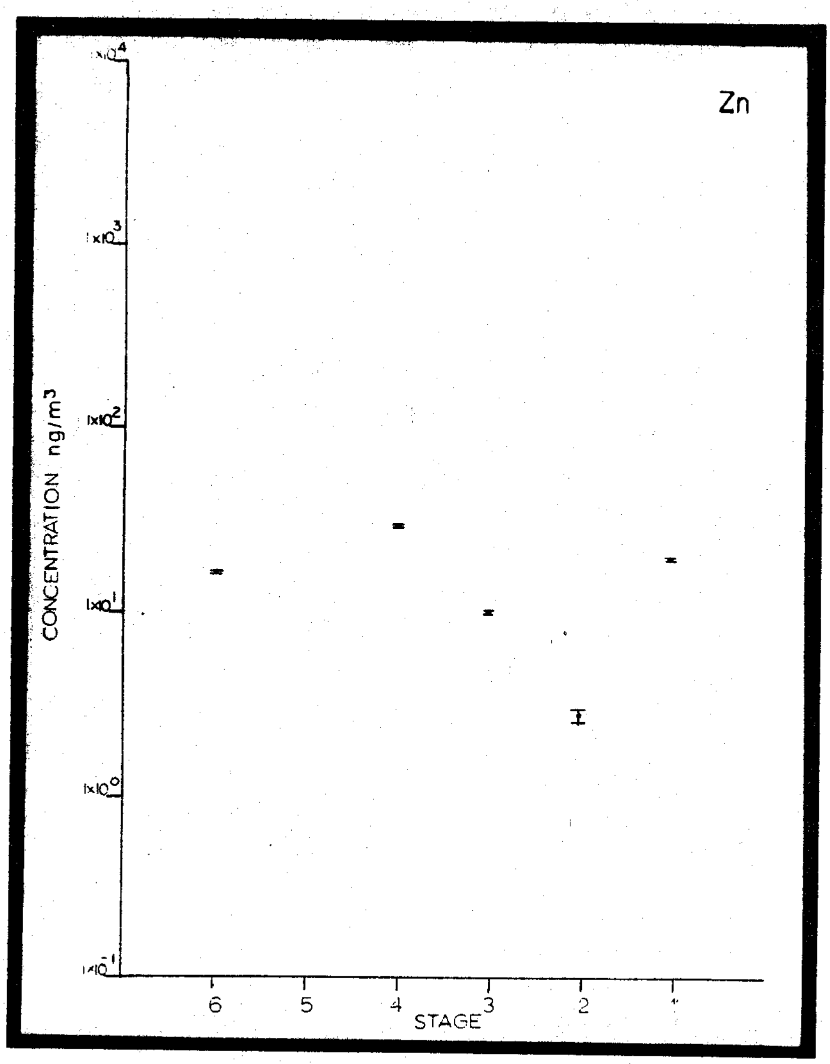

Figure 77 St. Louis Municipal Court B. Size Distribution Br

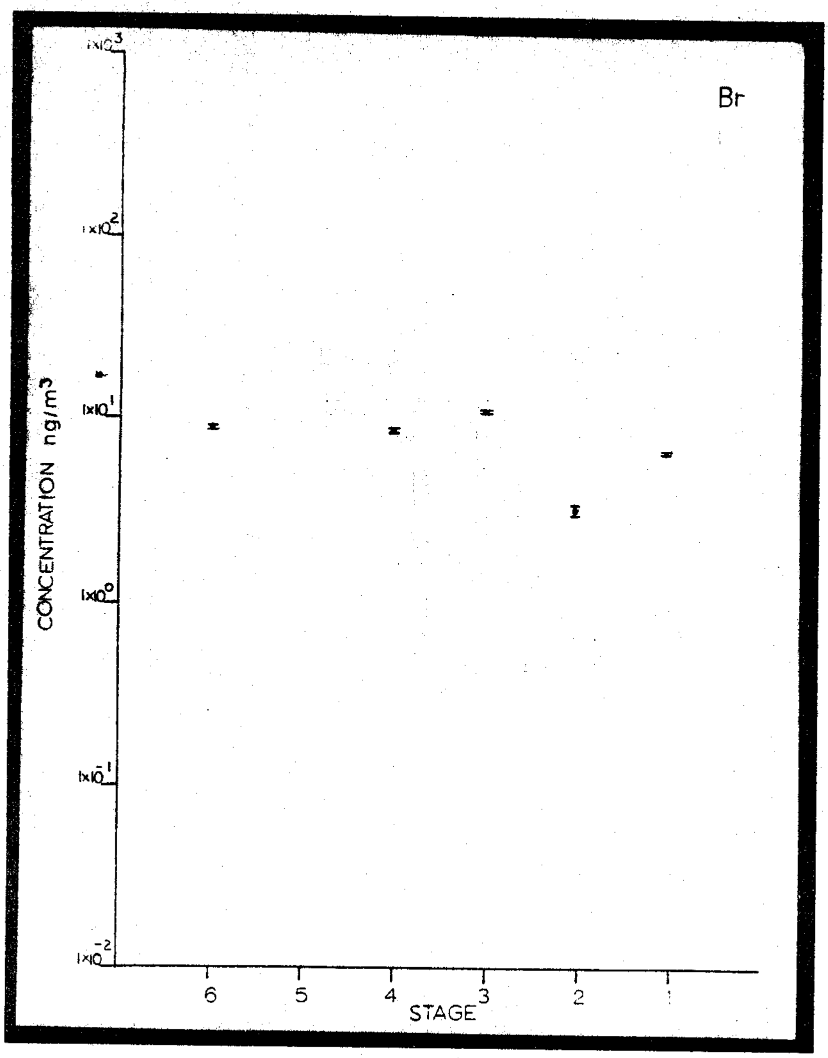

Figure 78 St. Louis Municipal Court B. Size Distribution Pb

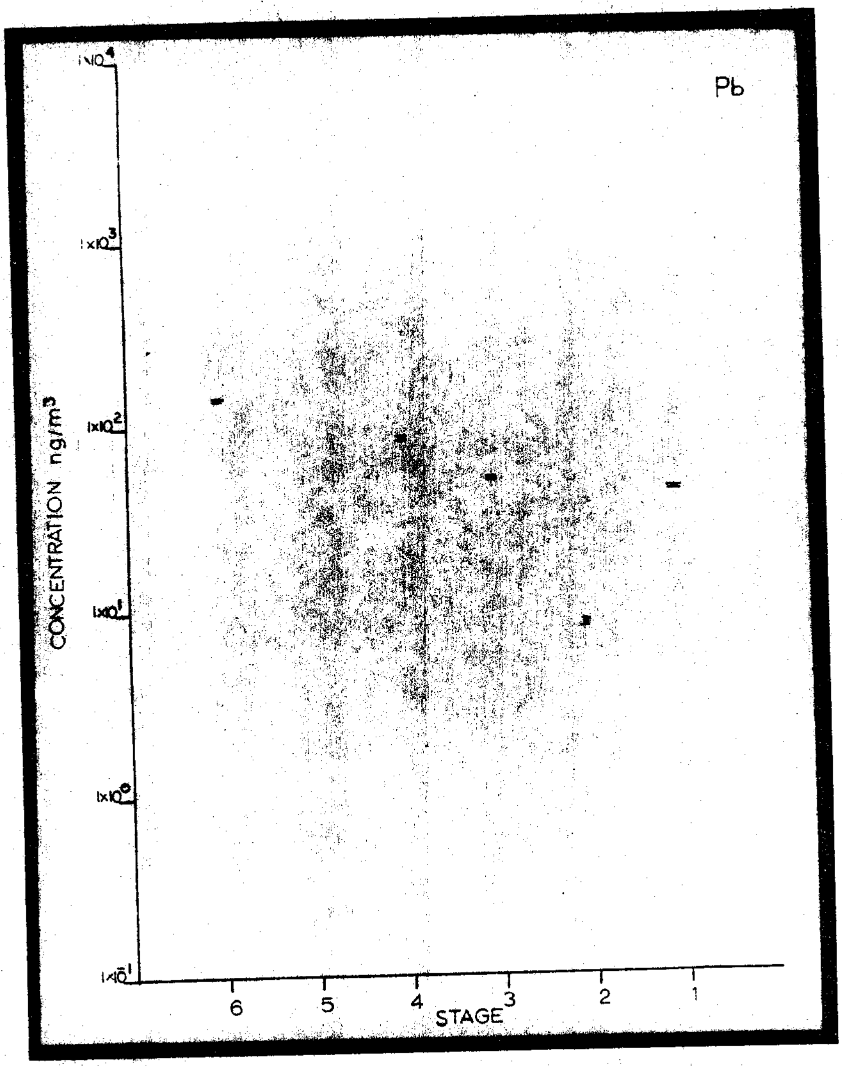

Figure 79 St. Louis Municipal Court C. Size Distribution P

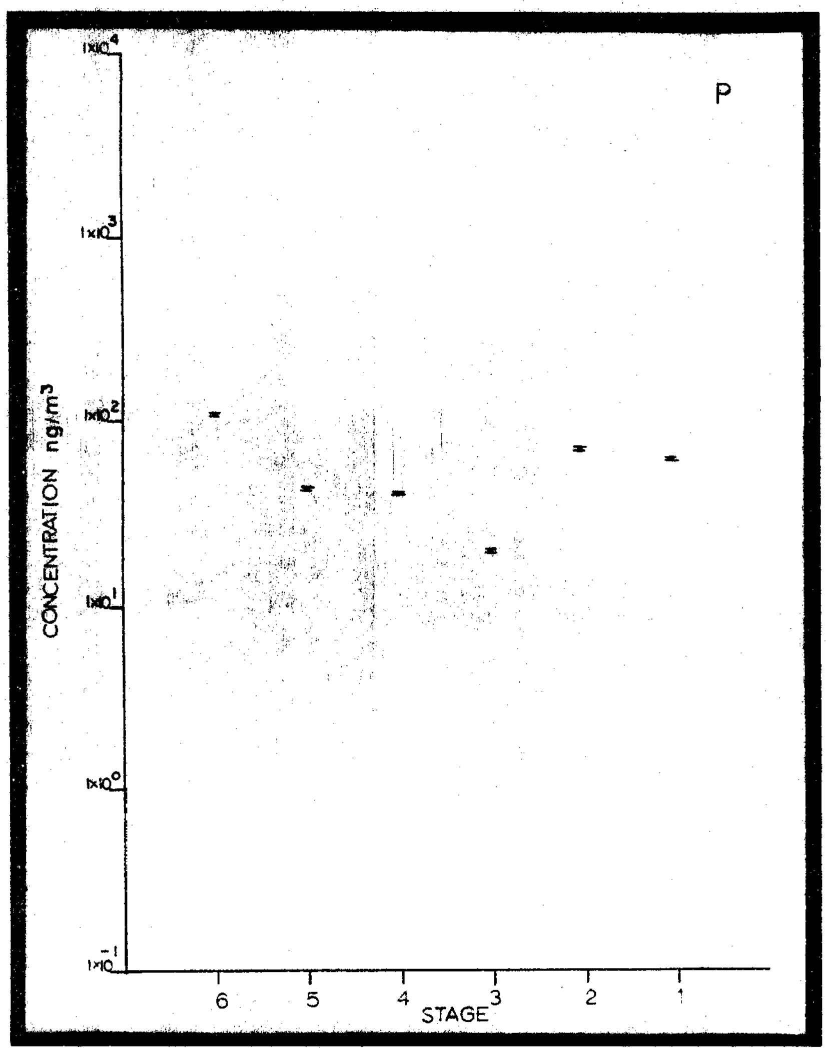

Figure 80 St. Louis Municipal Court C. Size Distribution S

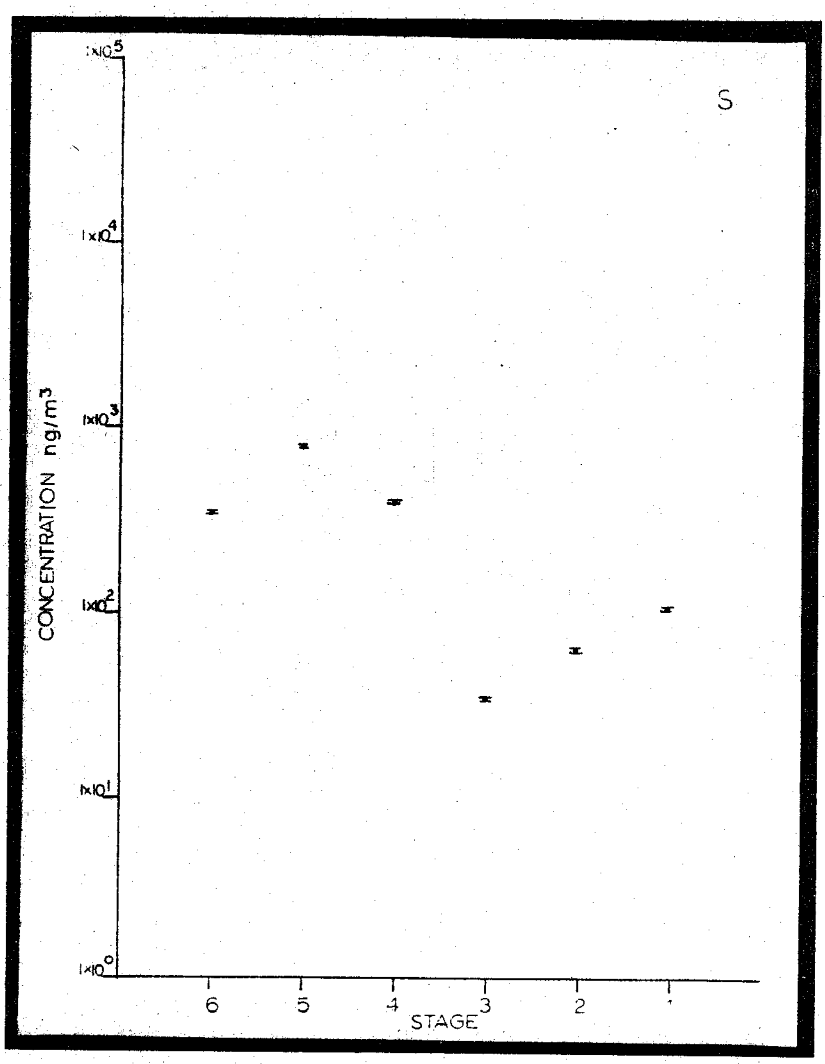

Figure 81 St. Louis Municipal Court C. Size Distribution Cl

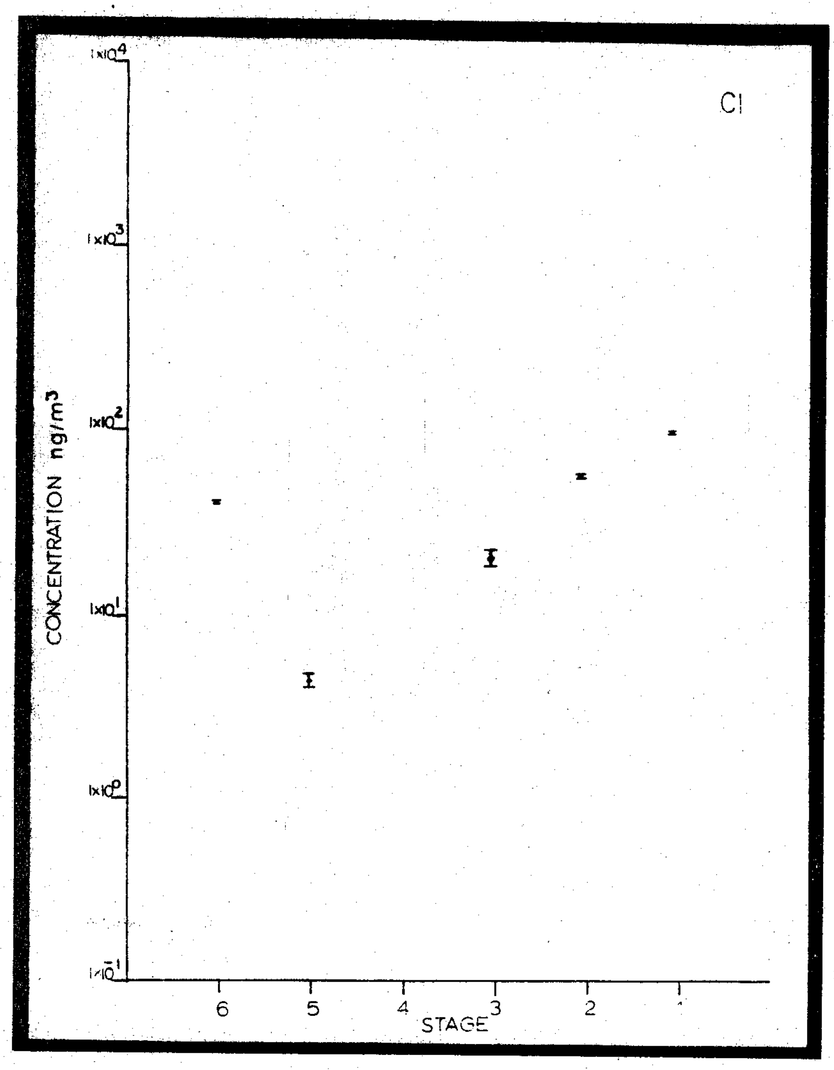

Figure 82 St. Louis Municipal Court C. Size Distribution K

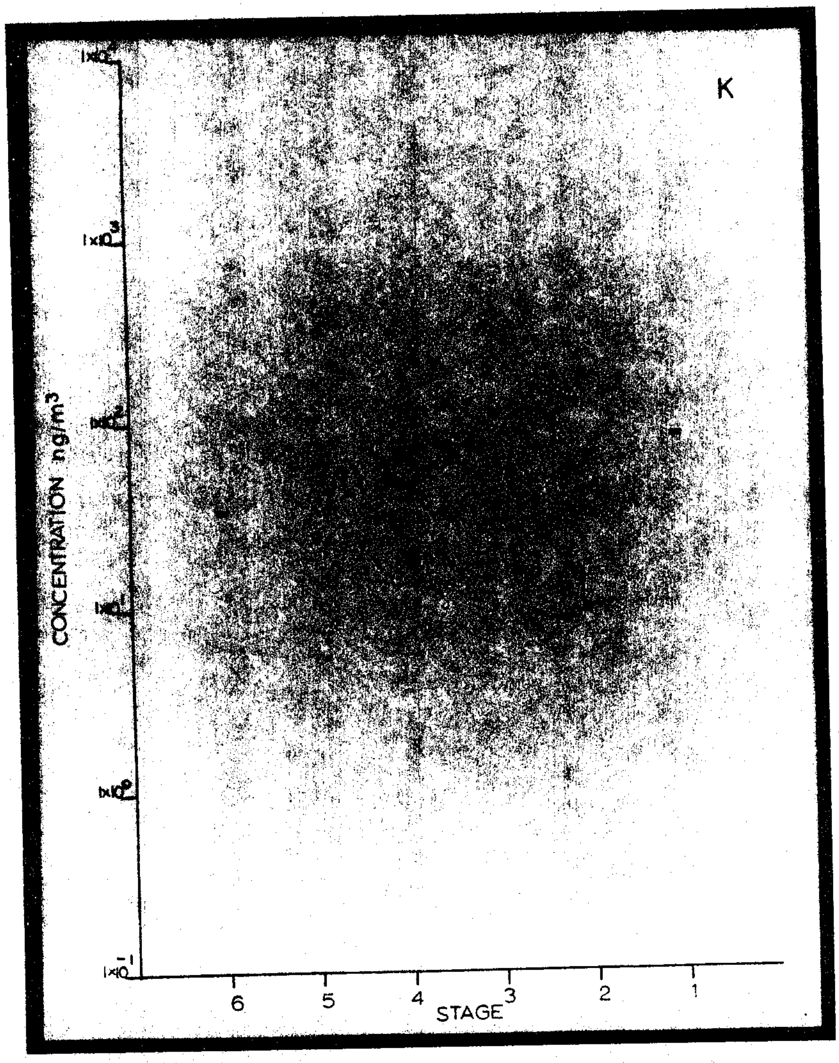

Figure 83 St. Louis Municipal Court C. Size Distribution Ca

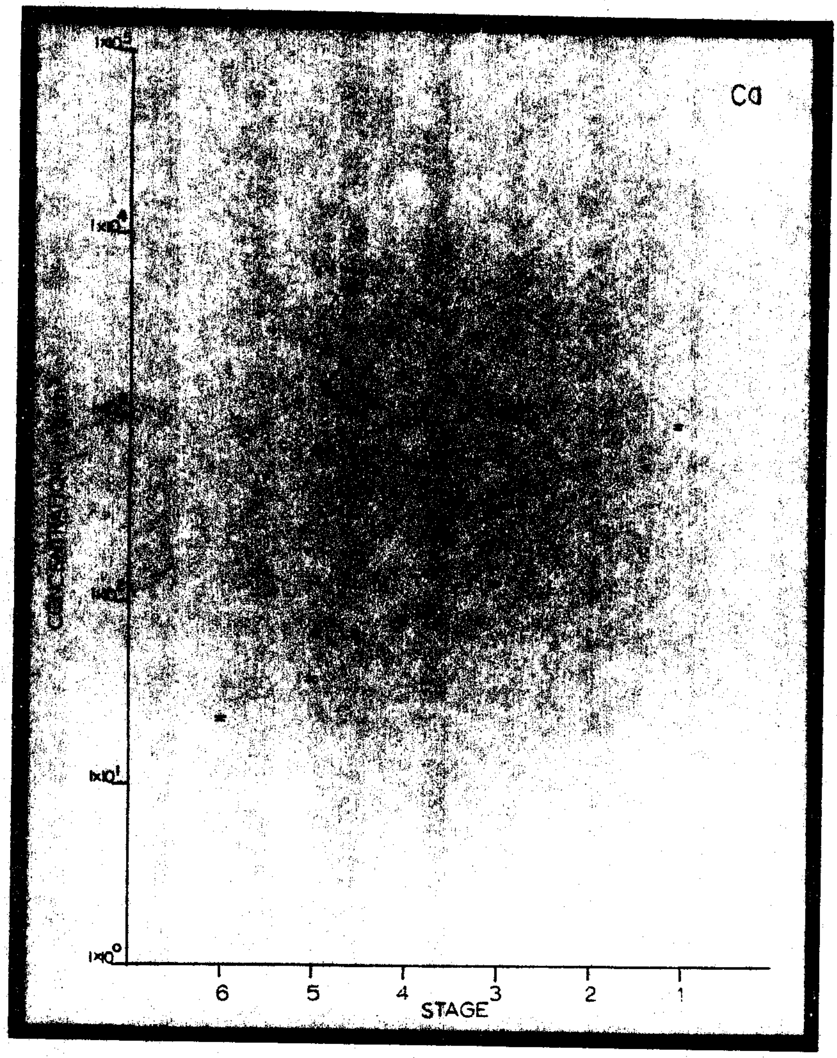

Figure 84 St. Louis Municipal Court C. Size Distribution Ti

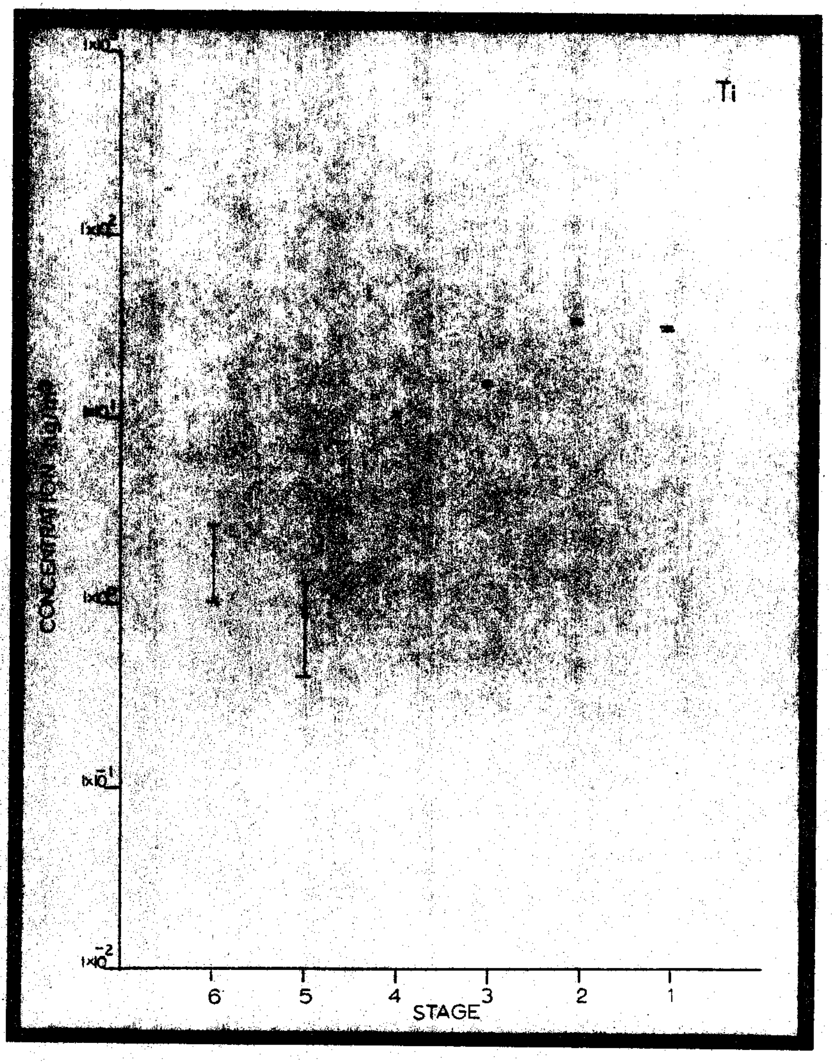

Figure 85 St. Louis Municipal Court C. Size Distribution V

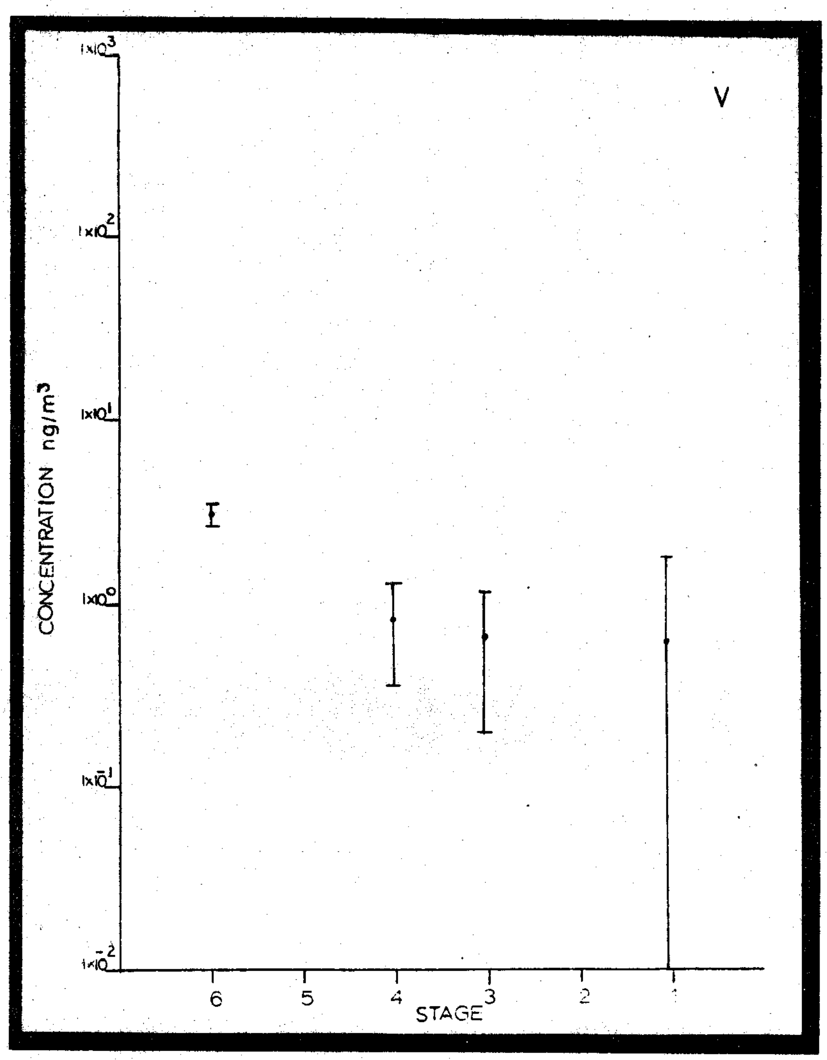

Figure 86 St. Louis Municipal Court C. Size Distribution Mn

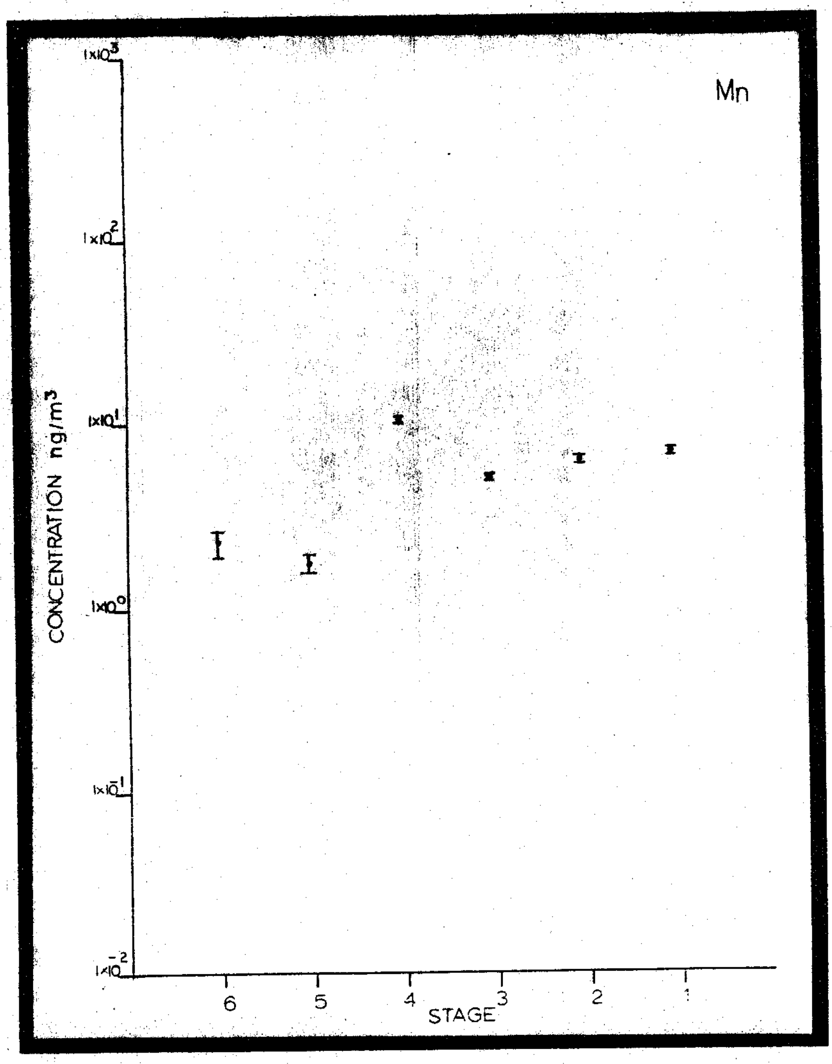

Figure 87 St. Louis Municipal Court C. Size Distribution Fe

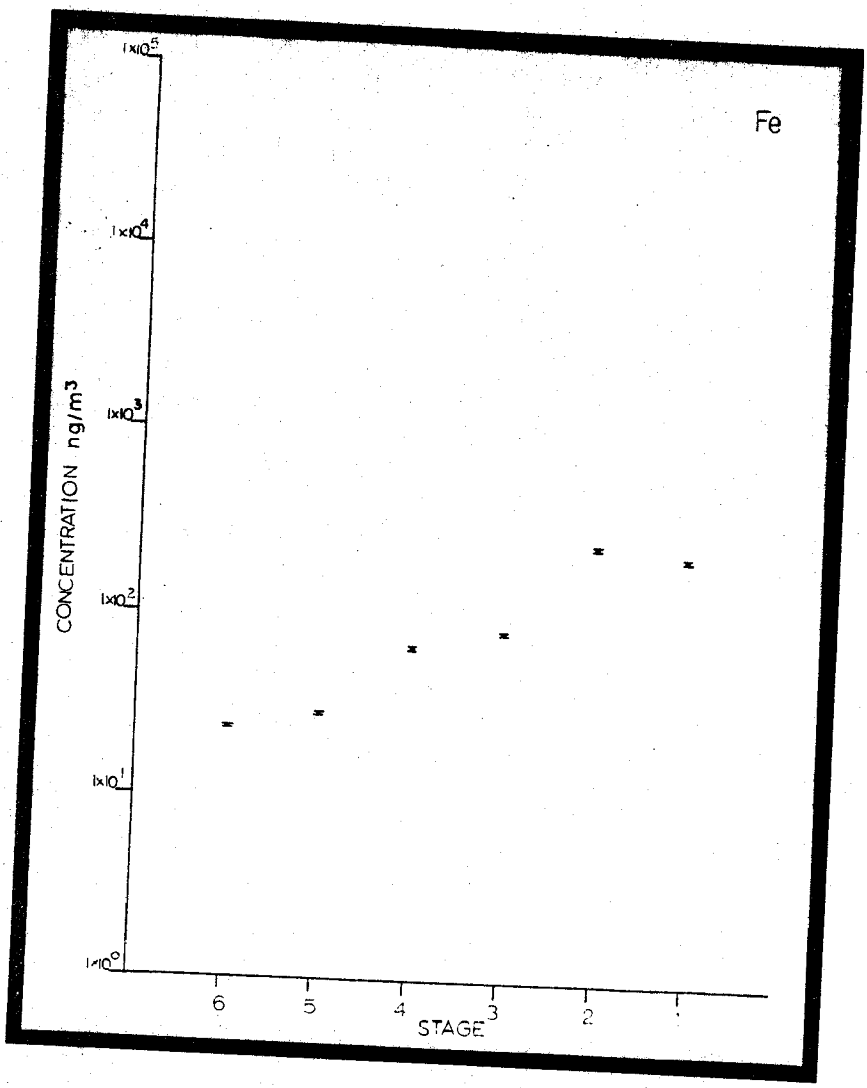

Figure 88 St. Louis Municipal Court C. Size Distribution Cu

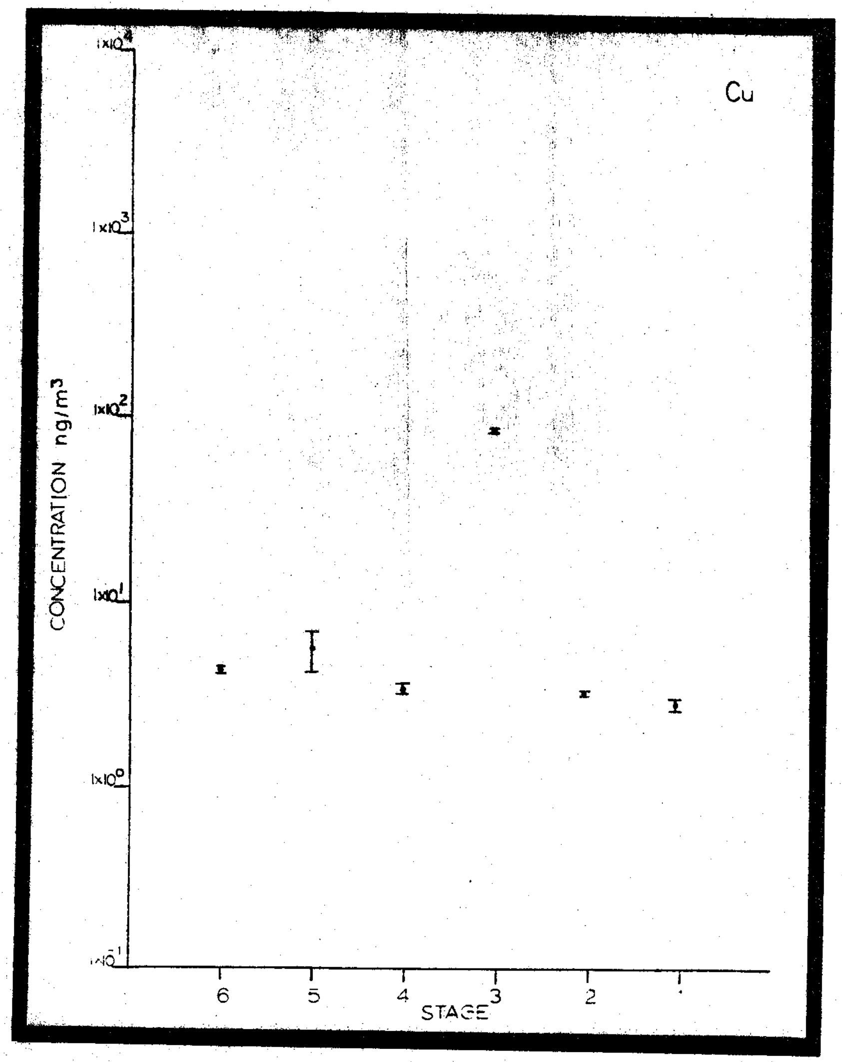

Figure 89 St. Louis Municipal Court C. Size Distribution Zn

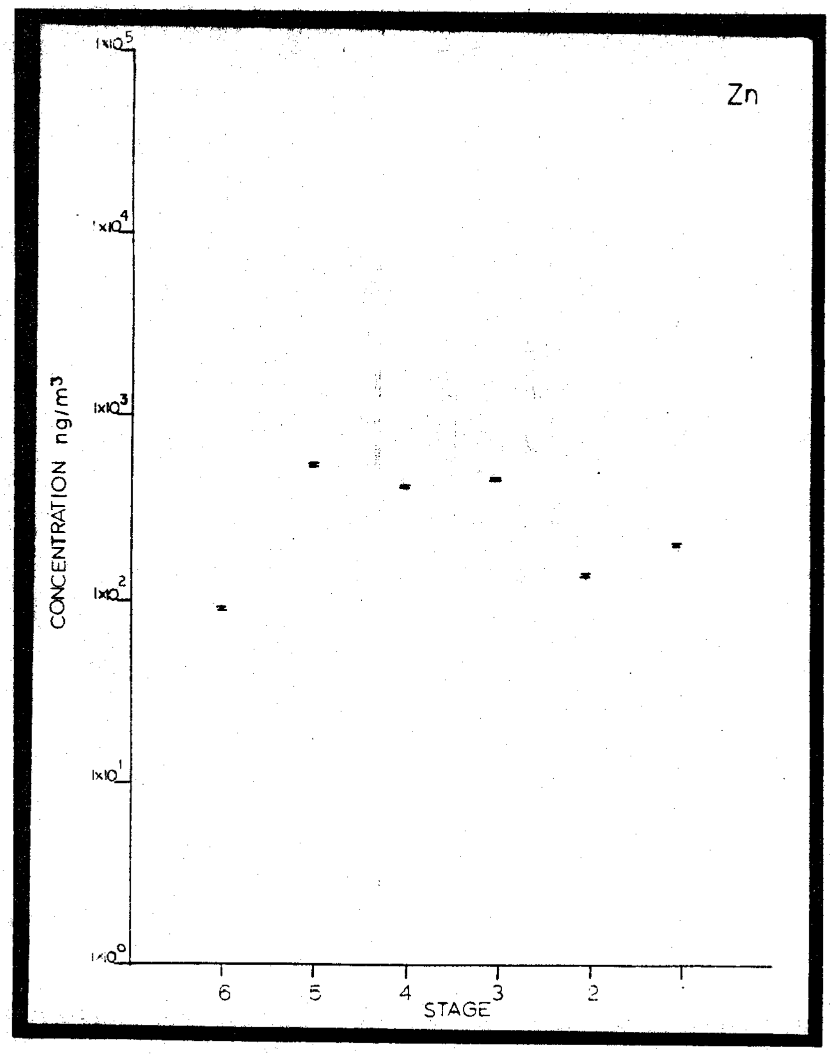

Figure 90 St. Louis Municipal Court C. Size Distribution Br

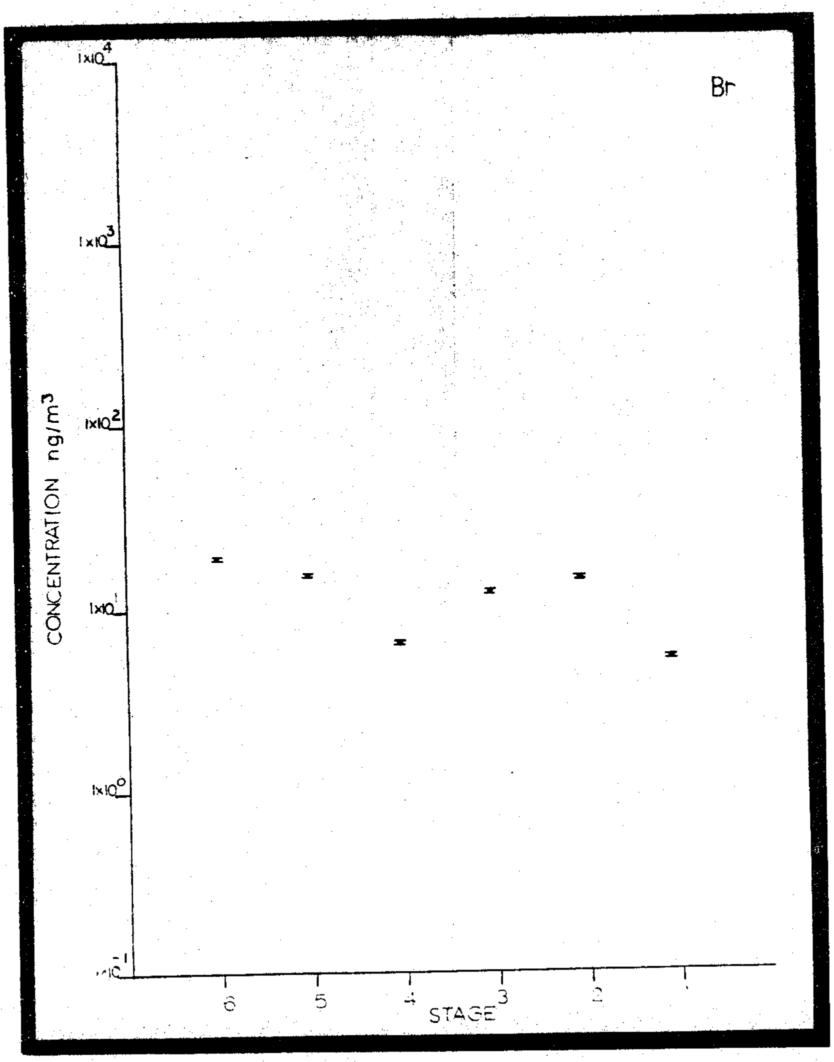

Figure 91 St. Louis Municipal Court C. Size Distribution Pb

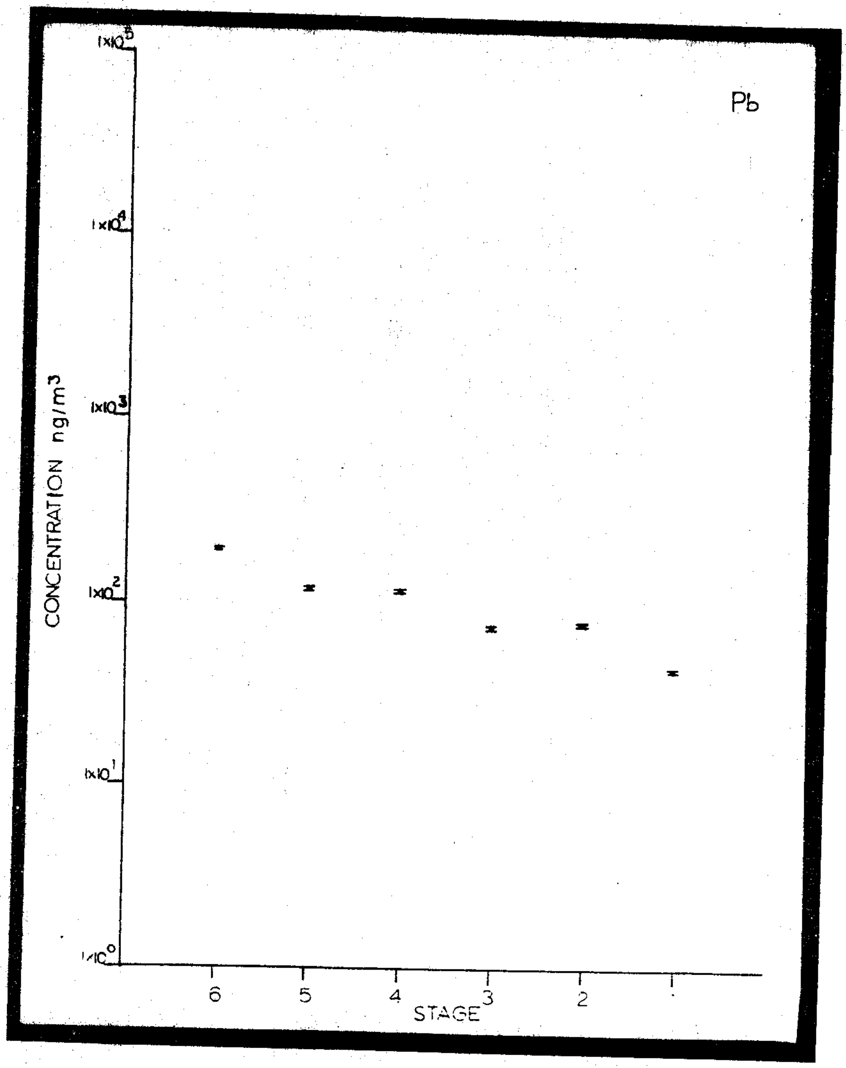

Figure 92 Time Distribution Data Cl

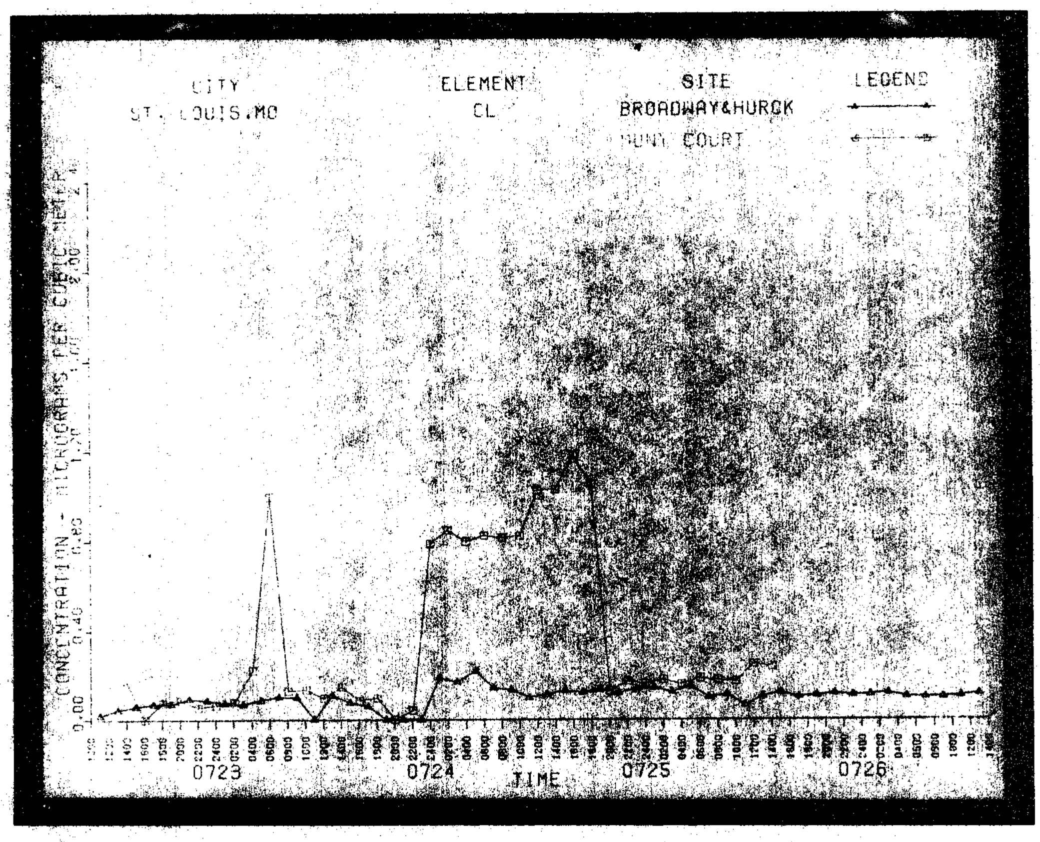

Figure 93 Time Distribution Data K

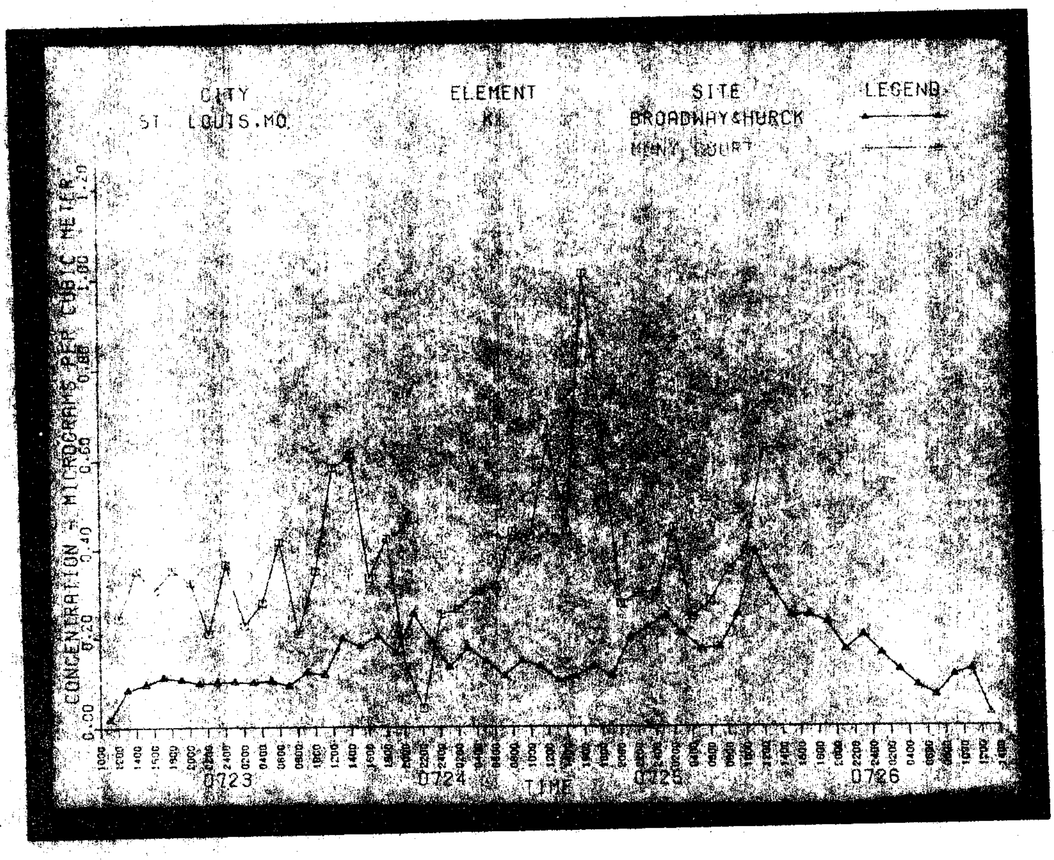

Figure 94 Time Distribution Data Ca

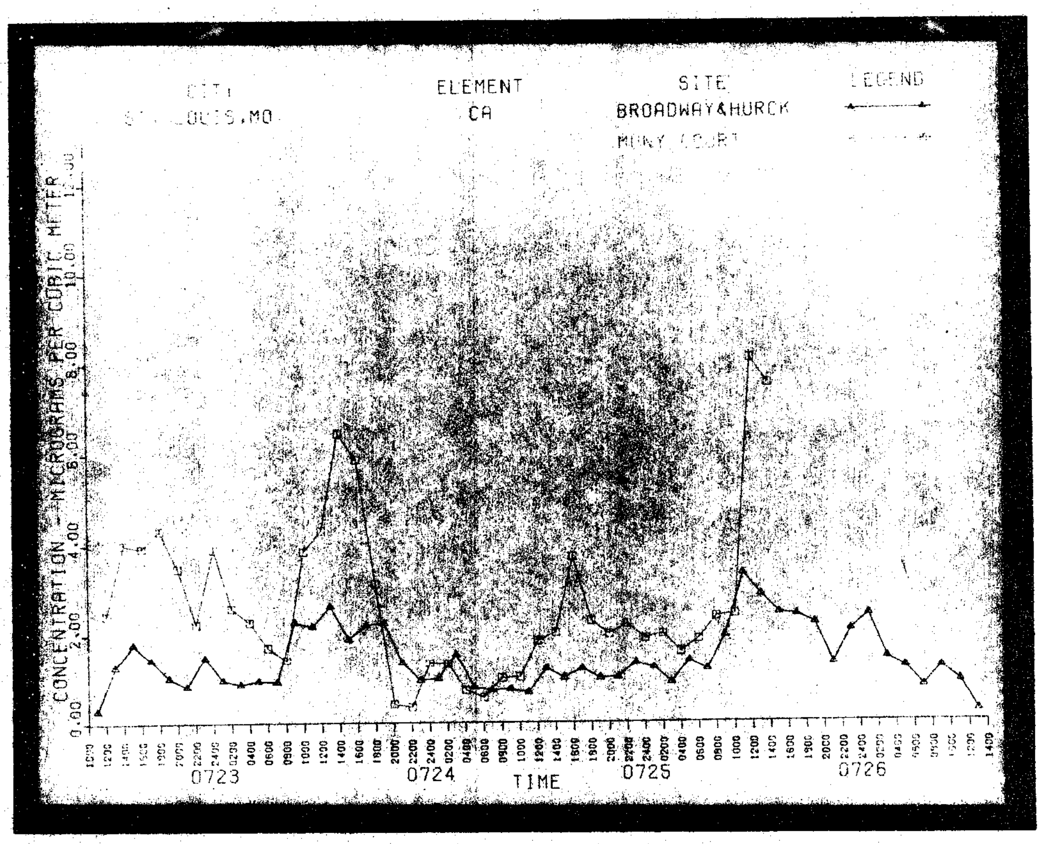

Figure 95 Time Distribution Data Ti

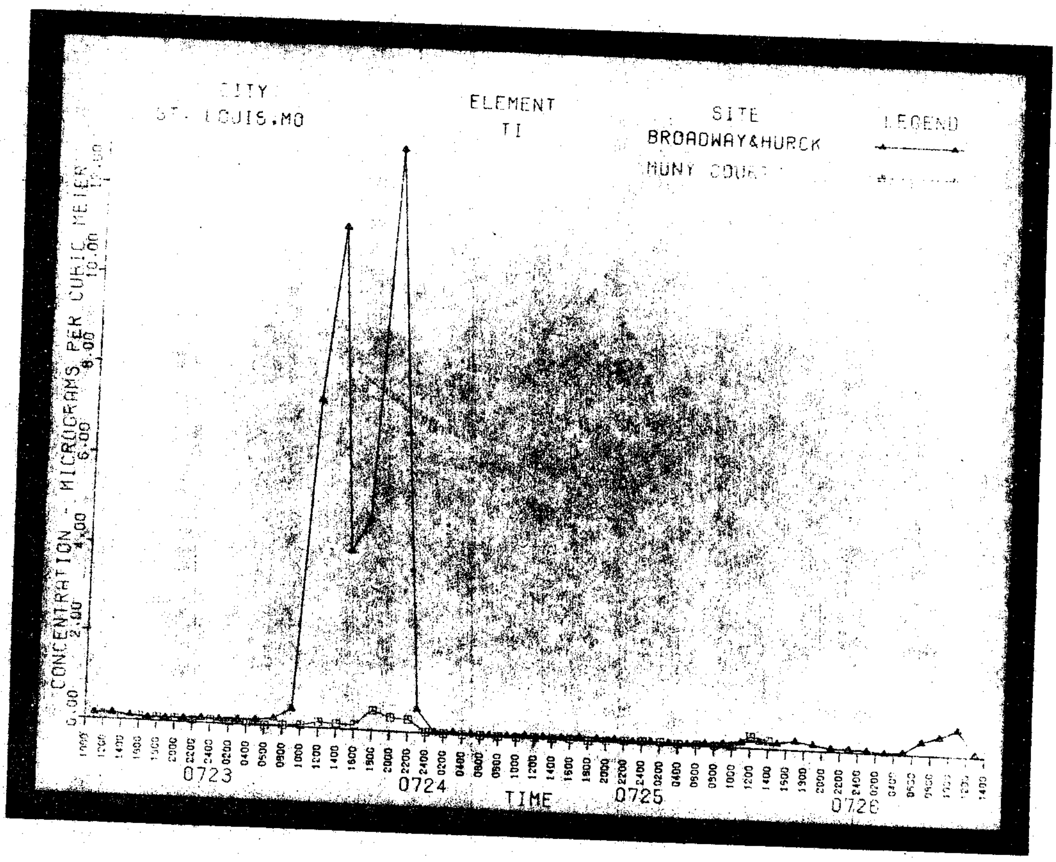

Figure 96 Time Distribution Data V

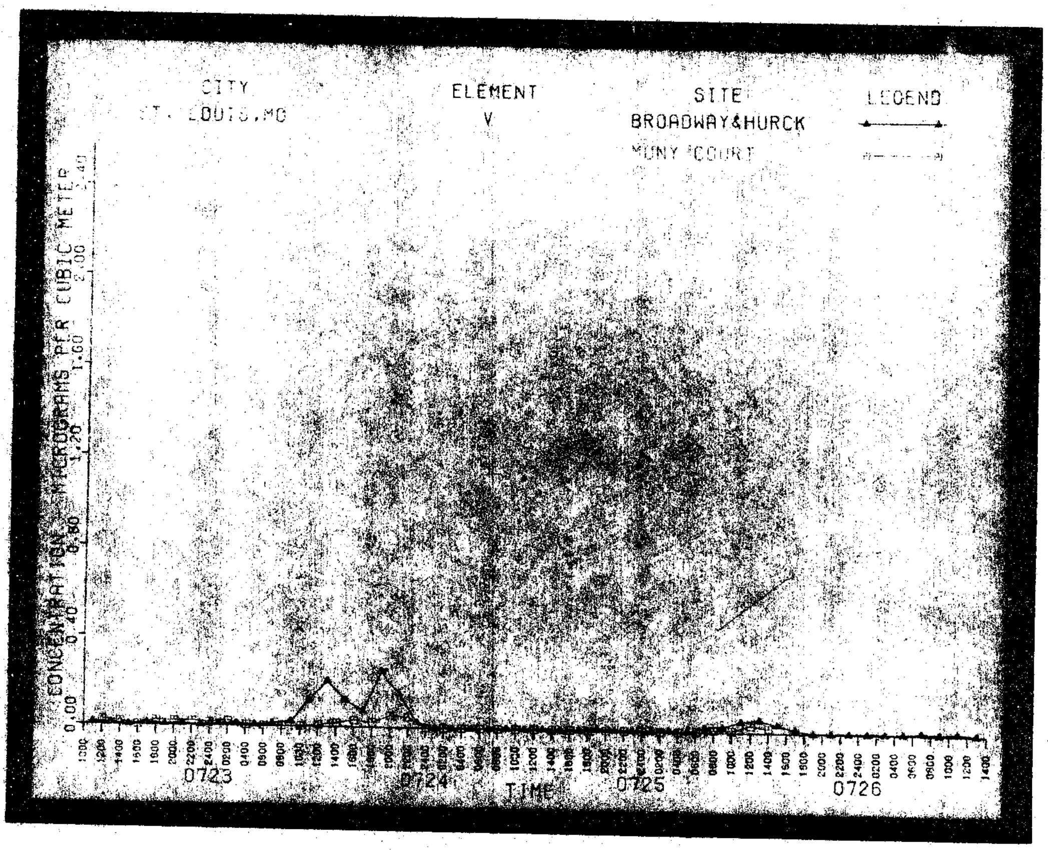

Figure 97 Time Distribution Data CR

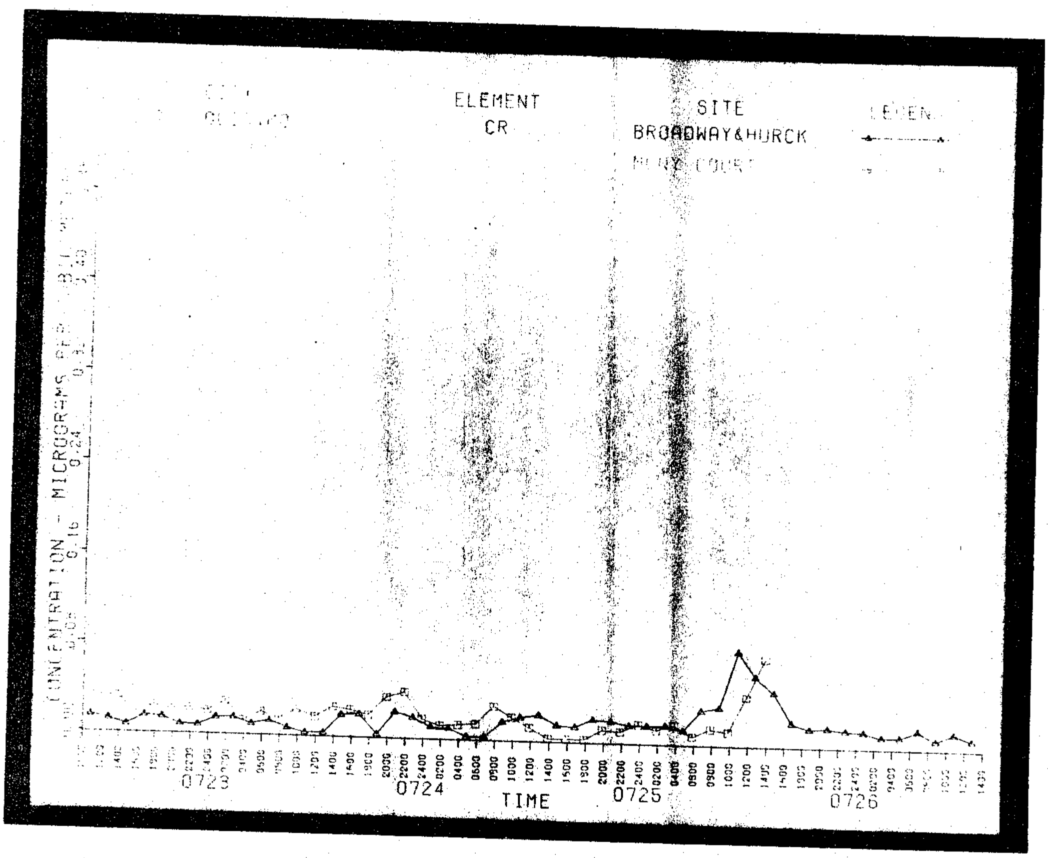

Figure 98 Time Distribution Data Mn

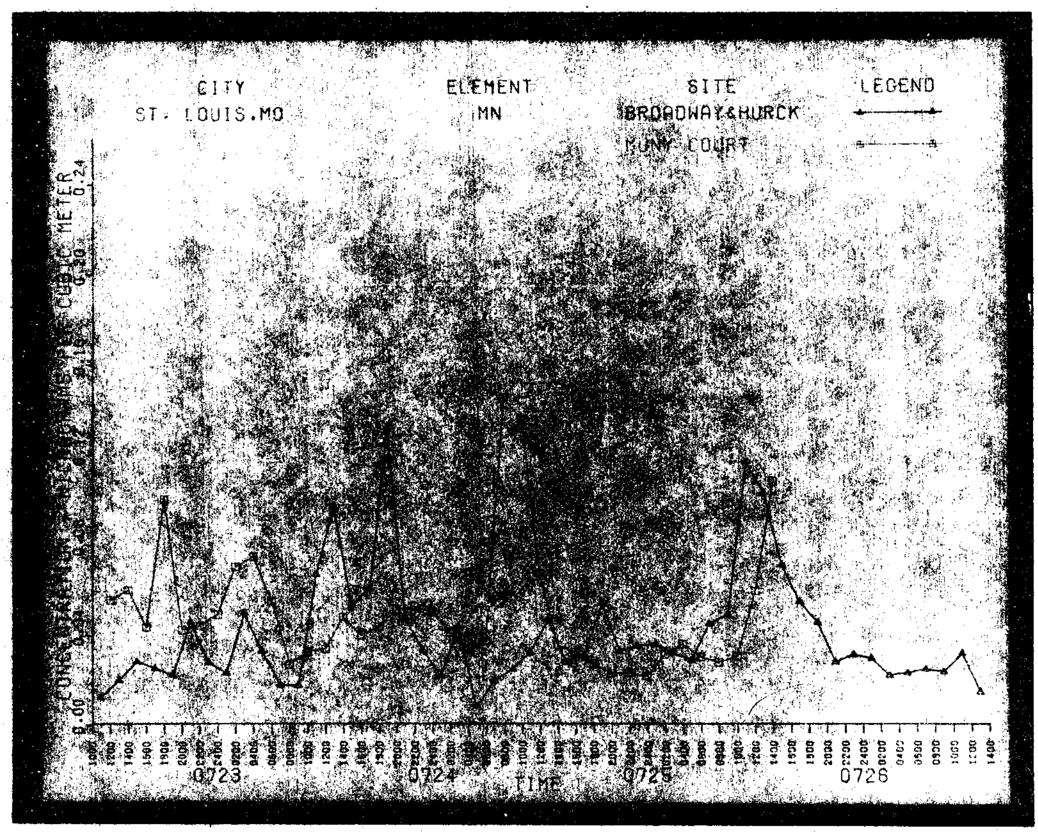

Figure 99 Time Distribution Data Fe

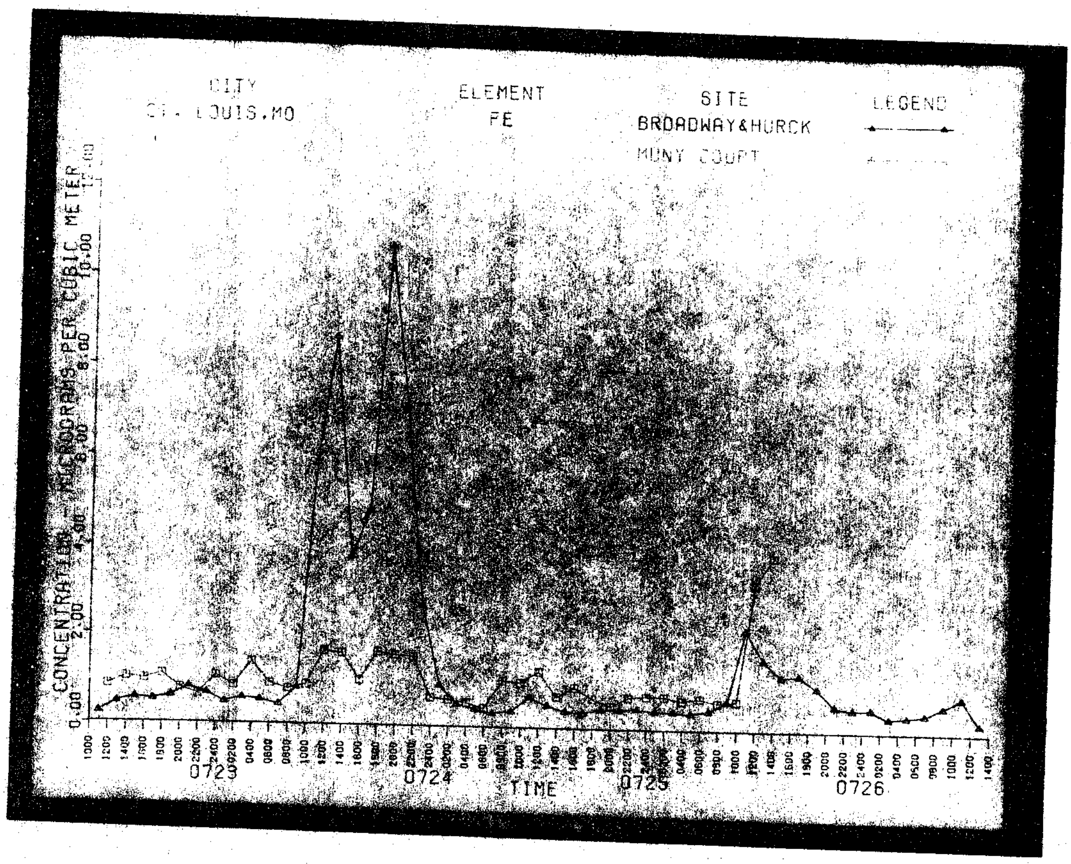

Figure 100 Time Distribution Data Ni

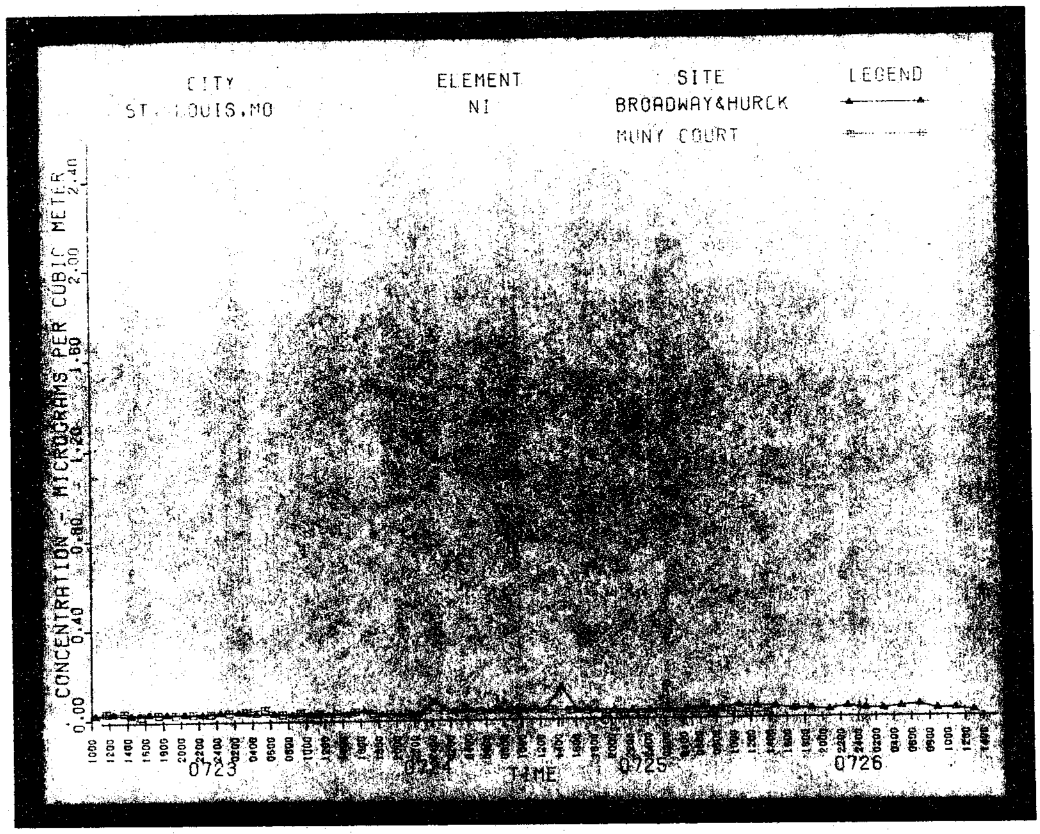

Figure 101   Time Distribution Data   Cu

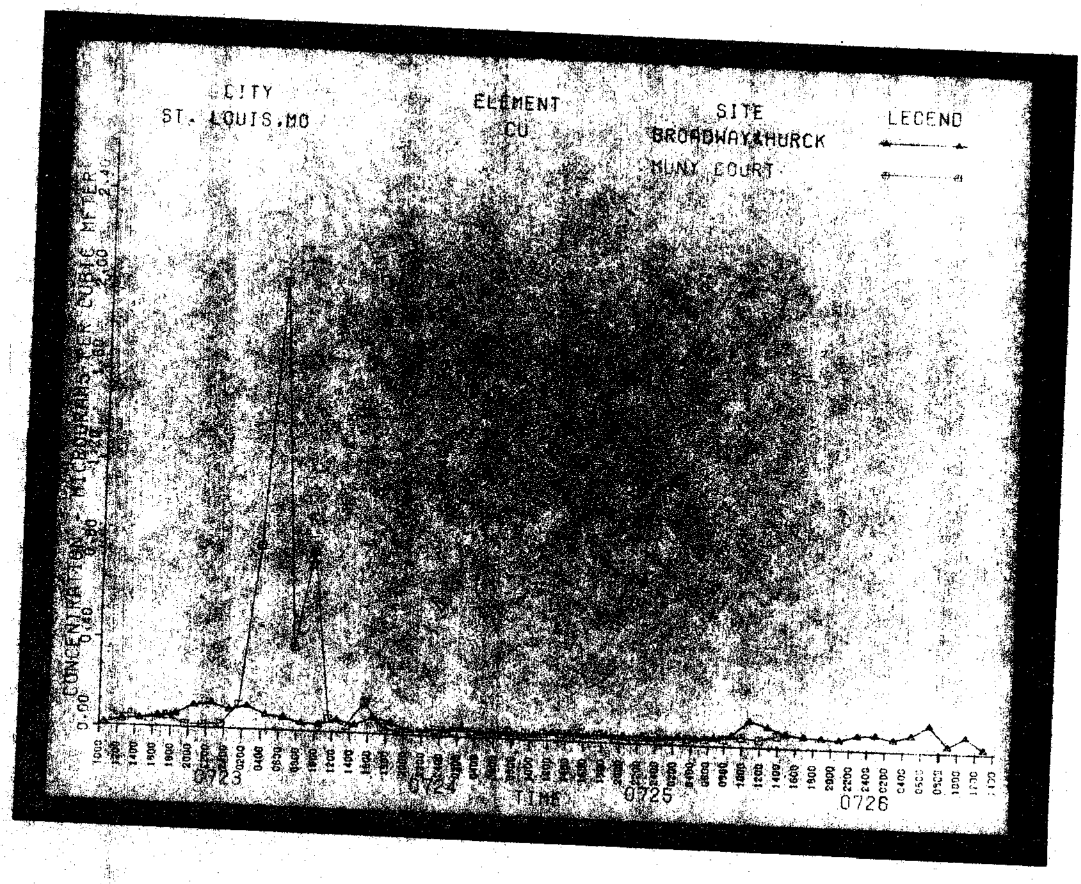

Figure 102 Time Distribution Data Zn

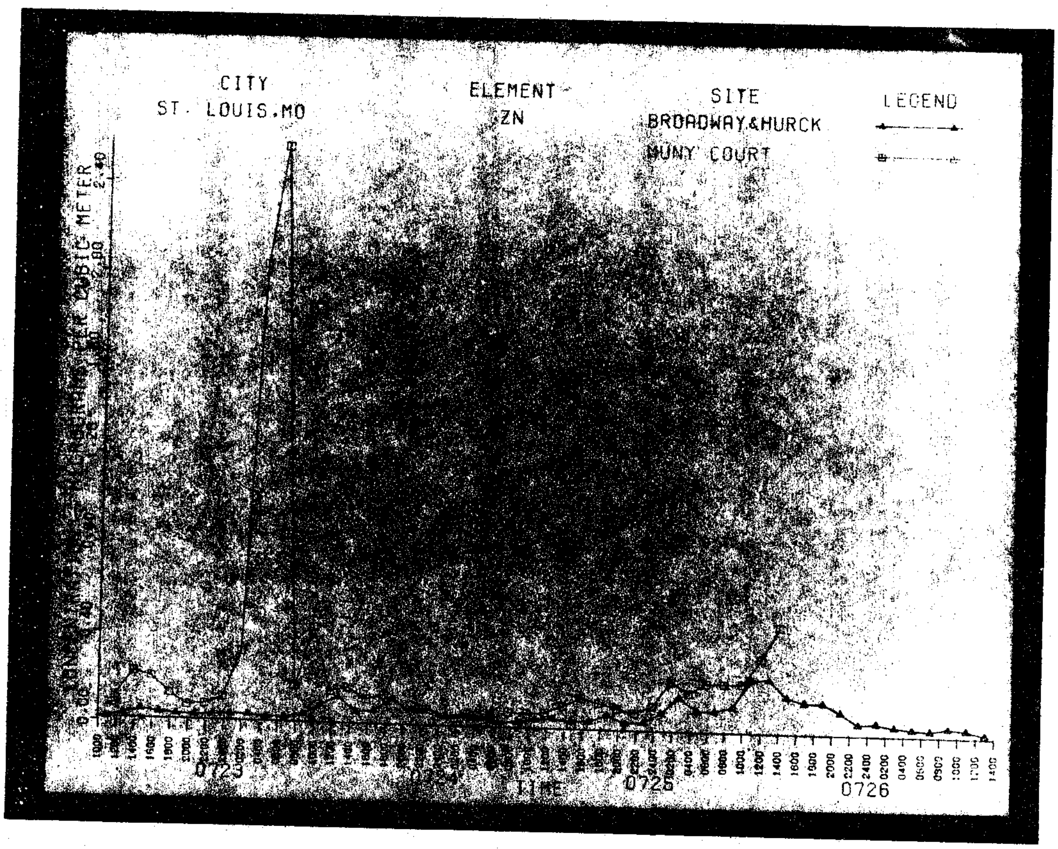

Figure 103 Time Distribution Data Br

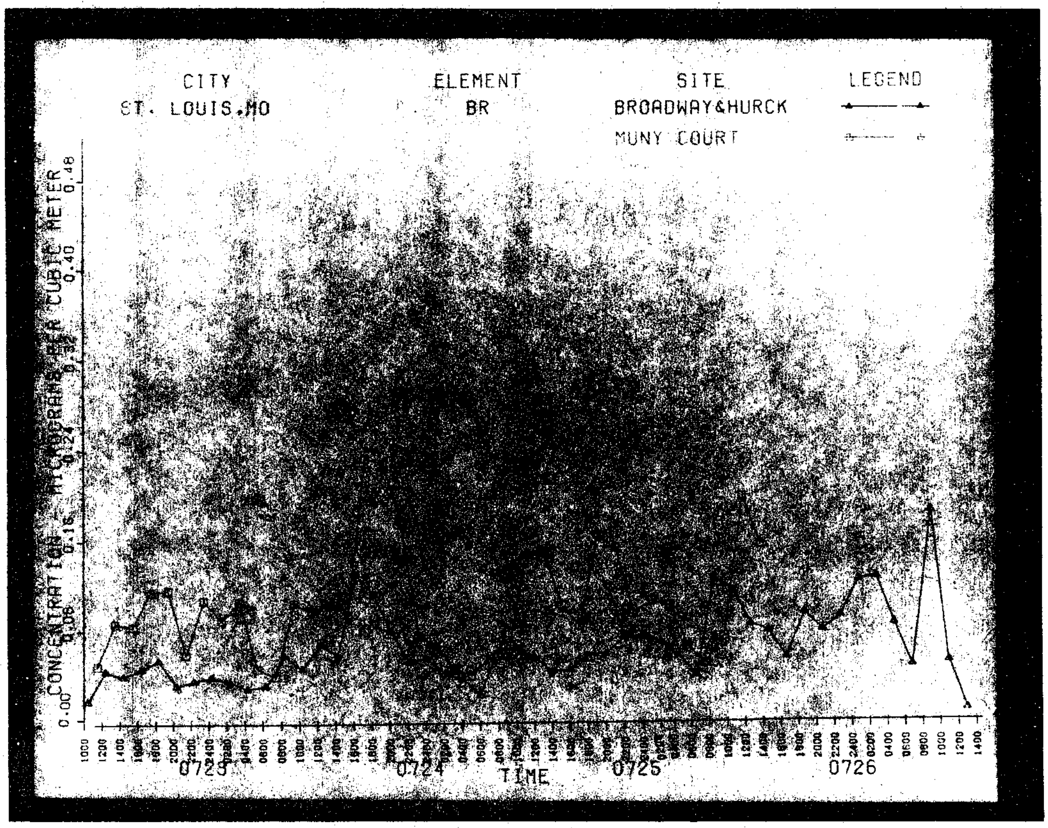

Figure 104 Time Distribution Data Pb

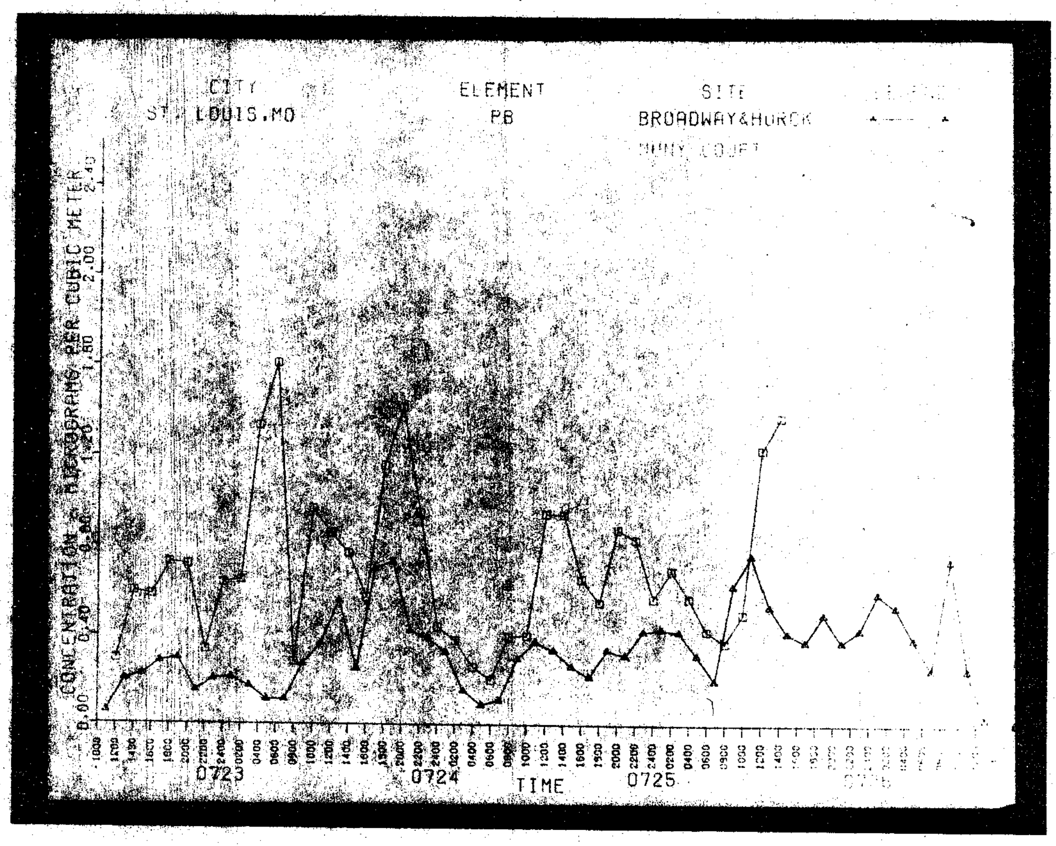

Figure 105 St. Louis Municipal Court. Directional Distribution P

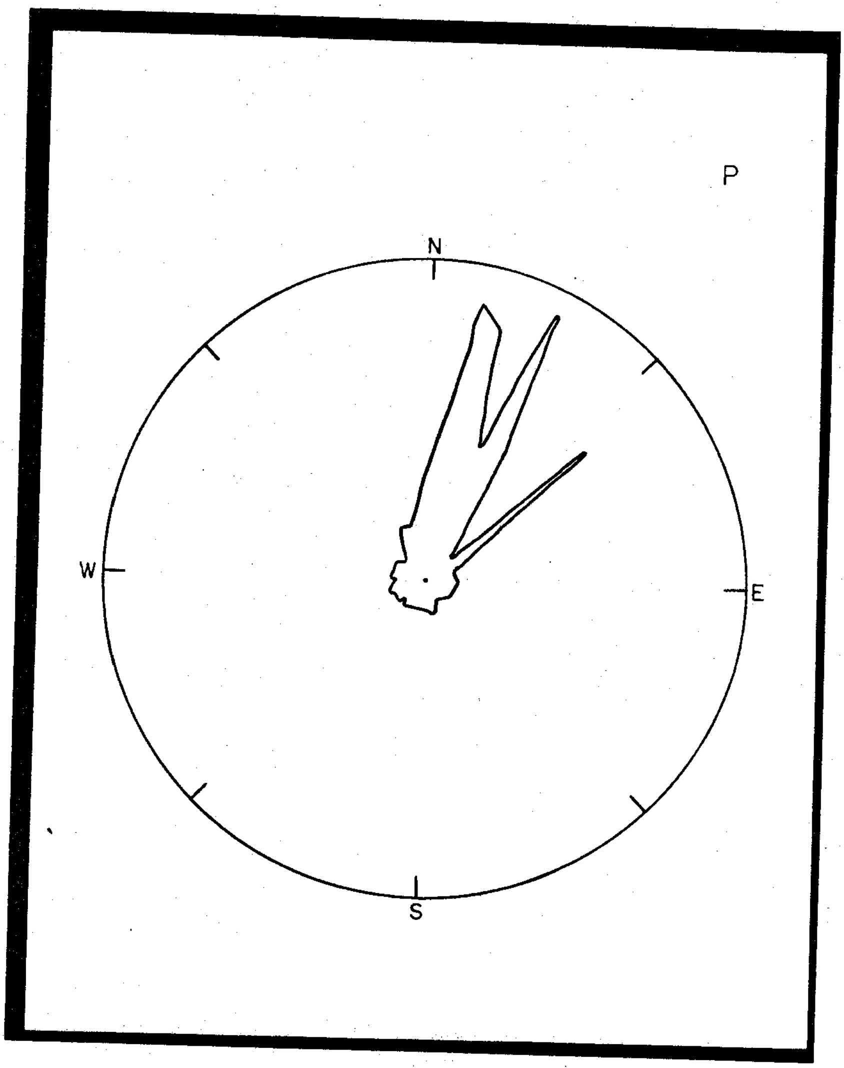

Figure 106 St. Louis Municipal Court. Directional Distribution S

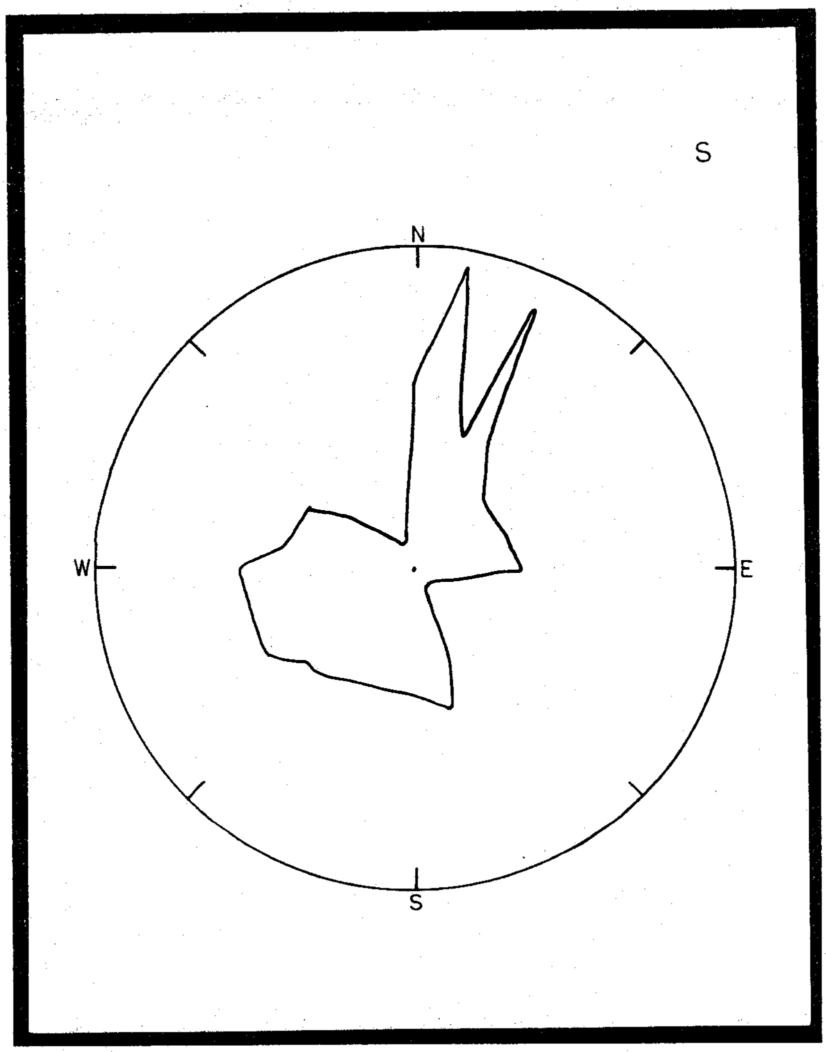

Figure 107 St. Louis Municipal Court. Directional Distribution Cl

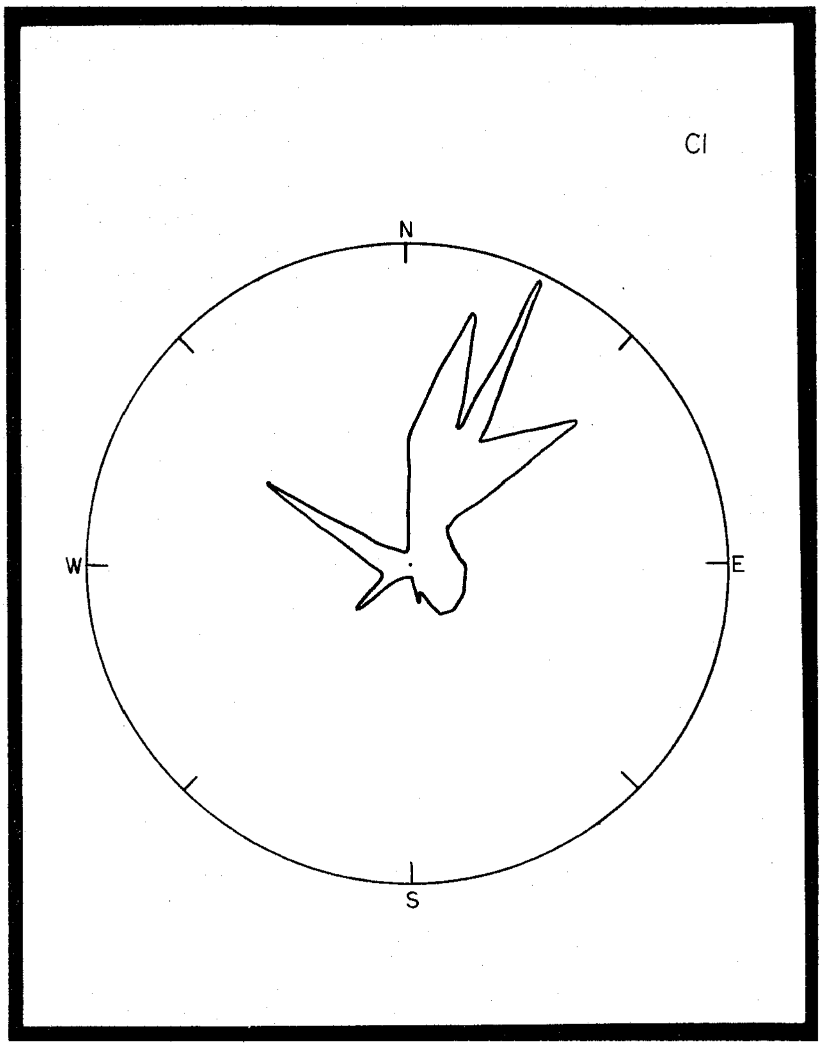

Figure 108 St. Louis Municipal Court. Directional Distribution K

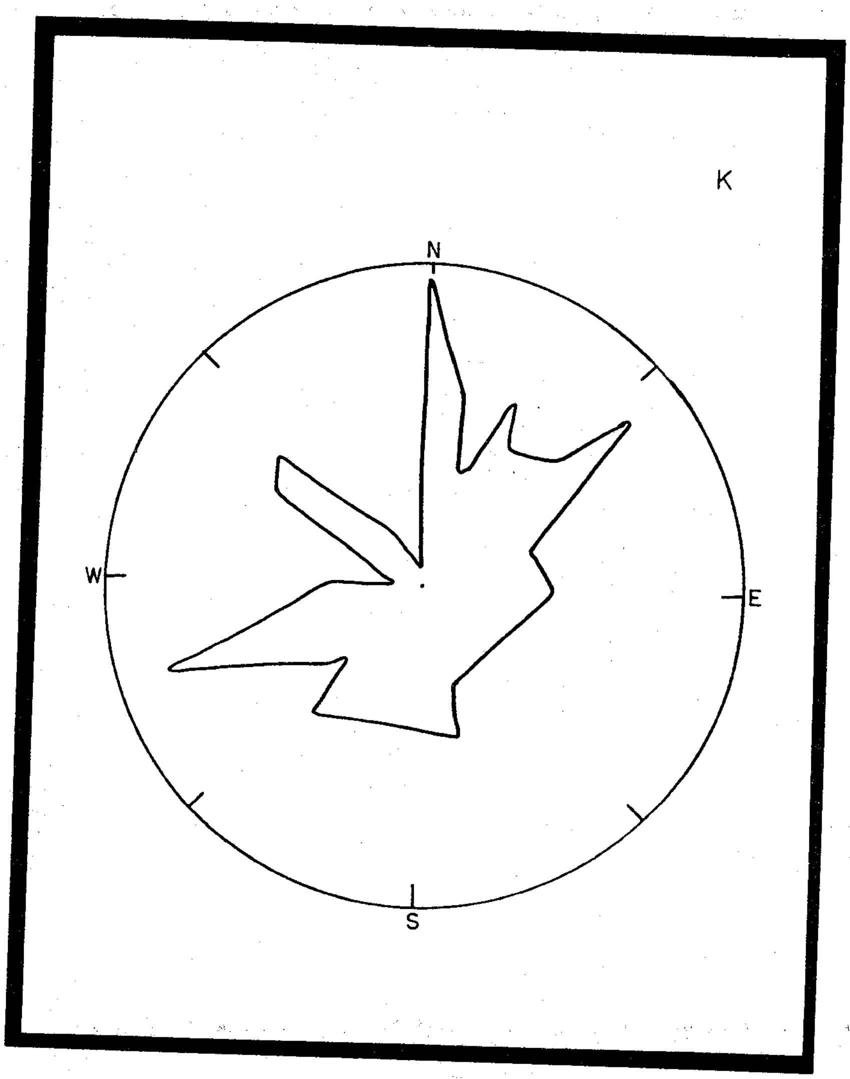

Figure 109 St. Louis Municipal Court. Directional Distribution Ca

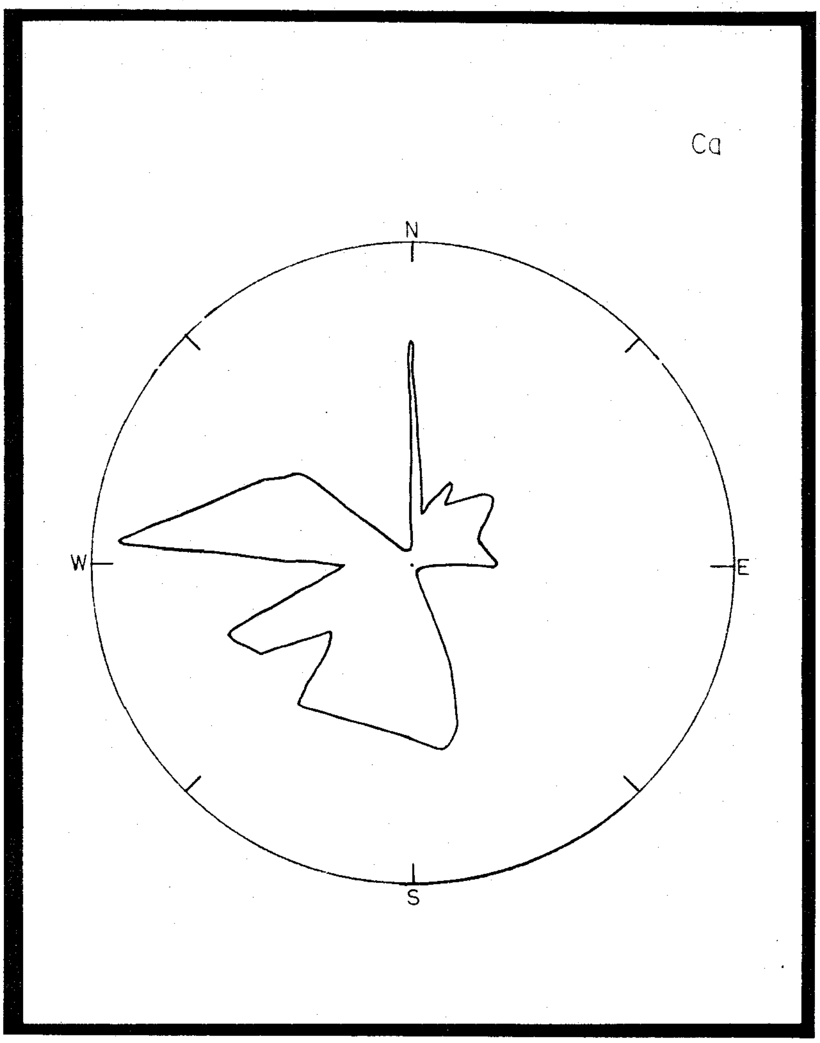

Figure 110 St. Louis Municipal Court. Directional Distribution Ti

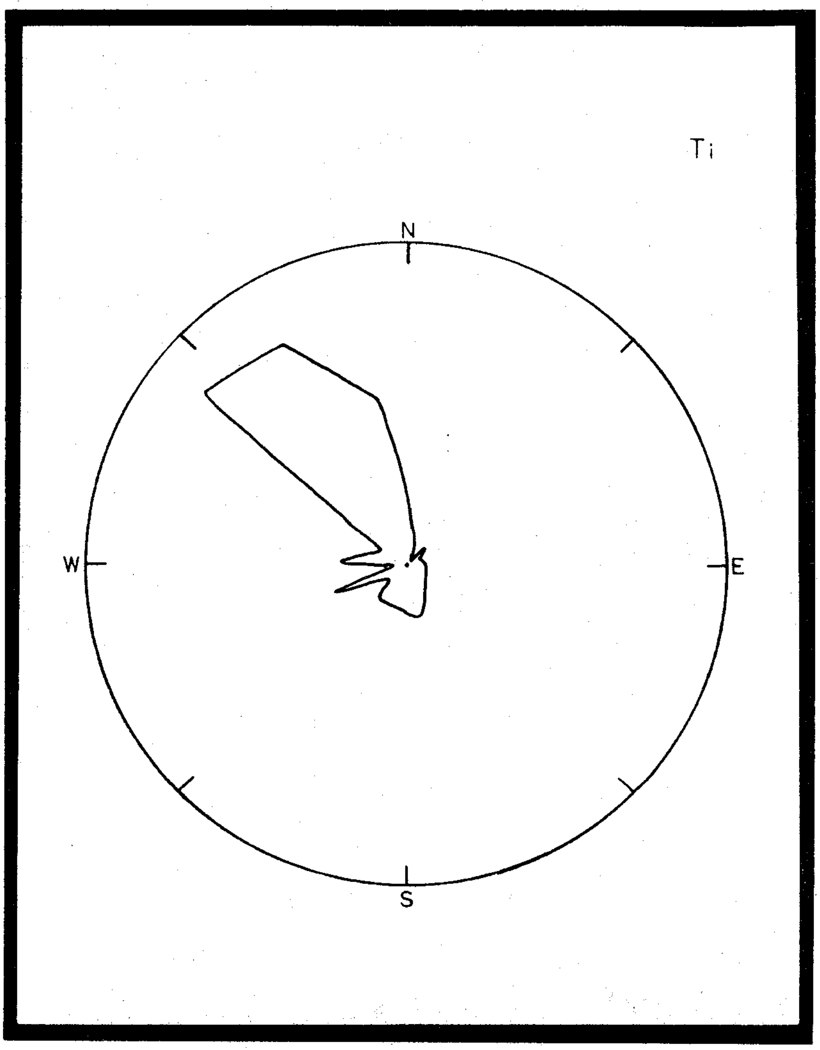

Figure 111 St. Louis Municipal Court. Directional Distribution V

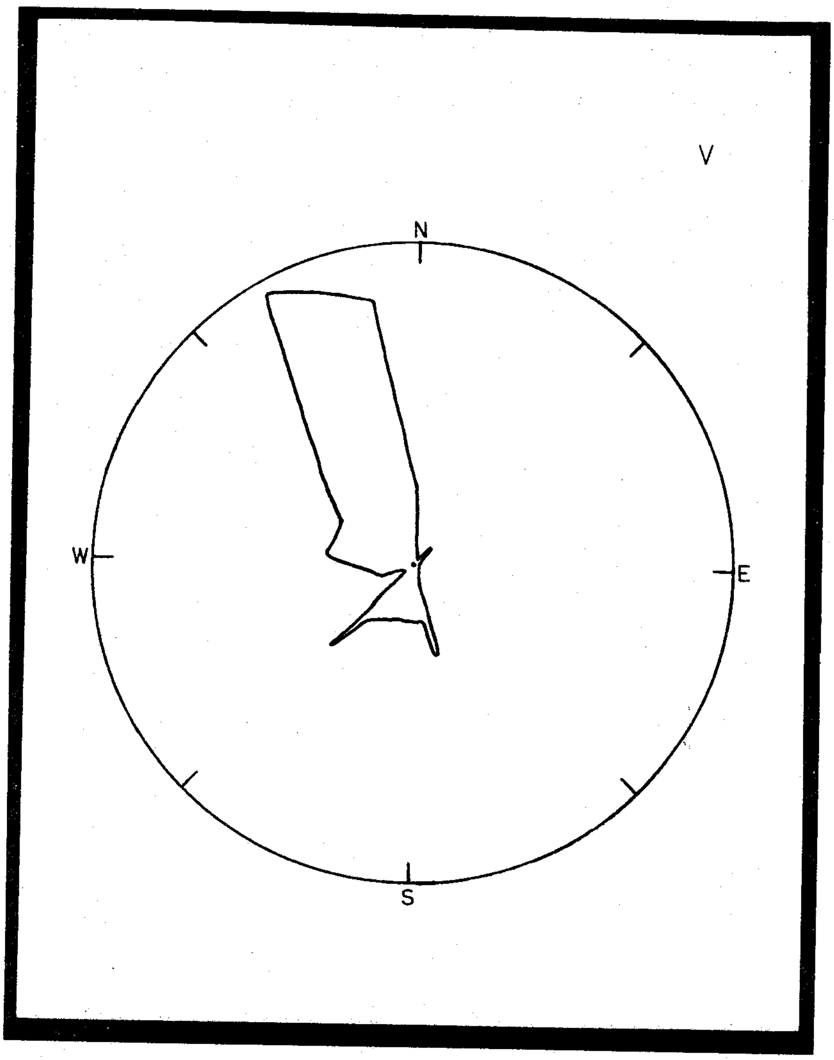

Figure 112 St. Louis Municipal Court. Directional Distribution Cr

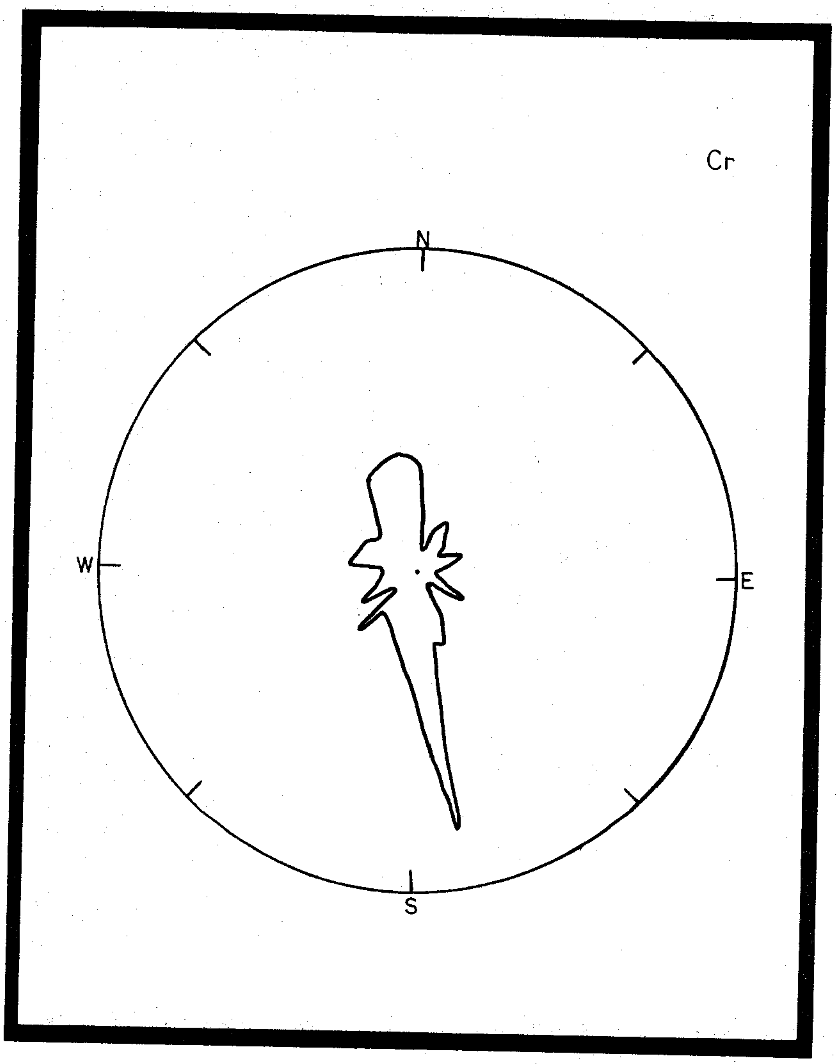

Figure 113 St. Louis Municipal Court. Directional Distribution Mn

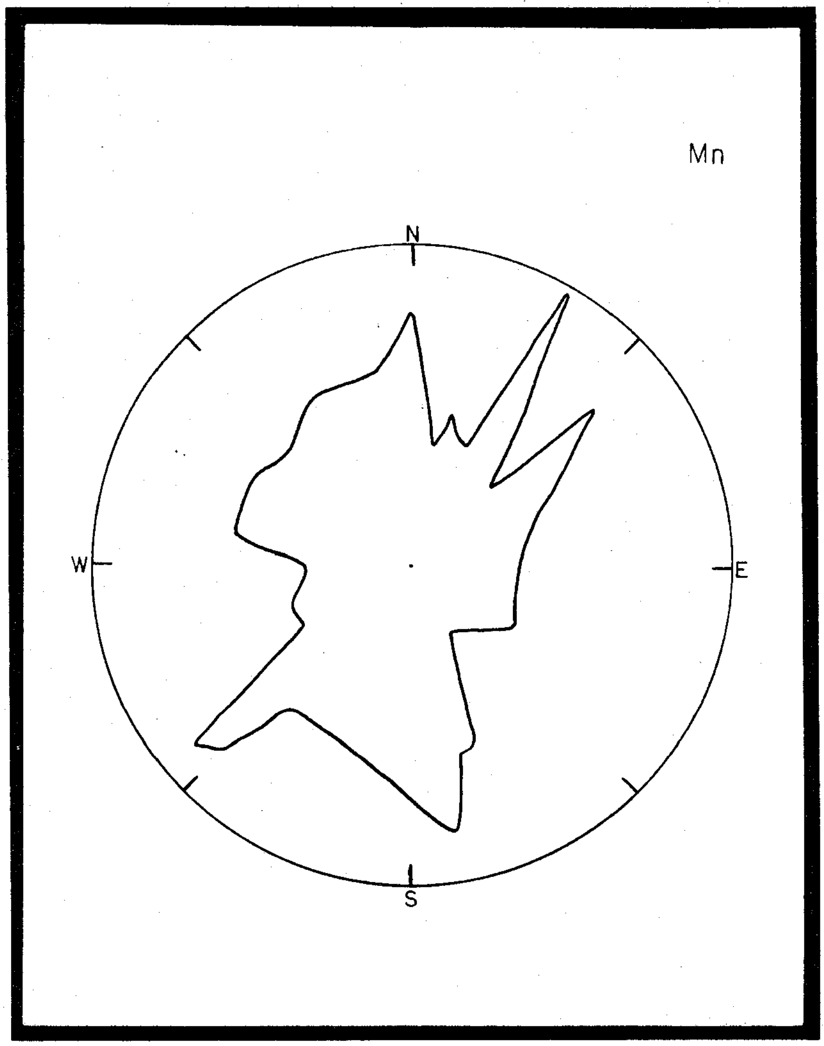

Figure 114 St. Louis Municipal Court. Directional Distribution Fe

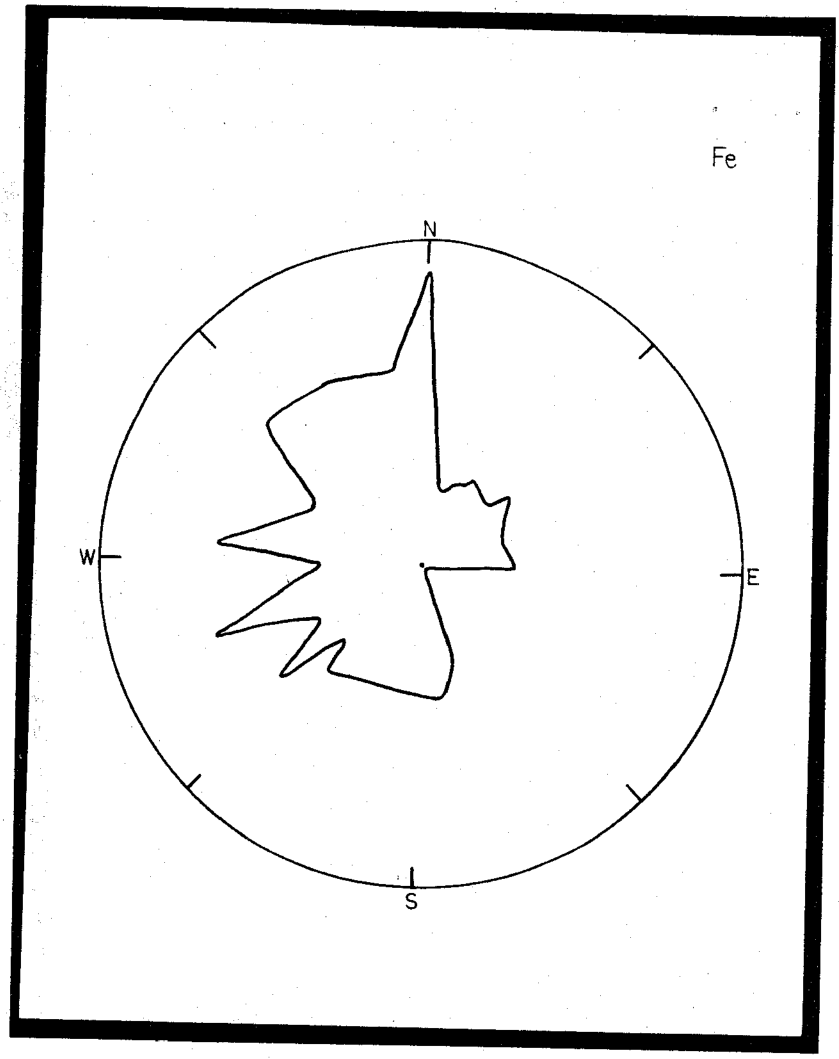

Figure 115 St. Louis Municipal Court. Directional Distribution Ni

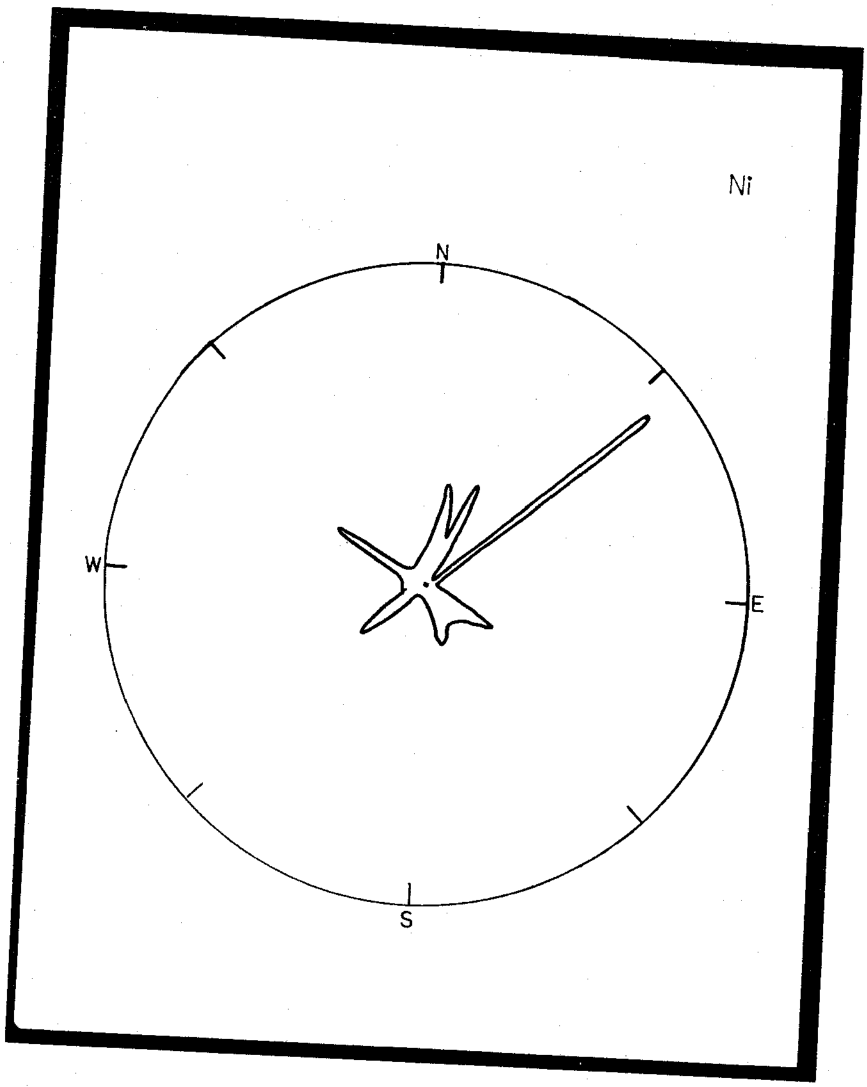

Figure 116 St. Louis Municipal Court. Directional Distribution Cu

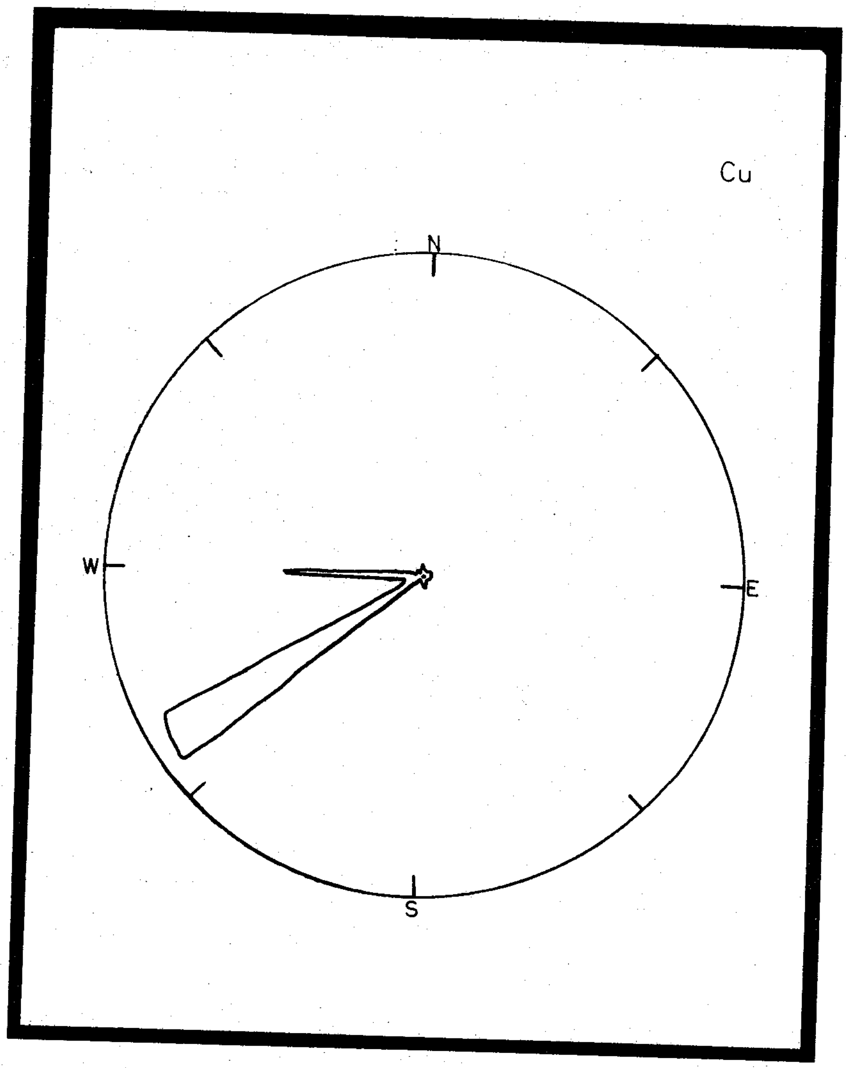

Figure 117 St. Louis Municipal Court. Directional Distribution Zn

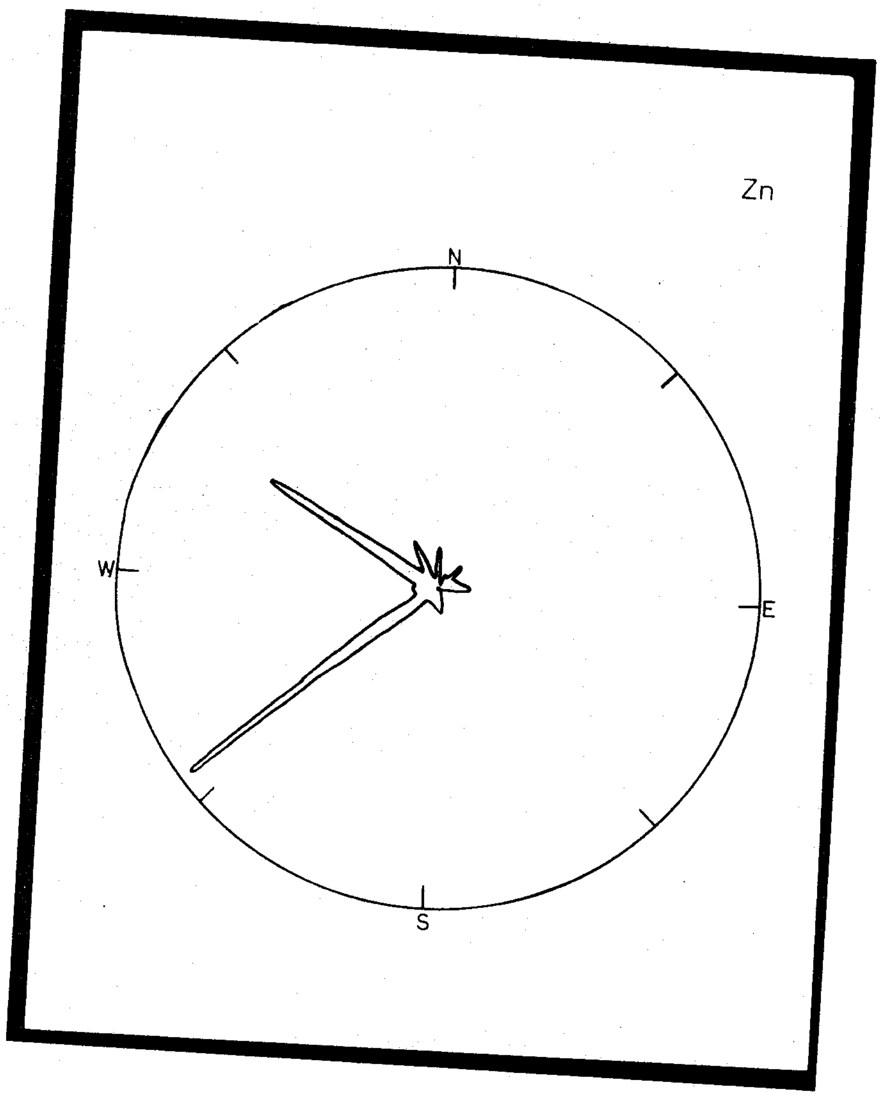

Figure 118 St. Louis Municipal Court. Directional Distribution Br

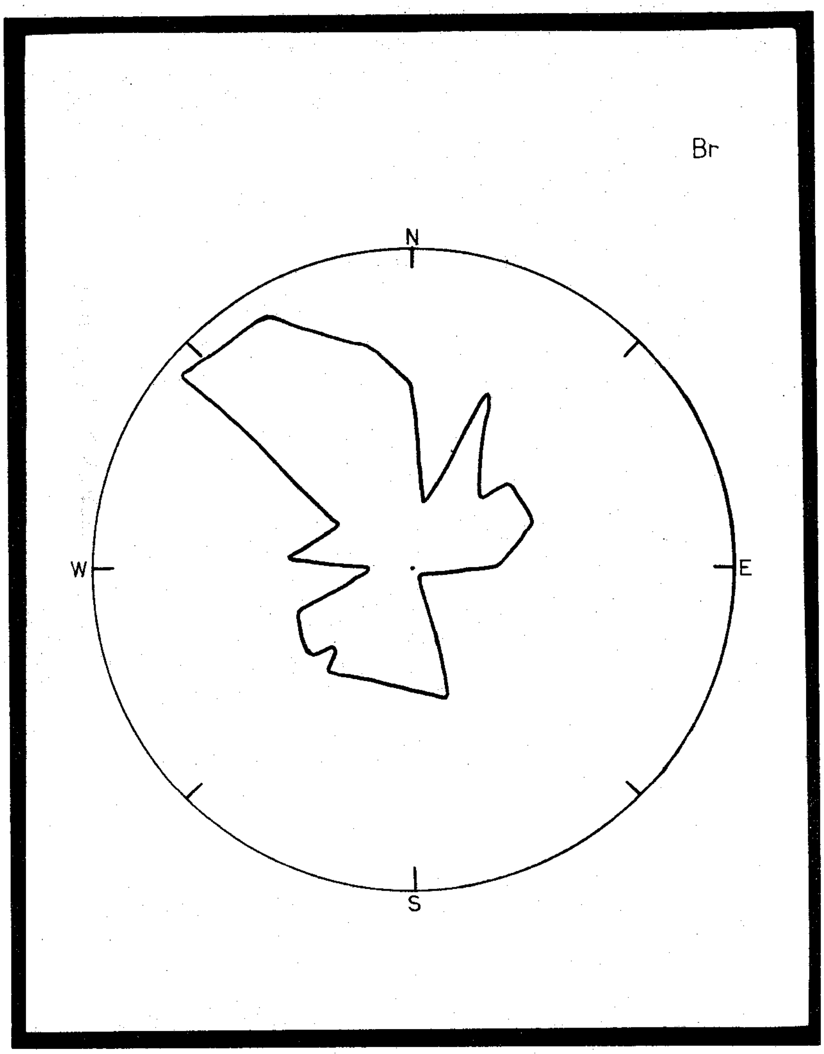

Figure 119   St. Louis Municipal Court. Directional Distribution Pb

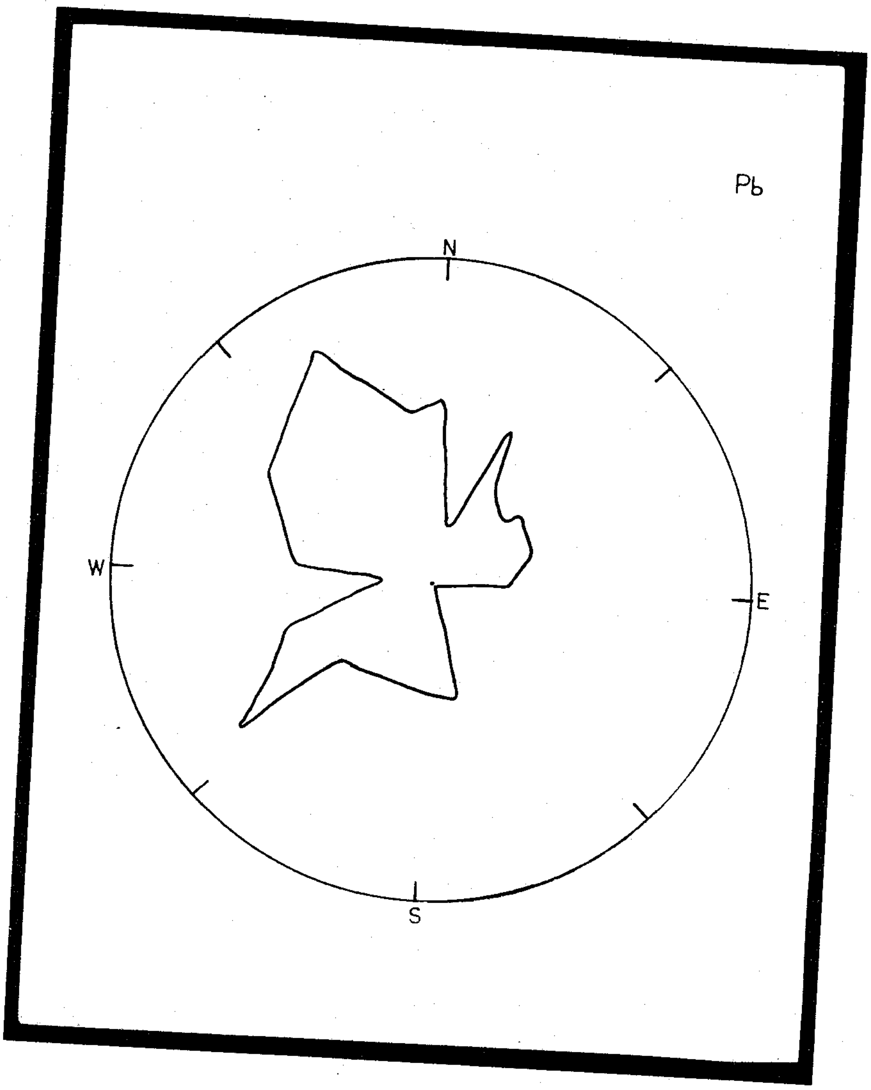

Figure 120 St. Louis Fire Station. Directional Distribution P

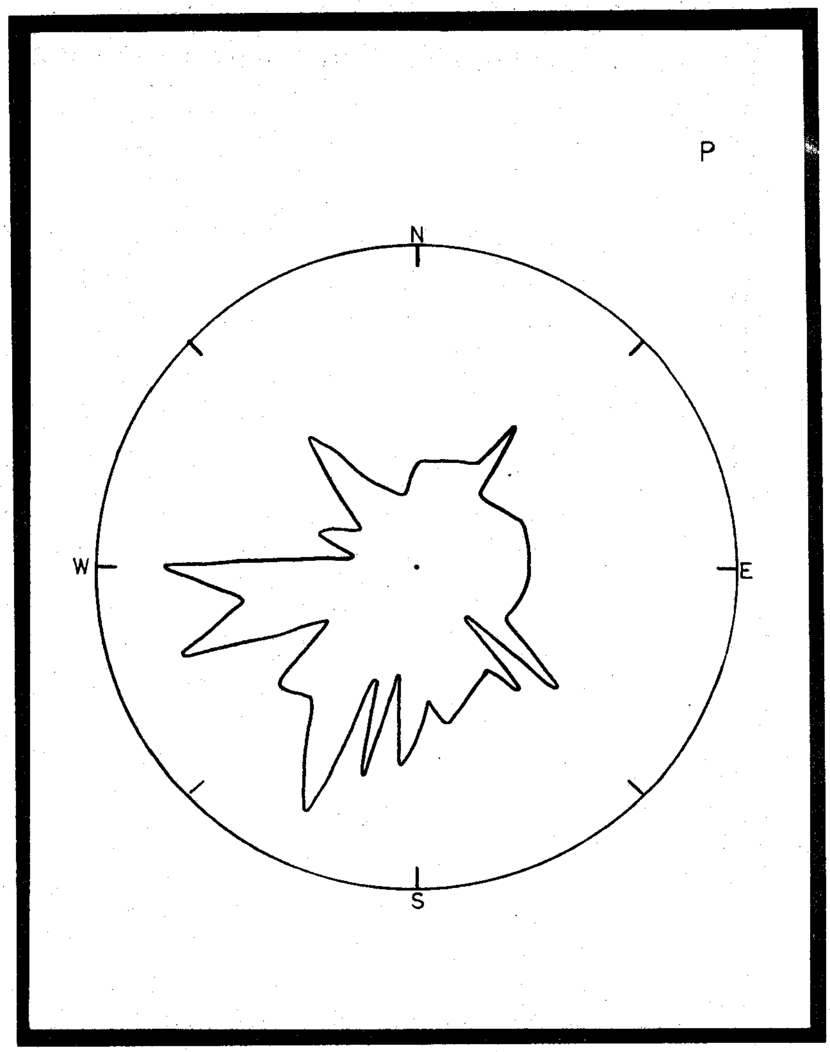

Figure 121 St. Louis Fire Station. Directional Distribution S

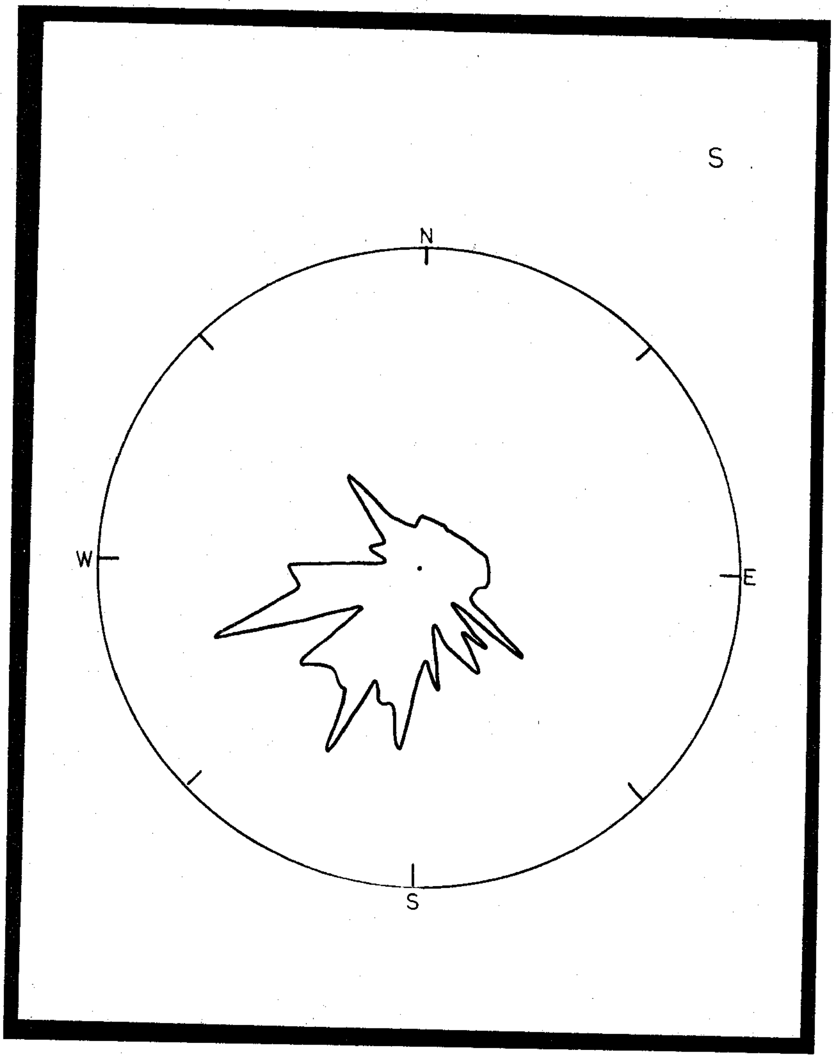

Figure 122 St. Louis Fire Station. Directional Distribution C1

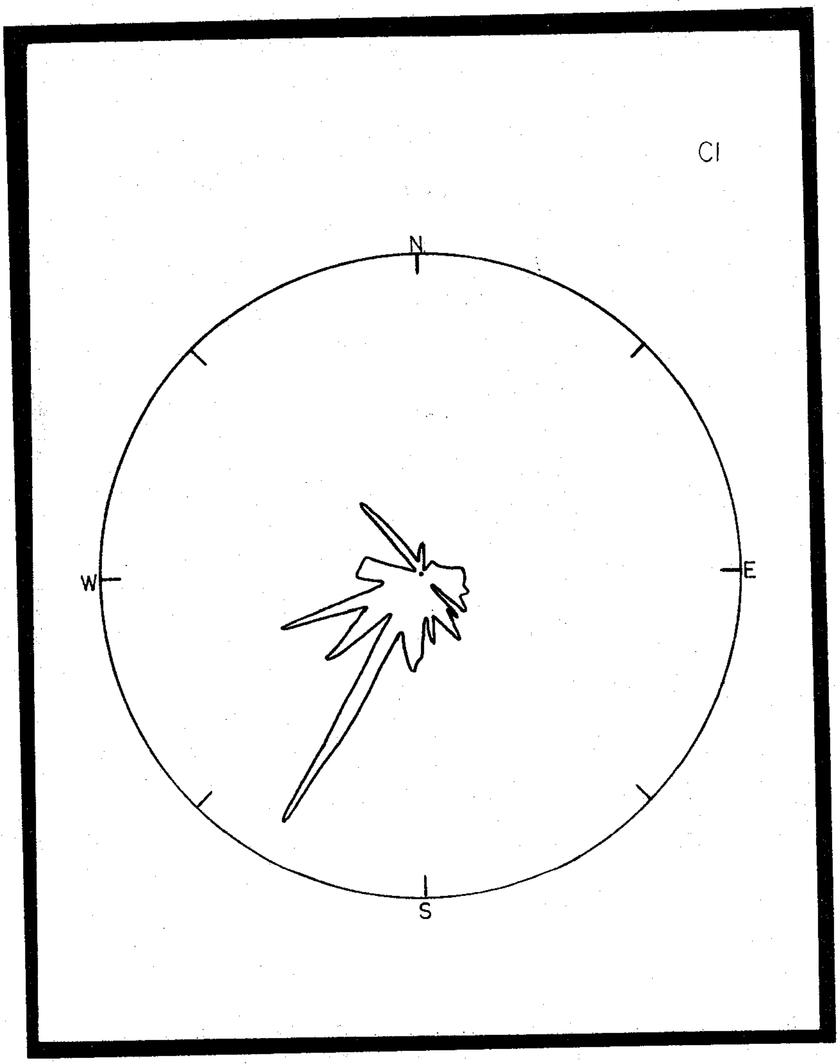

Figure 123 St. Louis Fire Station. Directional Distribution K

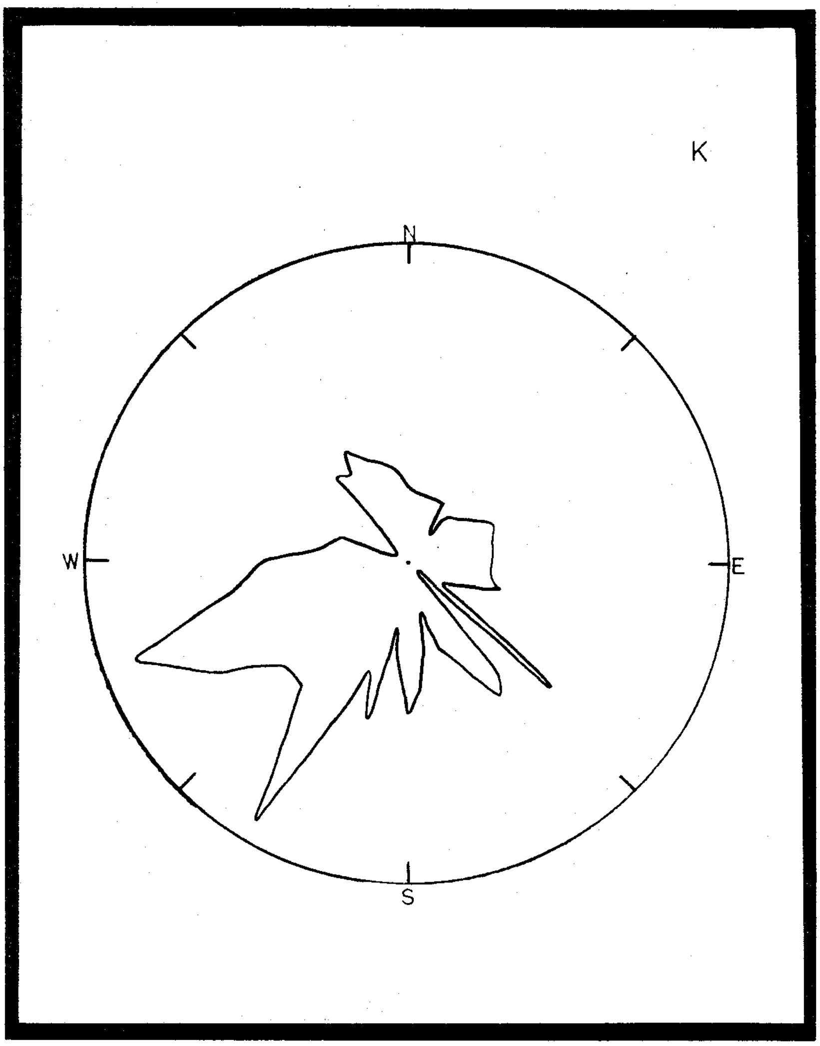

Figure 124 St. Louis Fire Station. Directional Distribution Ca

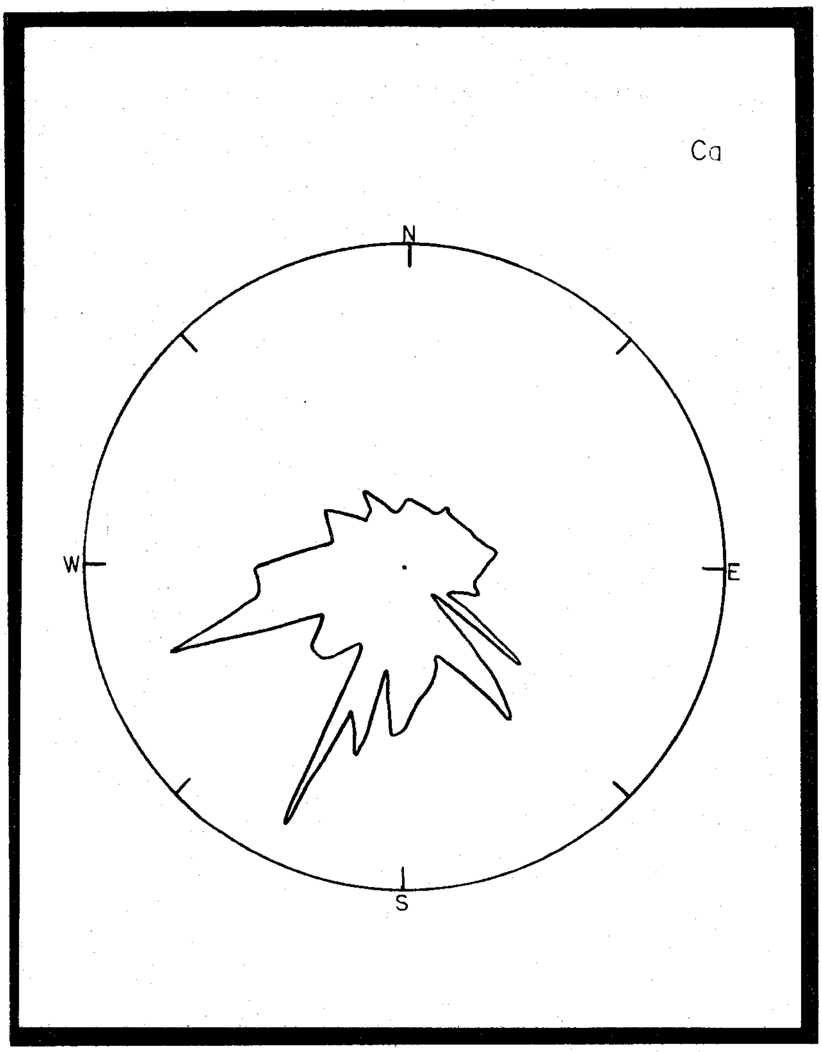

Figure 125 St. Louis Fire Station. Directional Distribution Ti

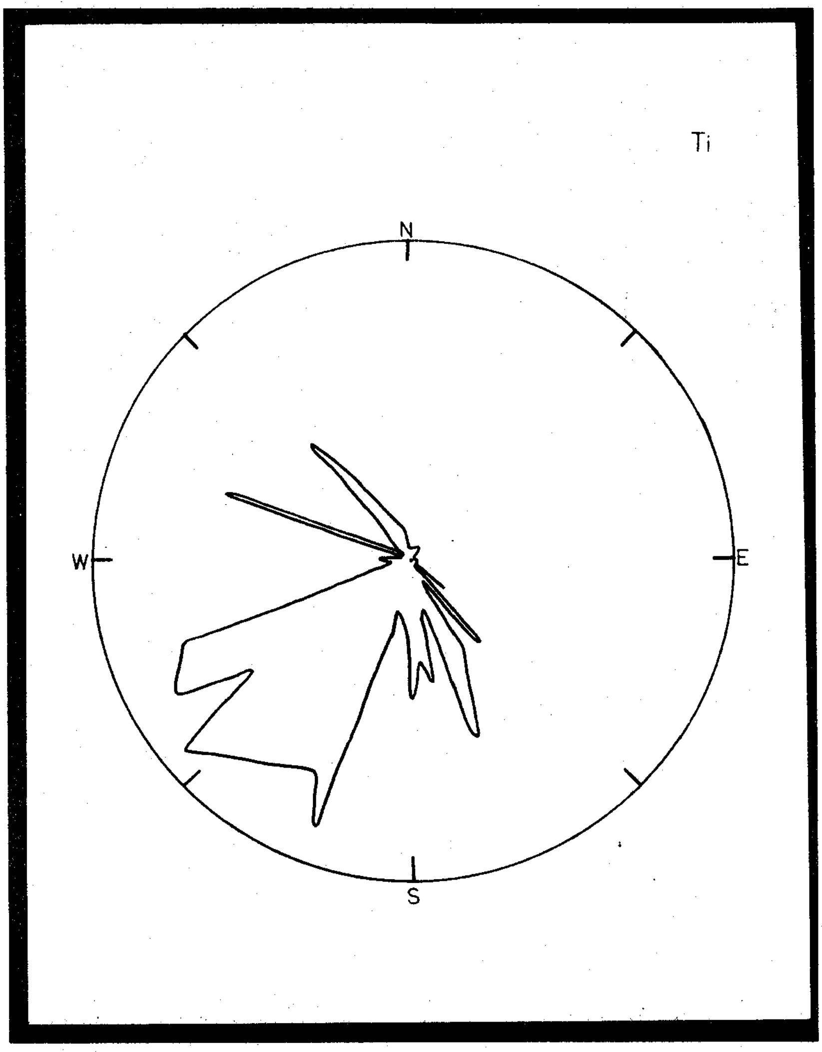

Figure 126 St. Louis Fire Station. Directional Distribution V

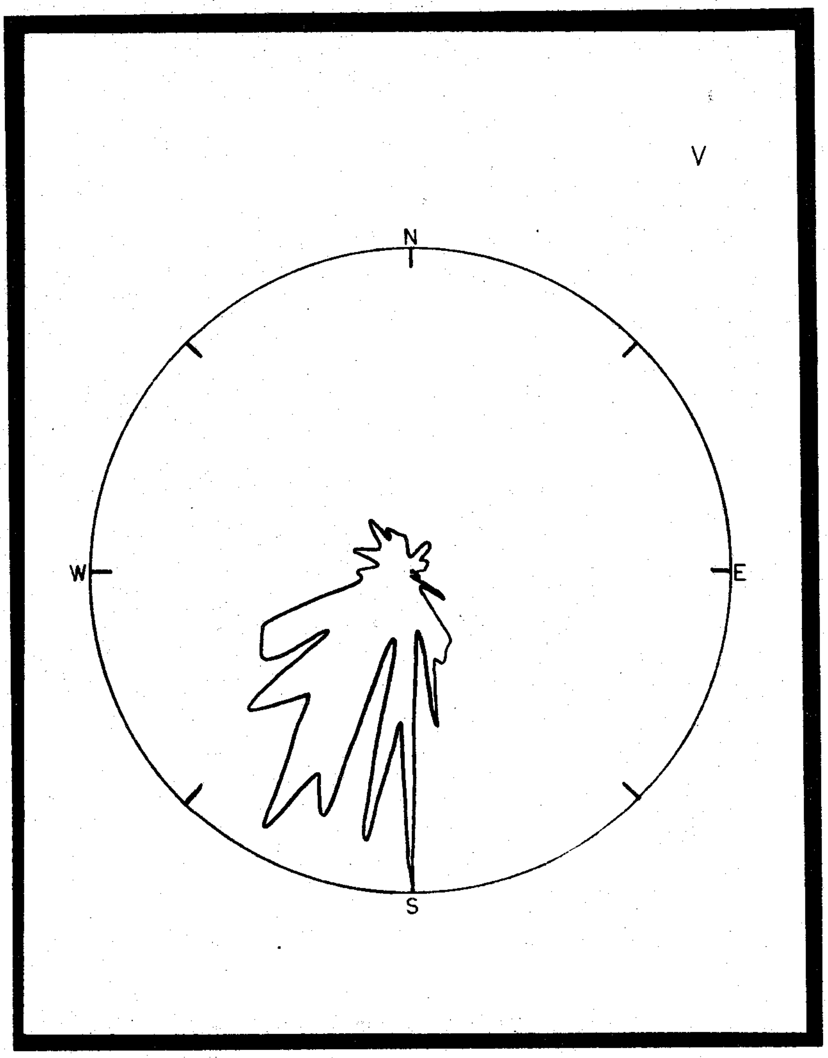

Figure 127 St. Louis Fire Station. Directional Distribution Cr

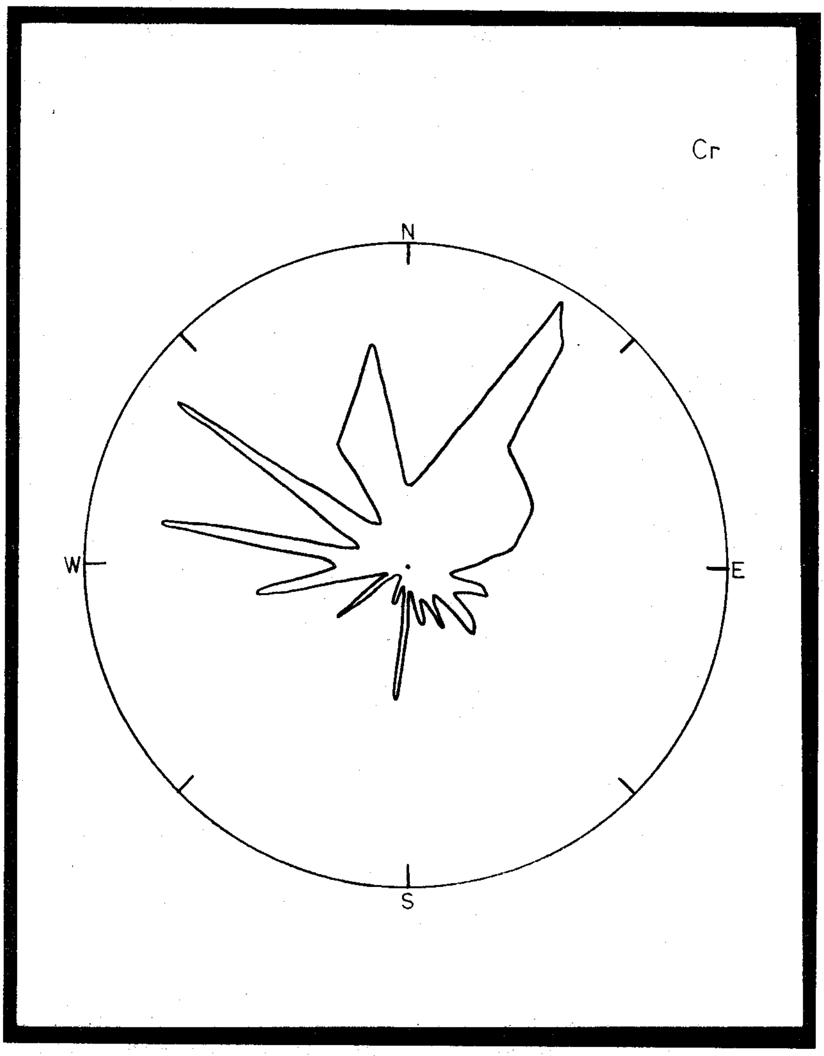

Figure 128 St. Louis Fire Station. Directional Distribution Mn

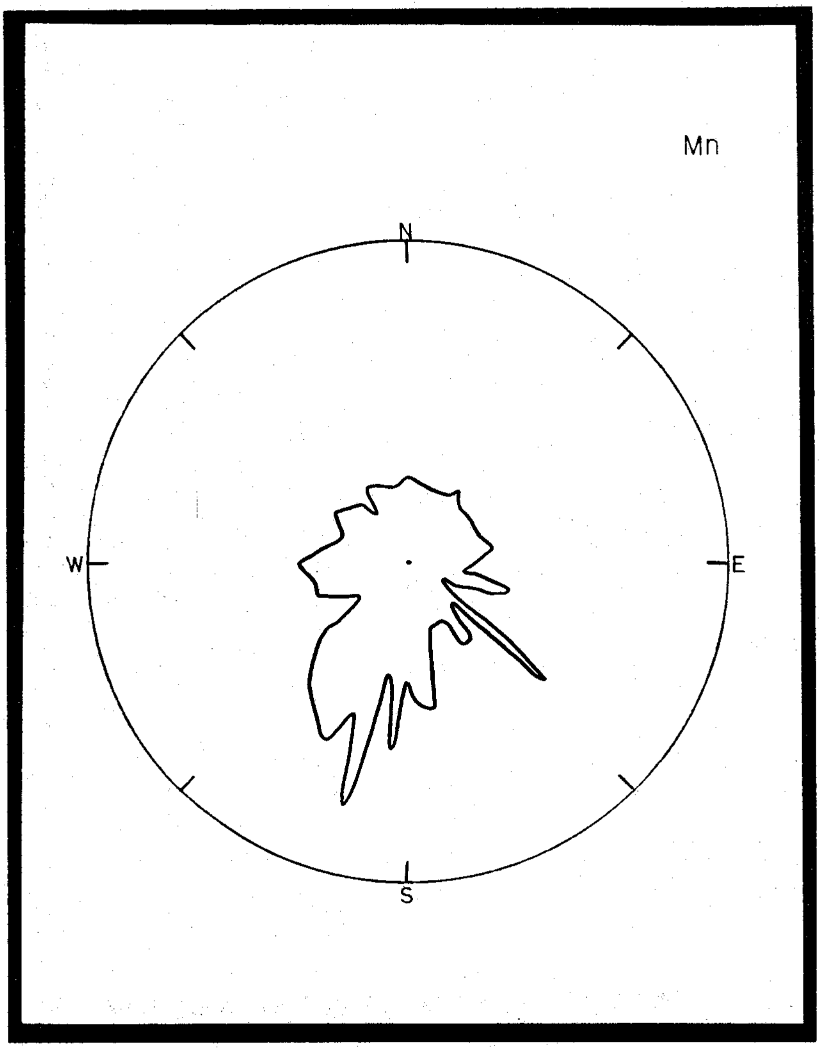

Figure 129 St. Louis Fire Station. Directional Distribution Fe

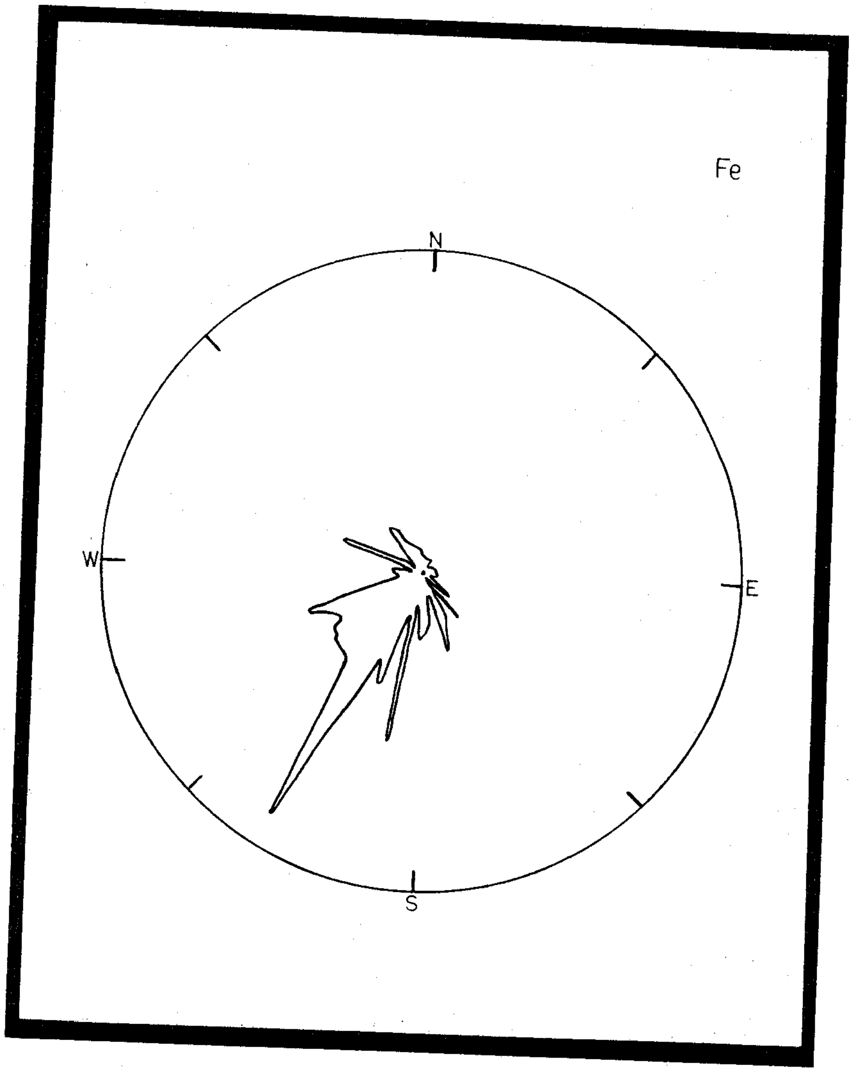

Figure 130 St. Louis Fire Station. Directional Distribution Ni

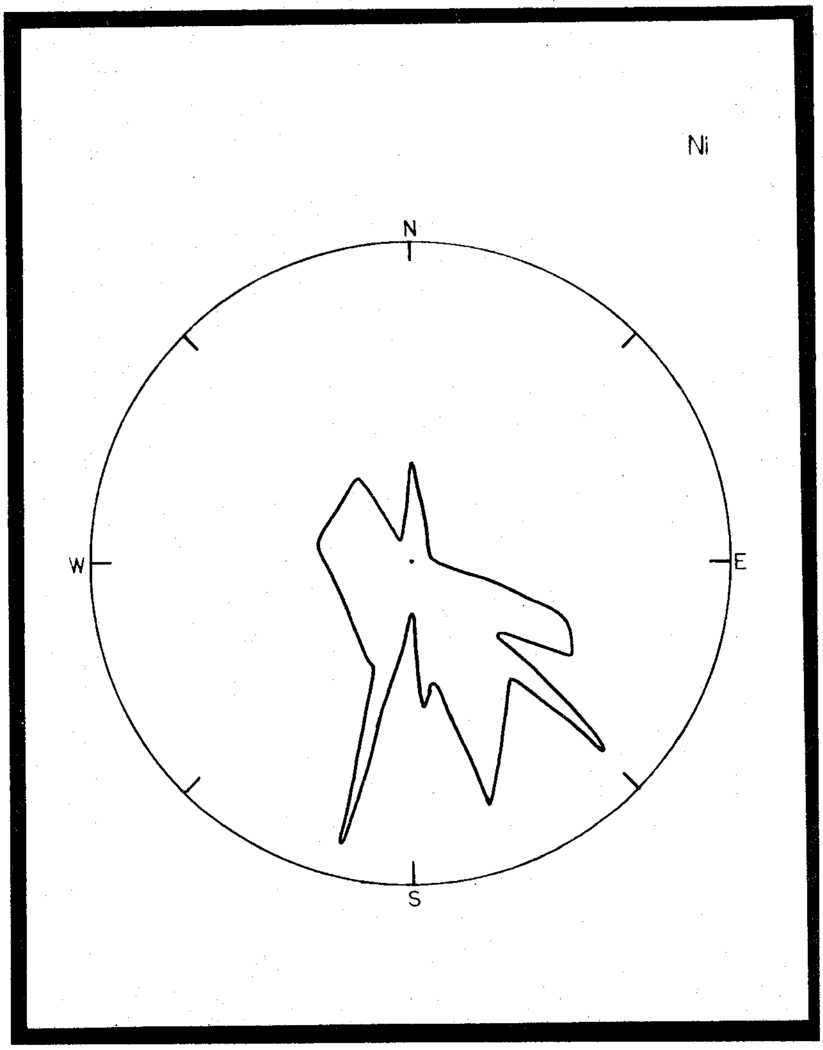

Figure 131 St. Louis Fire Station. Directional Distribution Cu

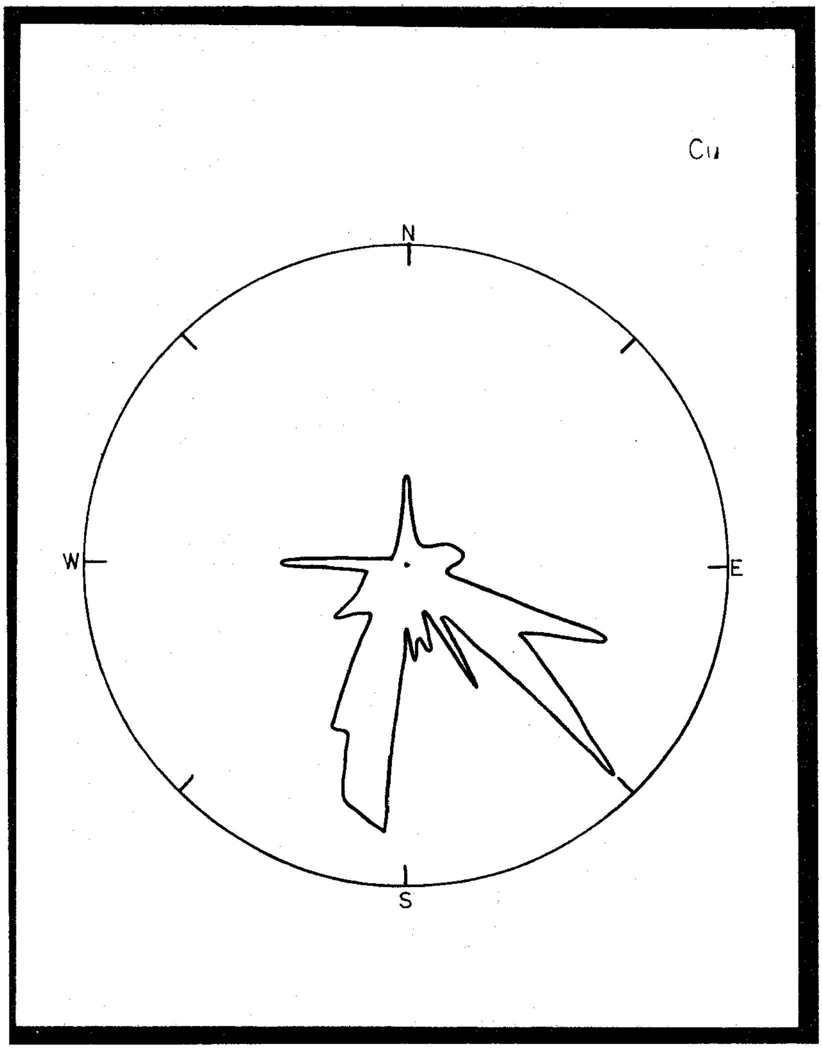

Figure 132 St. Louis Fire Station. Directional Distribution Zn

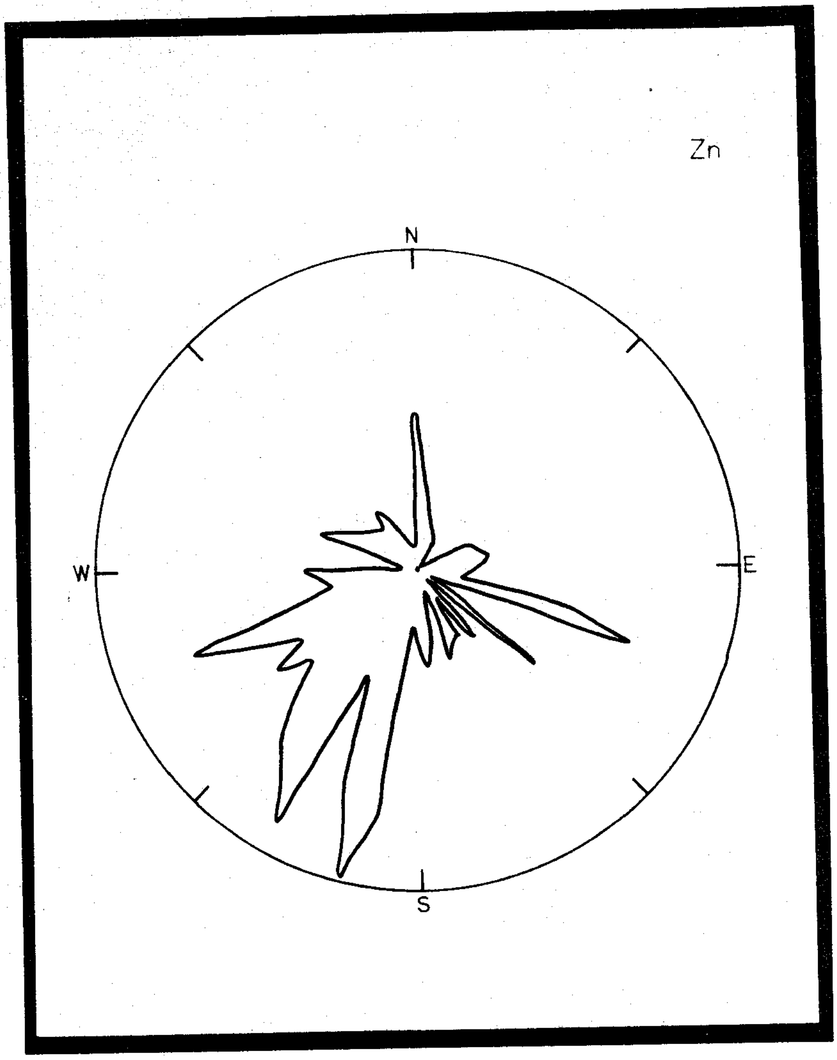

Figure 133 St. Louis Fire Station. Directional Distribution Br

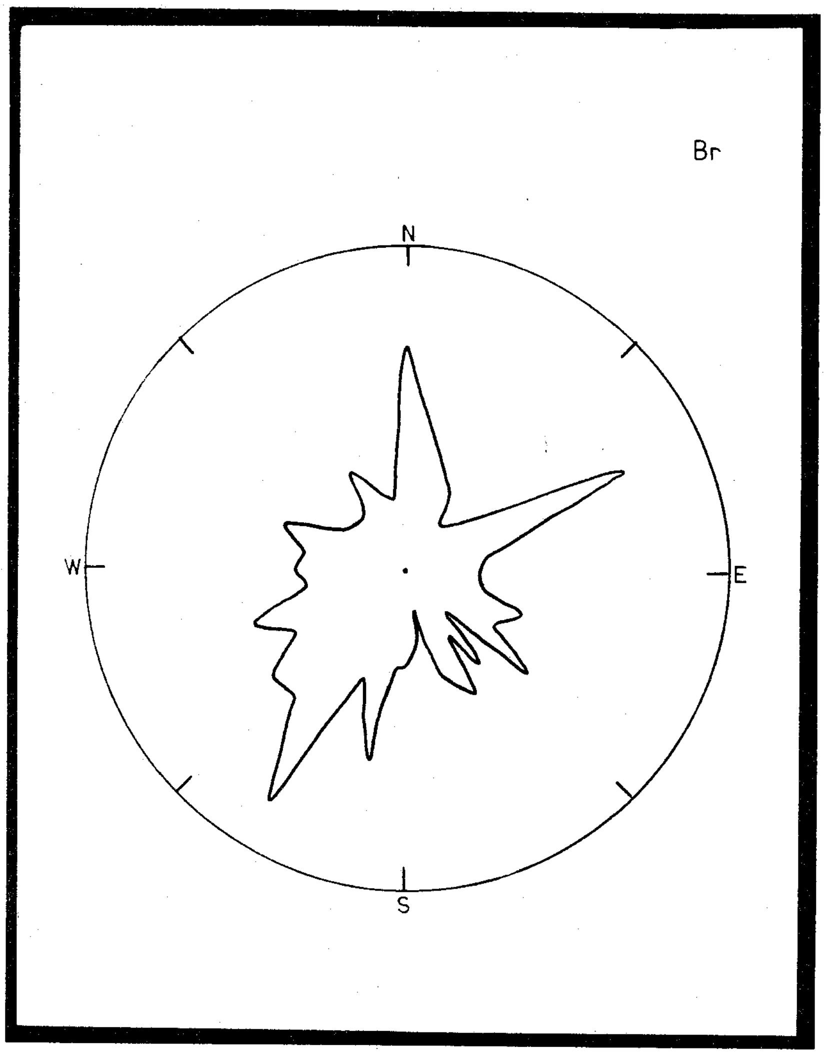

Figure 134 St. Louis Fire Station. Directional Distribution Pb

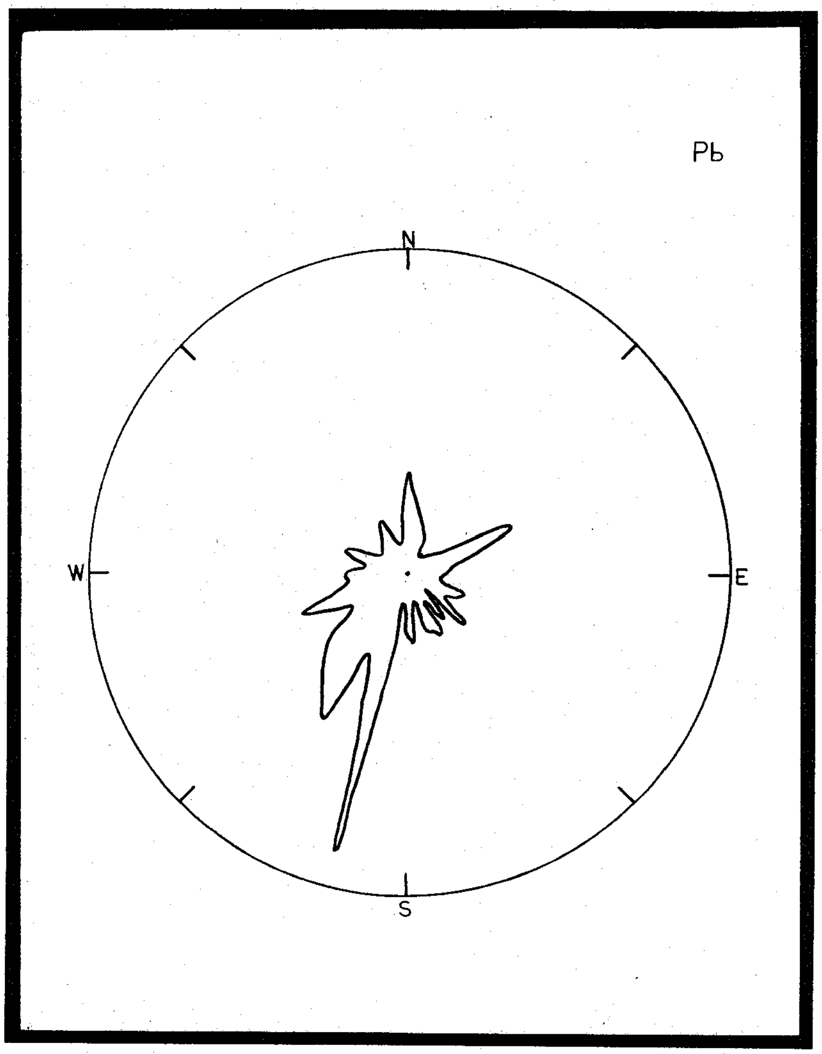

Figure 135 Wind Direction Sensitive Size Distributions. SLFS P

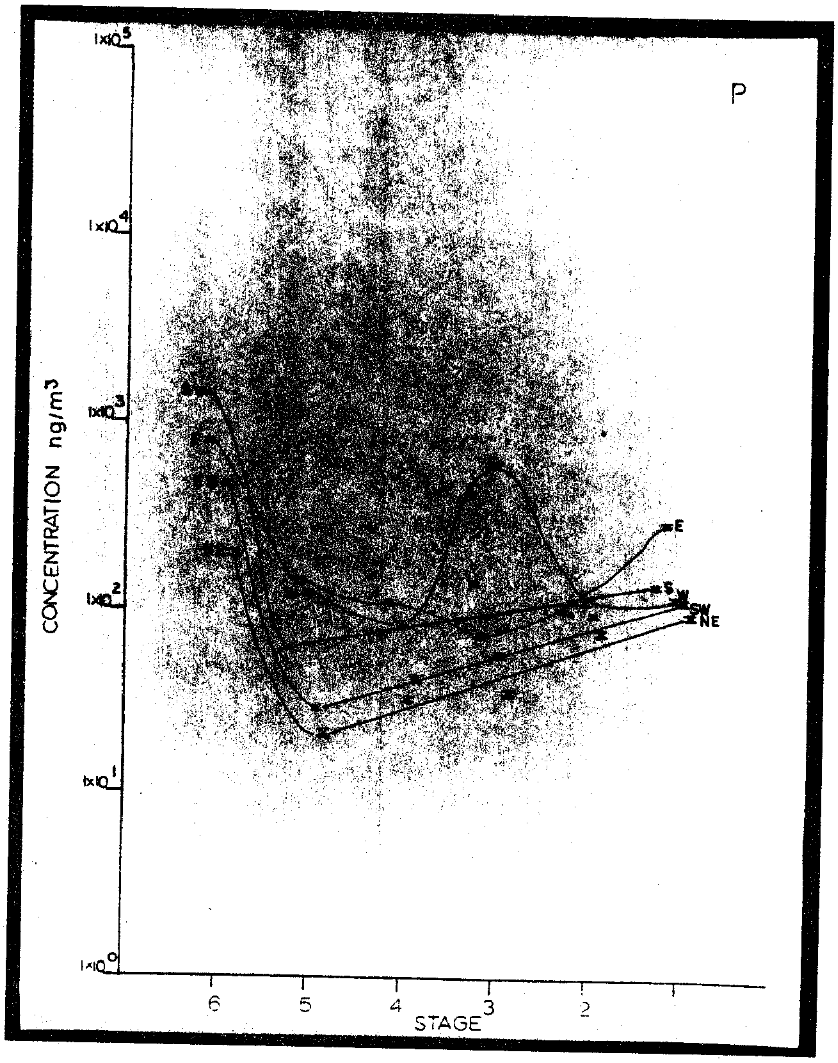

Figure 136 Wind Direction Sensitive Size Distributions. SLFS S

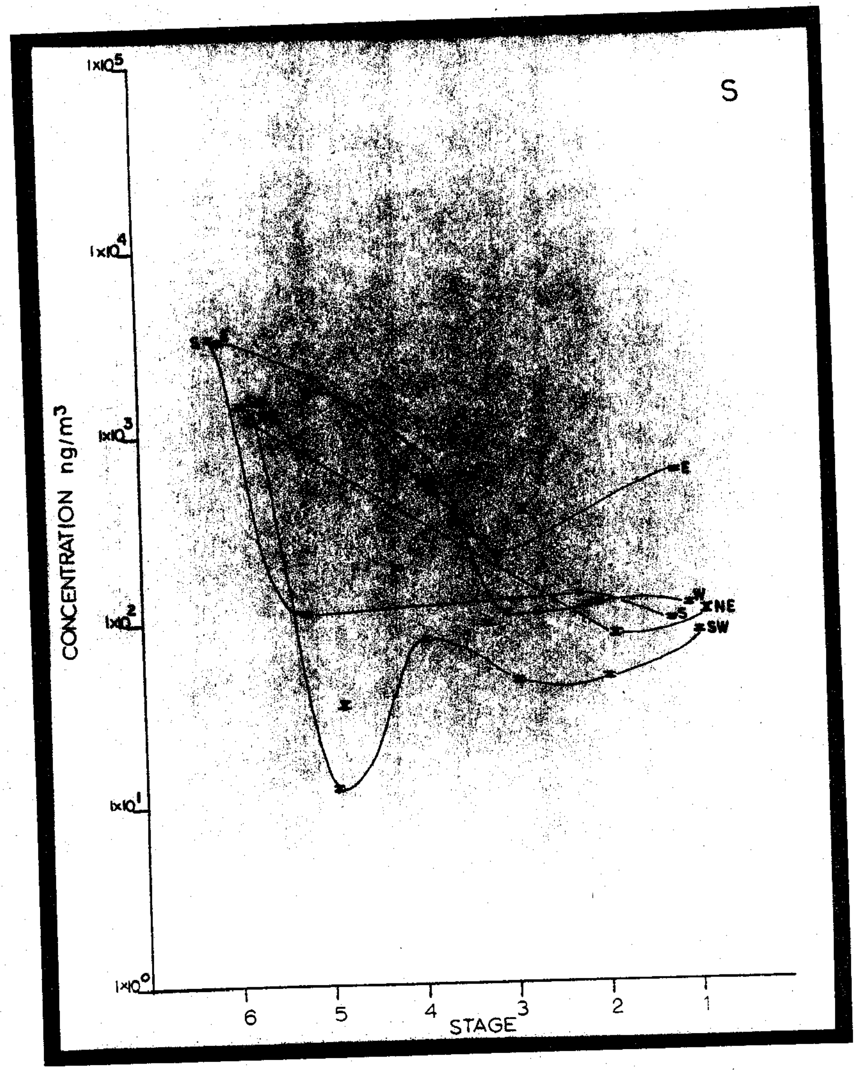

Figure 137 Wind Direction Sensitive Size Distributions. SLFS Cl

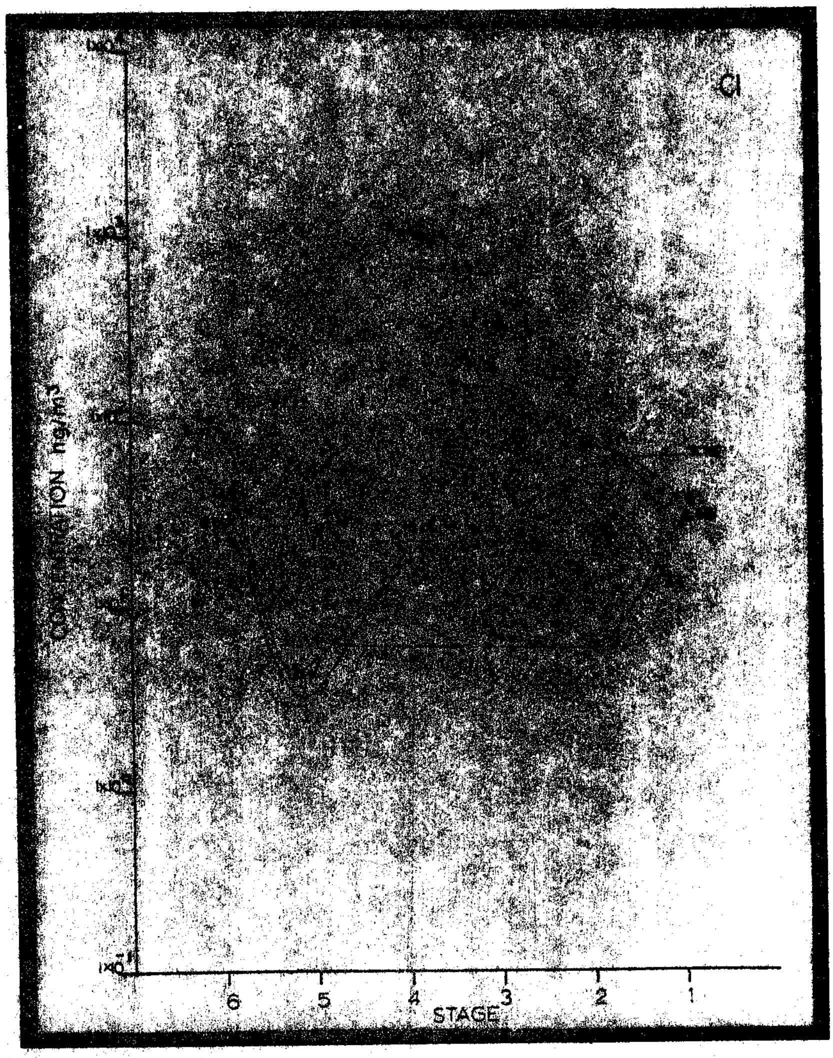

Figure 138 Wind Direction Sensitive Size Distributions. SLFS K

Figure 139 Wind Direction Sensitive Size Distributions. SLFS Ca

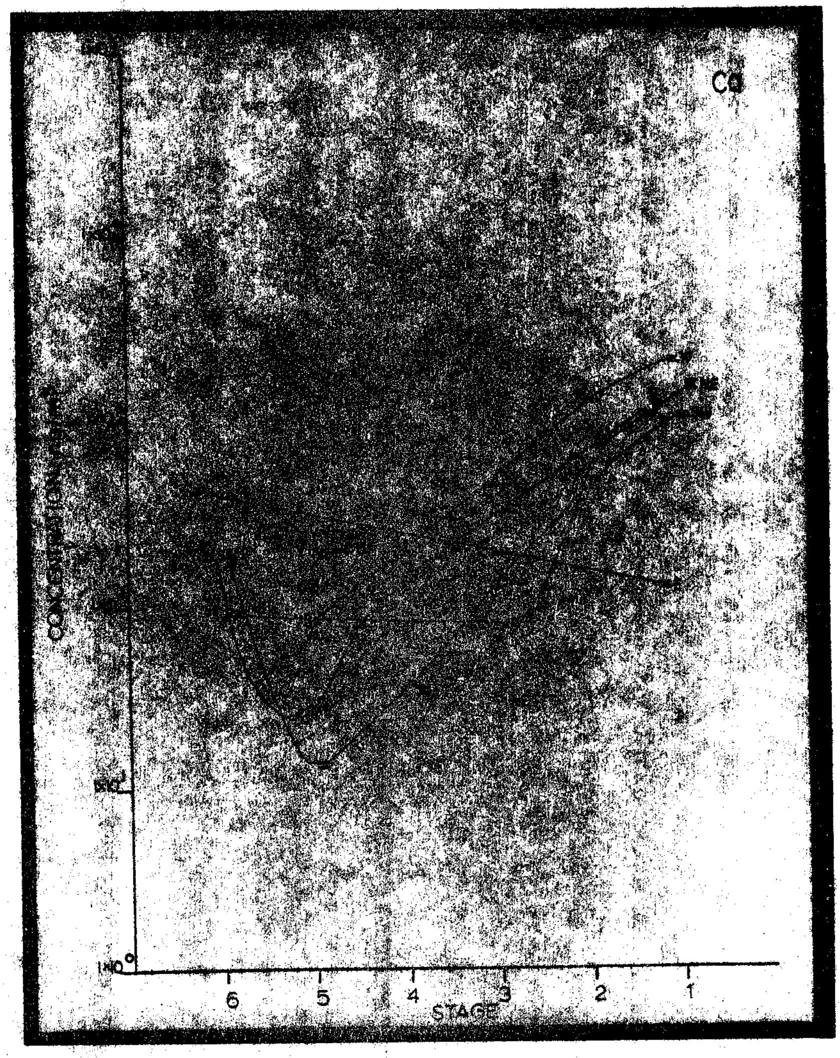

Figure 140   Wind Direction Sensitive Size Distributions.   SLFS   Ti

Figure 141 Wind Direction Sensitive Size Distributions. SLFS Mn

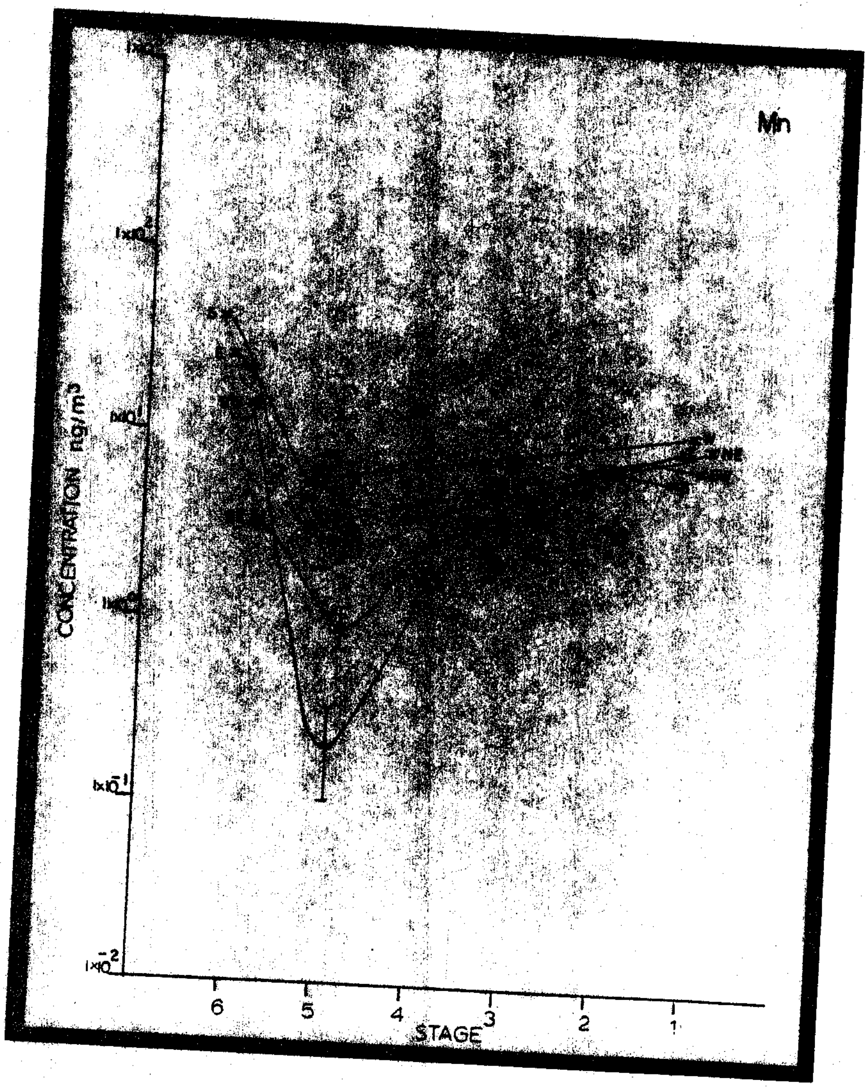

Figure 142 Wind Direction Sensitive Size Distributions. SLFS Fe

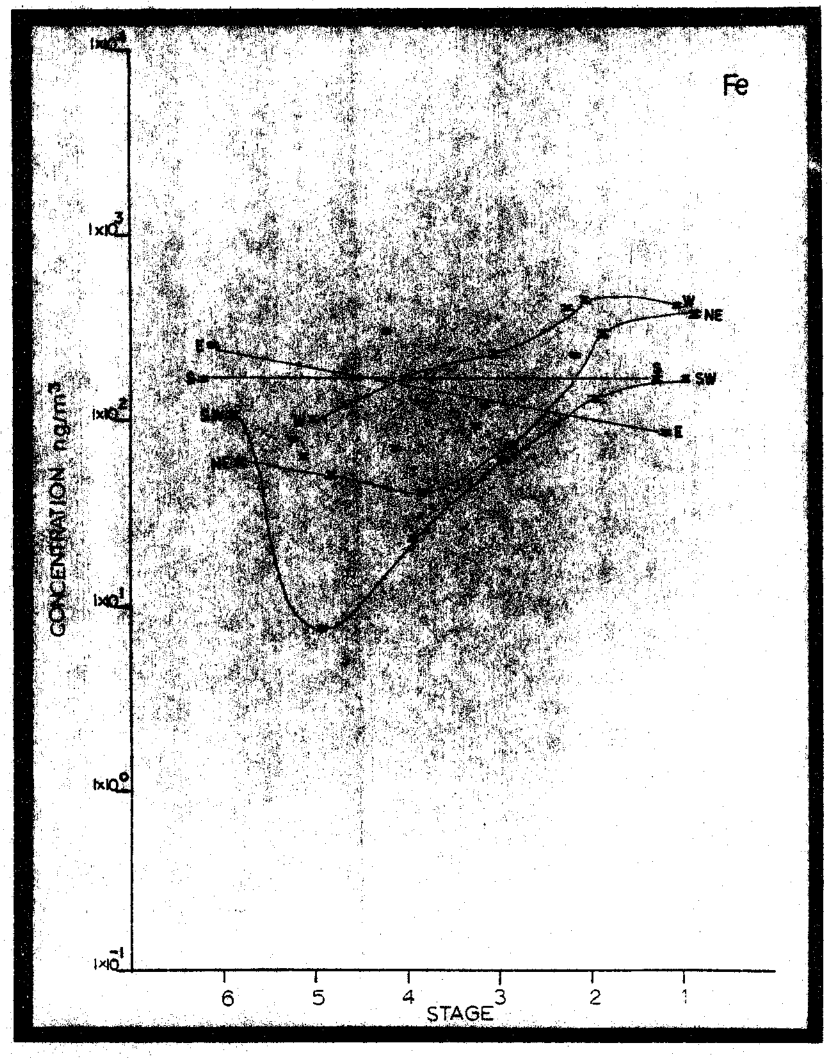

Figure 143 Wind Direction Sensitive Size Distributions. SLFS Ni

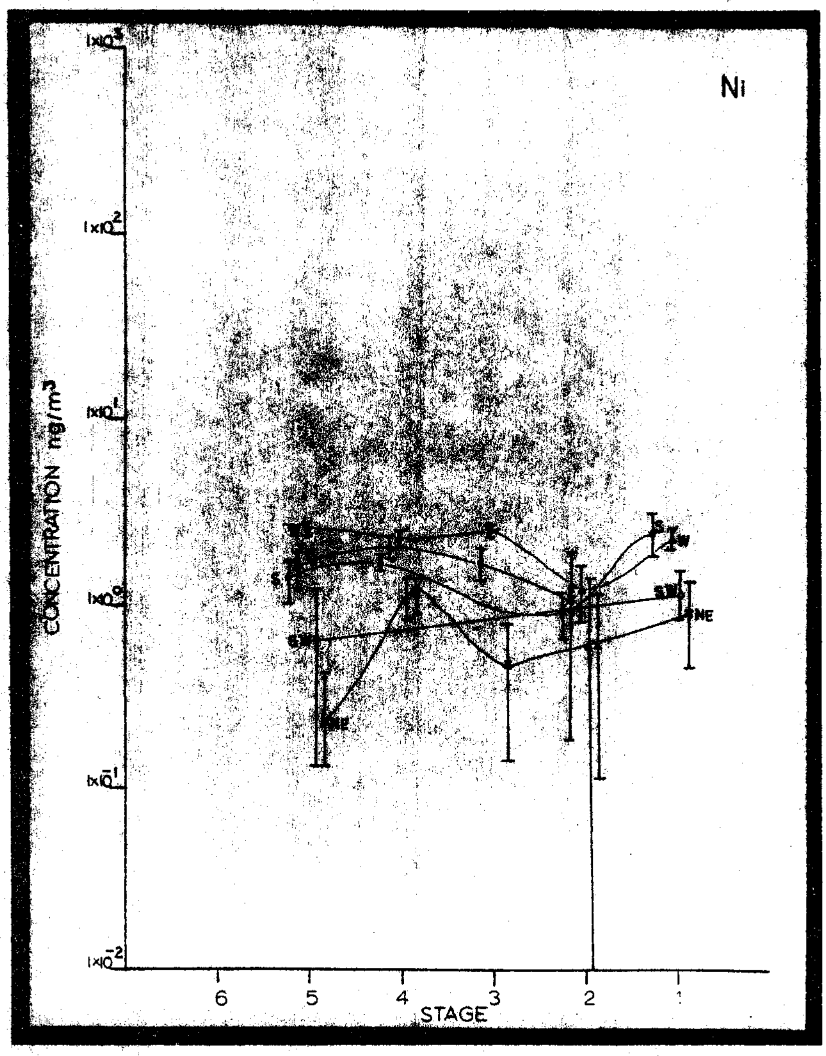

Figure 144 Wind Direction Sensitive Size Distributions. SLFS Cu

Figure 145 Wind Direction Sensitive Size Distributions. SLFS Zn

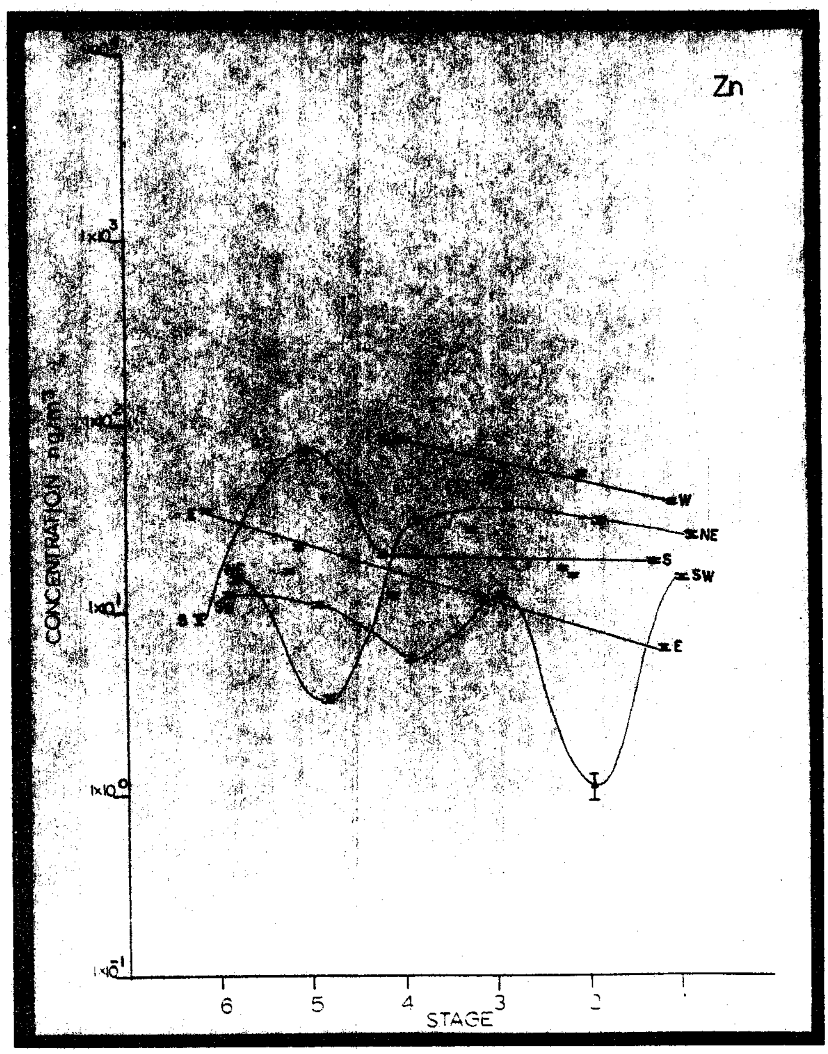

Figure 146 Wind Direction Sensitive Size Distributions. SLFS Br

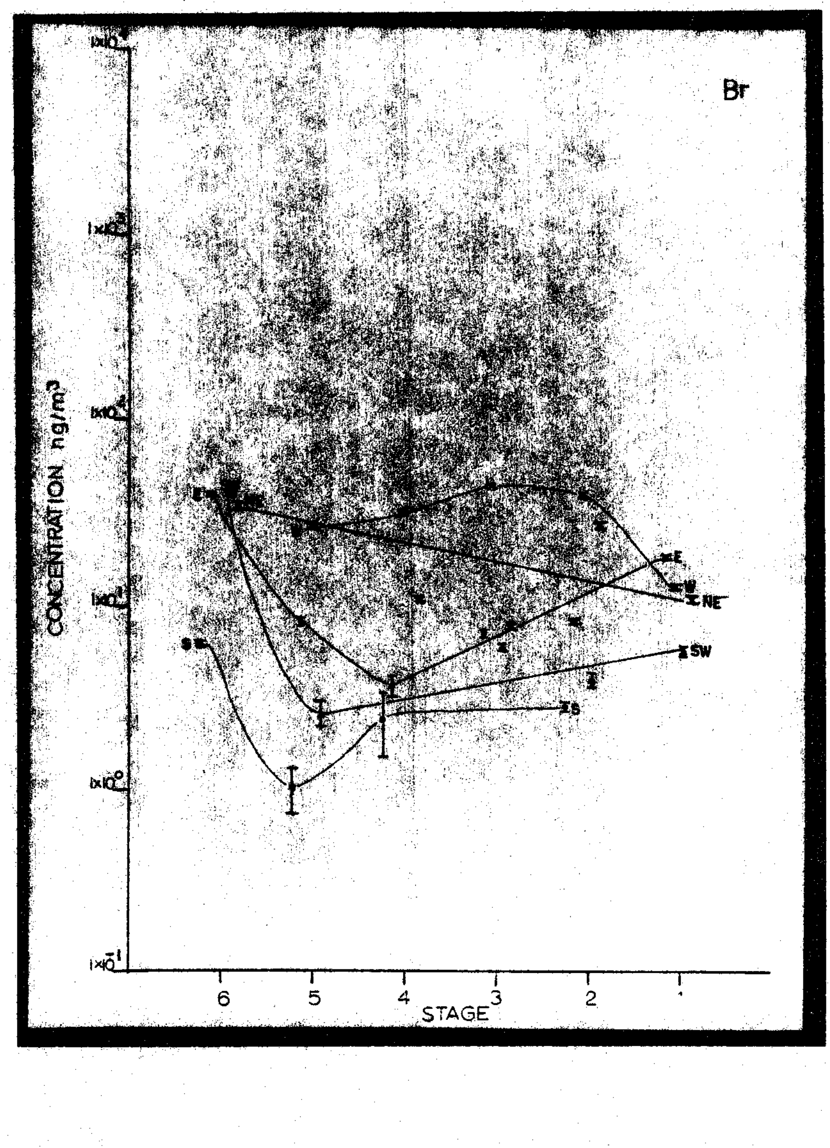

Figure 147 Wind Direction Sensitive Size Distributions. SLFS Pb

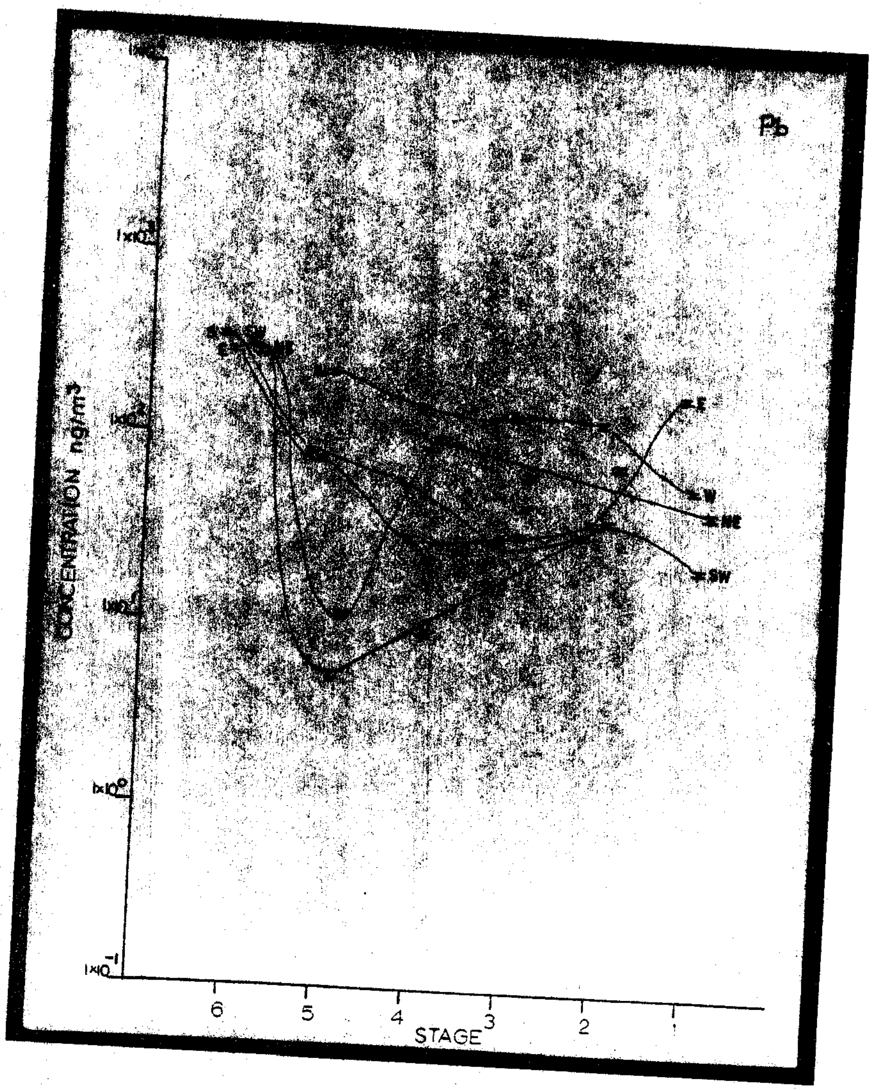

Figure 148 Wind Direction Sensitive Size Distributions. SLMC P

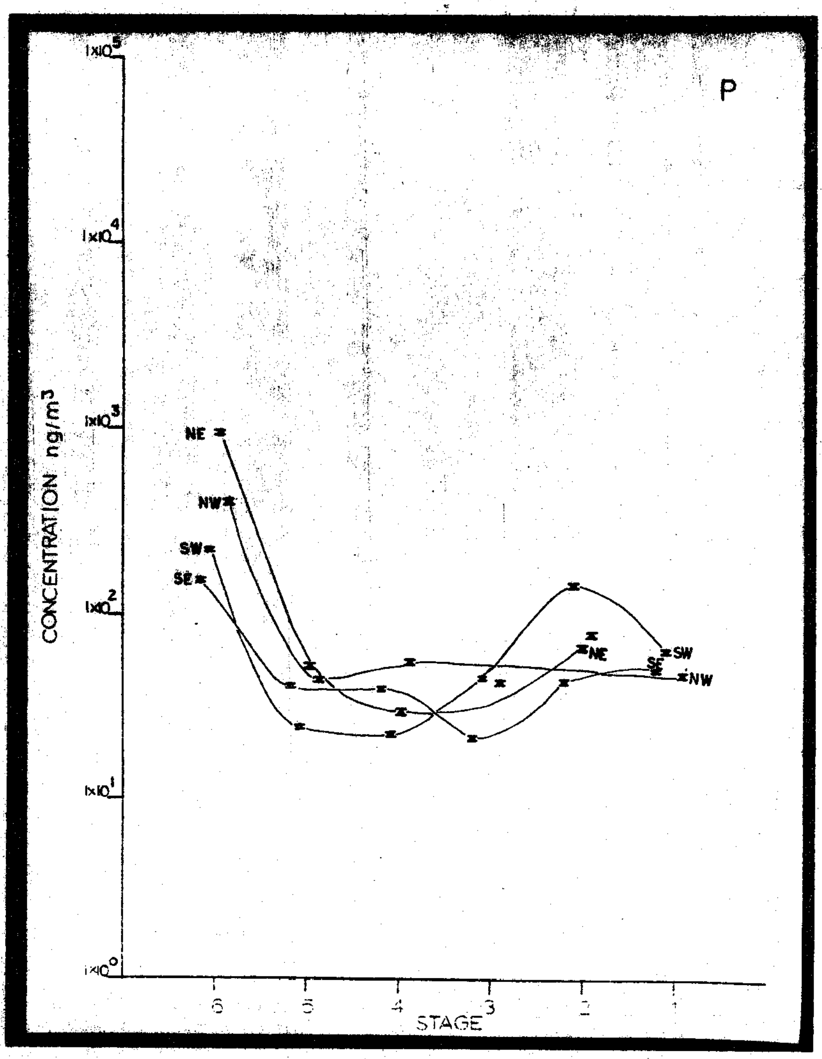

Figure 149 Wind Direction Sensitive Size Distributions. SLMC S

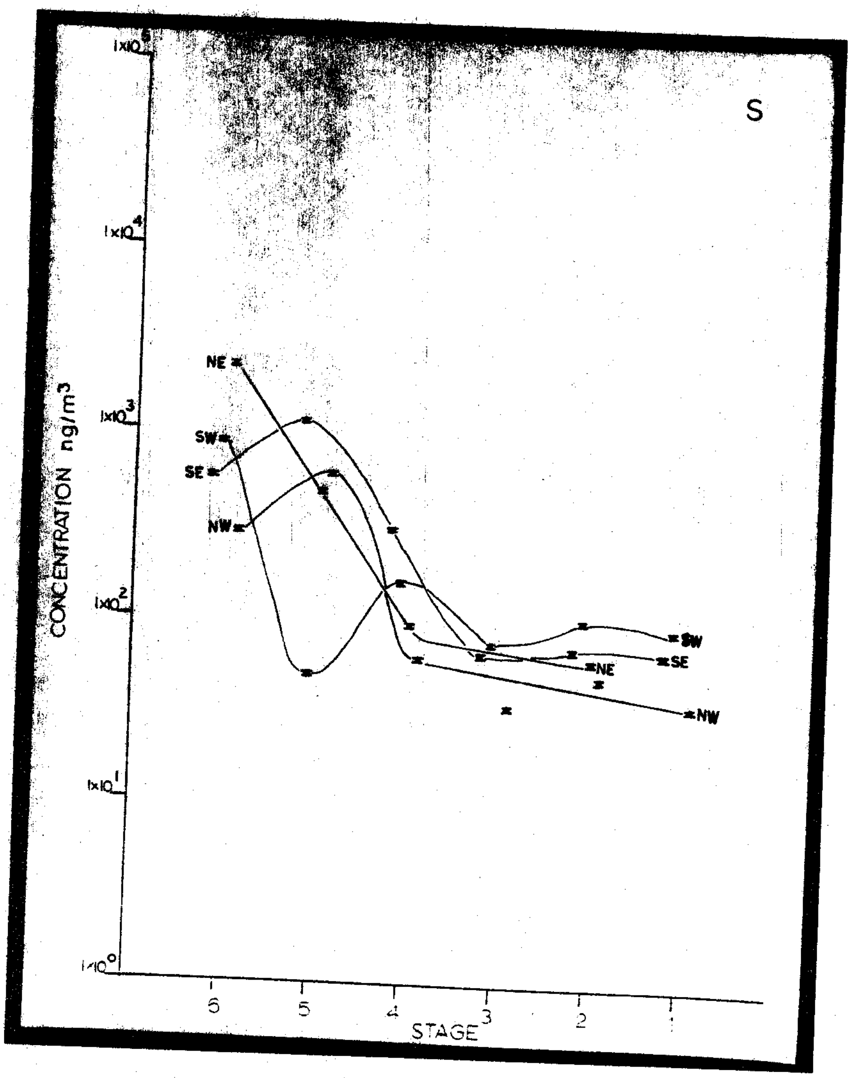

Figure 150 Wind Direction Sensitive Size Distributions. SLMC Cl

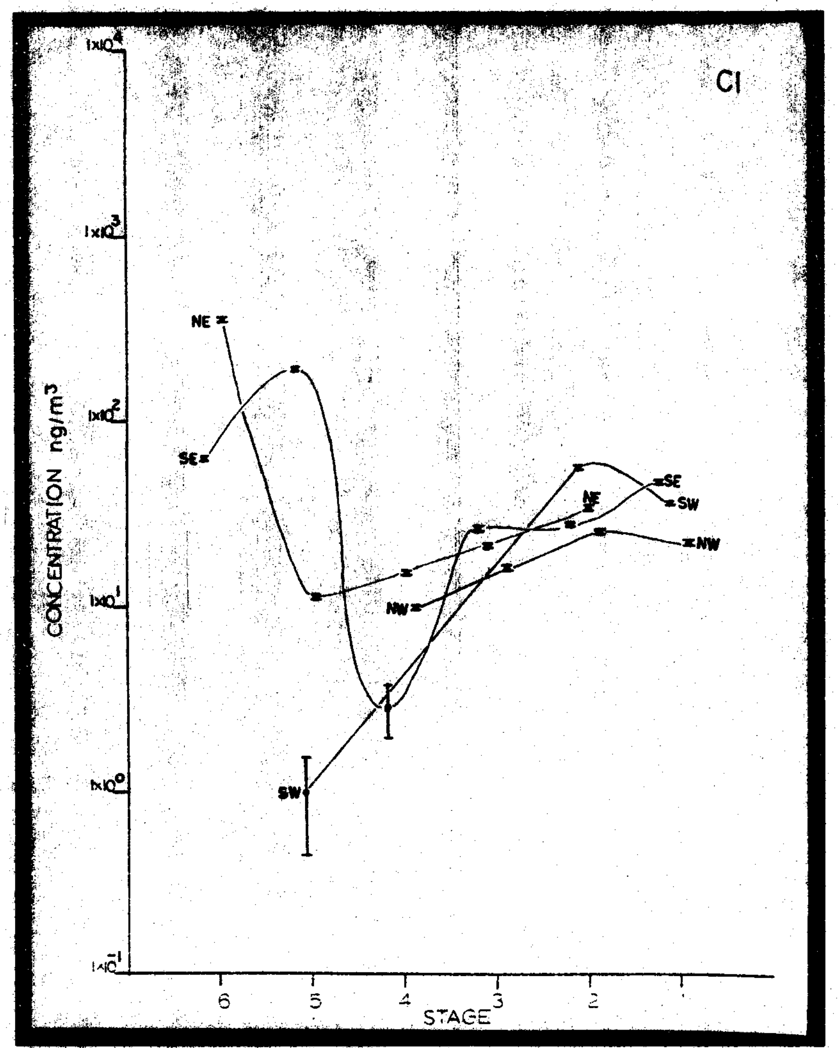

Figure 151 Wind Direction Sensitive Size Distributions. SLMC K

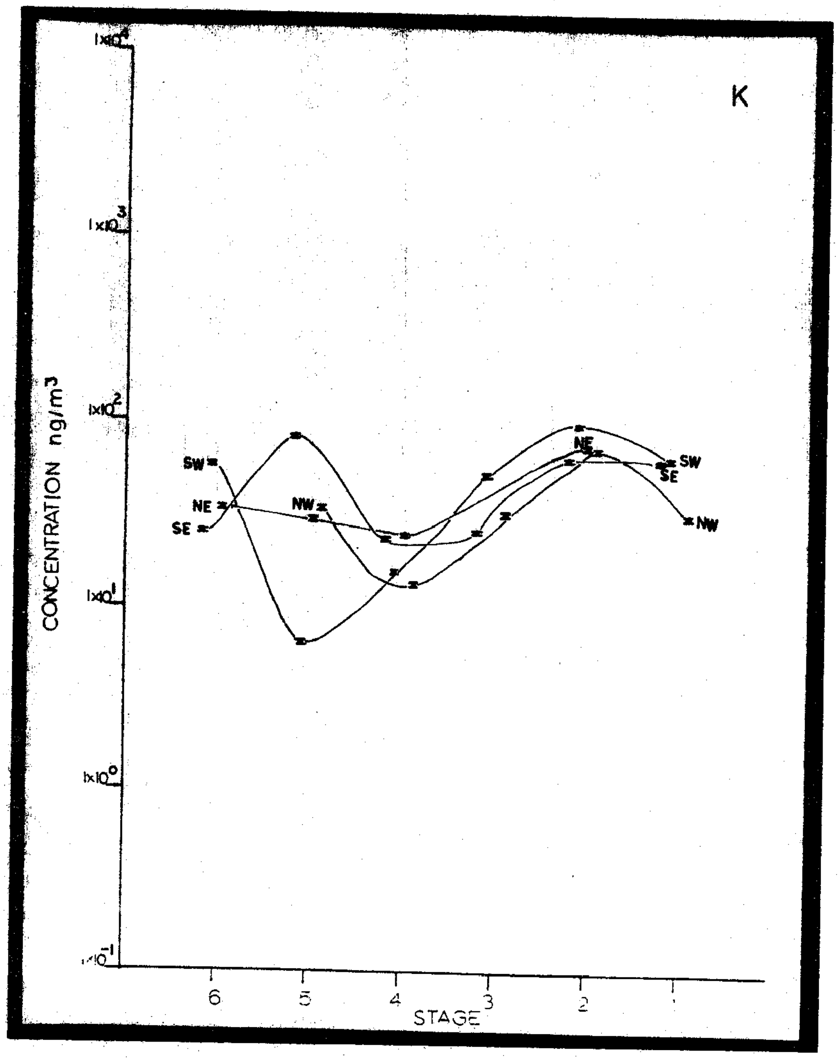

Figure 152 Wind Direction Sensitive Size Distributions. SLMC Ca

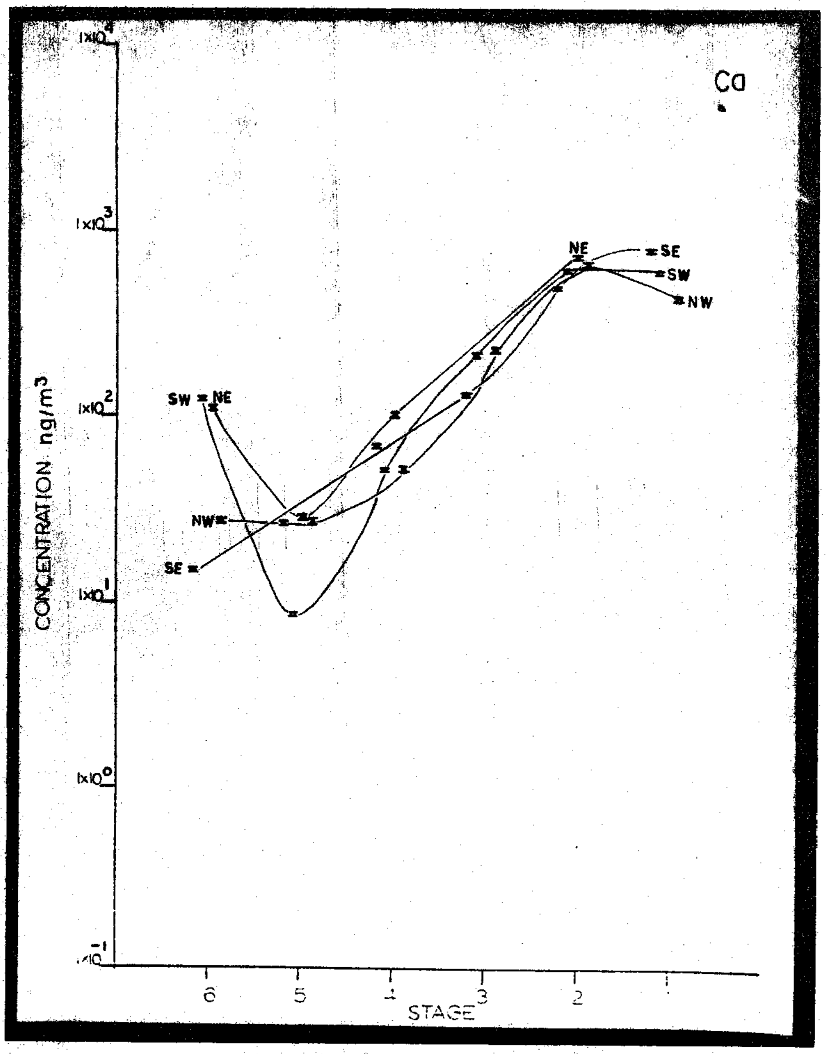

Figure 153 Wind Direction Sensitive Size Distributions. SLMC Ti

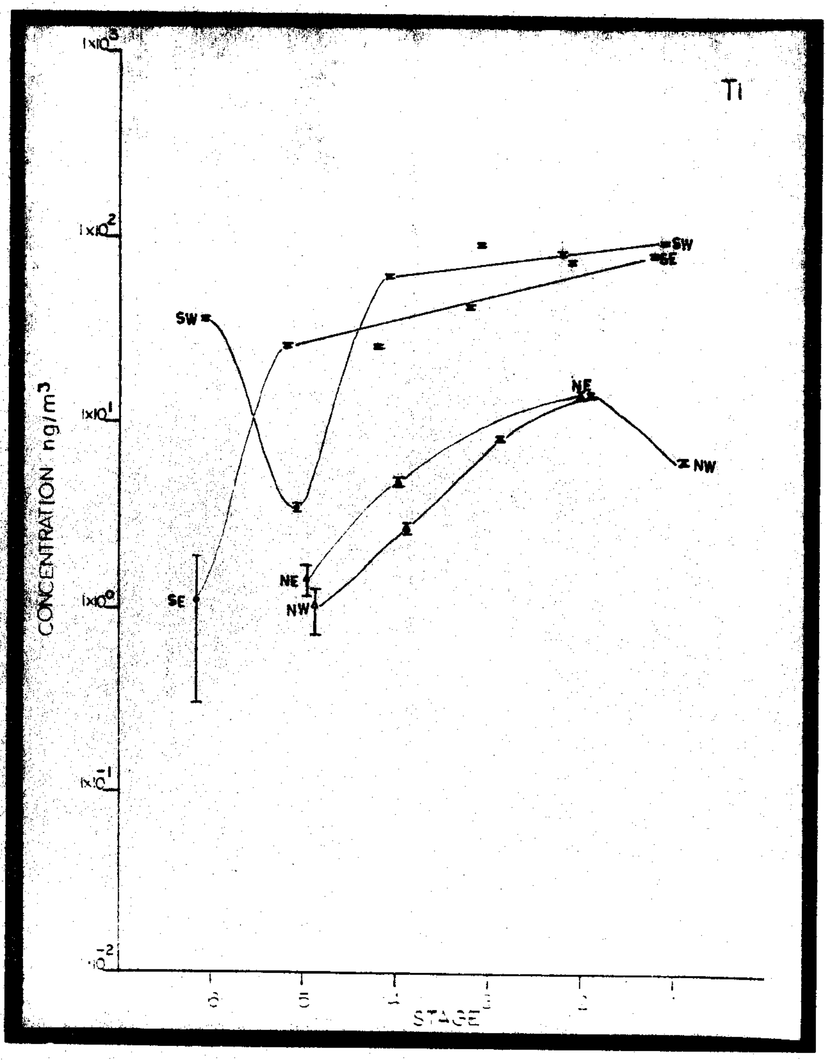

Figure 154 Wind Direction Sensitive Size Distributions. SLMC V

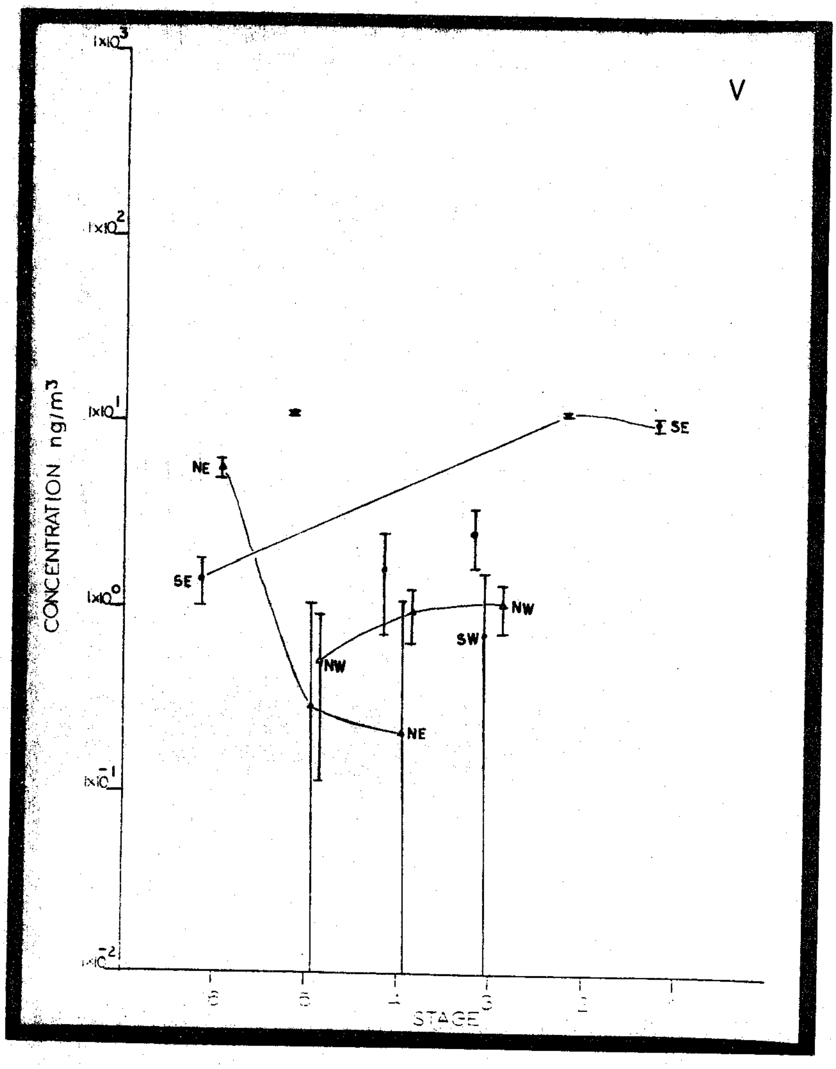

Figure 155 Wind Direction Sensitive Size Distributions. SLMC Mn

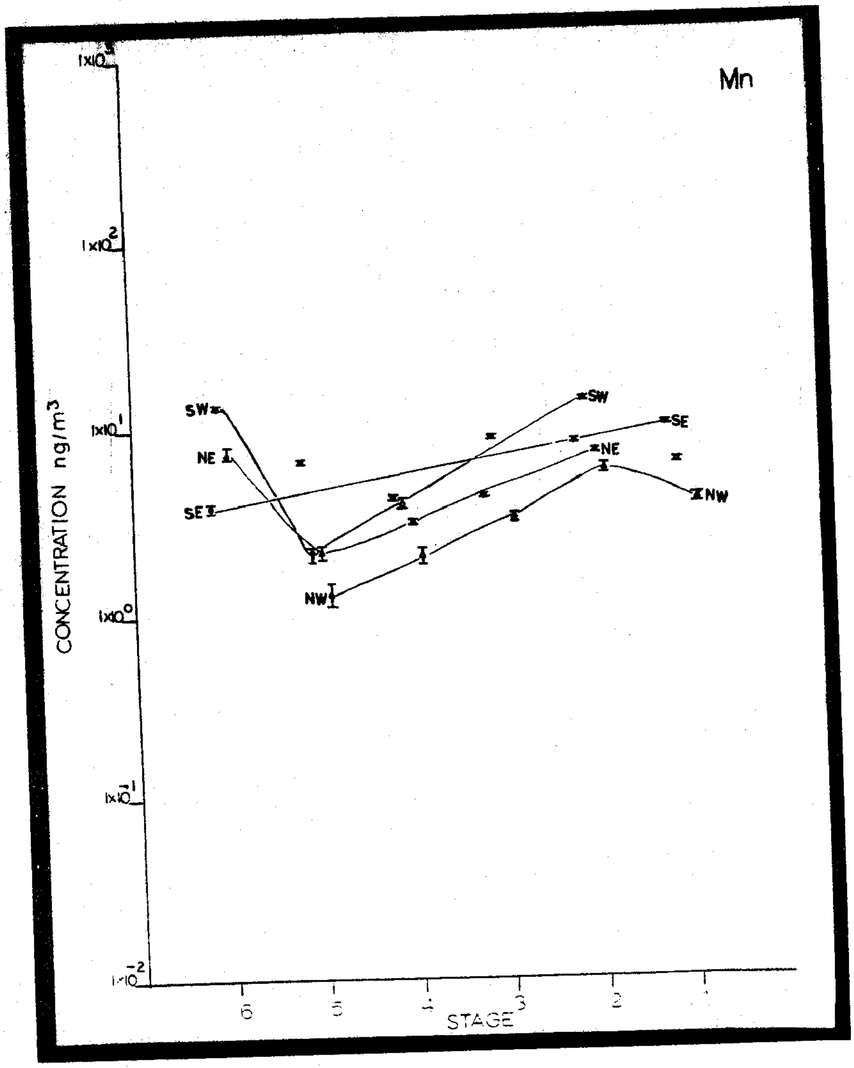

Figure 156 Wind Direction Sensitive Size Distributions. SLMC Fe

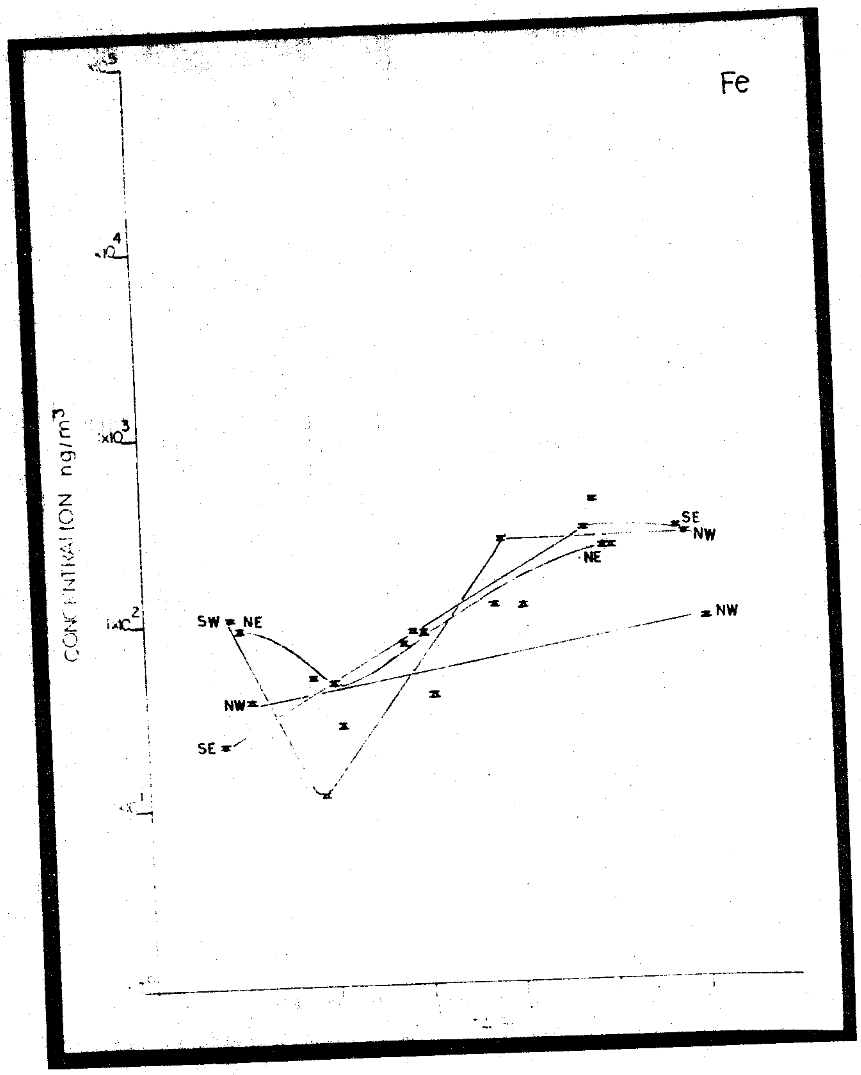

Figure 157 Wind Direction Sensitive Size Distributions. SLMC Cu

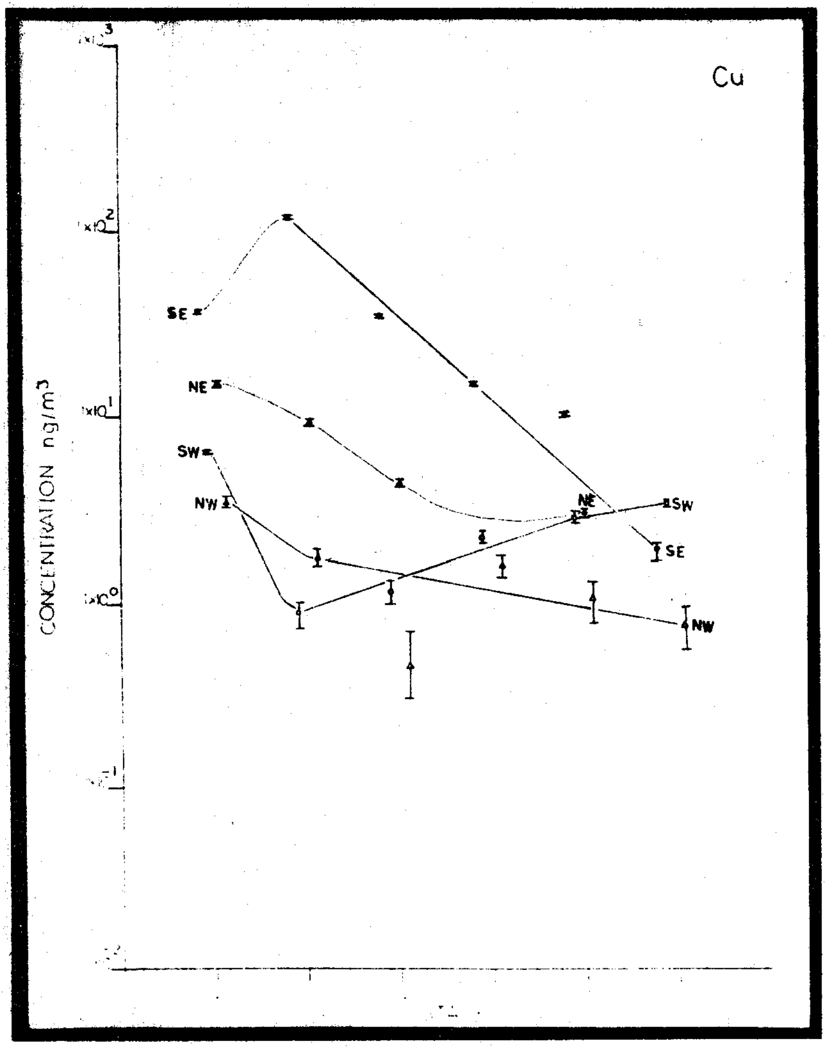

Figure 158 Wind Direction Sensitive Size Distributions. SLMC Zn

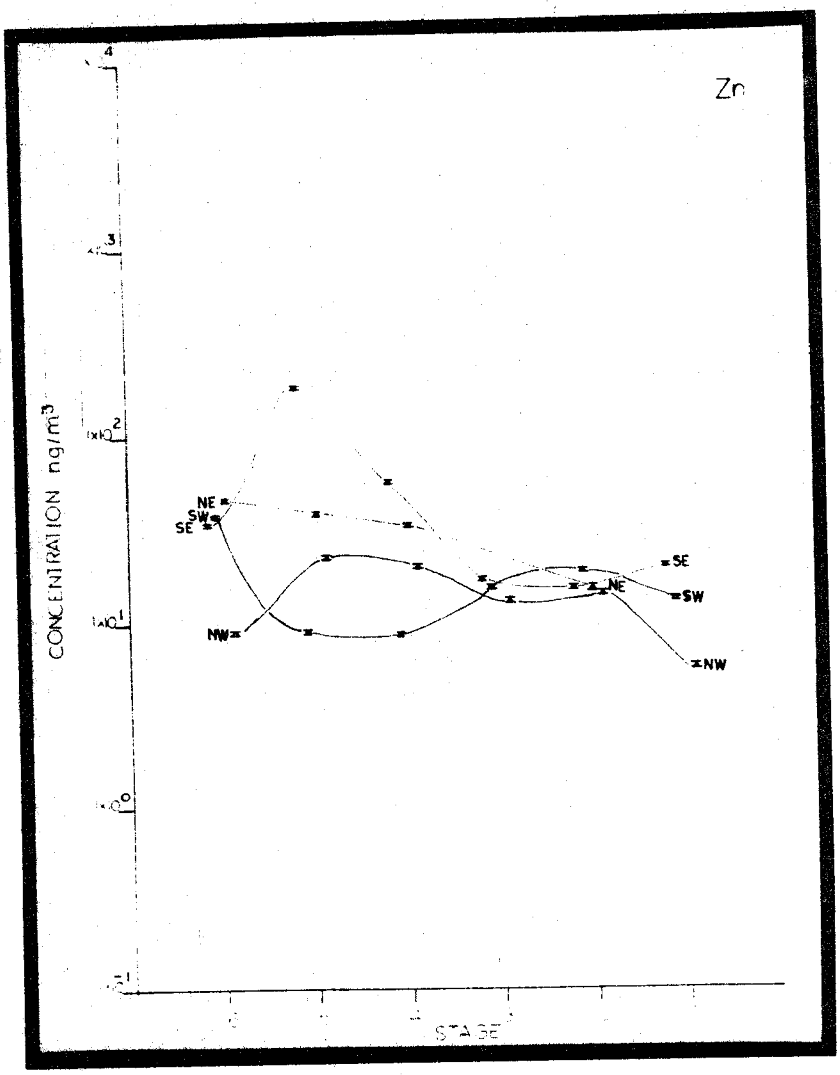

Figure 159 Wind Direction Sensitive Size Distributions. SLMC Br

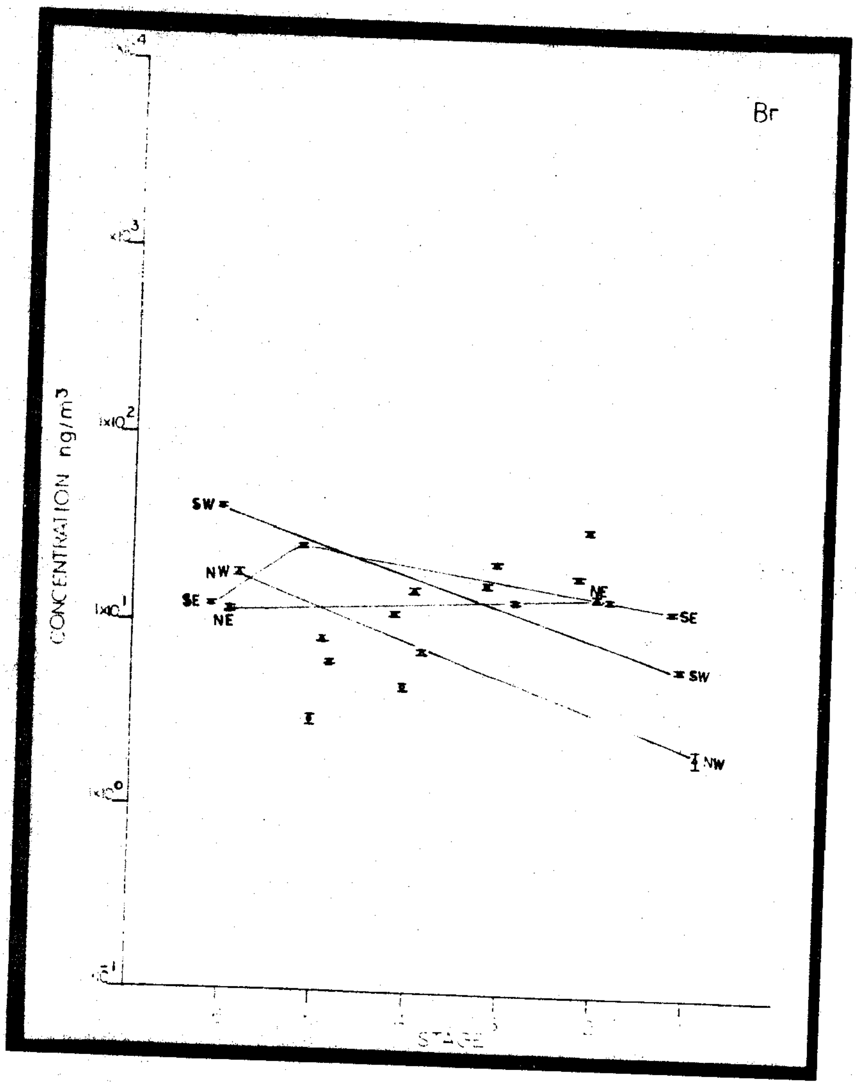

Figure 160 Wind Direction Sensitive Size Distributions. SLMC Pb

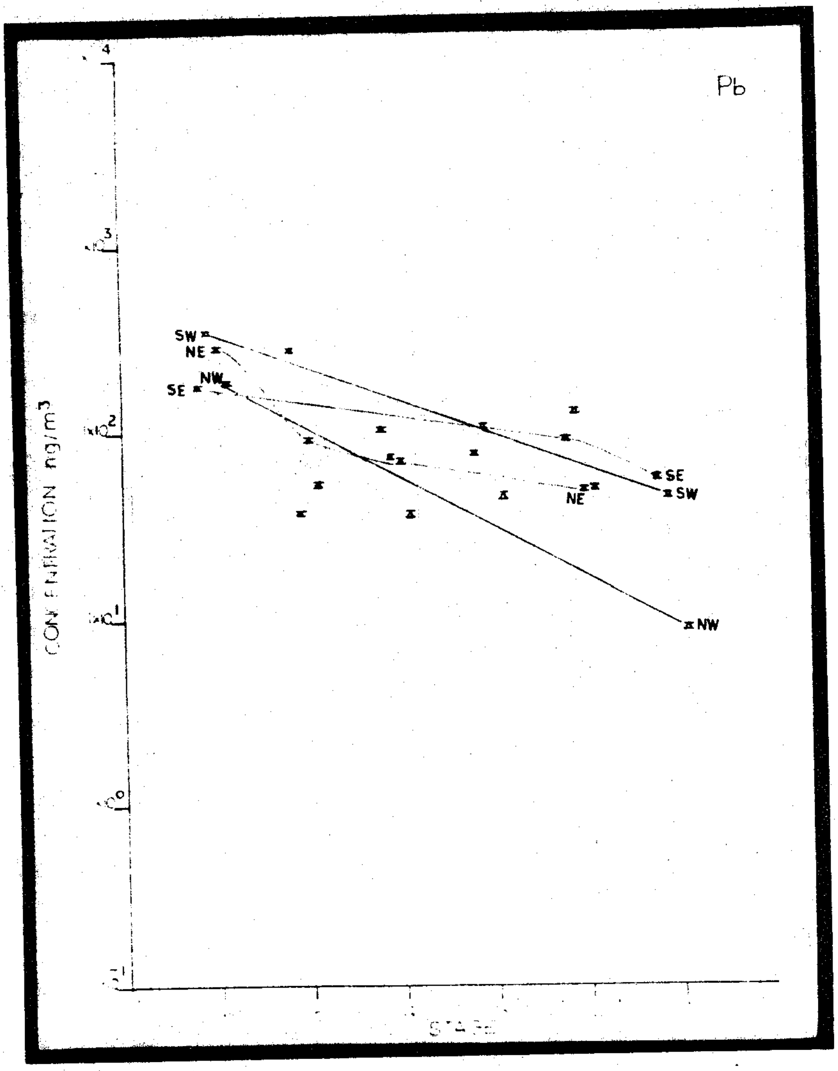

TECHNICAL REPORT DATA
(Please read Instructions on the reverse before completing)

1. REPORT NO. EPA-600/7-80-025	2.
3. RECIPIENT'S ACCESSION NO.	
4. TITLE AND SUBTITLE AEROSOL SOURCE CHARACTERIZATION STUDY IN ST. LOUIS Trace Element Analysis	5. REPORT DATE February 1980
	6. PERFORMING ORGANIZATION CODE
7. AUTHOR(S) Kenneth A. Hardy	8. PERFORMING ORGANIZATION REPORT NO.
9. PERFORMING ORGANIZATION NAME AND ADDRESS Department of Physical Sciences, Florida International University, Miami, Florida 33199	10. PROGRAM ELEMENT NO. EHE625 EA-011 (FY-76)
	11. CONTRACT/GRANT NO. 68-02-2406
12. SPONSORING AGENCY NAME AND ADDRESS Environmental Sciences Research Laboratory - RTP, NC; Office of Research and Development; U.S. Environmental Protection Agency; Research Triangle Park, North Carolina 27711	13. TYPE OF REPORT AND PERIOD COVERED
	14. SPONSORING AGENCY CODE EPA/600/09
15. SUPPLEMENTARY NOTES	

16. ABSTRACT

The aerosol in St. Louis was sampled in July 1975 to better characterize the aerosol in an urban environment with moderate dispersion characteristics and heavy industrial activity. Two sampling sites were chosen, one in downtown St. Louis and a second close to the industrialized section in south St. Louis.

Aerosol source coefficients show that the aerosol from the downtown site is primarily from coal (60-80%), cement dust (17%), steel manufacturing (6-7%) and auto emissions (3%). The aerosol from the industrialized site is primarily due to coal combustion products and dust (75%), and cement dust (15%), while auto emissions and heavy industrial processes account for ∿5% of the aerosol mass. Determining the directional distribution of the aerosol trace elements allowed pinpointing of strong local sources.

17. KEY WORDS AND DOCUMENT ANALYSIS

a. DESCRIPTORS	b. IDENTIFIERS/OPEN ENDED TERMS	c. COSATI Field/Group
*Air pollution *Aerosols *Chemical elements *Chemical analysis *Sources Identifying	St. Louis, MO	13B 07D 07B

18. DISTRIBUTION STATEMENT RELEASE TO PUBLIC	19. SECURITY CLASS (This Report) UNCLASSIFIED	21. NO. OF PAGES 198
	20. SECURITY CLASS (This page) UNCLASSIFIED	22. PRICE

EPA Form 2220-1 (9-73)

United States
Environmental Protection
Agency

Center for Environmental Research
Information
Cincinnati OH 45268

Please make all necessary changes on the above label, detach or copy, and return to the address in the upper left-hand corner.

If you do not wish to receive these reports CHECK HERE □; detach, or copy this cover, and return to the address in the upper left-hand corner.

EPA-600/7-80-025